QUINONE METHIDES: MULTIFUNCTIONAL TOOLS FOR CHEMICAL BIOLOGY AND MATERIAL SCIENCE

by

MARIIA VLADIMIROVNA SUTTON

(Under the Direction of Vladimir V. Popik)

ABSTRACT

Efficient generation of quinone methides (QMs) from quinone methide precursors (QMPs) under mild conditions, such as reagent free UV-light irradiation, and exceptional reactivity of QMs towards nucleophiles and, in case of *o*-QMs, towards dienophiles have attracted a lot of attention to these compounds in computation, chemical, biological and engineering spheres. Our research group has demonstrated successful application of *o*-napthoquinone methide precursors (*o*-NQMPs) as photolabile protecting groups (PPGs) and linkers, that can be employed in the design of multifunctional surfaces, used as PPGs for biological molecules that carry different functional groups and as a linker for peptide and protein reversible modification.

o-QMs and *p*-QMs demonstrate different chemical properties and different reactivity. However, to the best of our knowledge, the molecules containing competing *o*-NQM and *p*-QM moieties, have not been studied. Thus, the major goal of the first project was to develop and synthesize novel QMPs with ability to generate *o*-NQM and *p*-QM under light irradiation. Physical properties, chemical properties, such as ability to react with nucleophiles and undergo inter- and intra-molecular Diels-Alder reaction, as well as kinetic behavior of new QM-system have been studied.

We were also interested in investigating the ability of *o*-NQMPs decorated with thiol moieties to form “smart” polymers, that could be generated upon UV-light irradiation. The photo-induced degradation of the polymers could be achieved on demand upon light irradiation in the presence of vinyl ethers. Unfortunately, light-induced polymerization of the synthesized monomers resulted in exclusive formation of oligomers.

Another project has been focused on the development of a novel photocleavable analog of calcium-selective chelating ligand, which was based on the combination of properties of photolabile 3-(hydroxymethyl)-2-naphthol core and high calcium affinity of 1,2-*bis*(*o*-aminophenoxy)ethane-*N,N,N’,N’*-tetraacetic acid (BAPTA).

Finally, we have worked towards the design of a new fluorogenic PPG that could also serve as an intracellular pH indicator. 9*H*-xanthene-1,8,9-triol derivatives can be considered as photoactivatable fluorophores and fluorogenic PPGs, as 9*H*-xanthen-1,8,9-triols are expected to generate relatively stable quinone methide upon UV-light irradiation. Due to its structural similarity with fluorescein derivatives, we expected 8-hydroxy-1*H*-xanthen-1-one to be highly fluorescent. However, attempted synthesis resulted in the formation of a different unexpected product.

INDEX WORDS: quinone methides, QMs, quinone methide precursors, QMPs, *o*-naphthoquinone methides, *o*-NQMs, o-naphthoquinone methide precursors, *o*-NQMPs, BAPTA, NQMP-BAPTA, *hetero*-Diels-Alder reaction

QUINONE METHIDES: MULTIFUNCTIONAL TOOLS FOR CHEMICAL BIOLOGY AND MATERIAL SCIENCE

by

MARIIA VLADIMIROVNA SUTTON

BS, State Saint Petersburg University, Russia, 2015

A Dissertation Submitted to the Graduate Faculty of The University of Georgia in Partial Fulfillment of the Requirements for the Degree

DOCTOR OF PHILOSOPHY

ATHENS, GEORGIA

2019

QUINONE METHIDES: MULTIFUNCTIONAL TOOLS FOR CHEMICAL BIOLOGY AND MATERIAL SCIENCE

by

MARIIA VLADIMIROVNA SUTTON

Major Professor:	Vladimir V. Popik
Committee:	Robert S. Phillips
	Jason Locklin

Electronic Version Approved:

Suzanne Barbour
Dean of the Graduate School
The University of Georgia
August 2019

DEDICATION

I would like to dedicate this work to my parents, Evgeniia Vladimirovna Sorokina and Vladimir Anatolievich Sorokin, and my husband, Dewey Sutton for their love and support.

ACKNOWLEDGEMENTS

I would like to thank my research advisor, Dr. Vladimir V. Popik, for giving me interesting and diverse projects, for always being available to discuss the research problems and for his continuous support.

I would like to thank my committee members, Dr. Jason Locklin and Robert S. Phillips, for their assistance in review of this work.

I would also like to thank Dr. Chris McNitt, Dr. Dewey Sutton, Nannan Lin and Chris Molnar for their assistance in troubleshooting the teaching and research problems over the years.

TABLE OF CONTENTS

Page

LIST OF TABLES

Page

LIST OF FIGURES

Page

LIST OF SCHEMES

Page

CHAPTER 1

INTRODUCTION AND LITERATURE REVIEW

1.1. Introduction and Literature Review

Quinone methides (QMs) represent a unique class of molecules, that demonstrate a combination of properties of zwitterionic aromatic and neutral valence non-aromatic compounds. Quinone methides exist in three isomeric forms: 1,2-, 1,3- and 1,4-quinone methides, however, their distinctive high chemical reactivity, such as ability to react as Michael acceptors, can be only attributed to *ortho*-quinone methide (*o*-QM) and *para*-quinone methide (*p*-QM). o-QMs and p-QMs are relatively stable neutral molecules, that resemble the structure of simple Michael acceptors.[1] They readily react with nucleophiles in 1,4- and 1,6-addition, respectively. And if 1,4-addition of protonated nucleophiles to α,β-unsaturated ketones **1.1** results in a small decrease in product stabilization by a loss of a conjugated π-bond compare to starting material, in case of o-QM increase in stabilization occurs due to formation of aromatic system. Similarly, 1,6-addition of nucleophiles to α,β,γ,δ-unsaturated ketones results in a decrease in product stabilization by a loss of two conjugated π-bonds compared to starting material. On the other hand, addition of nucleophiles to *p*-QM **1.4** results in increase of stability.[1,2] Additionally, **o**-QMs **1.7** undergo fast and efficient Diels-Alder reaction with electron-rich alkenes (Scheme 1.1).[3]

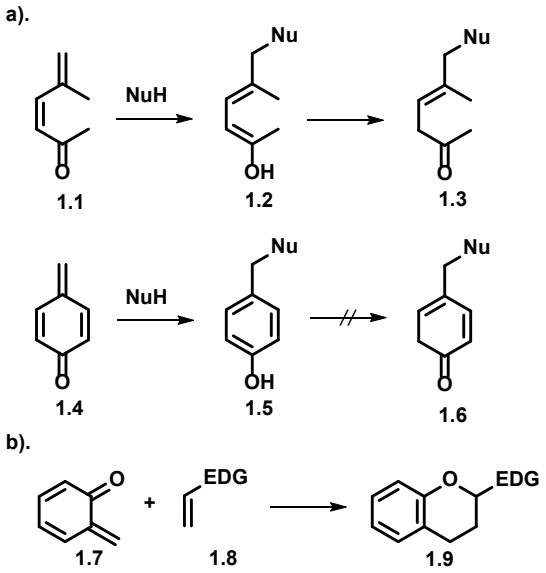

Scheme 1.1. a). Comparison of α,β,γ,δ-unsaturated ketones with p-QM in the reaction with protonated nucleophiles. **b).** Hetero-Diels-Alder reaction between o-QM and electron-rich alkene.

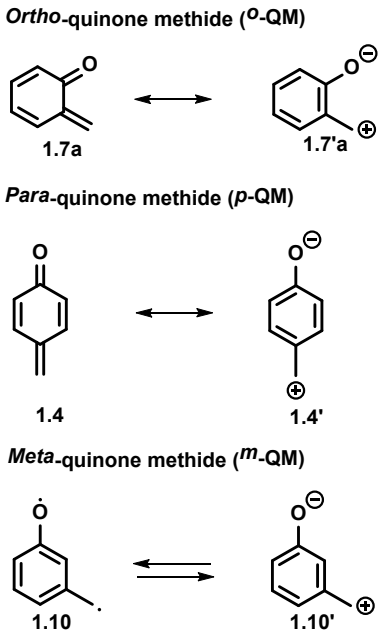

Scheme 1.2. Resonance structures of *o*-QM and *p*-QM, and equilibrating forms of *m*-QM.

Meta-quinone methides (m-QMs) **1.10** exhibit completely different properties compare to their 1,2- and 1,4-analogues, and that can be easily explained by their structural differences. In 1,3-isomers there is no direct orbital interaction between oxygen in *meta*-position and carbon substituent. Additionally, in neutral

form *m*-QMs exist as a triplet biradical (Scheme 1.2). Thus, compare to 1,2- and 1,4-isomers, *m*-QMs are chemically unstable and hard to generate.[4]

Unique chemical behavior and high reactivity of *o*- and *p*-QMs attracted significant attention to these core structures, and different methods of generation of these highly reactive species were reported. Thermal methods of generation of quinone methides are based on the elimination of substituents in benzylic position in a form of a stable molecule. The major downfall of these methods is a requirement of high temperature, which cannot be tolerated by a lot of nucleophiles.[3] The most commonly used thermal methods are summarized in Scheme 1.3 on the example of generation of *o*-QM **1.11**.

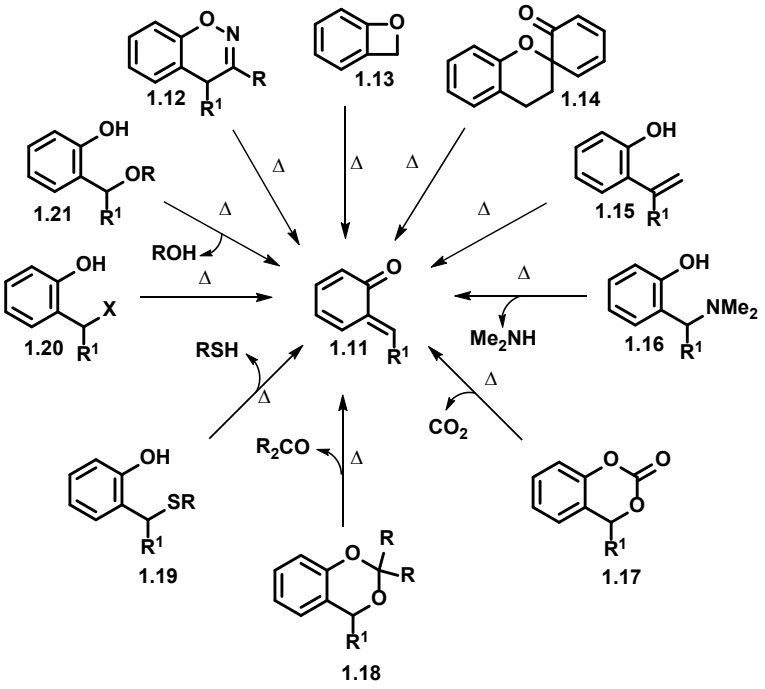

Scheme 1.3. Thermal methods of synthesis of *o*-QMs.

Alternatively, QMs can be generated photochemically under mild conditions. The first simple and general method of photogeneration of all three isomers of QMs have been reported by Wan in 1995 and involved photolysis of hydroxybenzyl alcohols **1.23** in aqueous solutions.[4] Later Kresge[5,6], Popik[7,8] and Freccero[9-12] have shown that QMs could be also generated via photoheterolysis of hydroxybenzyl ethers **1.21**, Mannich bases **1.16** and quaternary ammonium salts **1.22** (Scheme 1.4). In all cases photogeneration of

QMs happened within a nanosecond laser pulse, however, efficiency of photoactivation and solubility in aqueous solutions strongly depend on the leaving group. For instance, quaternary ammonium salts demonstrated better water solubility and higher quantum yield (Φ ~ 0.98).[13]

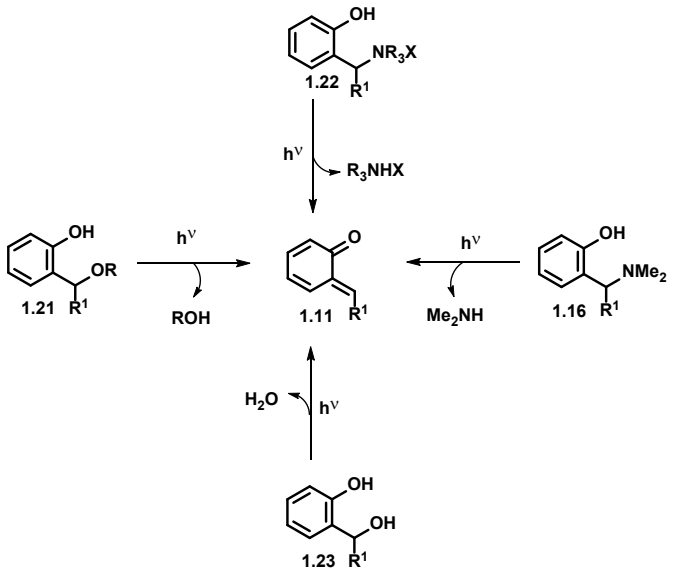

Scheme 1.4. Photochemical methods of synthesis of *o*-QMs.

Even though many research groups have been studying the mechanism of photogeneration of QMs, the mechanism is still not fully understood. Phenols and naphthols are strong acids in the excited state (pKa* of phenol and 2-naphthol in the excited state are ~4.0 and 2.8, respectively),[14,15] thus excited state intramolecular proton transfer (ESIPT) of a phenolic proton to an oxygen atom in the benzylic position can occur. Thus, C-O heterolysis in the benzylic position most likely happens in a concerted fashion with excited state intermolecular proton transfer.[7] Recently, it has been proposed that photogeneration *o*-QMs and *p*-QMs happens via different pathways. Mechanistic studies performed by Popik on *o*-naphthoquinone methide precursors (*o*-NQMPs) **1.24** and **1.28** suggested the absence of ESIPT from phenolic oxygen to an oxygen atom in the benzylic position, and oxetanes **1.27** and **1.31** are believed to be o-QMs precursors (Scheme 1.5).[7]

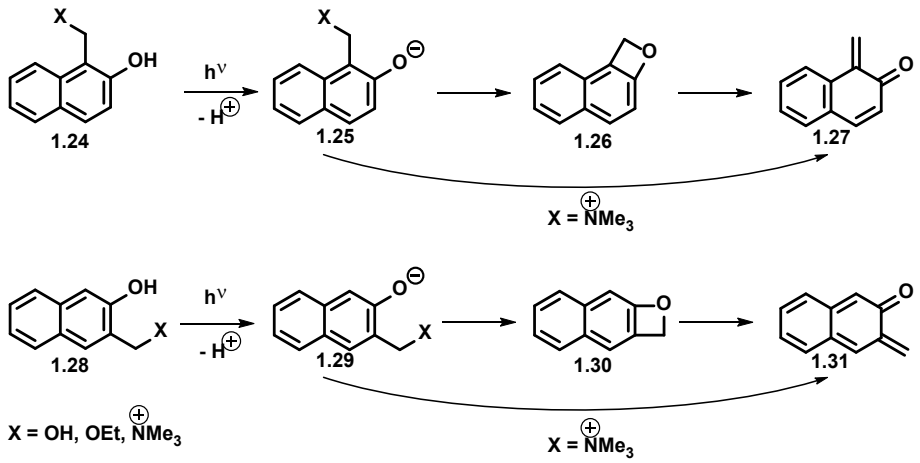

Scheme 1.5. Proposed mechanism of photochemical formation of *o*-NQMs from various *o*-NQMPs.

At the same time, Basaric performed time-resolved fluorescence studies on 2-hydroxy-3-(diphenylhydroxymethyl)anthracene **1.32** and observed formation of two short-living species. Thus, he believed that photodissociation of the anthrol hydroxyl in singlet excited state **1.33** caused elimination of benzylic hydroxyl and resulted in the formation of corresponding *o*-QM **1.34** (Scheme 1.6). However, as it is mentioned in the publication, neither mechanism that involve ESIPT nor formation of benzoxete intermediates could be ruled out.[16]

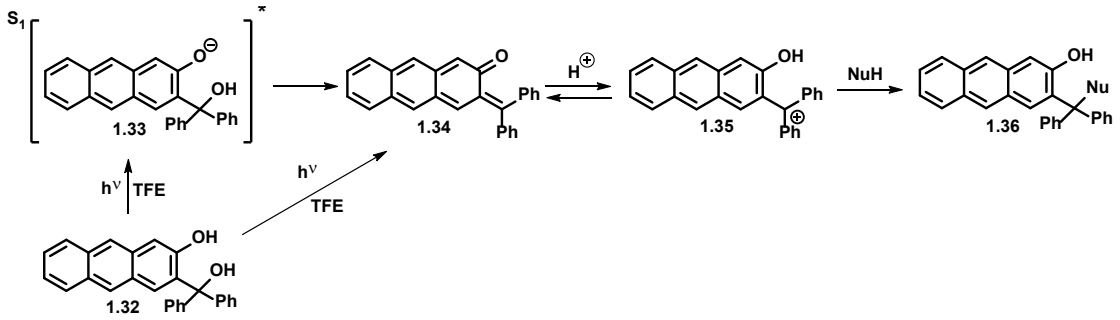

Scheme 1.6. Proposed mechanism of photochemical formation of *o*-anthra-QM from *o*-anthra-QMP.

In 2018 Basaric presented theoretical and experimental data regarding photogeneration of *o*-QM from 2-hydroxymethylphenol **1.37a**. Upon photoexcitation **1.37a** underwent homolytic cleavage of the phenolic hydroxyl with formation of phenoxyl radical **1.38a** in S_0 state and simultaneous elimination of water, that gave QM **1.7a** in S_0 state. The first process occurred in nanosecond range, the second process happened

in femtosecond time scale. High energy barrier of formation of benzoxete intermediate **1.13** in S_0 state, as well as its lower stability compare to QM, it is considered highly unlikely to be an intermediate in photogeneration of *o*-QM (Scheme 1.7).[17]

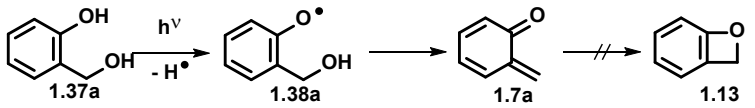

Scheme 1.7. Proposed mechanism of photochemical formation of *o*-QM from *o*-NQP.

The most recent mechanistic studies of *p*-QMs, performed on 6,6'-bis(hydroxymethyl)-1,1'-binaphthyl-2,2'-diol **1.39** (*p*-BQMP), suggested that that in aqueous solution solvent-assisted intramolecular excited state proton transfer takes place. It was proposed that water and deuterium oxide solvents would cause solvent kinetic isotope effect if solvent is involved in ESIPT. Indeed, Phillips observed kinetic isotope effect of k_H/k_D ~ 2 for the process of generation of excited QM. Thus, water-mediated proton transfer (τ ~ 125 ps) resulted in formation of excited state QM **1.40**, then was followed by the loss of water (τ ~ 906 ps) and formation of *p*-binaphthylquinone methide (*p*-BQM) **1.44** through ground state intramolecular proton transfer (GSIPT) process (τ ~ 1.7 μs) (Scheme 1.8).[18]

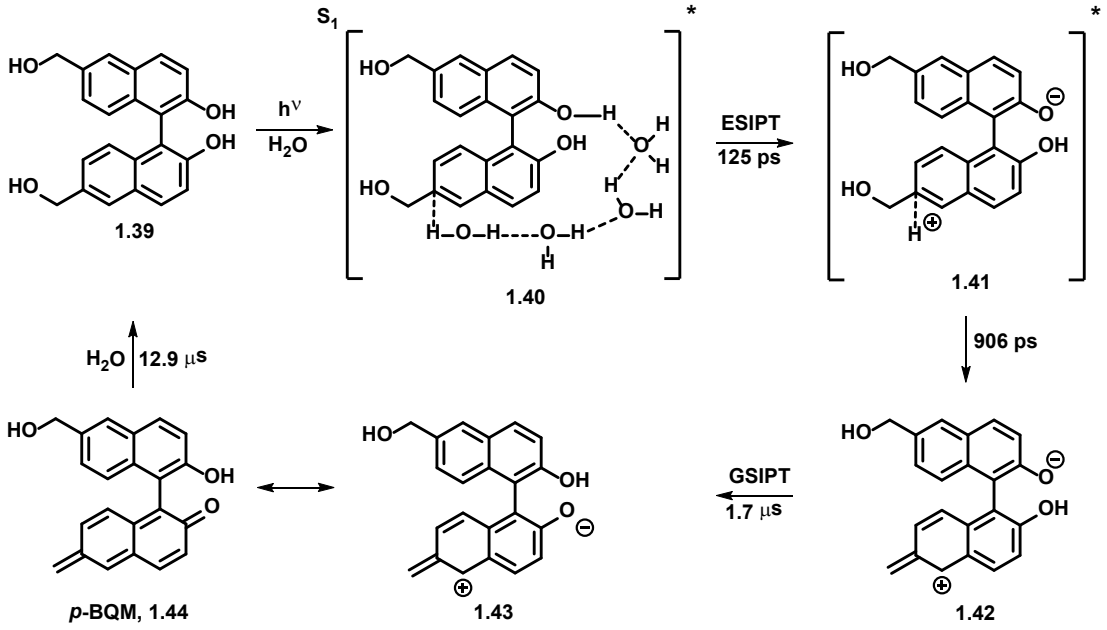

Scheme 1.8. Proposed mechanism of photochemical formation of *p*-BQM from *p*-BQMP.

This chapter will focus on the physical and chemical properties of the derivatives of *o*- and *p*-quinone methides, as well as their precursors. Applications of these reactive species in material sciences and chemical biology that were studied by our group will be also discussed. Finally, the goals and the importance of current projects will be presented. In the first part, we will discuss properties of QMPs, such as absorption and fluorescence spectra, pKa and their effectiveness in generating QMs upon light irradiation. Then reactivity of QMs towards nucleophilic attack (including hydration) and [4+2] cycloaddition to dienophiles will be presented. The emphasis will be placed on the relationship between the structure and properties of the compounds. The second part will focus on the versatility of QMPs applications demonstrated by our group. For instance, QMPs can be used for surface derivatization, as photolabile linkers and as photolabile protecting groups (PPGs). Finally, this literature review will introduce our current projects, which include both fundamental and applied studies.

1.2. Properties of Some QMPs

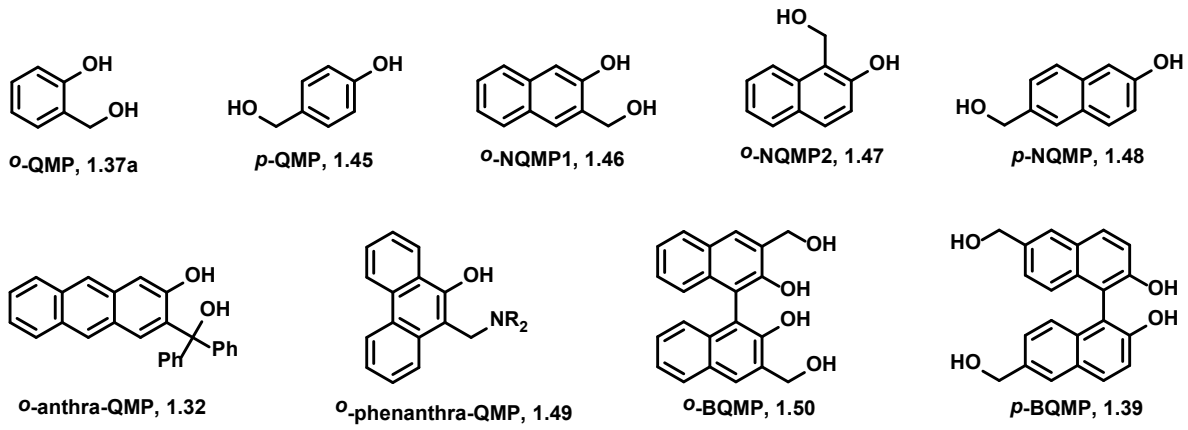

Scheme 1.9. Structures of QMPs.

Absorption spectra of QM precursors in aqueous acetonitrile solutions are predictably similar due to the presence of analogous chromophores. In general, UV spectra of QM precursors resemble spectrum of phenol, similarly naphtho-, anthra- and phenanthra-QM precursors exhibited spectra similar to 2-naphthol, 2-anthrol and 9-phenanthrol, respectively (Scheme 1.9). For instance, *o*- and *p*-hydroxybenzyl chromophores have the lowest energy absorbance at λ_{max} = 275 nm (log ε = 3.30).[19] Absorbance spectra

of 3-hydroxy-2-naphthalene methanol **1.46**, 2-hydroxy-1-naphthalenemethanol **1.47**, 6-(hydroxymethyl)naphthalen-2-ol **1.48** and 6,6'-bis(hydroxymethyl)-1,1'-binaphthyl-2,2'-diol **1.39** are bathochromically shifted and have two major absorbance bands at λ_{max} ~ 275-277 nm (log ε = 4.06) and at λ_{max} ~ 325 nm (log ε = 3.70-3.83).[7,20] UV spectrum of 2-hydroxy-3-(diphenylhydroxymethyl)anthracene **1.32** has multiple absorbance bands centered at 350-400 nm: at λ_{max} = 330 nm log ε = 3.46, at λ_{max} = 350 nm log ε = 3.50, at λ_{max} = 375 nm log ε = 3.45 and at λ_{max} = 390 nm log ε = 3.43.[16] Its phenanthra-QM precursor (*N,N*-dialkyl-9-aminomethyl-10-phenanthrols) **1.49** has major absorbance bands at λ_{max} = 300 nm log ε = 4.21, at λ_{max} = 335 nm log ε = 3.40, at λ_{max} = 355 nm log ε = 3.65 and λ_{max} = 380 nm log ε = 2.24.[21] All QM precursors show strong fluorescence, expectedly similar to their analogs phenol, 2-naphthol, 2-anthrol and 9-phenanthrol. However, fluorescence lifetimes of QM precursors are found to be shorter than for their analogs. The observation can be explained by the new pathway for the decay of excited state. For example, emission spectra of NQMPs demonstrate major bands at 360 nm and 423 nm with fluorescence quantum yields similar to the one of 2-naphthol (Φ_{Fl} = 0.27):[22] *o*-NQMP1 (Φ_{Fl} = 0.230±0.002) and *o*-NQMP2 (Φ_{Fl} = 0.30±0.01).[7] Fluorescence intensity was found to decay with the time constant of τ_{Fl} ~ 7 ns,[7] which was faster compare to 2-napthol (τ_{Fl} ~ 11 ns).[23] BQMPs are reported to be much less fluorescent at 320-400 nm compare to their naphthols analogs. *p*-BQMP has emission maximum at λ_{max} = 356 nm in pure acetonitrile and at λ_{max} = 360 nm in aqueous acetonitrile. Additionally, it was found that fluorescence intensity decreased significantly in the presence of water. Current observation suggested water-assisted decay of excited state.[20] Emission spectrum of 2-hydroxy-3-(diphenylhydroxymethyl)anthracene **1.32** contains band at λ_{max} = 450 nm (Φ_{Fl} = 0.86±0.01) in pure acetonitrile and two bands at λ_{max} = 450 nm and 545 nm (Φ_{Fl} = 0.39±0.01) in aqueous acetonitrile (1:1). Decrease of fluorescence intensity at 450 nm was observed with increase of water content. Also, addition of water caused change in fluorescence lifetimes of *o*-anthra-QMP: fluorescence intensity was found to decay with the time constant of τ_{Fl} ~ 17.8±0.1 ns in pure acetonitrile and with the time constant of τ_{Fl} ~

1.7±0.2 ns in aqueous acetonitrile (1:1), which was much faster compare to 2-anthrol (τ_{FI} 25.3±0.1 ns).[16] Fluorescent spectra of *N,N*-dimethyl-9-aminomethyl-10-phenanthrol and *N,N*-diethyl-9-aminomethyl-10-phenanthrol are nearly identical and have emission bands at λ_{max} = 460 nm in pure acetonitrile and λ_{max} = 380 nm and at λ_{max} = 460 nm in aqueous acetonitrile (1:1). Increase of water concentration resulted in the decrease of fluorescence intensity at λ_{max} = 460 nm and caused the formation of new emission band at λ_{max} = 380 nm.[21] This observation is similar to the one described for of 2-hydroxy-3-(diphenylhydroxymethyl)anthracene **1.32**. Yasuda proposed that emission band dominated in pure acetonitrile could be attributed to the singlet excited state of the zwitter-ion generated via ESIPT process. Additionally, appearance of new emission band in aqueous solutions could be explained via protonation of singlet excited state anion by water. The proposed mechanism was supported by similarity of emissions bands of phenanthra-QMPs (λ_{max} = 390 nm) and 9-phenanthrol (λ_{max} =384 nm) in aqueous solutions.[21]

The ground-state acidities of QM precursors are similar to their analogs: phenol (pKa = 9.99),[24] 2-naphthol (pKa = 9.6),[25] 2-anthrol (pKa = 9.4)[16] and 9-phenanthrol (pKa = 10.15).[26] In case of *o*-QMPs intermolecular hydrogen-bonding with the benzyl alcohol increases their acidity. For instance, pKa of 2-hydroxymethylphenol **1.37a** is 9.93, pKa of 3-hydroxy-2-naphalenemethanol **1.46** and 2-hydroxy-1-naphthalenemethanol **1.47** are 9.01 and 8.93, respectively.[7] Similarly pKa* of the excited state is much lower, than of their excited analogs phenol (pKa* = 4.0),[14] 2-naphthol (pKa* = 2.8),[15] 2-anthrol (pKa* = 2.13)[16] and 9-phenanthrol (pKa* = 3.5).[26] For example, pKa* of 2-hydroxymethylphenol is ~ 2.5 and pKa* of 3-hydroxy-2-naphalenemethanol is 0.77.[7]

1.3. Reactivity of some QMPs

As it was mentioned earlier photolysis of aqueous solutions of QMPs results in rapid consumption of substrate and formation of QMs, which readily react with nucleophiles and dienophiles (Scheme 1.10). In general, chemical yields are almost quantitative at low conversion (~ 20-30 %), however, the yields of photoproducts are reduced at longer irradiation time.[6,7,10] Secondary biproducts are believed to be QM

oligomers.[13] Quantum yields for some QM precursors (Scheme 1.11) obtained in aqueous acetonitrile (1:1) are summarized in Table 1.1.

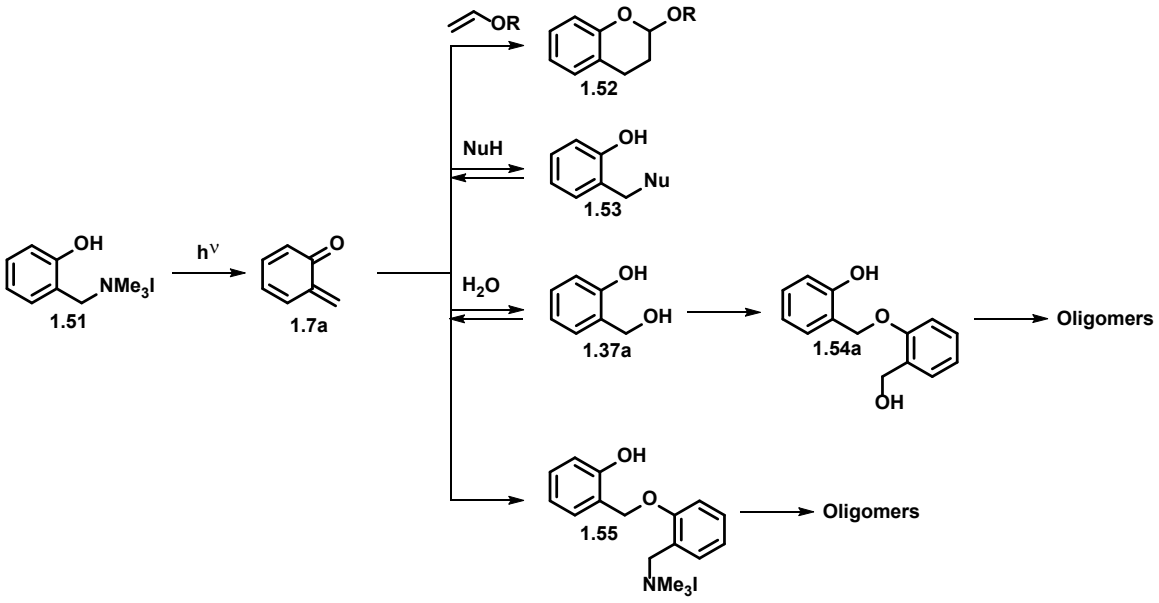

Scheme 1.10. Reactivity of *o*-QM under various conditions.

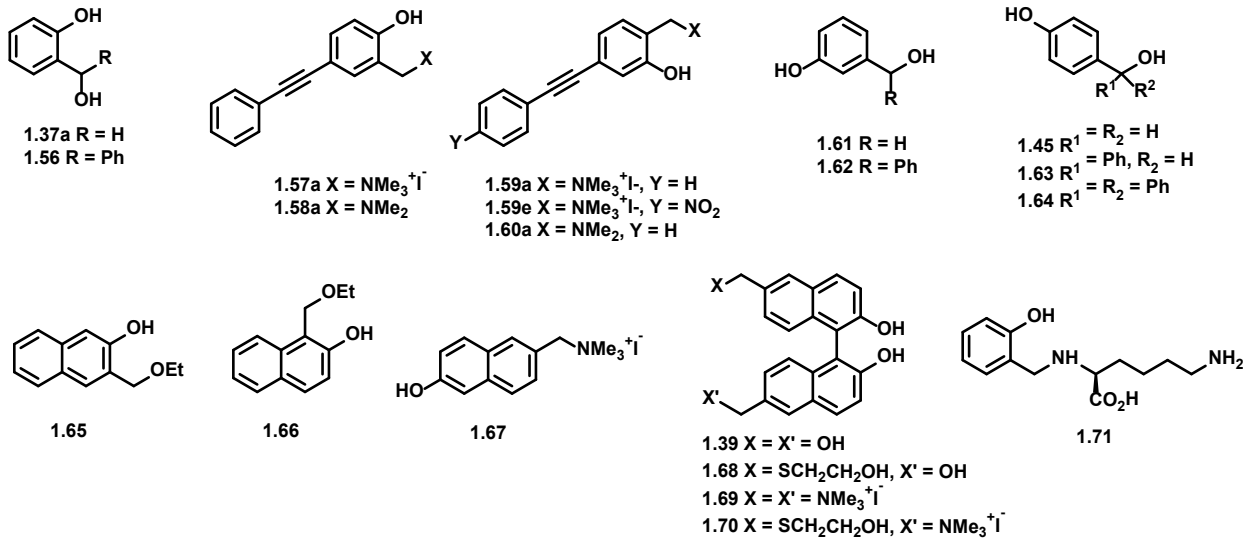

Scheme 1.11. Structures of QMPs.

Table 1.1 Quantum yields of photochemical generation of QMs from corresponding precursors. Quantum yields have been determined in aqueous acetonitrile solution (1:1).

QM precursor	**Φ**	**Ref.**
2-hydroxymethylphenol **1.37a**	0.23	[4,13]
(2-hydroxybenzyl)trimethylammonium iodide **1.51**	0.98	[13]
2-(hydroxy(phenyl)methyl)phenol **1.56**	0.46	[4]
1-(2-hydroxy-5-(phenylethynyl)phenyl)-N,N,N-trimethylmethanaminium iodide **1.57a**	0.48	[27]
2-((dimethylamino)methyl)-4-(phenylethynyl)phenol **1.58a**	0.06	[27]
1-(2-hydroxy-4-(phenylethynyl)phenyl)-N,N,N-trimethylmethanaminium iodide **1.59a**	0.25	[27]
2-((dimethylamino)methyl)-5-(phenylethynyl)phenol **1.60a**	0.02	[27]
1-(2-hydroxy-5-(4-nitrophenylethynyl)phenyl)-N,N,N-trimethylmethanaminium iodide **1.59e**	$7x10^{-4}$	[27]
3-hydroxymethylphenol **1.61**	0.12	[4]
3-(hydroxy(phenyl)methyl)phenol **1.62**	0.23	[4]
4-hydroxymethylphenol **1.45**	0.007	[4]
4-(hydroxy(phenyl)methyl)phenol **1.63**	0.1	[4]
4-(hydroxy(diphenyl)methyl)phenol **1.64**	n.d.	[6]
3-ethoxymethyl-2-naphthol **1.65**	0.17	[7]
1-ethoxymethyl-2-naphthol **1.66**	0.20	[7]
2-hydroxy-3-(diphenylhydroxymethyl)anthrcene **1.32**	0.023	[16]
N,N-dialkyl-9-aminomethyl-10-phenantrol **1.49**	n.d.	[21]
1-(6-hydroxynaphthalen-2-yl)-N,N,N-trimethylmethanaminium iodide **1.67**	0.28	[20]
6,6'-bis(hydroxymethyl)-1,1'-binaphthyl-2,2'-diol **1.39**	0.87	[20]
6-(2-hydroxyethylthio)methyl]-6'-(hydroxymethyl)-1,1'-binaphthyl-2,2'-diol **1.68**	0.15	[20]
1,1'-(2,2'-dihydroxy-1,1'-binaphthyl-6,6'-diyl)bis(N,N,N-trimethylmethanaminium) bromide **1.69**	0.61	[20]
[2,2'-dihydroxy-6'-(2-hydroxyethylsulfanylmethyl)-[1,1']binaphthalenyl-6-ylmethyl]-trimetylammonium **1.70**	0.24	[20]

Efficiency of photoactivation process was found to depend on several factors, such as nature of the chromophore and leaving group, solubility of the compound and type of solvent. Indeed, 2-hydroxymethylphenol **1.37a** demonstrated higher quantum yield (Φ = 0.23), compare to analogues *m*-QMP **1.61** (Φ = 0.12), and *p*-QMP **1.45** had the lowest quantum yield (Φ = 0.007).[4] Additionally, BQMPs exhibited higher efficiency of photoactivation than their naphtho-analogs (Φ = 0.87 vs. 0.17 for **1.39** and **1.65**, respectively).[20] Nature of leaving group as well as solubility of the compound in aqueous solution also played an important role. For example, quaternary ammonium salts demonstrated better water

solubility and higher quantum yield compare to benzylic alcohols and Mannich bases (Φ = 0.98 vs. 0.23 for **1.51** and **1.37a**, respectively).[13] Type of the solvent and pH also affected the quantum yield of formation QMs. For instance, photolysis of quaternary ammonium salts was found to be more efficient in aqueous acetonitrile (1:1), than in buffered aqueous solution at pH = 7 without organic co-solvent (Φ = 0.25 vs. 0.06 for **1.59a**).[27] Additionally, o-QM could be obtained with higher quantum yield under mild acidic conditions (3 < pH < 7) than under basic conditions (pH = 12): Φ = 0.73 in acidic solvent and Φ = 0.13 in basic solvent for *N*-(hydroxybenzyl)-*L*-lysine hydrochloride **1.71**.[13]

1.4. Transient QMPs and QMs

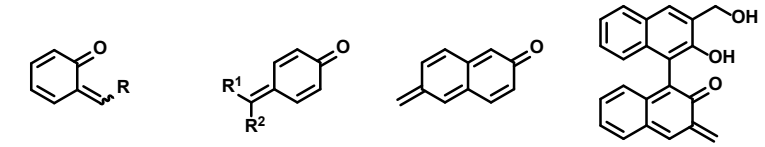

o-QMs
1.7a R =H
1.72 R = Ph
1.73 R = 4-MeO-C_6H_4

p-QMs
1.4 R^1 = R_2 = H
1.74 R^1 = Ph, R_2 = H
1.75 R^1 = R_2 = Ph

p-NQM, 1.76

o-BQM, 1.77

Scheme 1.12. Structures of QMs.

Laser flash photolysis (LFP) of QMPs in aqueous acetonitrile solution (1:1) allowed to obtain a full spectroscopic characterization of QMs. Majority of transient species were found to be QMs in S_0 state, however, in some cases formation of T_1 transients of QMPs were reported (Scheme 1.12).

1.4.1. Transients of o-QMs

Transient of unsubstituted *o*-QM **1.7a** demonstrated a characteristic absorption band at λ_{max} = 400 nm and had a lifetime of τ >1 s in pure acetonitrile and τ = 2.3 ms in water at pH = 7.[13] Long-lived transient of o-quinone α-phenylmethide **1.72** had two characteristic absorption bands at λ_{max} = 350 nm and λ_{max} = 450 nm. [4]

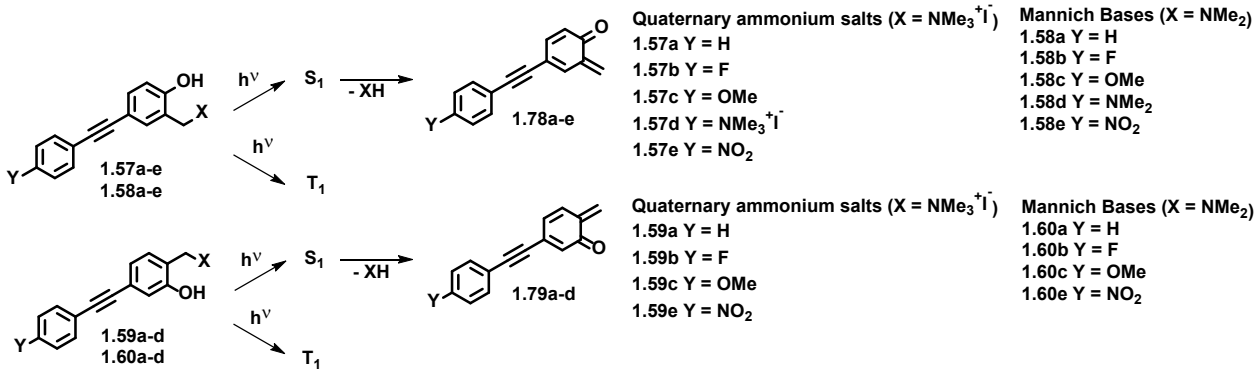

Scheme 1.13. Proposed mechanism of photochemical formation of *o*-arylethynyl-*Q*Ms from corresponding quaternary ammonium salts and Mannich bases.

Acetonitrile solutions of 4- and 5-arylethynylquinone 1-methides **1.78** and **1.79** exhibited very similar transient spectra with λ_{max} at 430-600 nm, and absorption bands were efficiently quenched by oxygen. Thus, observed transients were assigned to a triplet state T_1. Other transient species were detected in aqueous acetonitrile solution. They were characterized by longer lifetime and were not quenched by oxygen. Current transients had absorption maximum at λ_{max} ~365 nm and were assigned to *o*-QMs. QMs and T_1 of the QMPs were found to be cogenerated species. However, introduction of electron-donating substituents, such as 4- and 5-(4'-methoxyphenyl)ethynyl, and conduction the experiment in protic solvent resulted in formation of longer living transients of o-QMs and nearly complete suppression of T_1 transients. On the other hand, introduction of electron-withdrawing substituents and performing the photolysis in polar aprotic solvent resulted in nearly exclusive generation of T_1 transients (Scheme 1.13).[27] LFP of 3-hydroxy-2-naphthalenemethanol and 2-hydroxy-1-naphthalenemethanol in aqueous acetonitrile resulted in formation of short-lived transients (τ = 12-13 μs) with absorption maximum at λ_{max} = 370 nm. Decay of these transients give arise to formation of longer living-species with λ_{max} = 330 nm and lifetime τ = 4-8 ms. Comparison of current observations with previously reported data may suggest that longer-living transients could be assigned to *o*-NQM1 and *o*-NQM2.[7]

Excitation of 3,3'-bis(hydroxymethyl)-1,1'-binaphthyl-2,2'-diol **1.50** in biphosphate buffer solution (pH = 7) resulted in the formation of short-lived transient with absorption band at λ_{max} = 360 nm. The transient was successfully quenched by nucleophiles and was assigned to *o*-BQM.[18]

Behavior of transient species generated from 2-hydroxy-3-(diphenylhydroxymethyl)anthrcene **1.32** by LFP were studied in pure acetonitrile, aqueous acetonitrile (1:1) and in TFE. In acetonitrile and aqueous acetonitrile transient with λ_{max} ~400-500 nm and lifetime τ ~ 0.1-2 s and τ ~ 10-100 μs have been detected and assigned to *o*-anthra-QM. In pure acetonitrile shorter living transient was detected. It was characterized by absorption band at λ_{max} = 700 nm and lifetime τ = 1 μs. Since the transient was not quenched by oxygen, it was assigned to a radical structure. Experiments performed in TFE detected primary transient, characterized by absorption band at λ_{max} = 580 nm (τ = 690 ns) and secondary transient with λ_{max} = 520 nm (τ = 84 μs). Since quenching with nucleophiles only affected secondary transient and only primary transient was affected by pH, it was proposed that long-living transient could be assigned to carbocation and short-living transient to *o*-anthra-QM. However, there was not enough data presented to confirm the proposal.[16]

1.4.2. Transients of m-QMs

Transients of *m*-quinone α-phenylmethide **1.62** and *m*-quinone α,α-diphenylmethide exhibited one absorption band at λ_{max} = 420 nm and λ_{max} = 445 nm, respectively, and were characterized as short living species with τ = 30 ns and τ = 10 μs in aqueous acetonitrile.[6]

1.4.3. Transients of *p*-QMs

Transient of unsubstituted *p*-QM **1.4** demonstrated a characteristic absorption band at λ_{max} = 300 nm, transient of *p*-quinone α-phenylmethide **1.74** had one characteristic absorption band at λ_{max} = 380 nm and had a relatively long lifetime (τ > 5 s) in aqueous acetonitrile.[4]

LFP of 6-hydroxy-2-naphthalenemethanol in aqueous acetonitrile resulted in formation of two transients with absorbance bands at λ_{max} = 370 nm and λ_{max} = 310-330 nm. The decay rate of both transients was not

affected by oxygen. Lifetime of a longer living intermediate (λ_{max} = 310-330 nm) was too long to be determined with the laser equipment, however, the intermediate was successfully quenched by 2-ethanthiol, thus, was assigned to *p*-NQM **1.76**.[7]

Excitation of 6,6'-bis(hydroxymethyl)-1,1'-binaphthyl-2,2'-diol **1.39** in biphosphate buffer solution (pH = 7) resulted in the formation of short-lived transient ($\tau_{1/2}$ = 2 μs) with absorption band at λ_{max} = 360 nm. The transient was successfully quenched by nucleophiles and was assigned to *p*-BQM.[18]

1.5. Reactions of QMs

1.5.1. Hydration Rate Profile

As it was mentioned earlier QMs are very reactive species and in the absence of nucleophiles or dienophiles they undergo hydration to produce corresponding 2-hydroxymethylphenol derivatives. Rates of hydration are generally measured in dilute aqueous solutions of perchloric acid, sodium hydroxide, acetate, biphosphate and bicarbonate buffers, all at a constant ionic strength of 0.1 M. Laser flash photolysis of QM precursors in aqueous solution produces short-living transient species (QM) with characteristic absorbance band at ~ 400 nm. Thus, the rate of hydration can be determined by following the decay of the absorbance band over time. In all reported experiments, obtained kinetic data obeyed the first-order rate law and observed pseudo-first order rate constants were determined by least-squares fitting to a single exponential function. The measurements in buffers are usually conducted in series of solutions of constant buffer ratio but at different buffer concentrations. Extrapolation of the data to zero buffer concentration gives an intercept that can be used in building of a pH-dependent rate profile. Buffer catalysis can be described via equation 1.1:

Eq. 1.1 $$k_{obs.} = k_{int} + k_{buff}[Buffer]$$

where $k_{obs.}$ is experimentally observed pseudo-first order rate constant, s^{-1}; k_{int} is a zero buffer concentration intercept, s^{-1}; k_{buff} is a buffer catalytic coefficient, $M^{-1}s^{-1}$.[5,6,28]

In hydration of QMs three processes are involved: acid catalysis, uncatalyzed water reaction and hydroxide-ion catalyzed process (Scheme 1.14). Thus, rate profile of hydration can be described via equation 1.2:

Eq. 1.2 $$k = k_{H+}[H^+] + k_w + k_{OH-}[OH^-]$$

where k_{H+} is a second order rate constant of acid-catalyzed process, k_w is a pseudo-first order rate of uncatalyzed water reaction, s^{-1}; k_{OH-} is a second order rate of hydroxide-ion catalyzed process, $M^{-1}s^{-1}$.

The uncatalyzed hydration reaction in rate profile is represented by horizontal region and can be described via k_w.[5,6,28]

Second-order rate constant of acid-catalyzed process, k_{H+}, is determined via eq. 1.3:

Eq. 1.3 $$k_{H+} = \frac{k_{obs}}{[H^+]} = \frac{k'_w}{K_{SH}}$$

where k_w' is rate constant for carbocation ion capture by water, s^{-1}; and K_{SH} is acid dissociation constant of the protonated QM

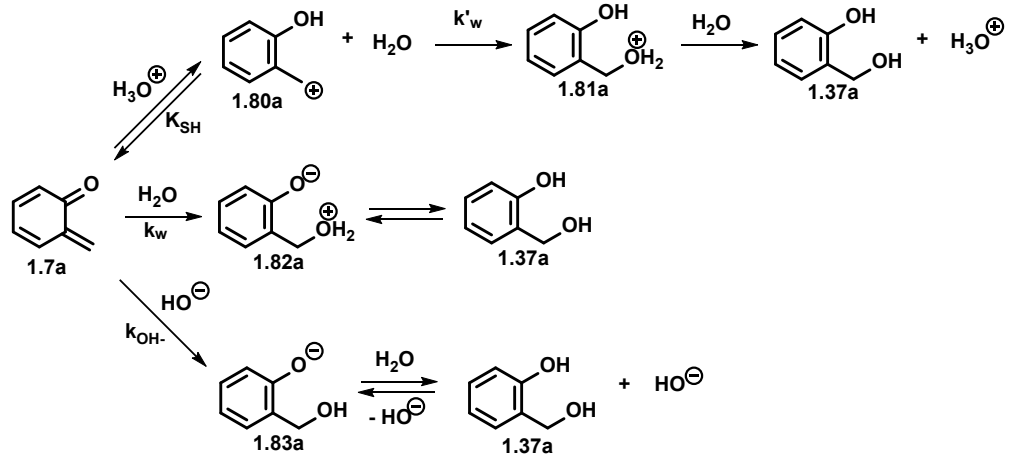

Scheme 1.14. Proposed mechanism of hydration of *o*-QM at different pH.

In case of o-quinone methide **1.7a** rate of hydration was independent of the acidity of aqueous solutions in the pH range of 4-8. The rate of hydration demonstrated a pronounced specific acid catalysis, which could be explained by the rapid pre-equilibrium protonation of *o*-QM. General acid and general base catalysis in biphosphate buffer were weak and reliable k_{buff} have not been reported.[28] *p*-QM **1.4**, *p*-quinone

α-phenylmethide **1.74** and *p*-quinone α,α-diphenylmethide **1.75** had rate of hydration being independent of the acidity of aqueous solutions in the pH range of 6-10. Pronounced specific acid and base catalysis were observed. Buffer catalysis was not detected for *p*-quinone α,α-diphenylmethide, however, weak general base catalysis in biphosphate buffer was present in hydration of *p*-QM and *p*-quinone α-phenylmethide. Current observation was explained by steric hindrance of diphenyl substituted compound compare to unsubstituted and monosubstituted analogs. Buffer base was believed to serve as a nucleophile, thus substituted methylene group was less accessible.[6]

Attempts to analyze hydration profile of o-quinone α-phenylmethide **1.72** were unsuccessful, however, analysis of its closest analog *o*-quinone α-(4-methoxyphenyl)methide **1.73** was reported.[28] Kinetic parameters of hydration of *o*-QMs and *p*-QMs are summarized in Table 1.2.

Table 1.2. Hydration rate constants of *o*-QMs and *p*-QMs, and acidity constants of protonated substrates.

QM	k_w, s^{-1}	k_{OH^-}, $M^{-1}s^{-1}$	k_{H^+}, $M^{-1}s^{-1}$	K_{SH}, M	k_w', s^{-1}
o-QM[5,28]	2.6×10^{2}	3.0×10^{4}	8.4×10^{5}	5.2×10^{1}	4.4×10^{7}
p-QM[5,6]	3.3	n.d.	5.3×10^{4}	1.1×10^{2}	5.8×10^{6}
1.74[6]	5.1×10^{-2}	8.2×10^{1}	2.9×10^{4}	1.5×10^{1}	4.4×10^{5}
1.75[6]	3.7×10^{-4}	6.5×10^{-1}	2.1×10^{3}	1.9×10^{-1}	3.9×10^{2}
1.73[28]	n.d.	n.d.	5.6×10^{6}	8.2×10^{-2}	4.6×10^{5}

The rate constant of the uncatalyzed hydration, k_w, was found to be 78 times greater for *o*-QM, than for *p*-QM.[5] This observation pointed on the increased stability of *p*-quinoid core, compare to *o*-quinoid one. Indeed, *p*-benzoquinone is known to be much more stable than *o*-benzoquinone. Introduction of phenyl substituents into the α-carbon of *p*-QM caused even further decrease in rate of uncatalyzed hydration. Water acted as a nucleophile in uncatalyzed hydration, thus substituted methylene group was less accessible in sterically hindered mono- and diphenyl substituted *p*-QMs. Reaction rate with hydroxide ion, described via rate constant k_{OH^-}, demonstrated the same tendency as the one of uncatalyzed hydration. Hydroxide ion acted as a nucleophile, thus stability of quinoid core toward nucleophilic attack as well as accessibility of α-carbon played a crucial role. Similar effect was mentioned earlier: an absence

of buffer catalysis was observed in diphenyl substituted *p*-QMs, compare to weak general catalysis described for *o*-QM and unsubstituted and mono-substituted *p*-QMs.[5,6]

Hydronium ion - catalyzed addition of water, described as catalytic coefficients k_{H+}, also decreased with introduction of phenyl-substituents into α-position. However, observed rate decrease was less pronounced compared to uncatalyzed and hydroxide ion - catalyzed hydration. According to Eq. 1.3, k_{H+} is a complex value, which depends on the ratio of two parameters: rate of QM conjugate acid reaction with water, k_w', and conjugate acid dissociation constant $K_{SH.}$ Change from *o*-QM to *p*-QM, as well as introduction of α-substituents in *p*-QM resulted in the reduction of both parameters. Influence of structure of QM and accessibility of α-carbon in carbocations determined k_w' value. Same effects as those described for k_w took place. Since the decrease in k_w' value is more significant than the decrease of K_{SH}, overall decrease of k_{H+} was observed in the row of *o*-QM, p-QM, *mono*- and *bis*-substituted *p*-QMs.[6]

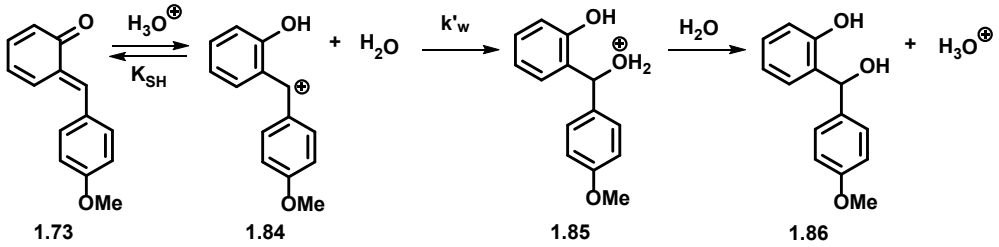

Scheme 1.15. Proposed mechanism of hydration of *o*-quinone α-(4-methoxyphenyl)methide.

Comparison of hydration data of unsubstituted *o*-QM **1.7a** with *o*-quinone α-(4-methoxyphenyl)methide **1.73** allowed us to understand better the role of stabilization of the cationic intermediate formed by protonation of *o*-QM. Change from *o*-QM to its *p*-anisyl derivative resulted in decrease of K_{SH} and k_w'. Significant decrease in K_{SH} parameter could be explained via increased acidity of *p*-anisyl substituted *o*-QM compare to *o*-QM. Introduction of 4-methoxyphenyl group stabilized carbocation and corresponding QM, however, the greater stabilization of carbocation took place, thus caused significant decrease in K_{SH}. Accessibility of α-carbon in carbocations determined k_w' value. Since the decrease in k_w' value is less significant than the decrease of K_{SH}, overall increase of k_{H+} was observed (Scheme 1.15).[28]

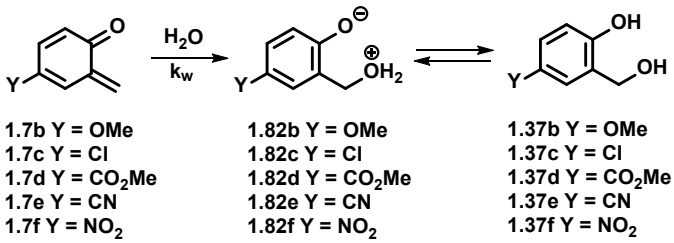

1.7b Y = OMe
1.7c Y = Cl
1.7d Y = CO_2Me
1.7e Y = CN
1.7f Y = NO_2

1.82b Y = OMe
1.82c Y = Cl
1.82d Y = CO_2Me
1.82e Y = CN
1.82f Y = NO_2

1.37b Y = OMe
1.37c Y = Cl
1.37d Y = CO_2Me
1.37e Y = CN
1.37f Y = NO_2

Scheme 1.16. Effect of electron-donating and electron-withdrawing substituents on reactivity of *o*-QMs in hydration reaction.

Effect of electron-donating and electron-withdrawing substituents on reactivity of *o*-QM **1.7** in hydration reaction has been studied by Rokita. Incorporation of electron-withdrawing substituent, such Cl, CO_2Me, CN and NO_2, progressively decreased lifetime of *o*-QM in water (Scheme 1.16). For example, introduction of CO_2Me, CN and NO_2 resulted in increase of second-order rate constant in 47, 256 and 3256 times, respectively. On the other hand, incorporation of OMe resulted in decrease of second-order rate constant in 4 times, compare to unsubstituted *o*-QM.[29]

Another study of effect of electron-donating and electron-withdrawing substituents on the reactivity of *o*-QM in hydration reaction has been conducted by Freccero.[27] Two series of *o*-QMs, 4- and 5-arylethynyl-1-quinone methides **1.78** and **1.79**, with electron-donating and electron-withdrawing substituents have been analyzed. Rate constants of uncatalyzed hydration process are summarized in Table 1.3. In general, electron-withdrawing substituents, such as 4-fluoro- and 4-nitrophenylethynyl, have been found to increase the rate of hydration. On the other hand, electron-donating substituents, such as 4-methoxy- and 4-dimethylaminophenylethynyl, decreased the rate of hydration. Introduction of arylethynyl substituents in position 5 resulted in much stronger effect on electrophilicity of *o*-QM than introduction of substituent in position 4.[27]

Table 1.3. Effect of electron-donating and electron-withdrawing substituents on the rate constant in uncatalyzed hydration.

Y-substituent in 1.78	**k_w, s^{-1}**
a H	$5.9x10^2$
b F	$3.5x10^2$
c OMe	$2.6x10^2$
d NMe_2	$2.0x10^2$
e NO_2	$3.4x10^4$
f NMe_3^+	$1.8x10^3$
Y-substituent in 1.79	**k_w, s^{-1}**
a H	9.8
b F	$6.6x10^2$
c OMe	$5.31x10^1$
e NO_2	$4.4x10^4$

In case of 2,3-napthoquinone-3-methide and 1,2-napthoquinone-1-methide (*o*-NQM1 and *o*-NQM2), generated from 3-hydroxy-2-naphthalene methanol and 2-hydroxy-1-naphthalenemethanol, rate of hydration was independent of the acidity of aqueous solutions in the pH range of 1-8. Rate constants of uncatalyzed hydration of o-NQM1 and o-NQM-2 were determined to be $k_w = (1.5x10^2)\ s^{-1}$ and $k_w = (2.3x10^2)\ s^{-1}$, respectively. Reported values were very similar to the one of *o*-QM $(2.6x10^2)\ s^{-1}$. Specific acid catalysis of o-NQMs was very weak and became pronounced only at pH < 1. Hydronium ion catalyzed addition of water, described as catalytic coefficients k_{H+}, was determined only for o-NQM1 ($k_{H+} = (2.99x10^2)\ M^{-1}s^{-1}$) and appeared to be much smaller than the one recorded for *o*-QM. It could be explained by the lower reactivity of protonated *o*-NQM compare to *o*-QM due to an increased delocalization of positive charge. On the other hand, a significant rate increase was observed at pH > 10. The rate constants for hydroxide-ion catalyzed hydration were determined to be $k_{OH-} = (3.30x10^4)\ M^{-1}s^{-1}$ for o-NQM1 and $k_{OH-} = (3.74x10^4)\ M^{-1}s^{-1}$ for o-NQM2. Rates of nucleophilic attack of o-NQM by hydroxide ion are very similar to the rate reported for o-QM ($k_{OH-} = (3.30x10^4)\ M^{-1}s^{-1}$). General acid and general base catalysis in biphosphate buffer were not observed.[7]

To the best of our knowledge, hydration rate profiles of *p*-NQM, o-BQM and p-BQM, *o*-anthra-QM and *o*-phenanthra-QM have not been reported. However, rate constants of uncatalyzed hydration were reported for *o*-BQM and *p*-BQM $k_w = (7.1x10^5)\ s^{-1}$,[20] and *o*-anthra-QM $k_w = (1.6x10^3)\ s^{-1}$.[16] *o*-BQM and *p*-BQM were reported to be much more reactive with nucleophiles. It could be explained by specific intramolecular acid catalysis due to the presence of hydroxyl-group of 2'-naphthol.[20]

Further investigation of the reaction mechanism of hydration of QMs at various pH was performed via determination of isotope effect on rates of decay of QMs. Thus, rates of decay of QMs were studied in solutions of perchloric acid in H_2O and deuterated perchloric acid in D_2O. According to reported experiments, in acid-catalyzed hydration was slower in H_2O than in D_2O, which meant inverse isotope effect (k_H/k_D <1). [5,6,28] The inverse isotope effect could be explained via pre-equilibrium proton-transfer reaction mechanism, where protonation of the oxygen atom is fast and reversible. This step transforms a relatively weak O-H bond of the hydronium ion into a strong O-H bond in water molecule, which results in inverse isotope effect. For example, inverse isotope effect on the rate of acid-catalyzed hydration was observed in case of *o*-QM (k_{H+}/k_{D+} = 0.416±0.079),[5] *p*-QM (k_{H+}/k_{D+} = 0.409±0.005),[5,6] *p*-quinone α-phenylmethide (k_{H+}/k_{D+} = 0.408±0.011) and *p*-quinone α,α-diphenylmethide (k_{H+}/k_{D+} = 0.387±0.022) at acidities $pK_{SH} < pH < 3$.[6] The uncatalyzed hydration reaction was characterized by rate-determining nucleophilic addition of water. In this case, in positively charged intermediates O-H bonds were weaker than uncharged O-H bonds of water molecules, thus conversion of H_2O into ROH_2^+ resulted in overall loosening of involved O-H bonds. That would cause normal solvent isotope effect. Indeed, all studied reactions demonstrated normal solvent isotope effect: *o*-QM (k_{H2O}/k_{D2O} = 1.42±0.06),[5] *p*-QM (k_{H2O}/k_{D2O} = 1.46±0.07),[5] *o*-NQM1 (k_{H2O}/k_{D2O} = 1.85±0.14) and *o*-NQM2 (k_{H2O}/k_{D2O} = 1.42±0.07.[7] Solvent isotope effect for *p*-quinone α-phenylmethide and *p*-quinone α,α-diphenylmethide have not been reported.[6]

1.5.2. Reactions of QMs with Nucleophiles

QMs are very reactive species and readily react with nucleophiles. Rate constant of this process depends on the electrophilicity of generated QM and on nucleophilicity of nucleophile (Scheme 1.17). The second-order rate constants of QMs reactions with 2-aminoethylthiol hydrochloride are summarized in Table 1.4. Comparison of rate constants measured by LFP allowed to generate electrophilicity scale of QMs towards thiol: *o*-BQM ≈ *p*-BQM >> *o*-(4-EWG-Q)M > *o*-NQM > *o*-(5-EWG-Q)M > *p*-QM ≥ *o*-(4-EDG-Q)M.[5,7,20,29] In 2001 Mella analyzed second-order rate constants of reaction between o-QM and various nucleophiles. Comparison of the data allowed to generate a nucleophilicity scale towards o-QM: $RS^- >> R_3N > PhO^- > RSH \approx RNH_2 > HO^- \approx N_3^- >> H_2O \geq Cl^-, AcO^-, ROH$.[13]

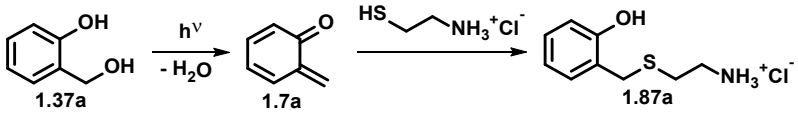

Scheme 1.17. Reaction between o-QM and 2-aminoethylthiol hydrochloride.

Table 1.4. The second-order rate constants of QMs reactions with 2-aminoethylthiol hydrochloride in aqueous biphosphate buffer at pH = 7.0 unless otherwise noted.

QM	k, $M^{-1}s^{-1}$ $HSCH_2CH_2NH_2 \cdot HCl$	Ref.
1.7a	$1.9x10^5$ (pH = 6.9) $2.8x10^8$ (pH = 12.1)	[13]
1.78a	$1.18x10^5$	[27]
1.78c	$1.29x10^3$	[27]
1.78d	$7.0x10^2$	[27]
1.78e	$1.45x10^5$	[27]
1.79b	$7.7x10^2$	[27]
1.79e	$3.5x10^4$	[27]
1.7b	$4.0x10^4$ (pH=9.0)	[29]
1.7c	$4.4x10^4$ (pH = 9.0)	[29]
1.7d	$5.9x10^6$ (pH = 9.0)	[29]
1.7e	$5.01x10^7$ (pH = 9.0)	[29]
1.4	$1.3x10^3$	[20]
1.44	$2.0x10^7$	[20]
1.77	$2.0x10^7$	[20]
1.31	$2.24x10^5$	[7]
1.27	$3.34x10^5$	[7]

1.5.3. o-QMs in Diels-Alder reaction

Unlike *m*-QMs and *p*-QMs, o-QMs can be considered as *hetero*-diene system. Indeed, *o*-QMs are known to react with electron rich dienes via [2+4] cycloaddition to give various substituted chromanes with moderate to high yields.[3,7,30] These *hetero*-Diels-Alder products are a key ring system in myriad of natural products.[31,32] The intermolecular Diels–Alder reactions between *o*-QMs and less-reactive electron-deficient alkenes are known to be less clean and result in the oligomerization of the *o*-QMs.[3] The selectivity of formation of Diels – Alder reaction products depends on three factors: diene and dienophile orientation in the transition state (endo- or exo-approach), o-QM geometry (E- or Z-configuration) and stability of the corresponding diastereomers. Reactivity of the dienophiles is dependent on steric effect, for example, ethyl vinyl ether (EVE) was found to be more reactive than *E*-1-propenyl ethyl ether and than *Z*-1-propenyl ethyl ether. The reaction between EVE and *o*-QMs usually happens via an *endo* attack through a transition state stabilized by secondary attractive interactions between the carbonyl group of o-QM and the oxygen of the ethoxy group (Scheme 1.18).[33] The second order rate constants were determined for the reaction between EVE and 2,3-napthoquinone-3-methide and 1,2-napthoquinone-1-methide by Popik and were found to be k = (4.07±0.19)x10^4 $M^{-1}s^{-1}$ and k = (6.05±0.34)x10^4 $M^{-1}s^{-1}$, respectively.[7]

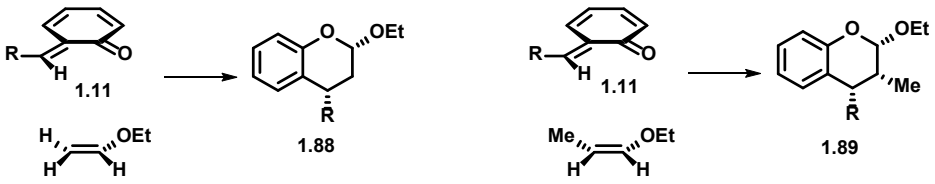

Scheme 1.18. Geometry of intermolecular *hetero*-Diels-Alder reaction.

Intramolecular *hetero*-Diels-Alder reactions is very uncommon for *o*-QMs. However, in 1974 Padwa reported intermolecular cyclization of *o*-quinone α-phenylmethide **1.72** generated from 2-(methoxy(phenyl)methyl)phenol **1.90** under light irradiation in pure methanol, which resulted in formation of 9H-xanthene **1.92**. The formation of xanthene **1.92** (Φ = 0.02) occurred as an intramolecular

[4+2] pericyclic reaction of *Z*-isomer of o-quinone α-phenylmethide **1.72**, followed by 1,3-hydrogen shift. The efficiency of the reaction was low due to ability of only *Z*-isomer to undergo cyclization, however, both *Z*- and *E*-isomers reacted with methanol and water, and were also involved in formation of *o*-benzylphenol **1.93** via radical pathway (Scheme 1.19).[34]

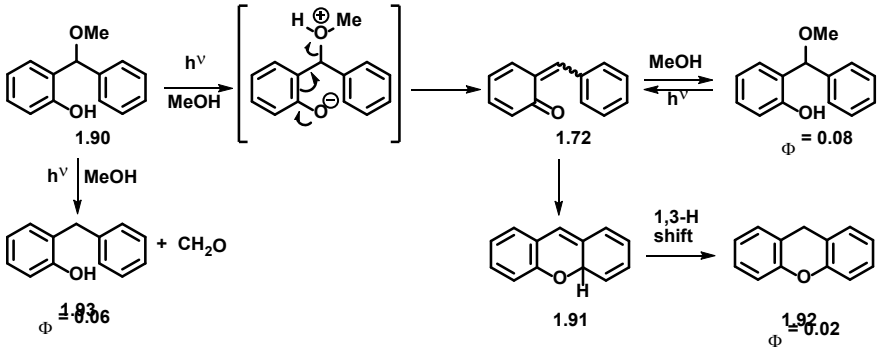

Scheme 1.19. Intramolecular *hetero*-Diels-Alder reaction.

1.5.4. Selectivity of Reactions Involving *o*-QMs

As it was shown above on multiple examples, photogenerated *o*-QMs readily react with nucleophiles, electron-rich dienophiles, and in the absence of those undergo hydration. However, conditions providing opportunity for competing processes, such as Diels-Alder reaction and nucleophilic attack, as well as factors determining the selectivity of the reactions have not been discussed. In 1997 Wan investigated the selectivity between intramolecular [4+2] cycloaddition reaction and nucleophilic substitution of photogenerated *o*-QMs decorated with dienophile moieties under various conditions. It was found that photolysis of the compound **1.94** in aqueous acetonitrile resulted in exclusive formation of hydration product and formation of [4+2] adduct was not observed. Similarly, light irradiation of **1.94** in aqueous methanol yielded benzylic ether **1.95**, which underwent secondary photoreaction to produce **1.96**. However, the Diels-Alder product of the reaction was not detected (Scheme 1.20). The lack of intramolecular [4+2] cycloaddition could be explained by the fact that the dienophile was only mono-alkyl-substituted and, thus, not sufficiently electron-rich to react with the *hetero*-diene of the *o*-QM.[35]

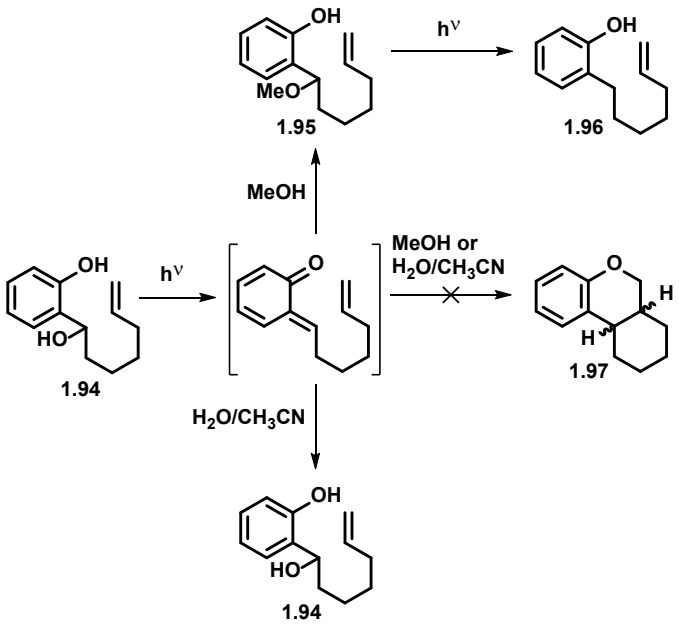

Scheme 1.20. Photolysis of substituted *o*-QMP in various solvent systems.

Analogous experiments were conducted with *o*-QMP **1.98** decorated with sufficiently electron-rich tri-alkyl-substituted dienophile. They resulted in the formation of expected Diels-Alder adduct **1.101** (Scheme 1.21). Photolysis of the compound **1.98** in aqueous acetonitrile resulted in exclusive formation of the **1.101** in high yields (> 80 %). Increase of water content was reported to increase quantum yield of the photolysis due to reduction of radical processes. For example, in pure acetonitrile quantum yield was 0.048 and in 4:1 water/acetonitrile quantum yield was measured to be 0.10 (Scheme 1.21).[35]

Photolysis of **1.98** in aqueous methanol allowed authors to study the competition between intramolecular [4+2] cycloaddition and nucleophilic attack by methanol of photogenerated *o*-QM. Performed photolysis yielded methyl ether **1.99** and [4+2] adduct **1.101.** Maximal chemical yield of the **1.101** was reported to be ~ 60 %, and the chemical yield of the methyl ether never exceeded 12 %. Higher chemical yield of the Diels-Alder adduct could be explained via reversibility of nucleophilic addition upon irradiation, and irreversibility of cyclization reaction. Interestingly, secondary photoproduct **1.100** was not formed (Scheme 1.21).[35]

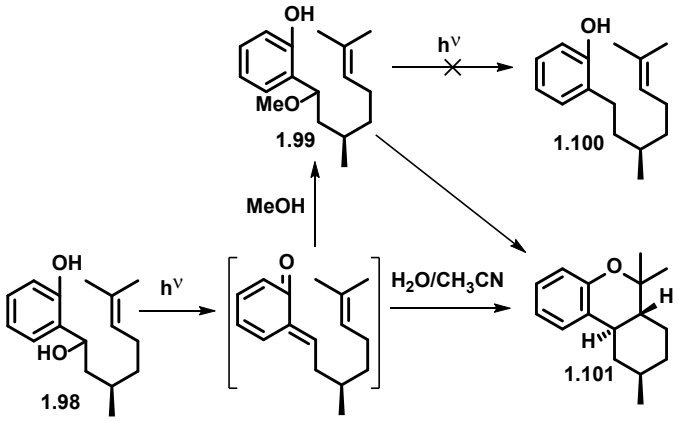

Scheme 1.21. Competing processes of photolysis of substituted *o*-QMP in various solvent systems.

Two years later in 1999 Wan reported that not only nature of dienophile but also steric factor determined selectivity of the reaction conducted under competing conditions. For instance, photolysis of *o*-hydroxy-α-phenylstyrene **1.102** in methanol and in aqueous acetonitrile with added ethyl vinyl ether resulted in the quantitative formation of methyl ether **1.105** and benzylic alcohol **1.103**, respectively, and formation of the Diels-Alder adduct **1.104** was not observed.[36] The steric hindrance due to the presence of the *syn* methyl group blocked the approach of the dienophile (EVE), thus the [4+2] product was not produced (Scheme 1.22). However, the photolysis of *o*-QMP without *syn* methyl group in aqueous acetonitrile with added EVE resulted in exclusive formation of the [4+2] product (Scheme 1.22).[4,37]

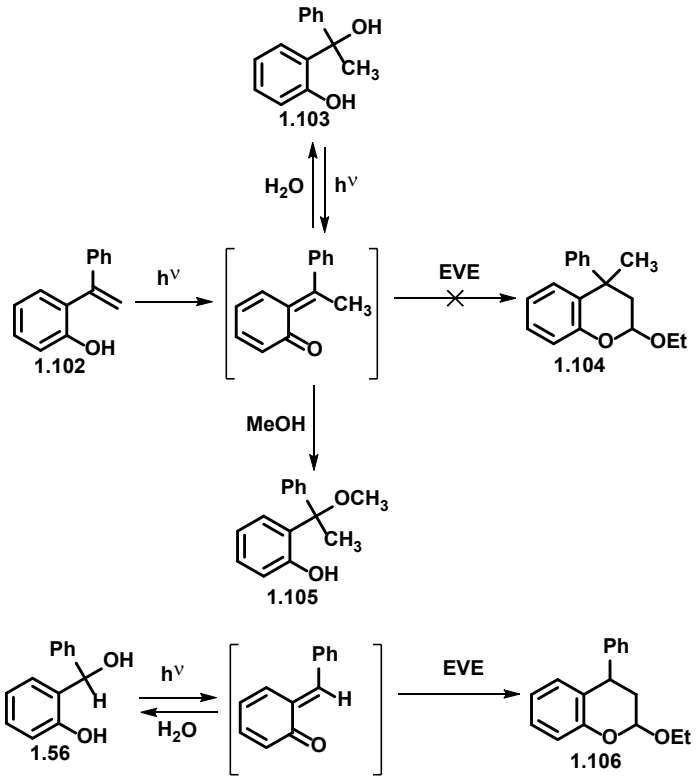

Scheme 1.22. Steric effect on the selectivity between the Diels-Alder reaction and hydration.

1.6. Application of QMPs and QMs

Quinone methides represent a unique class of molecules, that demonstrate a combination of properties of zwitterionic aromatic and neutral non-aromatic compounds.[1] As it was mentioned earlier they can be successfully generated via photolysis of aqueous solutions of QMPs.[6-12] *O*-hydroxybenzyl chromophore has little absorbance beyond 250 nm, and thus not suitable for biological applications. Alternatively, 2-hydroxynaphthyl chromophore exhibit absorbance above 350 nm.[7,16,20] Nowadays research is more focused on QMs and their precursors with extended conjugation systems, such as naphthyl, binaphthyl, anthryl and phenanthryl. Additionally, o-QMs provide opportunity to be applied not only via reactions with nucleophiles but also via *hetero*-Diels-Alder reaction. Thus, research in our group has been focused on studying the photogeneration of o-NQMs and demonstration of versatility of these reactive species as photolabile protecting groups.

One of the areas of application of o-NQMs and their precursors is postpolymerization modification (PPM) of the surface.[38] This technique allows to immobilize multiple different chemical functionalities onto substrates of covalently grafted polymer films. In 2012 Popik reported a novel approach of surface photoderivatization, which was based on the reaction between 2-napthoquinone-3-methide (o-NQM1) and thiols ($k_{RSH} \approx 2.2 \times 10^5\ M^{-1}s^{-1}$) (Scheme 1.20).[7,39] Majority of photoimmobilization techniques, as well as "dark" immobilization methods are irreversible and result in the formation of the surface that cannot be reused. The first group can be represented by surface modification via UV-initiated thiol–ene[40-42] and thiol–yne[43,44] chemistry and photoreduction of Cu (II) to Cu (I) in copper-catalyzed azide click reaction.[45] It results in the formation of covalent bond between surface and a substrate. The second method can be illustrated by "dark" immobilized surface with photosensitive *o*-nitrobenzyl groups.[46-48] In this case irradiation cleaves the bond between the surface and the substrate, thus releasing the substrate from the surface. However, the surface is not reusable. The unicity of the strategy arises from the ability to perform photoimmobilization and further photoreplacement of NQMP derivatized substrates on a thiol-functionalized surface.[39,49]

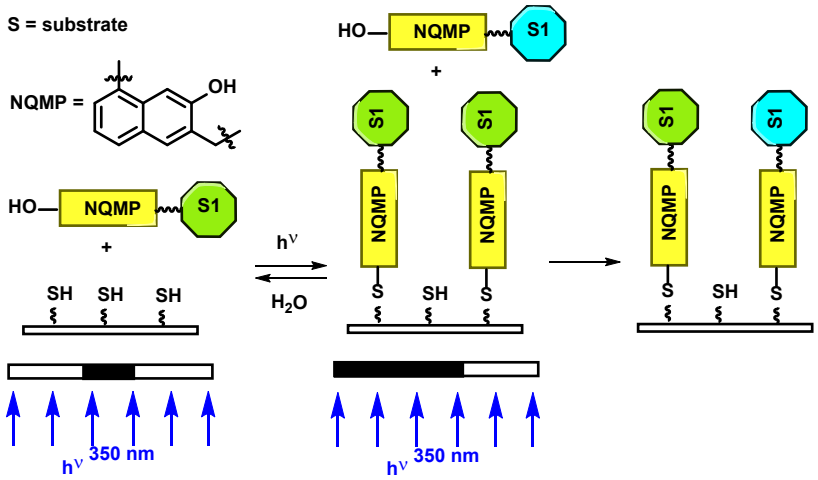

Scheme 1.23. Surface derivatization and further modification based on the reaction between o-NQMs and thiols.

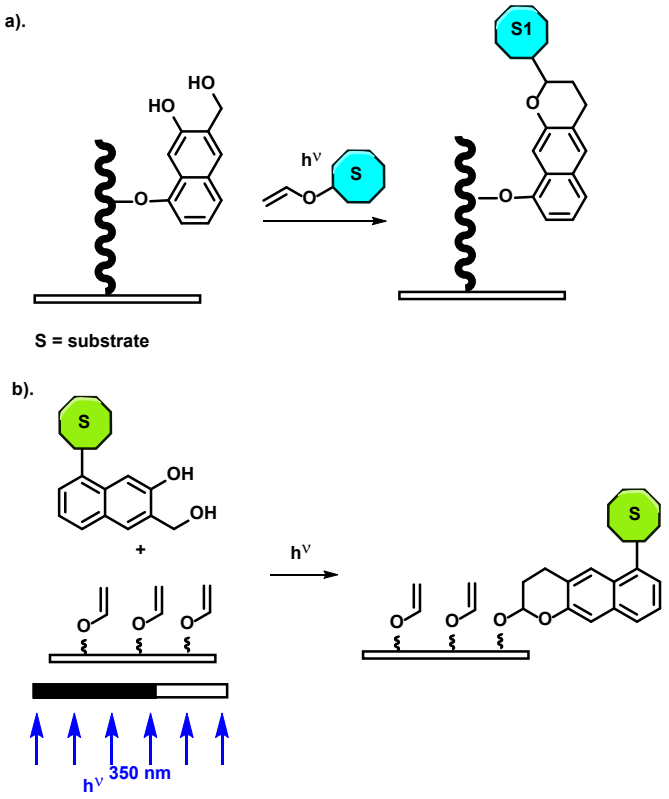

Scheme 1.24. a). Surface modification based on the reaction between *o*-NQMs and thiols. **b).** Surface modification based on the *hetero*-Diels-Alder reaction.

Another example of surface photoderivatization was based on the Diels-Alder reaction between surface immobilized 2-napthoquinone-3-methide and vinyl ether groups attached to a substrate ($k \approx 4.1 \times 10^4$ $M^{-1}s^{-1}$) (Scheme 1.21a).[7,50] Alternatively, surface immobilized with vinyl ether groups could be decorated with 2-napthoquinone-3-methides as a substrate (Scheme 1.21b).[51]

The nucleophilic addition of thiols to *o*-NQMs, as well as Diels–Alder photoclick reaction have been shown to be orthogonal to azide–alkyne click chemistry. This feature enables to perform surface derivatization followed by azide/alkyne click modification to create multifunction surface. Additionally, photolithographic methods allow to perform high-resolution surface patterning.[39.49-51]

Another area of application of *o*-NQMs and their precursors is the design of photolabile protecting groups (PPGs).[8,52,53] This technique allows to "cage" a molecule of interest and later restore its properties on

demand upon light irradiation. This feature is based on the ability of o-NQMPs to generate o-NQMs upon light irradiation, followed by efficient hydrolysis. The benefits of using o-NQMPs as PPGs include low cytotoxicity of "caged" compounds as well as of their photoproducts,[52] ability to protect multiple functional groups, such as alcohols, phenols and carboxylic acids,[8] fast rate of cleavage ($k \approx 10^5\ s^{-1}$), good quantum (Φ = 0.17-0.26) and chemical (>90%) yields.[7,8] Application of (3-hydroxy-2-naphthalenyl)methyl as a PPG was successfully demonstrated for progesterone, estrone, 3'-*O*-3-dimethylthymidine and *N*-Boc-*L*-phenylalanine (Scheme 1.25).[8]

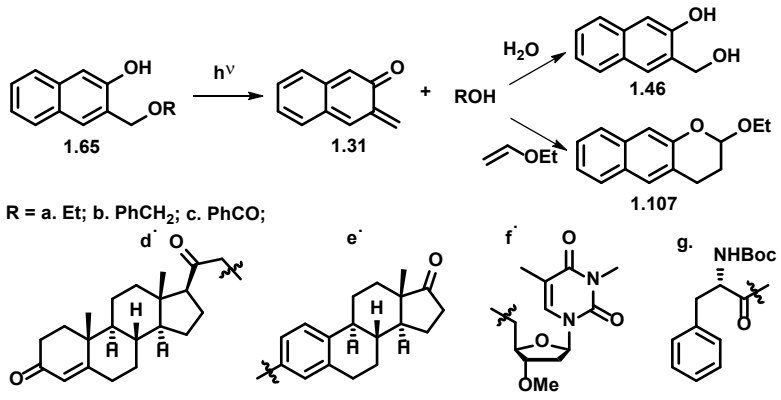

Scheme 1.25. Application of (3-hydroxy-2-naphthalenyl)methyl as a PPG for alcohols, phenols and carboxylic acids.

(3-hydroxy-2-naphthalenyl)methyl has been also shown to "cage" fluorescein. Photoactivation of nonfluorescent NQMP-caged fluorescein with 300-350 nm light produced a highly emissive fluorescein monoether (Scheme 1.26).[56]

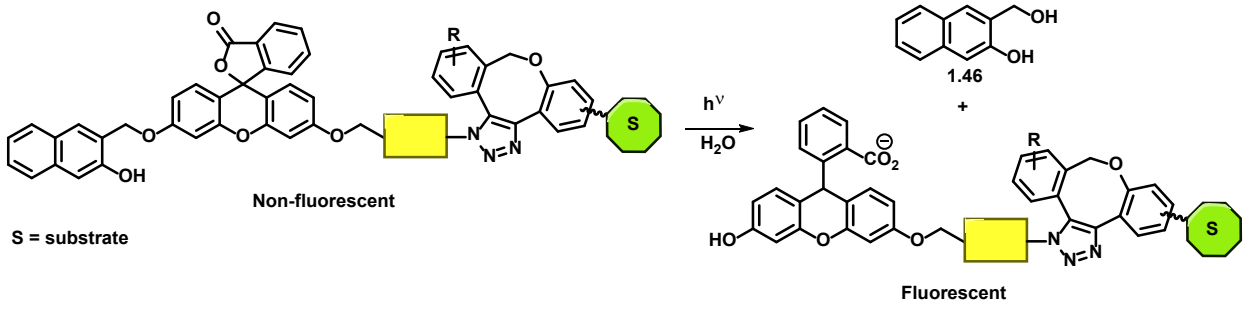

Scheme 1.26. Application of (3-hydroxy-2-naphthalenyl)methyl as a "cage" for fluorescein.

Application of (3,5-dihydroxynaphthalen-2-yl)methyl as PPG provided an extra handle for properties modulation, enabling to create a bichromophoric fluorescent PPG. For instance, in 2012 (5-dansyloxy-3-hydroxynaphthalen-2-yl)methyl has been reported as a novel fluorescent PPG for alcohols and carboxylic acids. Irradiation of protected compounds **1.108** with UV-light resulted in fast and efficient substrate release. Beneficially, both "caged" substrates and 5-dansyloxy-3-hydroxynaphthalen-2-yl)methyl **1.109** exhibited green fluorescent emission at λ_{max} = 559 nm (fluorescence quantum yield Φ_{Fl} = 0.21) upon excitation with 400 nm light (Scheme 1.27).[54]

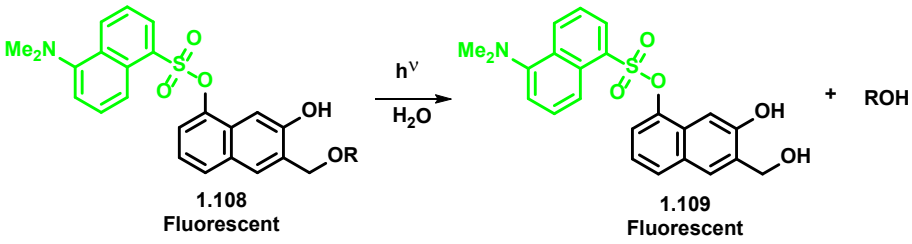

Scheme 1.27. Application of 5-dansyloxy-3-hydroxynaphthalen-2-yl)methyl as a fluorescent PPG for alcohols and carboxylic acids.

Finally, o-NQMPs have been employed as linkers for various systems. In 2011 a new photoclick platform based on light-induced *hetero*-Diels-Alder click reaction has been used for efficient ligation. (3,5-Dihydroxynaphthalen-2-yl)methyl derivatives were modified via conjugation with various functional moieties in the 5th position and then underwent fast and efficient *hetero*-Diels-Alder with electron-rich alkenes. That technique resulted in the formation of permanent linker (Scheme 1.28).[52]

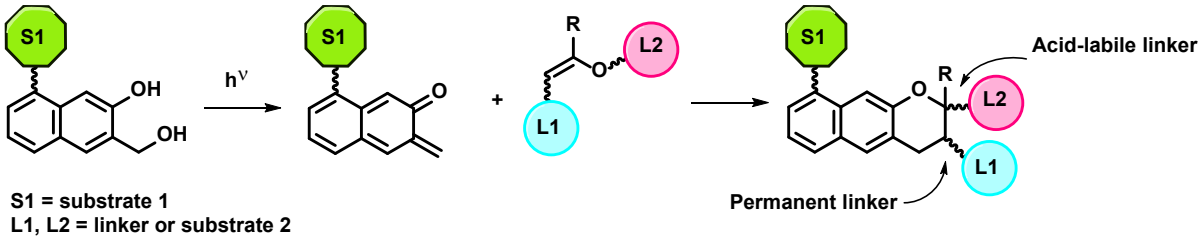

Scheme 1.28. Application of (3,5-dihydroxynaphthalen-2-yl)methyl derivatives as a permanent linker.

In 2014 example of photolabile linker have been reported: 3,5-dihydroxynaphthalen-2-yl)methyl derivatives have been employed as selective, photolabile linkers in derivatization of cysteine residues in peptides and proteins.[55,56] The technique is based on exceptionally fast reaction between o-NQMs and thiols ($k_{RSH} \approx 2.2 \times 10^5\ M^{-1}s^{-1}$).[7] Hydroxyl group in position 5 of (3,5-dihydroxynaphthalen-2-yl)methyl have been used as an extra handle for conjugation with various moieties, such as PEG, dyes, carbohydrates, biotin, azide and alkyne. The last three functional groups could be used in further orthogonal modifications. The photo-release of the free cysteine residues could be achieved on demand upon light irradiation, when vinyl ethers are employed as o-NQM trapping agents (Scheme 1.29).[55,56]

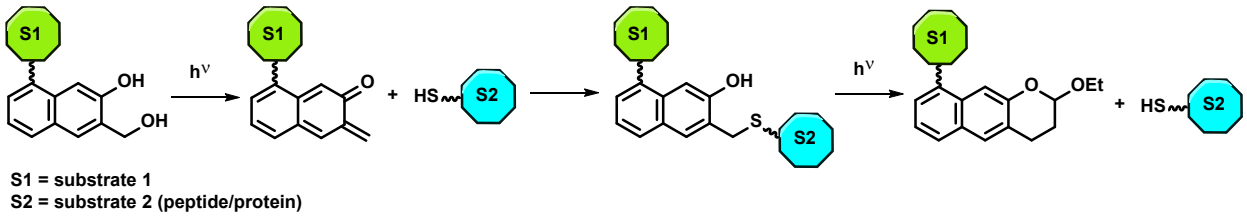

Scheme 1.29. Application of (3,5-dihydroxynaphthalen-2-yl)methyl derivatives as a photolabile linker.

1.7. Conclusions and Goals of the Projects

Efficient generation of QMs from QMPs under mild conditions, such as reagent free UV-light irradiation, and exceptional reactivity of QMs towards nucleophiles and, in case of *o*-QMs, towards dienophiles have attracted a lot of attention to these compounds in computation, chemical, biological and engineering spheres. Our research group demonstrated successful application of o-NQMPs as photolabile protecting groups and linkers, that can be employed in the design of multifunctional surfaces, used as PPGs for biological molecules that carry different functional groups and as a linker for peptide and protein reversible modification.

As it was discussed earlier, o-QMs and p-QMs demonstrated different chemical properties and different reactivity. However, to the best of our knowledge, the molecules containing competing o-naphthoquinone methide and p-quinone methide moieties, have not been studied. Thus, the major goal

of the project was to develop and synthesize novel QMPs **1.110** with ability to generate *o*-NQM and *p*-QM under light irradiation (Scheme 1.30). Physical properties, chemical properties, such as ability to react with nucleophiles and undergo inter- and intra-molecular Diels-Alder reaction, as well as kinetic behavior of new QM-system have been studied.

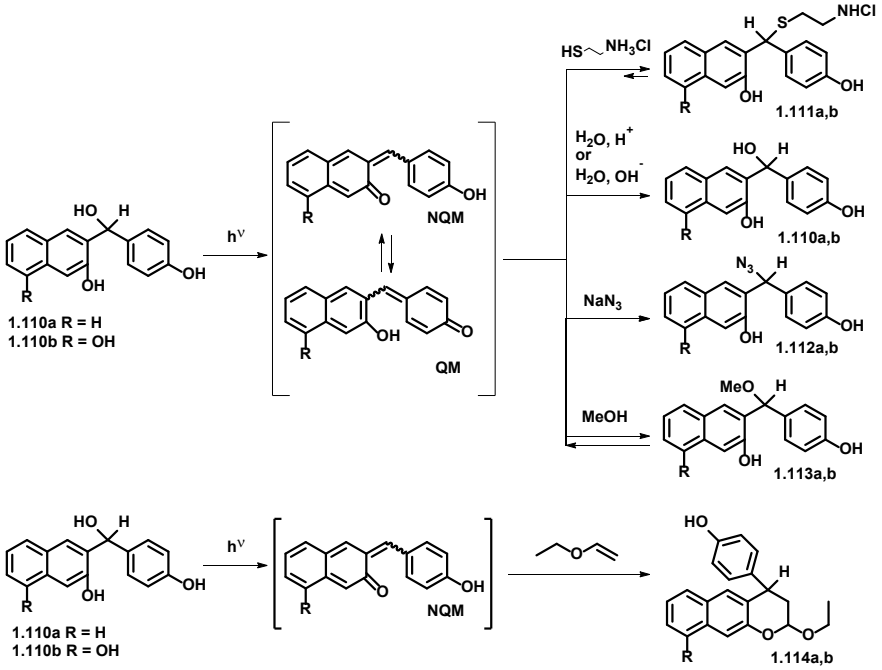

Scheme 1.30. Chemical reactivity of QMs under various conditions.

We were also interested to investigate the ability of *o*-NQMPs **1.115** and **1.118** to form "smart" polymers, that could be generated upon UV-light irradiation of (3,5-dihydroxynaphthalen-2-yl)methyl derivatives decorated with thiol moieties. The photo-induced degradation of the polymers could be achieved on demand upon light irradiation, when vinyl ethers were employed as *o*-NQM trapping agents (Scheme 1.31).

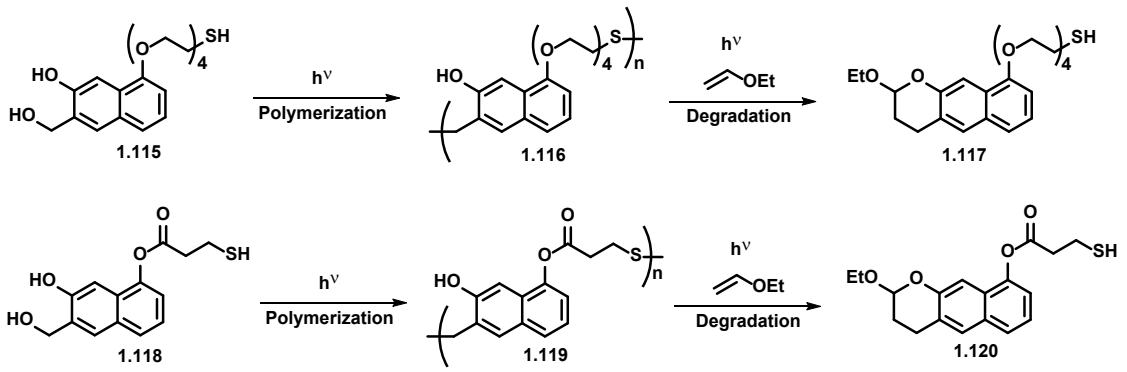

Scheme 1.31. "Smart" polymers from (3,5-dihydroxynaphthalen-2-yl)methyl derivatives decorated with thiol moieties.

Another project has been focused on the development of a novel photocleavable analog of calcium-selective chelating ligand **1.119**, based on the combination of properties of photolabile 3-(hydroxymethyl)-2-naphthol core and high calcium affinity of 1,2-*bis*(*o*-aminophenoxy)ethane-*N,N,N',N'*-tetraacetic acid (BAPTA) (Scheme 1.32).

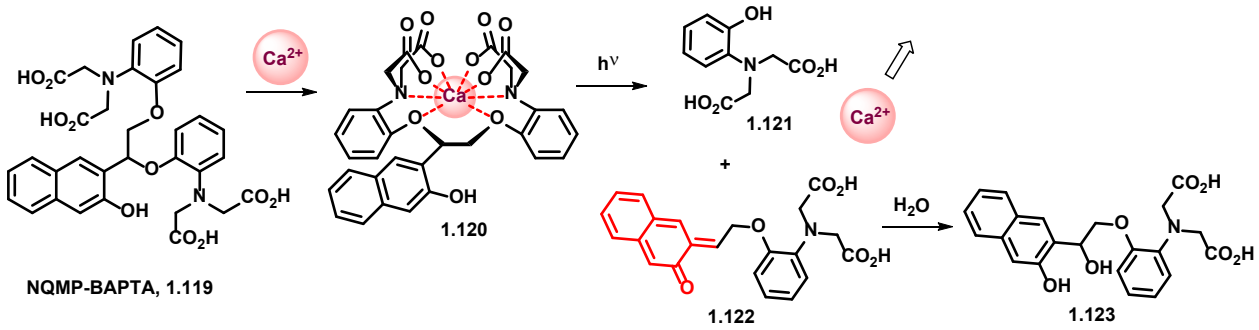

Scheme 1.32. Novel photocleavable analog of calcium-selective chelating ligand NQMP-BAPTA.

Finally, we were working on the design of a new fluorogenic PPG that could also serve as an intracellular pH indicator.[54] 9*H*-xanthene-1,8,9-triol derivatives **1.124** can be considered as photoactivatable fluorophores and fluorogenic PPGs, as 9*H*-xanthen-1,8,9-triols are expected to generate relatively stable quinone methide **1.125** upon UV-light irradiation, one of the resonance structures of which **1.125'** is fully aromatic (Scheme 1.33). Due to its structural similarity with fluorescein derivatives, we expected 8-hydroxy-1*H*-xanthen-1-one **1.125** to be highly fluorescent.[58,59] Additionally, we expected 9*H*-xanthen-

1,8,9-triols to undergo hydronium-ion mediated reversible dehydroxylation which would yield highly fluorescent 8-hydroxy-1*H*-xanthen-1-one derivatives.

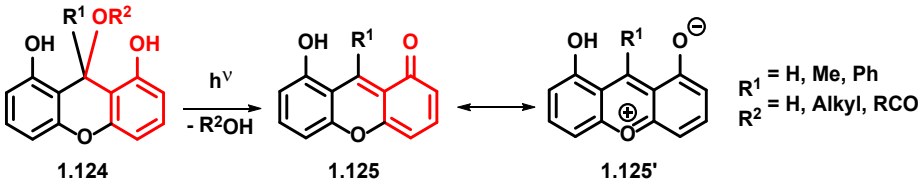

Scheme 1.33. Proposed mechanism of action of a new fluorogenic PPG.

1.8. References

1. Toteeva, M. M.; Richard, J. P. *Adv. Phys. Org. Chem.* **2011**, 45, 39-91.
2. Richard, J. P.; Toteeva, M. M.; Crugeiras, J. *J. Am. Chem. Soc.* **2000**, 122, 1664-1674.
3. Singh, M. S.; Nagaraju, A.; Anand, N., Chowdhuty, S. *RSC Adv.* **2014**, 4, 55924-55959.
4. Diao, L.; Yang, C.; Wan, P. *J. Am. Chem. Soc.* **1995**, 117, 5369-5370.
5. Chiang, Y.; Kresge, A. J.; Zhu, Y. *J. Am. Chem. Soc.* **2002**, 124, 6349-6356.
6. Chang, J. A.; Kresge, A. J.; Zhan, H.-Q.; Zhu, Y. *J. Phys. Org. Chem.* **2004**, 17, 579-585.
7. Arumugam, S.; Popik, V. V. *J. Am. Chem. Soc.* **2009**, 131, 11892-11899.
8. Kulikov, A.; Arumugam, S.; Popik, V. V. *J. Org. Chem*. **2008**, 73, 7611-7615.
9. Verga, D.; Richter, S. N.; Palumbo, M.; Gandolfi, R.; Freccero, M. *Org. Biol. Chem*. **2007**, 5, 233-235.
10. Richter, S.; Maggi, S.; Colloredo-Mels, S.; Palumbo, M.; Freccero, M. *J. Am. Chem. Soc*. **2004**, 126, 13973-13979.
11. Di Antoniu, M.; Doria, F.; Richter, S. N.; Bertipaglia, C; Mella, M.; Sissi, C.; Palumbo, M.; Freccero, M. J. *J. Am. Chem. Soc*. **2009**, 131, 131132-13141.
12. Colloredo-Mels, S.; Doria F.; Verga, D.; Freccero, M. J. *J. Org. Chem*. **2006**, 71, 3889-3895.
13. Modica, E.; Zanaletti, R.; Freccero, M.; Mella, M. *J. Org. Chem*. **2001**, 66, 41-52.
14. Wehry, E. L.; Rogers, L. B. *J. Am. Chem. Soc.* **1965**, 87, 4232-4238.
15. Tolbert, L. M.; Haubrich, J. E. *J. Am. Chem. Soc*. **1994**, 116, 10593-10600.

16. Skalamera, D.; Mlinaric-Majerski, K.; Martin-Kleiner, I.; Kralj, M.; Wan, P.; Basaric, N. *J. Org. Chem*. **2014**, 79, 4390-4397.
17. Skalamera, D.; Antol, I.; Mlinaric-Majerski, K.; Vancik, H.; Phillips, D. L.; Ma, J.; Basaric, N. *Chem. Eur. J*. **2018**, 24, 9426-9435.
18. Yan, Z.; Du, L.; Lan, X.; Zhang, X.; Phillips, D. L. *J. Mol. Sci*. **2018**, 1172, 102-107.
19. Aulin-Erdtman, G.; Sanden, R. *Acta Chem. Scand*. **1968**, 22, 1187-1209.
20. Verga, D.; Nadai, M.; Doria, F.; Percivalle, C.; Di Antonio, M.; Palumbo, M.; Richter, S. N.; Freccero, M. *J. Am. Chem. Soc*. **2010**, 132, 14625-14637.
21. Matsumoto, J.; Ishizu, M.; Kawano, R.-i.; Hesaka, D.; Shiragami, T.; Hayashi, Y.; Yamashita, T.; Yasuda, M. *Tetrahedron* **2005**, 61, 5735-5740.
22. Birks, J. B. *Photophysics of Aromatic Molecules*; Wiley Interscience: New York, 1970; 703 p.
23. Berlman, I. B. *Handbook of Fluorescence Spectra of Aromatic Molecules*; Academic Press: New York, 1971; 473 p.
24. Mikami, N. *Bull. Chem. Soc. Jpn.* **1995**, 68, 683-695.
25. Bryson, A.; Matthews, R. W. *Austral. J. Chem*. **1963**, 16 (3), 401-410.
26. Swaminathan, M. *Curr. Sci*. **1992**, 62 (4), 365-368.
27. Doria, F.; Lena, A.; Bargiggia, R.; Freccero, M. *J. Org. Chem*. **2016**, 81, 3665-3673.
28. a). Chiang, Y.; Kresge, A. J.; Zhu, Y. *J. Am. Chem. Soc.* **2000**, 122, 9854-9855; b). Chiang, Y.; Kresge, A. J.; Zhu, Y. *Pure Appl. Chem.* **2000**, 72 (12), 2299-2308.
29. Weinert, E. E.; Dondi, R.; Colloredo-Melz, S.; Frankenfield, K. N.; Mitchel, C. H.; Freccero, M.; Rokita, S. E. *J. Am. Chem. Soc.* **2006**, 128 (36), 11940-11947.
30. Popik, V. V.; Arumugam, S. *Methods for labeling a substrate using a hetero-Diels-Alder reaction*. US 2011/0257047 A1, Oct. 20, 2011.
31. Willis, N. J.; Bray, C. D. *Chem.: Eur. J.* **2012**, 18 (30), 9160-9173.

32. Yang, B.; Gao, S. *Chem. Soc. Rev*. **2018**, 47, 7926-7953.

33. Arduini, A.; Bosi, A.; Pochini, A.; Ungaro, R. *Tetrahedron* **1985**, 3095-3103.

34. Padwa, A.; Dehm, D.; One, T.; Lee, G. A. *J. Am. Chem. Soc.* **1975**, 97 (7), 1837-1845.

35. Barker, B.; Diao, L.; Wan, P. *J. Photochem. Photobiol. A: Chemistry* **1997**, 104, 91-96.

36. Foster, K. L.; Baker, S.; Brousmiche, D. W.; Wan, P. *J. Photochem. Photobiol. A: Chemistry* **1999**, 129, 157-163.

37. Wan, P.; Barker, B.; Diao, L.; Fischer, M.; Shi, Y.; Yang, C. *Can. J. Chem*. **1996**, 74, 465.

38. Arnold, R. M.; Patton, D. L.; Popik V. V.; Locklin, J. *Acc. Chem. Res.* **2014**, 47 (10), 2999-3008.

39. Arumugam, S.; Popik, V. V. *J. Am. Chem. Soc.* **2012**, 134 (20), 8408-8411.

40. De Forest, C. A.; Polizzotti, B. D.; Anseth, K. S. *Nat. Mater.* **2009**, 8, 659-664.

41. Fiore, M.; Marra, A.; Dondoni, A. *J. Org. Chem.* **2009**, 74, 4422-4425.

42. Fiore, M.; Chambery, A.; Marra, A.; Dondoni, A. *Org. Biomol. Chem.* **2009**, 7, 3910-3913.

43. Hensarling, R. M.; Doughty, V. A.; Chan, J. W.; Patton, D. L. *J. Am. Chem. Soc.* **2009**, 131, 14673-14675.

44. Norberg, O.; Lee, I. H.; Aastrup, T.; Yan, M.; Ramstrom, O. *Biosens. Bioelectron.* **2012**, 34, 51-56.

45. Chen, R. T.; Marchesan, S.; Evans, R. A.; Styan, K. E.; Such, G. K.; Postma, A.; McLean, K. M.; Muir, B. W.; Caruso, F. *Biomacromolecules* **2012**, 13, 889-895.

46. Shin, D.-S.; Seo, J. H.; Sutcliffe, J. L.; Revzin, A. Chem. Commun. 2011, 47, 11942-11944.

47. Nakanishi, J.; Kikuchi, Y.; Takarada, T.; Nakayama, H.; Yamaguchi, K.; Maeda, M. J. Am. Chem. Soc. 2004, 126, 16314-16315.

48. Agasti, S. S.; Chompoosor, A.; You, C. C.; Ghosh, P.; Kim, C. K.; Rotello, V. M. J. Am. Chem. Soc. 2009, 131, 5728-5729.

49. Popik, V. V.; Arumugam, S. *Methods for labeling a substrate having a plurality of thiol groups attached thereto*. US 2013/0281656 A1, Oct. 24, 2013.

50. Arumugam, S.; Orski, S. V.; Locklin, J.; Popik, V. V. *J. Am. Chem. Soc.* **2012**, 134 (1), 179-182.

51. Arumugam, S.; Popik, V. V. *J. Am. Chem. Soc.* **2011**, 133 (39), 15730-15736.

52. Arumugam, S.; Popik, V. V. *J. Am. Chem. Soc.* **2011**, 133, 5573-5579.

53. Nekongo, E. E.; Popik, V. V. *J. Org. Chem.* **2014**, 79 (16), 7665-7671.

54. Arumugam, S.; Popik, V. V. *Photochem. Photobiol. Sci.*, **2012**, 11, 518-521.

55. Arumugam, S.; Guo, J.; Mbua, N. E.; Friscourt, F.; Lin, N.; Nekongo, E.; Boons, G.-J.; Popik, V. V. *Chem. Sci*. **2014**, 5, 1591-1598.

56. Popik, V. V.; Boons, G.-J.; Guo, G.; Arumugam, S.; Nekongo, E.; Lin, N. *Methods for reacting cysteine residues in peptides and proteins*. US 2014/0054163 A1, Feb. 27, 2014.

57. Lavis, L. D.; Raines, R. T. *ACS Chem. Biol.* **2014**, 9, 855−866.

58. Leonhard, H.; Gordon, L.; Livingst, R. *J. Phys. Chem.* **1971**, 75, 245-249.

59. Nekongo, E. E.; Bagchi, P.; Fahrnib, C. J.; Popik, V. V. *Org. Biomol. Chem.* **2012**, 10, 9214-9218.

`

CHAPTER 2

PHOTOCHEMICAL GENERATION OF QUINONE METHIDES FROM 3-(HYDROXY(4-HYDROXYPHENYL)METHYL)NAPHTHALEN-2-OL AND 6-(HYDROXY(4-HYDROXYPHENYL)METHYL)NAPHTHALEN-1,7-DIOL AND THEIR REACTIVITY IN AQUEOUS SOLUTIONS*

2.1. Introduction

As it was mentioned in Chapter 1, photochemical generation of QMs from QMPs under catalyst free conditions and extraordinary reactivity of QMs towards nucleophiles and, in case of *o*-QMs, towards electron-rich dienophiles have attracted a lot of attention to these compounds. The research of our group has been conducted in two major directions. The fundamental studies of photochemical generation and the reactivity of o-NQMs have been performed.[1] Also, it has been successfully demonstrated that o-NQMPs could be used as photolabile protecting groups[2-4] and linkers[5,6] and be employed in the design of multifunctional surfaces.[7-10]

As it was discussed in Chapter 1, *o*-QMs and *p*-QMs, as well as their precursors exhibit different chemical properties and different reactivity. For instance, 2-hydroxymethylphenol and 3-ethoxymethyl-2-naphthol demonstrated higher quantum yields (Φ = 0.23 and 0.17, respectively)[1] than *p*-QMP 4-hydroxymethylphenol (Φ = 0.007).[11] Also, *o*-QMs have been found to be more reactive towards hydration and reactions with nucleophiles. For example *o*-QM and *o*-NQM1 (2,3-Naphthoquinone-3-methide) underwent uncatalyzed hydrolysis with rate constants $k_w = 2.6 \times 10^2\ s^{-1}$ and $k_w = 1.45 \times 10^2\ s^{-1}$ and reacted with 2-aminoethylthiol hydrochloride with second-order rate constants $k_{thiol} = 1.9 \times 10^5\ M^{-1}s^{-1}$ and $k_{thiol} = 2.24 \times 10^5\ M^{-1}s^{-1}$, respectively.[1,12,13] On the other hand, *p*-QM demonstrated much lower reactivity

*Sutton, M. V.; Popik, V. V., To be submitted to *J. Am. Chem. Soc.*

and was characterized by rate constants k_w = 3.3 s^{-1} and k = 1.3 x 10^3 $M^{-1}s^{-1}$ with 2-aminoethylthiol hydrochloride.[13,14] Additionally, only *o*-QMs can be involved in *hetero*-Diels-Alder reaction.

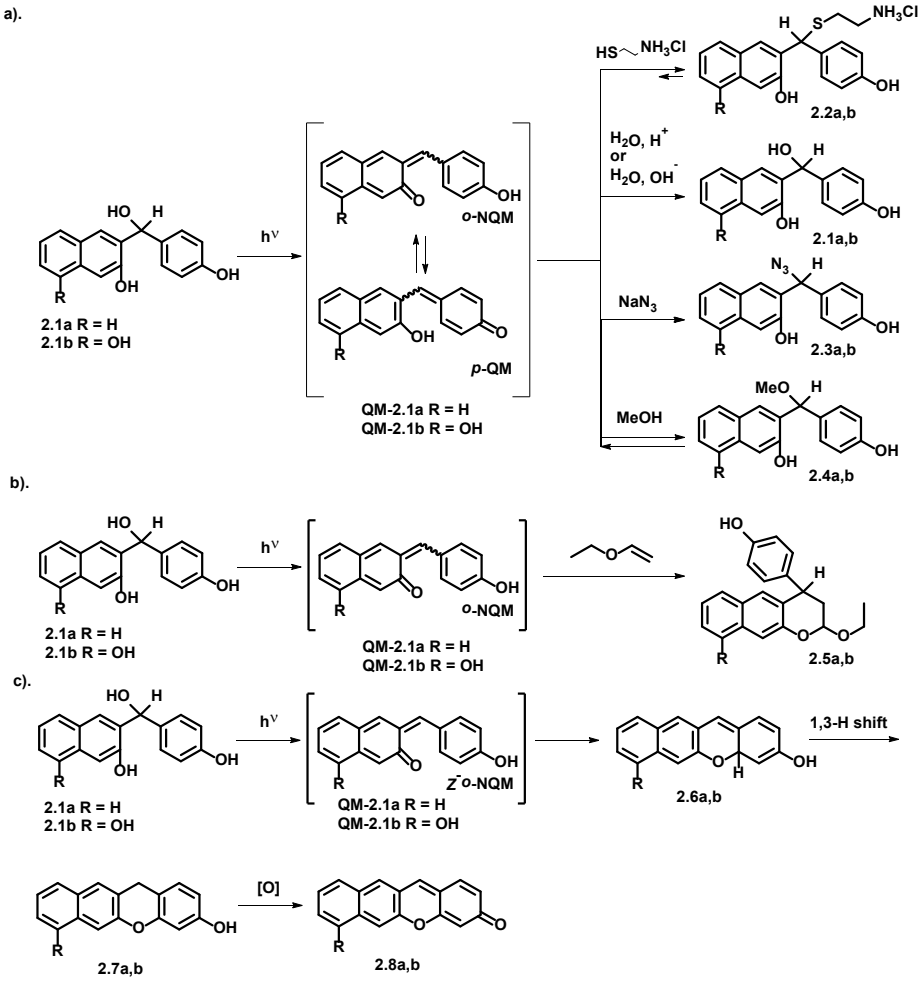

Scheme 2.1. Expected chemical reactivity of novel QMs under various conditions. a). Reaction with nucleophiles. b). Intermolecular Diels-Alder reaction with ethyl vinyl ether. c). Intramolecular Diels-Alder reaction.

To the best of our knowledge, the molecules containing competing *o*-naphthoquinone methide and *p*-quinone methide moieties, have not been studied. Thus, we decided to develop and synthesize novel QMPs (3-(Hydroxy(4-hydroxyphenyl)methyl)naphthalen-2-ol **2.1a** and 6-(Hydroxy(4-hydroxyphenyl)-methyl)naphthalene-1,7-diol **2.1b**), that could generate *o*-NQM and *p*-QM upon UV-light irradiation. Physical properties, chemical properties, such as ability to react with nucleophiles and undergo inter- and

intramolecular Diels-Alder reaction, as well as kinetic behavior of new QM-systems have been studied (Scheme 2.1).

2.2. Synthesis of 3-(Hydroxy(4-hydroxyphenyl)methyl)naphthalen-2-ol and 6-(Hydroxy(4-hydroxy-phenyl)methyl)naphthalene-1,7-diol

The synthesis of QMPs **2.1a** and **2.1b** was started from commercially available 3-hydroxy-2-naphthoic acid **2.9a** and 3,5-dihydroxy-2-naphthanoic acid **2.9b**, respectively. The protection of phenolic hydroxyls and esterification was followed by lithium aluminum hydride reduction of the esters **2.10** and produced compounds **2.11a** and **2.11b** in high yields. The oxidation with pyridinium chlorochromate gave naphthaldehydes **2.12a** and **2.12b** in 78 % and 94 % yields, respectively. Obtained aldehydes were converted with *n*-BuLi and 4-bromoanisole into the compounds **2.13a** and **2.13b**. Direct deprotection of phenolic hydroxyls under nucleophilic attack conditions with sodium ethanethiolate and under acidic conditions with BBr_3 did not succeed. Thus, deprotection was performed in two steps: compounds **2.13a,b** were first oxidized with manganese (IV) oxide into corresponding ketones **2.14**, and then demethylation was conducted with BBr_3. Reduction of obtained compounds **2.15a** and **2.15b** with lithium aluminum hydride resulted in the nearly quantitative formation of desired QMPs **2.1a** and **2.1b** (Scheme 2.2).

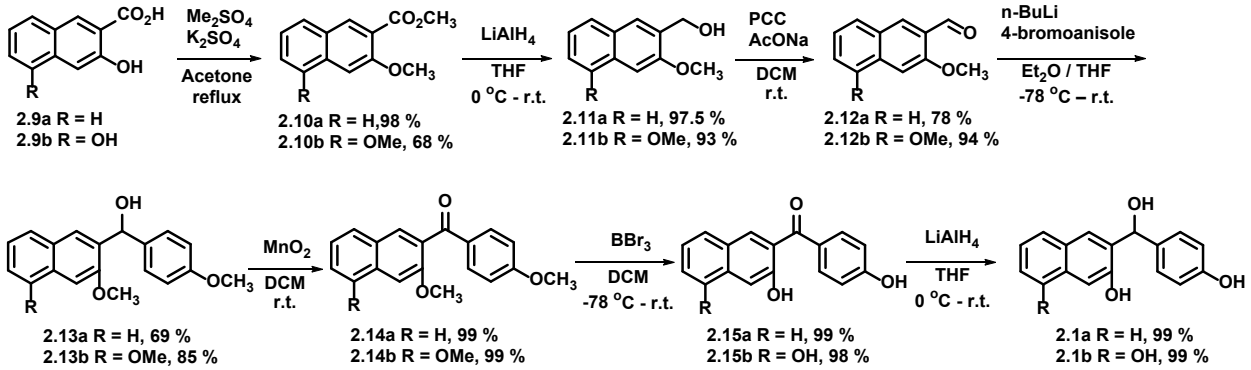

Scheme 2.2. Attempted synthesis of QMPs **2.1a** and **2.1b**.

2.3. Properties of QMPs 2.1a and 2.1b

Absorption spectra of QM precursors in acetonitrile solutions were found to be expectedly similar due to the presence of analogous chromophores, and resembled UV-spectrum of other NQMPs and 2-naphthol. Absorbance spectrum of 3-(hydroxy(4-hydroxyphenyl)methyl)naphthalen-2-ol **2.1a** has several major absorbance bands at λ_{max} ~ 230 nm (log ε = 5.13), λ_{max} ~ 275 nm (log ε = 4.15) and at λ_{max} ~ 330 nm (log ε = 3.76). UV spectrum of 6-(hydroxy(4-hydroxy-phenyl)methyl)naphthalene-1,7-diol **2.1b** has multiple absorbance bands located at λ_{max} ~ 220 nm (log ε = 5.05), λ_{max} ~ 248 nm (log ε = 5.01), λ_{max} ~ 280 nm (log ε = 4.24) and at λ_{max} ~ 335 nm (log ε = 3.82) (Figure 2.1).

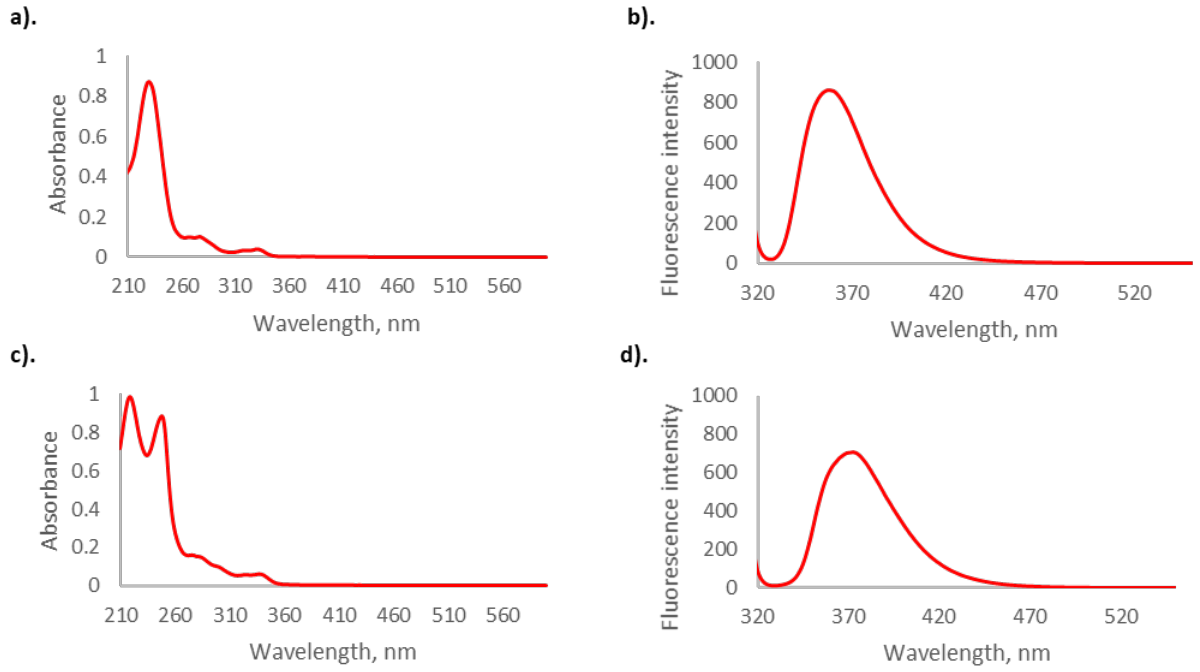

Figure 2.1. Absorption and emission spectra of **2.1a** and **2.1b. a).** UV-spectrum of **2.1a** in acetonitrile. **b).** Emission spectrum of **2.1a** in acetonitrile. **c).** UV-spectrum of **2.1b** in acetonitrile. **d)**. Emission spectrum of **2.1b** in acetonitrile.

Both QMPs **2.1a** and **2.1b** exhibit strong fluorescence, which is predictably similar to their analogs 2-naphthol (Φ_{Fl} = 0.27),[16] *o*-NQMP1 (Φ_{Fl} = 0.230±0.002) and *o*-NQMP2 (1,2-naphthoquinone-1-methide)

(Φ_{Fl} = 0.30±0.01).[1] QMPs **2.1a** and **2.1b** have emission maxima at λ_{max} = 358 nm and at λ_{max} = 371 nm in pure acetonitrile, respectively (Figure 2.1). Fluorescence quantum yields were measured by use of quinine sulfate (Φ_{Fl} = 0.546±0.02)[17] in 0.5 M aq. H_2SO_4 as a standard and were found to be Φ_{Fl} = 0.22±0.01 for **2.1a** and Φ_{Fl} = 0.30±0.01 for **2.1b** at excitation wavelength λ_{ex} = 305 nm. Due to the presence of additional hydroxyl group in the position 5 of naphthalene moiety, QMP **2.1b** is characterized by longer wavelength of emission and higher fluorescence efficiency.

The ground-state acidities of QMPs **2.1a,b** were determined by spectrophotometric titration in aqueous solution at 25 ± 0.1 °C and were determined to be pKa = 9.98 ± 0.02 for **2.1a** and pKa = 10.40 ± 0.03 for **2.1b** (Figure 2.2). These compounds appeared to be less acidic than other o-NQMPs.[1] For example, pKa of 3-hydroxy-2-naphalenemethanol and 2-hydroxy-1-naphthalenemethanol are 9.01 and 8.93, respectively.[1]

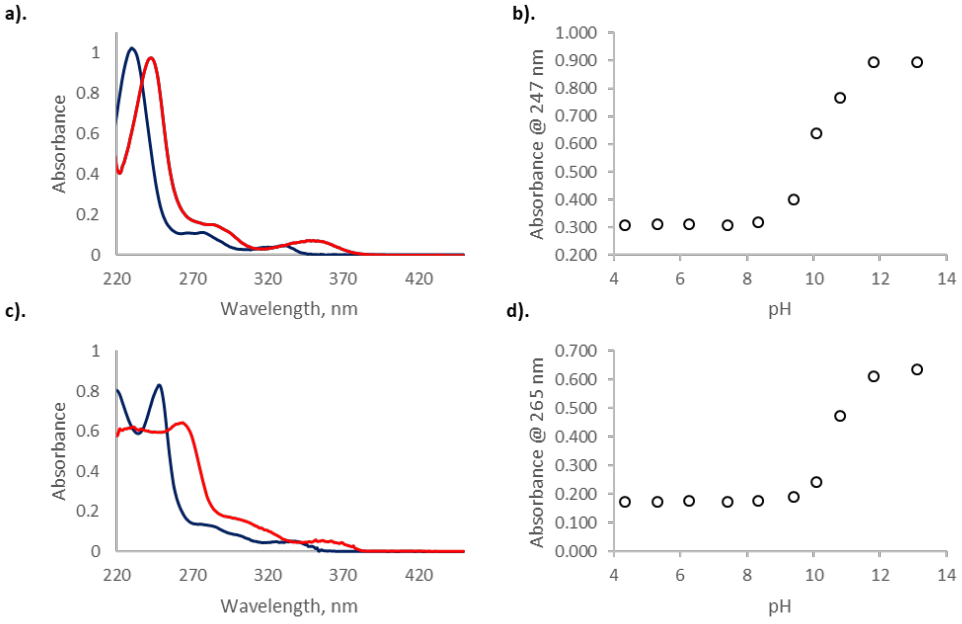

Figure 2.2. Spectrophotometric titration of **2.1a** and **2.1b. a).** UV-spectra of **2.1a** in neutral (blue) and anionic (red) forms. **b).** Spectrophotometric titration of **2.1a. c).** UV-spectra of **2.1b** in neutral (blue) and anionic (red) forms. **d).** Spectrophotometric titration of **2.1b**.

2.4. Reactivity of QMPs 2.1a and 2.1b

Photolysis of aqueous solutions of QMPs results in rapid consumption of substrate and formation of corresponding QMs, which readily react with nucleophiles and, in case of *o*-QMs, with electron-rich dienophiles. Irradiation of aqueous acetonitrile solutions (1:1, pH = 7.0) of NQMPs **2.1a** and **2.1b** with 300 nm light in the presence of a strong nucleophile, such as 2-aminoethylthiol hydrochloride, resulted in fast consumption of starting materials and formation of **2.2a** and **2.2b**, respectively. According to HPLC, at ~ 80 % conversion formation of oligomers was not observed, however, prolonged irradiation resulted in significant decrease of the peak areas corresponding to both **2.1** and **2.2**. Since formation of other new products was not detected, we believe that oligomerization of NQMPs occurred and those secondary products were apparently trapped in the column. The efficiency of the photolysis was determined by the use of 3,4-dimethoxynitrobenzene in 0.5 M aqueous KOH solution as an actinometer.[18] The quantum yields were found to be $\Phi = 0.157 \pm 0.002$ for **2.1a** and $\Phi = 0.064 \pm 0.005$ for **2.1b**.

2.5. Transient QMPs and QMs

Irradiation of QMPs **2.1a** and **2.1b** (0.0135 mM) in aqueous acetonitrile solution (1:1) with 300 nm light in Rayonet photoreactor resulted in formation of long-lived ($\tau_{1/2}$ ~ 30 s) and strongly absorbing species (λ_{max} = 400 nm) (Figure 2.3). Attempts to determine lifetimes of these species were unsuccessful, as decay of absorbance at λ = 400 nm over time gave the best fir to a three-exponential function and apparently corresponded to multiple processes. Generated species are characterized by significantly decreased fluorescence intensity at λ = 358 nm and λ = 371 nm compare to corresponding QMPs **2.1a** and **2.1b**. However, they show weak enhancement in fluorescence intensity at λ_{max} = 467 nm and λ_{max} = 465 nm, respectively (Figure 2.3).

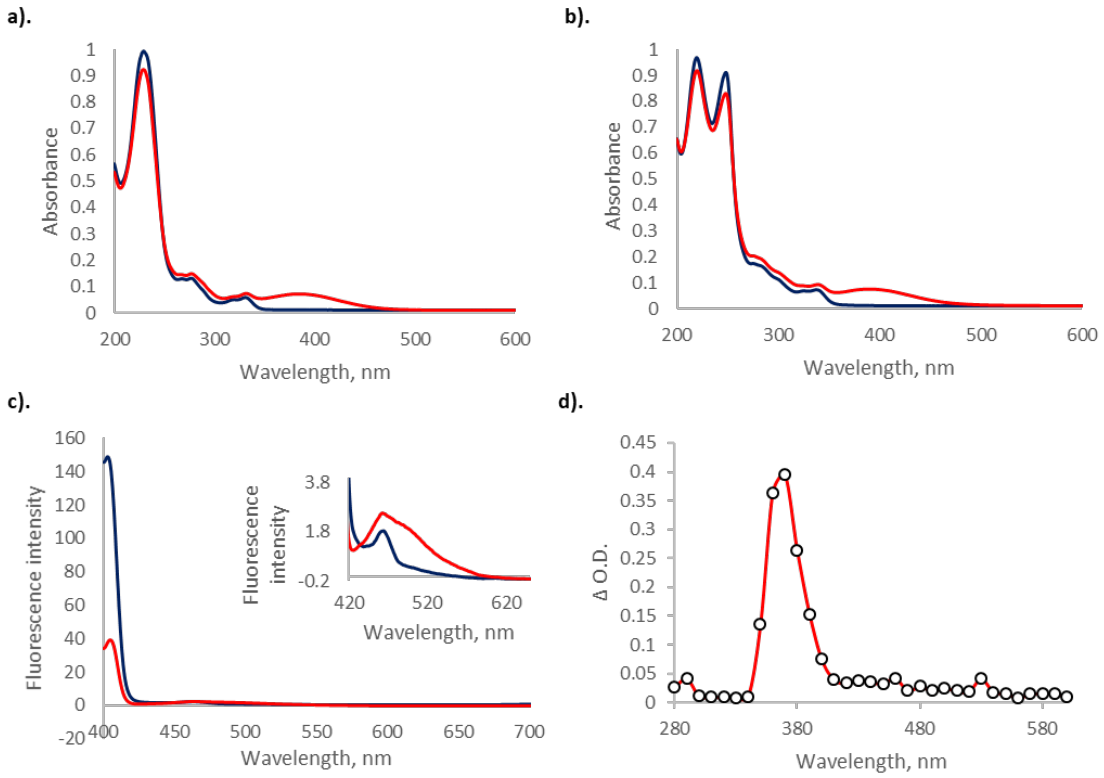

Figure 2.3. Spectroscopic properties of **2.1** and their transients. **a).** UV-spectra of **2.1a** prior (blue) and after 1 min (red) irradiation at 300 nm in acetonitrile/water, 1:1. **b).** UV-spectra of **2.1b** prior (blue) and after 1 min (red) irradiation at 300 nm in acetonitrile/water, 1:1. **c)**. Emission spectra of **2.1a** prior (blue) and after 1 min (red) irradiation at 300 nm in acetonitrile/water, 1:1. **d)**. Transient absorption spectra of **QM-2.1b** in acetonitrile (16 μs).

Laser flash photolysis (LFP) of QMP **2.1b** (0.033 mM) in aqueous acetonitrile solution (1:1) allowed to obtain a full spectroscopic characterization of the transient species. Transient generated from QMP **2.1b** demonstrated strong absorption band at λ_{max} = 375 nm and weak bands at λ_{max} = 460 nm and λ_{max} = 540 nm. It was characterized by a lifetime of τ ~ 18 ms and was not affected by oxygen (Figure 2.3). Thus, the transient did not exist in triplet state. Behavior of observed transient is very similar to one of the long-lived transient described for o-NQMPs: λ_{max} = 330 nm and broad absorption at λ_{max} = 430 nm, τ ~ 4-8 ms.[1]

Longer lifetime of observed by us QM compare to described earlier o-NQM can be explained by extended conjugation system.

2.6. Reactions of QMs

2.6.1. Hydration Rate Profile

As it was mentioned in Chapter 1 QMs undergo rapid hydration in the absence of nucleophiles or dienophiles, which results in the formation of corresponding hydroxymethylphenol derivatives. Rates of hydration of photochemically generated NQMs from **2.1a** and **2.1b** were determined in dilute aqueous solutions of perchloric acid, sodium hydroxide and biphosphate buffers (pH = 7.41, pH = 6.63 and at pH = 6.81). The ionic strength of all solutions was maintained at 0.1 M by the addition of sodium chloride. T Laser flash photolysis of QMPs in aqueous solution produced QMs with characteristic absorbance band at λ ~ 400 nm. Thus, the rate of hydration under various conditions were determined by following the decay of the absorption band at λ = 400 nm over time. The rate measurements were conducted using LKS.60 kinetic spectrometer (Applied Photophysics) equipped with Brilliant B Nd:YAG laser (pulse width = 4 ns) fitted with 2nd and 4th harmonic generators. All solutions had the same concentration of QMPs (0.033 mM), which corresponded to OD ~ 0.4 at 254 nm. The measurements were conducted at 25 ± 0.05 ºC. Obtained kinetic data obeyed the first-order rate law, thus observed pseudo-first-order rate constants were determined by least-squares fitting to a single exponential function.

Hydration can be described via three processes: acid catalysis, uncatalyzed water reaction and hydroxide-ion catalyzed process (Scheme 2.2). Thus, rate profile of hydration can be described via equation 2.1:[13-15]

Eq. 2.1 $$k = k_{H+}[H^+] + k_w + k_{OH-}[OH^-]$$

where k_{H+} is a second-order rate constant of acid-catalyzed process $M^{-1}s^{-1}$, k_w is a first-order rate of uncatalyzed water reaction, s^{-1}; k_{OH-} is a second-order rate of hydroxide-ion catalyzed process, $M^{-1}s^{-1}$. In case of **QM-2.1a** hydration occurred with τ ~ 29.5 s, however, in case of **QM-2.1b** two independent decays were observed: τ ~ 15 s and 0.27 ms. Both fast and slow processes were observed in buffered solutions at

neutral pH. Only slow process was detected at pH < 3.3 and at pH >11. We assume that under conditions of specific acid and specific base catalysis, the fast process becomes too fast to be detected via our instruments. Experiments conducted in dilute aqueous biphosphate buffer solution (pH = 7.41) in inert atmosphere, air and oxygen did not show significant effect on the rate constant of hydrolysis of the fast process. Thus, transients of the fast process did not exist in triplet state. The slow process was slightly affected by the presence of oxygen, however, full quenching of the process was not observed. In the inert atmosphere the hydration rate constant was $k_{Obs.}$ = 0.04 s^{-1}, but it was somewhat faster in the air and oxygen atmosphere: $k_{Obs.}$ = 0.067 s^{-1} and $k_{Obs.}$ = 0.115 s^{-1}, respectively. Current observation supported the assignment of transient species to QMs in S_0 state: QMs are known to be oxidized with singlet oxygen.[1]

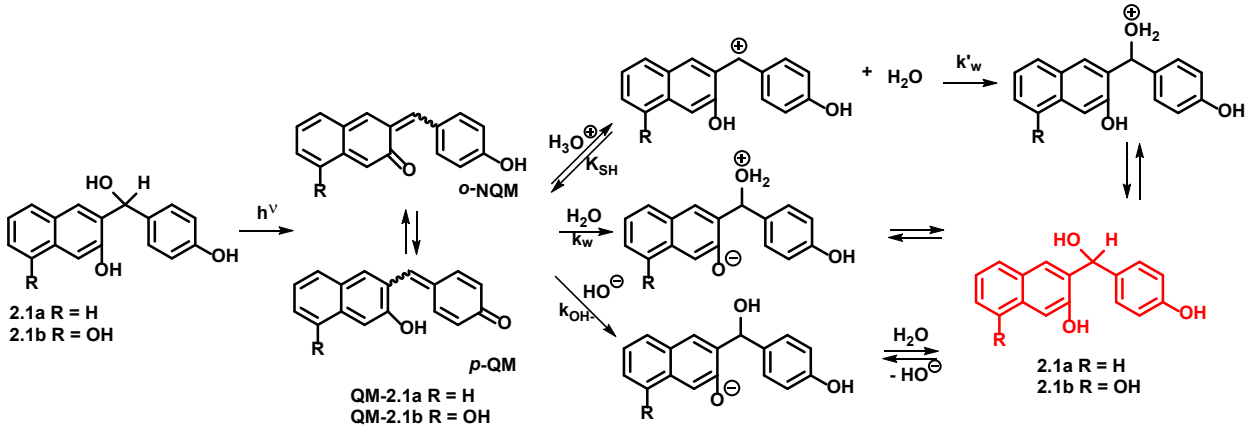

Scheme 2.3. Proposed mechanism of hydration of **QM-2.1** at different pH.

The buffer independent rate constants and observed rate constants determined in perchloric acid and sodium hydroxide solutions, are shown as the rate profile in Figure 2.4.

The rate of hydration of QMs generated from **2.1a** and **2.1b** were independent of the acidity of aqueous solutions in the pH range of 4-9. The obtained range is similar to the ones determined for *p*-QM (pH range of 6-10)[14,15] and for *o*-QM and *o*-NQMs (pH range of 4-8 and 1-8).[1,13,14] The observed rate constants on the plateau correspond to k_w = (2.1±0.1)x10^{-2} s^{-1} for **QM-2.1a** and k_w = (5.2±0.2)x10^{-2} s^{-1} for **QM-2.1b**. These values are very similar to uncatalyzed hydration of *p*-quinone α-phenylmethide (k_w = 5.1x10^{-2} s^{-1}).[12,14]

Obtained values were ~10,000-folds lower than the one of o-NQM (k_w = 2.3 x 10^2 s^{-1}).[1] That could indicate the domination of *p*-QM form over o-NQM form in uncatalyzed hydration.

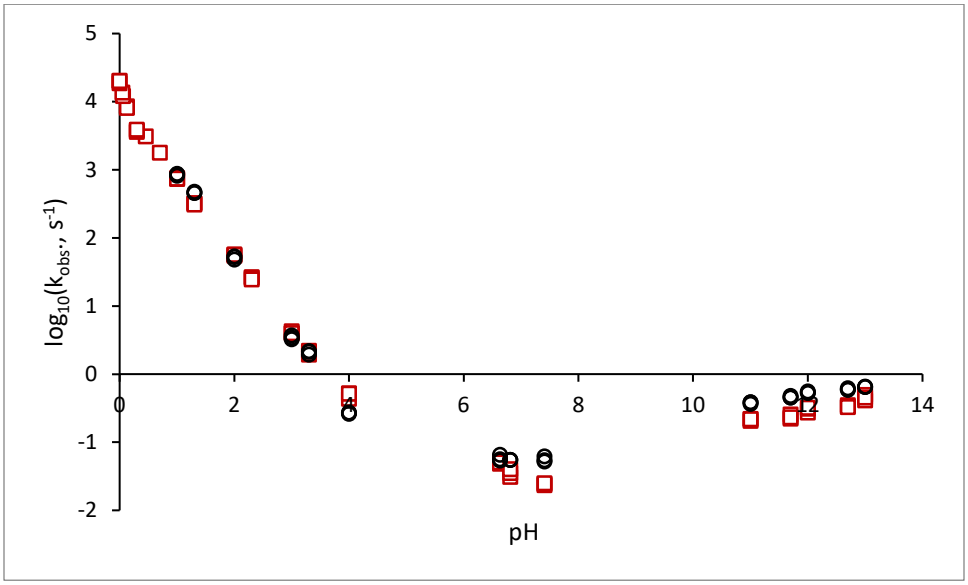

Figure 2.4. Rate profiles for the hydration of **QM-2.1a** (red squares) and **QM-2.1b** (black circles).

The rate of hydration demonstrated a pronounced specific acid catalysis (k_{H+} = (7.3±0.1)x10^3 $M^{-1}s^{-1}$ for **QM-2.1.a** and k_{H+} = (8.9±0.3)x10^3 $M^{-1}s^{-1}$ for **QM-2.1.b**), which was also observed for *o*-QM[12,13] and *p*-QM.[13-15] Obtained values were a little smaller than of the one reported for *p*-quinone α-phenylmethide (k_{H+} = 2.9x10^4 $M^{-1}s^{-1}$).[14] On the other hand, the values were greater than the one of o-NQM analog k_{H+} = 2.99x10^2 $M^{-1}s^{-1}$. Current observation indicated the contribution of both *p*-QM and *o*-NQM forms.

Specific base catalysis was present, however, was relatively weak. Hydroxide ion catalyzed addition of water, described as k_{OH-}, were determined to be k_{OH-} = 12.1±0.6 $M^{-1}s^{-1}$ for **QM-2.1.a** and k_{OH-} = 17.7±1.0 $M^{-1}s^{-1}$ for **QM-2.1.b**. Obtained values appeared to be much smaller than the ones recorded for *o*-NQMPs (k_{OH-} = (3.30x10^4) $M^{-1}s^{-1}$ for o-NQM1 and k_{OH-} = (3.74x10^4) $M^{-1}s^{-1}$ for o-NQM2),[1] however, they were similar to the one of *p*-quinone α-phenylmethide (k_{OH-} = 8.2x10^1 $M^{-1}s^{-1}$) (Table 2.1).[14] Hydroxide ion acted as a nucleophile, thus stability of quinoid core toward nucleophilic attack as well as accessibility of α-carbon played a crucial role. Thus, obtained values could be explained by domination of more stable *p*-QM form over *o*-NQM structure.

The presence of general catalysis was tested in dilute aqueous biphosphate buffer solutions at the same concentrations but of different buffer ratio (BR = 0.3, pH = 7.41; BR = 1.2, pH = 6.81 and BR = 1.8, pH = 6.63). The ionic strength of all solutions was maintained at 0.1 M by the addition of sodium chloride. Observed rate constants of hydration were found to be dependent on the buffer concentration, thus presence of general catalysis was assumed. To determine whether the reaction was catalyzed by general acid or general base, obtained observed rate constants were plotted vs. the concentration of general acid or general base, respectively. As a result, linear dependence of rate constant vs. general acid concentration was observed for hydration of **QM-2.1a** and **QM-2.1b** in case of a slow process (Figure 2.5). Thus, reaction was catalyzed by general acid and could be described via eq. 2.2,

Eq. 2.2. $$k_{Obs.} = k_{H^+}[H^+] + k_{HA}[HA] + k_w + k_{OH^-}[OH^-]$$

where HA is a general acid.[19]

On the other hand, presence of general acid catalysis in the fast process of hydrolysis of **QM-2.1b** and general base catalysis were not detected.

Table 2.1. Hydration rate constants of QMs.

QM	k_w, s^{-1}	k_{OH^-}, $M^{-1}s^{-1}$	k_{H+}, $M^{-1}s^{-1}$	k_{buffer}, $M^{-1}s^{-1}$ pH = 7.41	k_{buffer}, $M^{-1}s^{-1}$ pH = 6.81	k_{buffer}, $M^{-1}s^{-1}$ pH = 6.63
QM-2.1a	$(2.1\pm0.1)\times10^{-2}$	12.1±0.6	$(7.3\pm0.1)\times10^{3}$	2.4±0.2	6.4±0.5	7.5±0.5
QM-2.1b slow	$(5.2\pm0.2)\times10^{-2}$	17.7±1.0	$(8.9\pm0.3)\times10^{3}$	3.1±0.3	6.1±0.6	5.3±0.6
QM-2.1b fast	$(3.64\pm0.02)\times10^{3}$	n.d.	n.d.	$(2.9\pm0.2)\times10^{4}$	$(2.0\pm0.2)\times10^{4}$	$(2.2\pm0.2)\times10^{4}$

a).

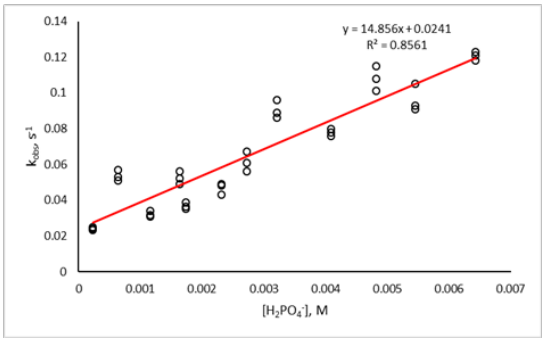

b).

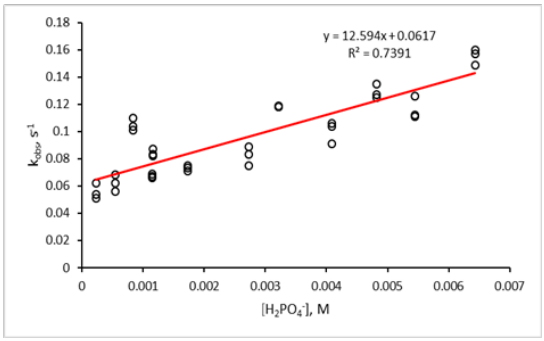

Figure 2.5. General acid catalysis of hydration of **QM-2.1a** and **QM-2.1b. a).** General acid catalysis of hydration of **QM-2.1a. b).** General acid catalysis of hydration of **QM-2.1b**.

Comparison of hydration rate constants of **QM-2.1a** and **QM-2.1b** allowed us to observe the influence of additional hydroxyl substituent in the 5th position on the hydration rate at various conditions. It was found that introduction of hydroxyl group increased the rate of the hydrolysis under neutral, acidic and basic conditions. However, significant effect was observed only under uncatalyzed and hydroxyl-ion catalyzed conditions.

2.6.2. Reactions of QMs with Nucleophiles

Photochemically generated QMs from **2.1a** and **2.1b** rapidly react with nucleophiles, such as methanol, 2-aminoethylthiol hydrochloride and sodium azide (Scheme 2.1).

UV-irradiation of **2.1a** and **2.1b** in aqueous solution of 2-aminoehylthiol hydrochloride (pH = 7.0) with 300 nm light resulted in the formation of corresponding thioethers **2.2a** and **2.2b**, respectively. According to HPLC analysis, maximum ratio between **2.2** and **2.1** was reached after 20 min of irradiation and was ~ 80 %. Formation of thioethers was confirmed by HR-MS analysis. The second-order rate constants of the reactions between photochemically generated QMs and 2-aminoehylthiol hydrochloride at pH = 7.00 were determined via LFP and were found to be k_{thiol} = (6.72±0.18)x10^4 $M^{-1}s^{-1}$ for **QM-2.1a** and k_{thiol} = (6.73±0.32)x10^4 $M^{-1}s^{-1}$ for **QM-2.1b**. Obtained rate constants were found to be lower than the ones determined for *o*-NQMs (k_{thiol} ~ 2.2x10^5 $M^{-1}s^{-1}$)[1] and higher than for *p*-QM (k_{thiol} ~ 1.3x10^3 $M^{-1}s^{-1}$).[13,14]

Likewise, azide ion was shown to trap photogenerated QMs. The second-order rate constants of the reactions between QMs and sodium azide in aqueous buffered solutions (pH 7.41) were determined via LFP and were found to be k_{N3} = (2.73±0.05)x10^3 $M^{-1}s^{-1}$ for **QM-2.1a** and k_{N3} = (2.13±0.06)x10^3 $M^{-1}s^{-1}$ for **QM-2.1b**. Similarly, obtained rate constants were found to be 10-folds lower than the ones determined for *o*-NQMs (k_{N3} ~ 2.0x10^4 $M^{-1}s^{-1}$).[1] HPLC analysis of the reaction mixture did not show formation of new peak corresponding to azide **2.3a,b**. Apparently, azide group is more labile under applied conditions and, thus, newly formed azides 2.3 form oligomers faster than alcohols **2.1**.

Photoirradiation of **2.1a** and **2.1b** in aqueous methanol with 300 nm light resulted in the formation of corresponding methyl ethers **2.4a** and **2.4b**. According to HPLC analysis, maximum ratio between **2.4** and **2.1** was reached after 35 min of irradiation and was ~ 80 %. Exhaustive irradiation resulted in decomposition of both compounds and the formation of QM oligomers. The prolonged irradiation resulted in broadening of absorption bands in the UV spectrum. Interestingly, **2.1b** was also found to undergo nucleophilic attack by methanol when kept as dilute solutions (5 mM) in methanol and methanol-d_4 at r.t. under white light. According to ^{1}H NMR spectra, ~17 % of the compound **2.1b** was converted into corresponding methoxy-derivates **2.4b** and **2.4b'** in 24 h. Prolonged storage of the solutions resulted in decomposition of **2.1b** and **2.4b**, **2.4b'**, however, the ratio between residual hydroxy-form **2.1b** and corresponding methoxy-forms stayed unchanged.

2.6.3. o-QMs in Diels-Alder reaction

As it was mentioned in Chapter 1, only o-QMs can be considered as *hetero*-diene system and react with electron rich dienes via [2 + 4] cycloaddition to give various substituted chromans with moderate to high yields.[1,20,21] The second-order rate constant was determined for the intermolecular Diels-Alder reaction between ethyl vinyl ether (EVE) and QM photochemically generated from **2.1a** in aqueous buffered solution (pH = 7.41) (Scheme 2.1). It was found to be k_{EVE} = 1.49±0.07 $M^{-1}s^{-1}$. Second-order rate constant for the reaction with **2.1b** was determined only for the fast process and was found to be k_{EVE} =

$(8.94\pm0.49)x10^2\ M^{-1}s^{-1}$, the rate of the slow process was not affected by the presence of EVE. Exceptionally small values of obtained rate constants could be explained by the domination of *p*-QM form over *o*-NQM form, as only *ortho*-isomer could be involved in [4+2] cycloaddition.

We expected **QMs-2.1** to undergo intramolecular *hetero*-Diels-Alder reaction, similar to the one described by Padwa,[22] which resulted in formation of 9*H*-xanthene. In our case irradiation of QMPs **2.1a** and **2.1b** in aqueous acetonitrile solution (1:1) resulted in the formation of short-lived QMs, followed by formation of oligomers. The formation of expected seminaphthofluorone (SNAFR) analogs was not observed (Scheme 2.1). Prolonged irradiation resulted in the formation of oligomers.

2.7. Conclusions and Future Directions

According to obtained rate constants of hydration and reactions between photochemically generated QMs and nucleophiles, it may be concluded that novel QM systems exhibit predominantly properties of *p*-QMs than *o*-NQMs. The extremely small rate constants of intermolecular Diels-Alder reaction also supported the formation of *p*-QMs in greater quantities than o-NQM form. Introduction of electron-donating hydroxyl-substituent into position 5 of naphthalene, was only observed in the uncatalyzed and specific base catalyzed hydrolysis. However, In the experiments performed with **QM-2.1b** two independent processes of decay of QM were observed: $\tau \sim 15$ s and $\tau \sim 0.27$ ms. In our opinion, it would be interesting to investigate if the presence of the fast process was due to the nature of hydroxyl-group in the 5th position of naphthalene or it was the result of electronic effect. Also, it would be interesting to study the influence of the substituents in the benzylic position on the reactivity of these QMP and QM systems towards nucleophiles and dienophiles. Unfortunately, our attempts to synthesize 6-(1-hydroxy-1-(4-hydroxyphenyl)ethyl)naphthalene-1,7-diol **2.16** were not successful. In addition, to study the role of *p*-QM moiety in our QM systems we attempted to synthesize 3-(hydroxy(4-methoxyphenyl)methyl)naphthalen-2-ol **2.17** from 3-(methoxymethoxy)-2-naphthaldehyde **2.18**, however, methoxymethyl group in the direct precursor was not labile.

2.8. Experimental Procedures

2.8.1. General Information

Column chromatography was performed using 40-63 μm silica gel. NMR spectra were recorded on a 400 MHz NMR spectrometer, unless otherwise noticed. Chemical shifts were referenced to residual solvent proton or carbon signals. Melting points were determined using a Fisher-Johns melting point apparatus. High resolution mass spectra were obtained using electron spray ionization and orbitrap mass analyzer. Solutions were prepared using HPLC grade water, methanol and acetonitrile. Photoreactions were conducted using a Rayonet photoreactor equipped with fifteen 4W 300 nm fluorescent lamps.

2.8.2. Experimental Procedures and Compounds Data

All reagents were obtained from commercial sources and were used without further purification unless otherwise noted. (3-(Methoxymethoxy)naphthalen-2-yl)methanol **2.23** was prepared as reported previously.[4]

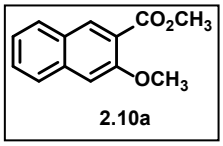

2.10a

Methyl 3-methoxy-2-naphthanoate (2.10a). Methyl 3-hydroxy-2-naphthoate **2.9a** (10 g, 50 mmol) and K_2CO_3 (34 g, 246 mmol) were mixed with acetone (120 mL). Me_2SO_4 (12 mL, 15.876 g, 126 mmol) was added dropwise, then reaction mixture was refluxed for 12 h. The reaction mixture was filtrated from salt, acetone was evaporated and the residue was dissolved in CH_2Cl_2. Obtained solution was washed with water, brine and dried over Na_2SO_4. Solvent was evaporated and the product **2.10a** was obtained as yellow oil (10.48 g, 98 %). No purification was required.

^{1}H NMR ($CDCl_3$, 400 MHz): 8.30 (1H, s), 7.79 (1H, d, *J* = 8.0 Hz), 7.71 (1H, d, *J* = 8.4 Hz), 7.52-7.47 (1H, m), 7.38 -7.33 (1H, m), 7.18 (1H, s), 3.97 (3H, s), 3.95 (3H, s).

^{13}C NMR ($CDCl_3$, 100 MHz): 166.5, 155.3, 135.9, 132.6, 128.5, 128.3, 127.3, 126.3, 124.2, 121.5, 106.6, 55.8, 52.1.

(3-methoxynaphthalen-2-yl)methanol (2.11a). Methyl 3-methoxy-2-naphthanoate **2.10a** (10.48 g, 48.5 mmol) was dissolved in anhydrous THF (500 mL), the solution was cooled to 0 ºC, and $LiAlH_4$ (10.78 g, 291 mmol) was added in small portions. The reaction mixture was allowed to react for 2 h at r.t., then 0.1 M solution of HCl was added and the product was extracted with EtOAc, washed with water, brine and dried over Na_2SO_4. Solvent was evaporated and the product **2.11a** was obtained as white solid (8.89 g, 97.5 %). No purification was required.

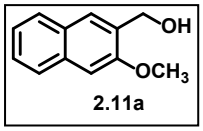

2.11a

^{1}H NMR ($CDCl_3$, 400 MHz): 7.77-7.72 (3H, m), 7.47-7.7.43 (1H, m), 7.38-7.34 (1H, m), 7.12 (1H, s), 4.83 (2H, s), 3.95 (3H, s).

^{13}C NMR ($CDCl_3$, 100 MHz): 155.8, 134.0, 130.4, 128.6, 127.6, 127.4, 126.4, 126.2, 123.8, 105.1, 62.3, 55.3.

3-methoxy-2-naphthaldehyde (2.12a). PCC (18.9 g, 73 mmol) was slowly added to 0 °C solution of alcohol **2.11a** (8.89 g, 47.3 mmol) and sodium acetate (6.05 g, 73 mmol) in DCM (400 mL). When addition was finished, the reaction mixture was left at r.t. overnight. The next day DCM was evaporated, and the residue was purified via column chromatography (CH_2Cl_2/Hexanes, 1:1). The product **2.12a** was obtained as yellow crystals (6.835 g, 78 %).

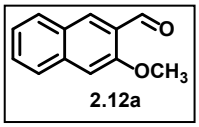

2.12a

^{1}H NMR ($CDCl_3$, 400 MHz): 10.56 (1H, s), 8.33 (1H, s), 7.85 (1H, d, *J* = 8.0 Hz), 7.72 (1H, s, *J* = 8.4 Hz), 7.55-7.51 (1H, m), 7.39-7.35 (1H, m), 7.16 (1H, s), 4.00 (3H, s).

^{13}C NMR ($CDCl_3$, 100 MHz): 190.2, 157.5, 137.4, 130.9, 129.8, 129.1, 127.6, 126.5, 125.5, 124.6, 106.3, 55.5.

(3-methoxynaphthalen-2-yl)(4-methoxyphenyl)methanol (2.13a). 4-Bromoanisole (2.442 g, 13 mmol) was dissolved in anhydrous diethyl ether (25 mL). Obtained solution was cooled to -78 ºC and n-BuLi (2.5 M in hexane, 4.80 mL, 12 mmol) was added dropwise. The mixture was allowed to react for 1 h at -78 ºC, then aldehyde **2.12a** (1.962 g, 10.6 mmol) in THF (20 mL) was added dropwise. The mixture was allowed to reach r.t. and was left overnight. The next day water (40 mL) was added, the product was extracted with ethyl acetate,

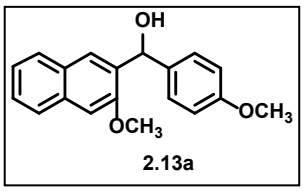

2.13a

washed with water, brine, and dried over Na_2SO_4. The product **2.13a** was isolated via column chromatography (EtOAc/Hexanes, 1:6) as pale yellow crystals (2.241 g, 69 %).

^{1}H NMR ($CDCl_3$, 400 MHz): 7.76-7.72 (3H, m), 7.45-7.43 (1H, m), 7.36-7.32 (3H, m), 7.14 (1H, s), 6.88-6.86 (2H, m), 6.11 (1H, d, *J* = 5.6 Hz), 3.90 (3H, s), 3.80 (3H, s), 3.04 (1H, d, *J* = 5.2 Hz).

^{13}C NMR ($CDCl_3$, 100 MHz): 158.8, 155.4, 135.1, 133.8, 133.4, 128.6, 128.0, 127.9, 126.8, 126.3, 123.9, 113.6, 105.6, 72.3, 55.4, 55.2.

HRMS (ESI), *m/z*: calcd. for $C_{19}H_{18}O_3Na$ $[M+Na]^+$ 317.1154, found 317.1149.

(3-methoxynaphthalen-2-yl)(4-methoxyphenyl)methanone (2.14a). Alcohol **2.13a** (2.111 g, 6.9 mmol) was dissolved in CH_2Cl_2 (200 mL), activated MnO_2 (12.3 g, 142 mmol) was added to the solution. The mixture was stirred at r.t. for 12 h, then precipitate was filtered off. The solvent was evaporated. The product **2.14a** was obtained as white crystals (2.080 g, 99 %). No purification was required.

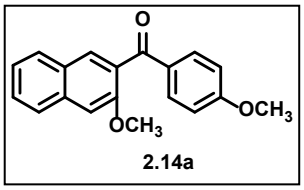

2.14a

M.p. = 88 ºC.

IR: 3674; 2988; 2900; 1645; 1600; 1582 cm^{-1}.

^{1}H NMR ($CDCl_3$, 400 MHz): 7.86-7.84 (2H, m), 7.80-7.78 (3H, m), 7.53-7.49 (1H, m), 7.41-7.37 (1H, m), 7.23 (1H, s), 6.92-6.90 (2H, m), 3.87 (3H, s), 3.86 (3H, s).

^{13}C NMR ($CDCl_3$, 100 MHz): 194.6, 163.6, 154.9, 135.1, 132.4, 130.9, 130.6, 129.1, 128.2, 127.9, 127.5, 126.6, 124.3, 113.5, 106.0, 55.6, 55.4.

HRMS (ESI), *m/z*: calcd. for $C_{19}H_{16}O_3H$ $[M+H]^+$ 293.1172, found 293.1175.

(3-hydroxynaphthalen-2-yl)(4-hydroxyphenyl)methanone (2.15a). A solution of ketone **2.14a** (1 g, 3.4 mmol) in CH_2Cl_2 (100 mL) was cooled to – 78 ºC, then BBr_3 (9.6 g, 3.7 mL, 39.1 mmol) was added dropwise. The reaction mixture was allowed to reach r.t. overnight. Water (40 mL) was added to the obtained solution, and obtained

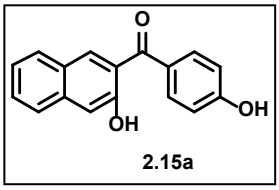

2.15a

precipitate was filtered off. Solution was extracted with EtOAc, washed with water, brine and dried over Na_2SO_4. The product **2.15a** was obtained as yellow crystals (897 mg, 99 %). No purification was required.

M.p. = 194 ºC.

IR: 3674; 3163 (broad); 2988; 2900; 1640; 1574; 1505; 1218; 899 cm^{-1}.

^1H NMR ($CDCl_3$, 400 MHz): 11.02 (1H, s), 8.18 (1H, s), 7.78-7.71 (4H, m), 7.55-7.51 (1H, m), 7.38 (1H, s), 7.35-7.31 (1H, m), 6.99-6.98 (2H, m), 5.62 (1H, s).

^{13}C NMR ($CDCl_3$, 100 MHz): 200.0, 159.6, 157.1, 137.6, 136.0, 132.5, 130.7, 129.5, 129.4, 126.7, 126.3, 124.0, 121.4, 115.3, 112.3.

HRMS (ESI), *m/z*: calcd. for $C_{17}H_{12}O_3H$ $[M+H]^+$ 265.0859, found 265.0860.

3-(hydroxy(4-hydroxyphenyl)methyl)naphthalen-2-ol (2.1a). The compound **2.15a** (100 mg, 0.38 mmol) was dissolved in anhydrous THF (15 mL), the solution was cooled to 0 ºC, and $LiAlH_4$ (38 mg, 1 mmol) was added. The reaction mixture was allowed to react for 1 h at r.t., then 2 mL of concentrated HCl was added and the product was extracted with EtOAc, washed with water, brine and dried over Na_2SO_4. Solvent was evaporated and the product **2.1a** was obtained as orange crystals (98 mg, 99 %). No purification was required.

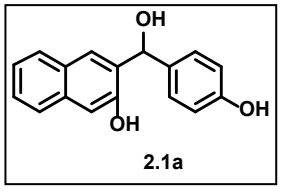

2.1a

The alcohol **2.1a** in neat was found to undergo decomposition (~5 % in a course of a week) at r.t. at white light. Decomposition rate was significantly reduced by storage of the compound **2.1a** in the dark at -10 ºC, resulting in ~2 % of decomposition in a course of a month according to ^1H NMR spectrum. However, decomposition of the compound was not observed upon storage as dilute solutions (1 mM) in non-nucleophilic solvents, such as acetonitrile and ethyl acetate, in the dark at -10 ºC.

M.p. = 83 ºC.

IR: 3675; 3292 (broad); 2988; 2901; 1698; 1599; 1507; 1224; 1032; 745 cm^{-1}.

^1H NMR (CD_3OD, 400 MHz): 7.79 (1H, s), 7.70 (1H, d, *J* = 8.0 Hz), 7.59 (2H, d, *J* = 8.0 Hz), 7.34-7.30 (1H, m), 7.24-7.21 (3H, m), 7.07 (1H, s), 6.74-6.71 (2H, m), 6.12 (1H, s), 4.63 (0.24H, s, broad).

^{13}C NMR (CD_3OD, 100 MHz): 157.6, 154.5, 136.0, 135.6, 134.6, 129.7, 129.5, 128.8, 127.1, 126.8, 126.7, 124.0, 116.0, 115.8, 110.1, 72.5.

HRMS (ESI), *m/z*: calcd. for $C_{17}H_{14}O_3$-H $[M-H]^-$ 265.0870, found 265.0867.

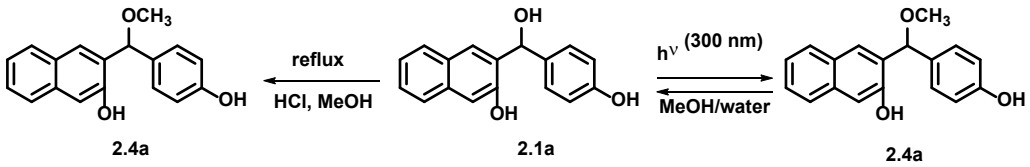

Scheme 2.4. Synthesis of compound **2.4a**.

3-((4-hydroxyphenyl)(methoxy)methyl)naphthalen-2-ol (2.4a).

"Dark" synthesis of **2.4a**.

Concentrated HCl (1 mL) was added to a solution of the compound **2.1a** (100 mg, 0.376 mmol) in methanol (10 mL). The reaction mixture was refluxed for 1 h, then cooled to r.t. and poured on ice. The mixture was extracted with EtOAc and washed with water and brine, then dried over Na_2SO_4. According to TLC, there were starting material and expected product **2.4a** present. Concentration of obtained solution resulted in partial decomposition. Isolation of the compound **2.4a** was attempted via column chromatography, however, total decomposition of **2.4a** was observed.

Photochemical synthesis of **2.4a***.*

The compound **2.1a** (100 mg, 0.376 mmol) was dissolved in methanol/water, 8:2 (380 mL) and irradiated in quartz reactor in Rayonet photoreactor equipped with fifteen 4W 300 nm fluorescent lamps for 35 min. Reaction progress was monitored by HPLC, and at 35 min of irradiation conversion of 80 % was achieved. Partial decomposition occurred upon concentration of the solution under vacuum. The mixture was extracted with EtOAc and washed with water and brine, then dried over Na_2SO_4. Concentration of obtained solution resulted in further decomposition. Isolation of the compound **2.4a** was attempted via column chromatography, however, total decomposition of **2.4a** was observed.

HRMS (ESI) spectra were obtained prior concentration of the reaction mixture.

HRMS (ESI) of **2.1a**, *m/z*: calcd. for $C_{17}H_{14}O_3$-H $[M-H]^-$ 265.0870, found 265.0867.

HRMS (ESI) of **2.4a**, *m/z*: calcd. for $C_{18}H_{16}O_3$-H $[M-H]^-$ 279.1027, found 279.1026.

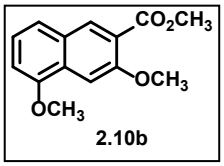

2.10b

Methyl 3,5-dimethoxy-2-naphthoate (2.10b). 3,5-Dihydroxynaphthoic acid **2.9b** (10.0 g, 49 mmol) and K_2CO_3 (33.95 g, 246 mmol) were mixed with acetone (250 mL). Me_2SO_4 (14.0 mL, 18.522 g, 147 mmol) was added dropwise, then reaction mixture was refluxed for 12 h. The reaction mixture was filtrated from salt, acetone was evaporated and the residue was dissolved in CH_2Cl_2. Obtained solution was washed with water, brine and dried over Na_2SO_4. The product **2.10b** was purified via column chromatography (EtOAc/Hexanes, 1:6) and was isolated as white crystals (8.2 g, 68 %).

^{1}H NMR ($CDCl_3$, 400 MHz): 8.27 (1H, s), 7.61 (1H, s), 7.40 (1H, d, *J* = 8.0 Hz), 7.29 (1H, t, *J* = 8.0 Hz), 6.85 (1H, d, *J* = 8.0 Hz), 4.02 (3H, s), 4.00 (3H, s), 3.95 (3H, s).

^{13}C NMR ($CDCl_3$, 100 MHz): 166.7, 155.4, 154.0, 132.3, 128.3, 128.0, 124.2, 121.8, 120.7, 105.9, 101.4, 56.0, 55.4, 52.2.

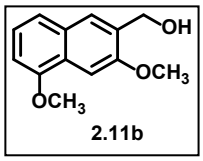

2.11b

(3,5-dimethoxynaphthalen-2-yl)methanol (2.11b). Methyl 3,5-dimethoxy-2-naphthanoate **2.10b** (6.63 g, 27 mmol) was dissolved in anhydrous THF (300 mL), the solution was cooled to 0 ºC, and $LiAlH_4$ (6.6 g, 179 mmol) was added in small portions. The reaction mixture was allowed to react for 2 h at r.t., then 0.1 M solution of HCl was added and the product was extracted with EtOAc, washed with water, brine and dried over Na_2SO_4. Solvent was evaporated and the product was obtained as white solid (5.474 g, 93 %). No purification was required.

^{1}H NMR ($CDCl_3$, 400 MHz): 7.70 (1H, s), 7.55 (1H, s), 7.38 (1H, d, *J* = 8.0 Hz), 7.30-7.27 (1H, m), 6.82 (1H, d, *J* = 7.6 Hz), 4.84 (2H, s), 4.02 (3H, s), 4.01 (3H, s).

^{13}C NMR ($CDCl_3$, 100 MHz): 155.6, 154.3, 130.7, 129.6, 127.2, 125.8, 123.7, 120.0, 104.3, 99.8, 62.5, 55.4, 55.4.

3,5-dimethoxy-2-naphthaldehyde (2.12b). PCC (10 g, 38.6 mmol) was slowly added to 0 °C solution of alcohol **2.11b** (5.474 g, 25 mmol) and sodium acetate (3.2 g, 38.6 mmol) in DCM (300 mL). When addition was finished, the reaction mixture was left at r.t. overnight. The next day DCM was evaporated, and the residue was purified via column chromatography (DCM/Hexanes, 1:1). The product was obtained as yellow crystals (5.065 g, 94 %).

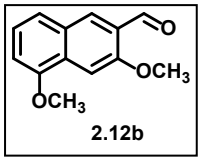

2.12b

^{1}H NMR ($CDCl_3$, 400 MHz): 10.58 (1H, s), 8.30 (1H, s), 7.59 (1H, s), 7.46 (1H, d, *J* = 8.4 Hz), 7.29 (1H, t, *J* = 8.0 Hz), 6.88 (1H, d, *J* = 7.6 Hz), 4.03 (3H, s), 4.01 (3H, s).

^{13}C NMR ($CDCl_3$, 100 MHz): 190.4, 157.4, 154.1, 130.4, 129.5, 128.6, 125.7, 124.4, 121.9, 106.7, 101.1, 55.7, 55.5.

(3,5-dimethoxynaphthalen-2-yl)(4-methoxyphenyl)methanol (2.13b). 4-Bromoanisole (2.442 g, 13 mmol) was dissolved in anhydrous diethyl ether (75 mL). Obtained solution was cooled to -78 ºC and n-BuLi (2.5 M in hexane, 5.75 mL, 14.4 mmol) was added dropwise. The mixture was allowed to react for 1 h at -78 ºC, then aldehyde **2.12b** (2.562 g, 11.9 mmol) in THF (75 mL) was added dropwise. The mixture was allowed to reach r.t. and was left overnight. The next day water (40 mL) was added, the product was extracted with ethyl acetate, washed with water, brine, and dried over Na_2SO_4. The product was isolated via column chromatography (EtOAc/Hexanes, 1:6) as pale yellow crystals (3.266 g, 85 %).

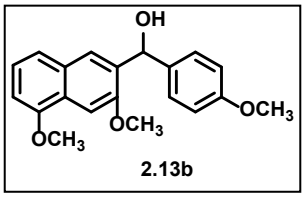

2.13b

^{1}H NMR ($CDCl_3$, 400 MHz): 7.70 (1H, s), 7.55 (1H, s), 7.37-7.32 (3H, m), 7.29-7.25 (1H, m); 6.89-6.85 (2H, m); 6.82 (1H, d, *J* = 7.6 Hz), 6.12 (1H, s), 4.00 (3H, s), 3.92 (3H, s), 3.80 (3H, s), 3.18 (1H, s, broad).

^{13}C NMR ($CDCl_3$, 100 MHz): 158.7, 155.1, 154.2, 135.2, 133.6, 129.5, 128.0, 126.5, 125.7, 125.6, 123.7, 120.2, 113.5, 104.2, 100.3, 72.2, 55.5, 55.4, 55.2.

HRMS (ESI), *m/z*: calcd. for $C_{20}H_{20}O_4$* $[M^*]^+$ 324.1356, found 324.1355.

(3,5-dimethoxynaphthalen-2-yl)(4-methoxyphenyl)methanone (2.14b).

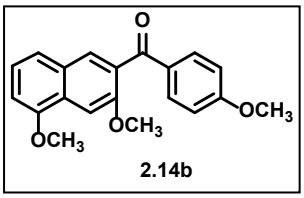

2.14b

Alcohol **2.13b** (3.0 g, 9 mmol) was dissolved in DCM (150 mL), activated MnO_2 (16.0 g, 184 mmol) was added to the solution. The mixture was stirred at r.t. for 12 h, then precipitate was filtered off. The solvent was evaporated. The product **2.14b** was obtained as white crystals (2.976 g, 99 %). No purification was required.

M.p. = 118 ºC.

IR: 3675; 2972; 2901; 1651; 1598; 1574; 1224; 851 cm^{-1}.

^1H NMR ($CDCl_3$, 400 MHz): 7.84 (2H, d, *J* = 8.4 Hz), 7.75 (1H, s), 7.63 (1H, s), 7.39 (2H, d, *J* = 8.4 Hz), 7.32-7.28 (1H, m), 6.92-6.87 (3H, m), 4.04 (3H, s), 3.87 (3H, s), 3.86 (3H, s).

^{13}C NMR ($CDCl_3$, 100 MHz): 194.8, 163.6, 154.7, 154.3, 132.4, 131.1, 130.6, 128.8, 128.7, 127.0, 124.2, 120.4, 113.5, 105.2, 100.7, 55.7, 55.5, 55.4.

HRMS (ESI), *m/z*: calcd. for $C_{20}H_{18}O_4H$ $[M+H]^+$ 323.1278, found 323.1279.

(3,5-dihydroxynaphthalen-2-yl)(4-hydroxyphenyl)methanone (2.15b).

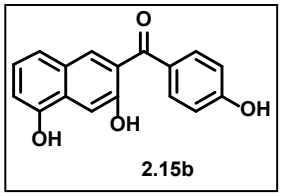

2.15b

A solution of **2.14b** (1.0 g, 3.1 mmol) in CH_2Cl_2 (60 mL) was cooled to – 78 ºC, then BBr_3 (14.5 g, 5.3 mL, 59.1 mmol) in CH_2Cl_2 (60 mL) was added dropwise. The reaction mixture was allowed to reach r.t. overnight. Water (100 mL) was added to the obtained solution and the mixture was stirred at r.t. for 3 h. Compound was extracted with CH_2Cl_2/MeOH (6:1), washed with water, brine and dried over Na_2SO_4. The product **2.15b** was obtained as yellow crystals (850 mg, 98 %). No purification was required.

M.p. = 242 ºC.

IR: 3675; 3224 (broad); 2971; 2900; 1640; 1602; 1509; 1221; 745 cm^{-1}.

^1H NMR (CD_3OD, 400 MHz): 7.91 (1H, s), 7.75-7.71 (2H, m), 7.60 (1H, s); 7.27 (1H, d, *J* = 8.0 Hz), 7.13-7.10 (1H, t, *J* = 8.0 Hz), 6.93-6.89 (2H, m), 6.84 (1H, d, *J* = 7.2 Hz).

^{13}C NMR (CD_3OD, 100 MHz): 199.8, 163.8, 155.3, 153.0, 133.8, 133.6, 130.5, 129.8, 129.5, 126.6, 125.2, 121.0, 116.2, 111.0, 107.1.

HRMS (ESI), *m/z*: calcd. for $C_{17}H_{12}O_3H$ $[M+H]^+$ 265.0859, found 265.0860.

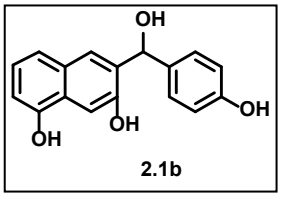

2.1b

6-(hydroxy(4-hydroxyphenyl)methyl)naphthalene-1,7-diol (2.1b). The compound **2.15b** (107 mg, 0.38 mmol) was dissolved in anhydrous THF (15 mL), the solution was cooled to 0 ºC, and $LiAlH_4$ (38 mg, 1 mmol) was added. The reaction mixture was allowed to react for 1 h at r.t., then 2 mL of concentrated HCl was added and the product was extracted with EtOAc, washed with water, brine and dried over Na_2SO_4. Solvent was evaporated and the product **2.1b** was obtained as orange glass (106 mg, 99 %). No purification was required.

The alcohol **2.1b** in neat was found to undergo relatively rapid decomposition (~10 % in a course of a week) at r.t. under white light. Decomposition rate was significantly reduced by storage of the compound **2.1b** in the dark at -10 ºC, resulting in ~2-5 % of decomposition in a course of a month according to ^{1}H NMR spectrum. However, decomposition of the compound was not observed upon storage as dilute solutions (1 mM) in non-nucleophilic solvents, such as acetonitrile and ethyl acetate, in the dark at -10 ºC.

IR: 3675; 3223 (broad); 2988; 2901; 1645; 1601; 1509; 1220; 742 cm^{-1}.

^{1}H and ^{13}C NMR spectra in the presence of ethyl acetate (spectra were recorded immediately after preparation):

^{1}H NMR (CD_3OD, 400 MHz): 7.71 (1H, s), 7.42 (1H, s), 7.25-7.20 (3H, m), 7.06-7.02 (1H, m), 6.74-6.69 (3H, m), 6.11 (1H, s).

^{13}C NMR (CD_3OD, 100 MHz): 157.6, 153.6, 152.9, 136.1, 134.6, 133.6, 131.1, 129.9, 129.5, 126.9, 126.8, 124.1, 120.1, 115.8, 108.7, 105.1, 72.5.

HRMS (ESI), *m/z*: calcd. for $C_{17}H_{14}O_4$-H $[M-H]^-$ 281.0814, found 281.0817.

Alcohol **2.1b** was found to undergo nucleophilic attack by methanol when kept as dilute solutions (5 mM) in methanol and methanol-d_4 at r.t. under white light.

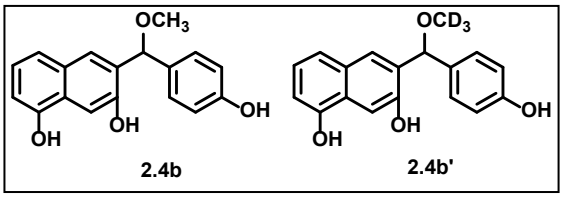

According to ^{1}H NMR spectra, ~17 % of the compound **2.1b** was converted into corresponding methoxy-derivates **2.4b** and **2.4b'** in 24 h. Prolonged storage of the solutions resulted in decomposition of **2.1b** and **2.4b**, **2.4b'**, however, the ratio between residual hydroxy-form **2.1b** and corresponding methoxy-forms **2.4b**, **2.4b'** stayed unchanged.

^{1}H and ^{13}C NMR spectra in the presence of methanol:

^{1}H NMR (CD_3OD, 400 MHz): 7.71 (1H, s, **2.1b**), 7.68 (0.2H, s, **2.4b**), 7.43 (0.2H, s, **2.4b**), 7.42 (1H, s, **2.1b**), 7.25-7.20 (3H, m, **2.1b** and 0.6H, m, **2.4b**), 7.06-7.02 (1H, m, **2.1b** and 0.2H, m, **2.4b**), 6.74-6.68 (3H, m, **2.1b** and 0.6H, m, **2.4b**), 6.11 (1H, s, **2.1b**), 5.68 (0.2H, s, **2.4b**), 3.40 (0.6H, s, **2.4b**).

^{13}C NMR (CD_3OD, 100 MHz): 157.8 (**2.4b**), 157.6 (**2.1b**), 153.8 (**2.4b**), 153.6 (**2.1b**), 152.9, 136.1, 134.6, 133.6, 132.3, 131.1, 130.1, 130.0, 129.9, 129.5, 126.9, 126.9, 126.8, 124.1, 120.1, 118.1, 115.8, 108.7, 105.1, 81.5 (**2.4b**), 72.5 (**2.1b**), 57.2 (**2.4b**).

HRMS (ESI), *m/z* (**2.4b**): calcd. for $C_{18}H_{16}O_4$-H $[M-H]^-$ 295.0976, found 295.0972.

^{1}H NMR spectrum in the presence of ethyl acetate in methanol-d_4 (spectrum was recorded in 24 h after preparation):

^{1}H NMR (CD_3OD, 400 MHz): 7.71 (1H, s, **2.1b**), 7.68 (0.2H, s, **2.4b'**), 7.43 (0.2H, s, **2.4b'**), 7.42 (1H, s, **2.4b**), 7.25-7.20 (3H, m, **2.1b** and 0.6H, m, **2.4b'**), 7.06-7.02 (1H, m, **2.1b** and 0.2H, m, **2.4b'**), 6.74-6.68 (3H, m, **2.1b** and 0.6H, m, **2.4b'**), 6.11 (1H, s, **2.1b**), 5.68 (0.2H, s, **2.4b'**), 4.63 (0.7H, s, broad).

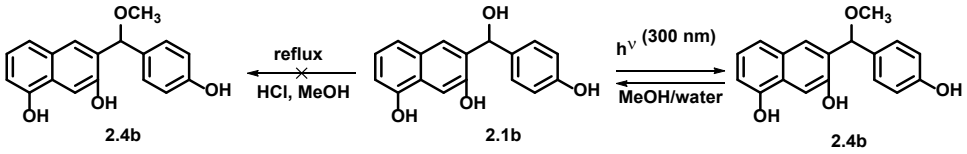

Scheme 2.5. Synthesis of compound **2.4b**.

6-((4-hydroxyphenyl)(methoxy)methyl)naphthalene-1,7-diol (2.4b).

"Dark" synthesis of **2.4b**.

Concentrated HCl (1 mL) was added to a solution of the compound **2.1b** (100 mg, 0.355 mmol) in methanol (10 mL). The reaction mixture was refluxed for 1 h; darkening of the solution has been observed. Then reaction mixture was cooled to r.t. and was poured on ice. Extraction was performed with EtOAc. According to TLC, there were no starting material and expected product **2.4b** present, but only polymerization/decomposition was observed.

Photochemical synthesis of **2.4b***.*

The compound **2.1b** (100 mg, 0.355 mmol) was dissolved in methanol/water, 8:2 (350 mL) and irradiated in quartz reactor in Rayonet photoreactor equipped with fifteen 4W 300 nm fluorescent lamps for 35 min. Reaction progress was monitored by HPLC, and at 35 min of irradiation conversion of 80 % was achieved. Partial decomposition occurred upon concentration of the solution under vacuum. The mixture was extracted with EtOAc and washed with water and brine, then dried over Na_2SO_4. Concentration of obtained solution resulted in further decomposition. Isolation of the compound **2.4b** was attempted via column chromatography, however, total decomposition of **2.4b** was observed.

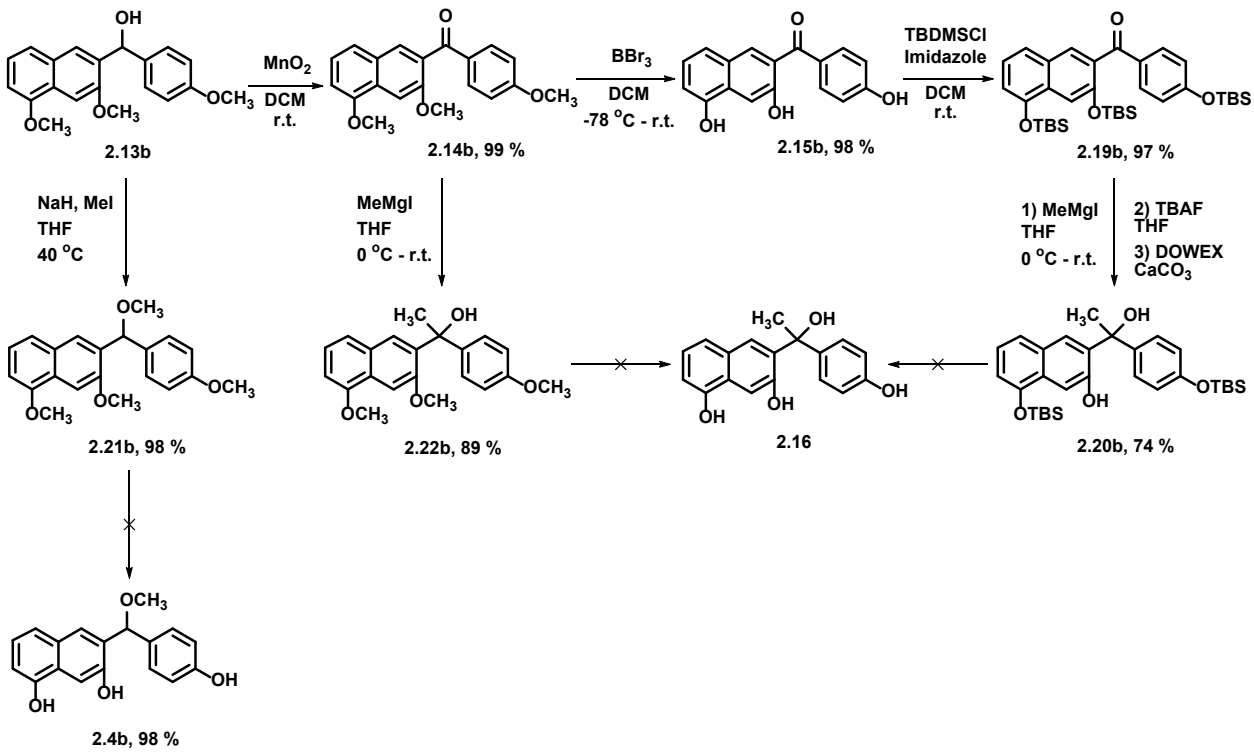

Scheme 2.6. Attempted synthesis of compounds **2.4b** and **2.16**.

1,7-dimethoxy-6-(methoxy(4-methoxyphenyl)methyl)naphthalene (2.21b).

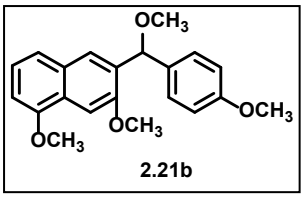

Alcohol **2.13b** (500 mg, 1.48 mmol) was dissolved in THF (50 mL), NaH (89 mg, 2.22 mmol) was added to the solution at r.t. The mixture was stirred at 40 ºC for 1 h, then iodomethane (420 mg, 0.18 mL, 2.96 mmol) was added and the reaction mixture was left at 40 ºC overnight. Reaction mixture was quenched with water, extracted with ethyl acetate. The organic layer was washed with water, brine and dried over Na_2SO_4. The product **10b** was purified via column chromatography (EtOAc/Hexanes, 1:6) and isolated as yellow crystals (508 mg, 98 %).

M.p. = 91 ºC.

IR: 2961; 2926; 1603; 1582; 1461; 1260; 1025; 732 cm^{-1}.

^1H NMR ($CDCl_3$, 400 MHz): 8.06 (1H, s), 7.60 (1H, s), 7.51 (1H, d, *J* = 8.0 Hz), 7.42 (2H, d, *J* = 8.0 Hz), 7.34-7.30 (1H, m), 6.90 (2H, d, *J* = 8.0 Hz), 6.83 1H, d, *J* = 7.6 Hz), 5.80 (1H, s), 4.02 (3H, s), 3.95 (3H, s), 3.80 (3H, s), 3.52 (3H, s).

^{13}C NMR ($CDCl_3$, 100 MHz): 158.7, 154.9, 154.2, 133.7, 132.4, 129.6, 128.6, 125.5, 125.1, 123.4, 120.2, 113.4, 103.9, 99.8, 79.0, 56.9, 55.3, 55.3, 55.0.

HRMS (ESI), *m/z*: calcd. for $C_{21}H_{22}O_4Na$ $[M+Na]^+$ 361.1410, found 361.1410.

1-(3,5-dimethoxynaphthalen-2-yl)-1-(4-methoxyphenyl)ethan-1-ol (2.22b).

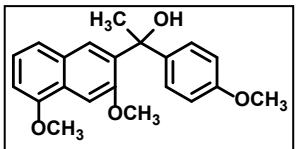

11b

Ketone **2.14b** (350 mg, 1.04 mmol) was dissolved in THF (3 mL) was added to the solution of MeMgI (0.55 mL, prepared from 1 g of Mg turnips, 2.7 mL of iodomethane in 6 mL of ether) at 0 ºC. The mixture was stirred at r.t. for 5 h, then water was added. The organic layer was washed with water, brine and dried over Na_2SO_4. The product **2.22b** was purified via column chromatography (EtOAc/Hexanes, 1:6) and isolated as yellow crystals (312 mg, 89 %).

M.p. = 51 ºC.

IR: 3533 (broad); 2971; 2901; 1600; 1581; 1507; 1462; 1246; 1029; 734 cm^{-1}.

^{1}H NMR ($CDCl_3$, 400 MHz): 7.83 (1H, s), 7.56 (1H, s), 7.43 (1H, d, *J* = 8.4 Hz), 7.34-7.30 (1H, m), 7.24-7.22 (2H, m), 6.83 (1H, d, *J* = 7.6 Hz), 6.80-6.77 (1H, m), 4.67 (1H, s), 4.00 (3H, s), 3.78 (3H, s), 3.76 (3H, s), 1.95 (3H, s).

^{13}C NMR ($CDCl_3$, 100 MHz): 158.0, 155.5, 154.2. 141.5, 136.1, 129.4, 126.0, 126.0, 125.5, 124.1, 120.3, 113.0, 104.4, 101.8, 76.1, 55.7, 55.5, 55.1, 30.3.

HRMS (ESI), *m/z*: calcd. for $C_{21}H_{22}O_4$* $[M^*]^+$ 338.1513, found 338.1514.

Attempts to deprotect methyl-protected hydroxyls in compounds **2.13a**, **2.13b**, **2.21b** and **2.22b** under acidic conditions (excess of BBr_3 in DCM) and under nucleophilic conditions (excess of 2-aminoethanethiol and sodium *t*-butylate in anhydrous DMF) were unsuccessful. Decomposition of starting materials was observed under acidic conditions, however, no reaction happened under nucleophilic conditions in a course of a week.

(3,5-bis((tert-butyldimethylsilyl)oxy)naphthalen-2-yl)(4-((tert-butyldimethylsilyl)oxy)phenyl)methanone (2.19b). Ketone **2.15b** (200 mg, 0.71 mmol), TBDMSCl (433 mg, 2.856 mmol) and imidazole (420 mg, 6.12 mmol) were dissolved in DMF (15 mL). The mixture was stirred at r.t. overnight, then water was added. The product **2.19b** was extracted with CH_2Cl_2, washed with water, brine and dried over Na_2SO_4. The compound was purified via column chromatography (Hexanes/EtOAc, 100:1). Silica gel was first worked up with Et_3N. The product **2.19b** was obtained as a yellow oil (430 mg, 97 %).

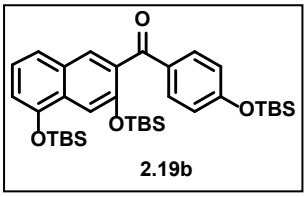

2.19b

IR: 2929; 1662; 1593; 1456; 1246; 756 cm^{-1}.

^1H NMR (CD_3OD, 400 MHz): 7.77-7.73 (3H, m), 7.59 (1H, s), 7.45 (1H, d, *J* = 8.4 Hz), 7.25 (1H, t, J = 8.4 Hz), 6.94-6.92 (1H, m), 6.92-6.89 (2H, m), 1.12 (9H, s), 0.99 (9H, s), 0.71 (9H, s), 0.34 (6H, s), 0.23 (6H, s), 0.16 (6H, s).

^{13}C NMR (CD_3OD, 100 MHz): 197.6, 162.2, 151.6, 151.2, 134.9, 133.6, 132.4, 131.5, 130.7, 130.1, 125.8, 122.4, 121.1, 114.9, 110.3, 26.5, 26.1, 25.9, 19.3, 19.1, 18.8, -4.1, -4.3.

HRMS (ESI), *m/z*: calcd. for $C_{35}H_{54}O_4Si_3H$ $[M+H]^+$ 623.3403, found 623.3407.

8-((tert-butyldimethylsilyl)oxy)-3-(1-(4-((tert-butyldimethylsilyl)oxy)phenyl)-1-hydroxyethyl)naphthalen-2-ol (2.20b). Ketone **2.19b** (285 mg, 0.46 mmol) was dissolved in THF (3 mL) was added to the solution of MeMgI (prepared from 1 g of Mg turnips, 2.7 mL of iodomethane in 6 mL of ether) at 0 ºC. The mixture was stirred at 40 ºC for 2 days, then water was added. Compound was extracted with ether. The organic layer was washed with water, brine and dried over Na_2SO_4. The product was purified via column chromatography (Hexanes/EtOAc, 100:1). Silica gel was first worked up with Et_3N. Product was obtained as a colorless oil (182 mg). Obtained compound was dissolved in THF (5 mL) and excess of TBAF (1M solution in THF, 8.2 mL, 8.2 mmol) was added. Solution was stirred at r.t. for 1 h, then ion-exchange resin Dowex (1 g) and

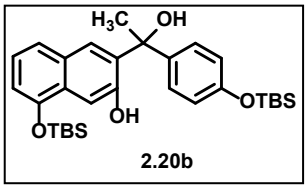

2.20b

$CaCO_3$ (1 g, 10 mmol) were added. The salts were filtered off, and the filtrate was evaporated. The product **2.20b** was obtained as a colorless oil (179 mg, 74 %).

IR: 2954; 2929; 2857; 1505; 1251; 834; 777 cm^{-1}.

^1H NMR (DMSO-d_6, 400 MHz): 9.85 (1H, s), 7.89 (1H, s), 7.41-7.39 (1H, dd, *J* = 8.0 and 0.8 Hz), 7.29 (1H, s), 7.24-7.22 (2H, dd, *J* = 7.6 and 1.6 Hz), 7.15-7.11 (1H, dd, m), 6.81-6.79 (1H, dd, *J* = 8.0 and 0.8 Hz), 6.73-6.71 (2H, dd, *J* = 7.6 and 1.6 Hz), 6.33 (1H, s), 1.93 (3H, s), 1.03 (9H, s), 0.91 (9H, s), 0.24 (6H, s), 0.15 (6H, s).

^{13}C NMR (DMSO-d_6, 100 MHz): 153.6, 153.4, 149.3, 140.8, 136.2, 129.1, 127.9, 127.0, 125.6, 123.0, 121.1, 118.8, 112.4, 105.1, 75.5, 29.4, 25.8, 25.6, 18.2, 18.0, -4.3, -4.4.

HRMS (ESI), *m/z*: calcd. for $C_{30}H_{44}O_4Si_2$-H $[M-H]^-$ 523.2700, found 523.2700.

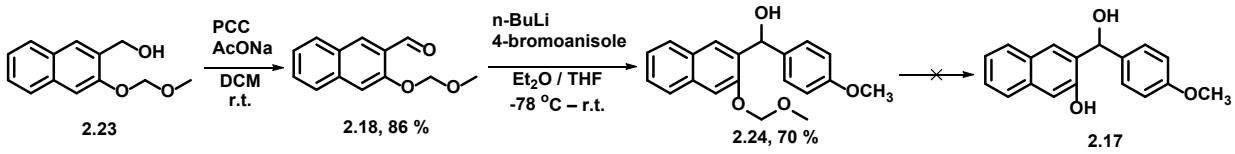

Scheme 2.7. Attempted synthesis of compound **2.17**.

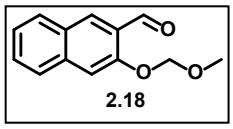

3-(methoxymethoxy)-2-naphthaldehyde (2.18). PCC (8.806 g, 34 mmol) was slowly added to 0 °C solution of alcohol **2.23** (5.0 g, 23 mmol), sodium acetate (2.788 g, 34 mmol), and molecular sieves Grade 564 8-12 mesh (0.5 g) in DCM (60 mL). When addition was finished, the reaction mixture was left at r.t. overnight. The next day the mixture was filtered through the plug of silica gel (~ 15 cm), washed with DCM, and fractions of about 50 mL were collected. The fractions with the product were combined, and solvent was evaporated to produce aldehyde **2.18** (4.3 g, 86 %) as white crystals.

^1H NMR ($CDCl_3$, 400 MHz): 10.61 (1H, s); 8.38 (1H, s); 7.87 (1H, d, *J* = 8.4 Hz); 7.74 (1H, d, *J* = 8.0 Hz); 7.55-7.51 (1H, m); 7.48 (1H, s); 7.41-7.37 (1H, m), 5.41 (2H, s); 3.57 (3H, s).

^{13}C NMR ($CDCl_3$, 100 MHz): 190.1, 155.0, 137.3, 130.6, 129.8, 129.1, 128.2, 126.9, 125.7, 125.0, 110,1, 94.7, 56.4.

(3-(methoxymethoxy)naphthalen-2-yl)(4-methoxyphenyl)methanol (2.24).

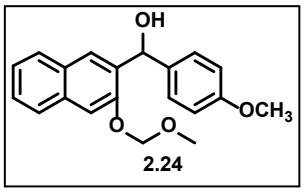

4-Bromoanisole (568 mg, 3.04 mmol) was dissolved in anhydrous THF (5 mL). Obtained solution was cooled to -78 ºC and n-BuLi (2.5 M in hexane, 1.22 mL, 3.04 mmol) was added dropwise. The mixture was allowed to react for 40 minutes at -78 ºC, then aldehyde **2.18** (500 mg, 1.9 mmol) in THF (5 mL) was added dropwise. The mixture was allowed to reach r.t. and was left overnight. The next day water (10 mL) was added, the product was extracted with ethyl acetate, washed with water, brine, and dried over Na_2SO_4. The product **2.24** was isolated via column chromatography (EtOAc/Hexanes, 1:6) as a colorless oil (431 mg, 70 %).

^{1}H NMR ($CDCl_3$, 400 MHz):7.87 (1H, s), 7.78 (1H, d, *J* = 8.0 Hz), 7.20 (1H, d, *J* = 8.0 Hz), 7.45-7.41 (1H, m), 7.39-7.31 (4H, m), 6.85 (2H, d, *J* = 8.0 Hz), 6.12 (1H, d, *J* = 5.2 Hz), 5.25-5.20 (2H, dd, *J* = 8.0 and 6.8 Hz), 3.79 (3H, s), 3.28 (3H, s), 2.85 (1H, d, *J* = 5.6 Hz).

^{13}C NMR ($CDCl_3$, 100 MHz): 158.9, 152.5, 135.5, 133.7, 133.5, 129.1, 128.1, 127.8, 126.6, 126.6, 126.3, 124.3, 113.6, 109.1, 94.1, 72.4, 56.1, 55.3.

Attempts to deprotect methoxymethyl-protected hydroxyl in compound **2.24** with Amberlyst-15H, TFA and HCl under various conditions were unsuccessful. Reaction progress was monitored by TLC for up to 24 h. Attempted conditions to synthesize the compound **2.17** are summarized in Table 2.2.

Table 2.2. Attempted conditions of deprotection of MOM-group in **2.24**.

Deprotecting reagent	**Solvent**	**Temperature, ºC**
Amberlyst-15H (1 g per 3 mmol, and 1 g per 1 mmol)	THF/water, 9:1	r.t.
	THF/water, 9:1	40 ºC
	THF/water, 9:1	reflux
	Methanol	r.t.
	Methanol	40 ºC
	Methanol	reflux
HCl (5 %, 10 %)	THF/water	r.t.
	THF/water	reflux
TFA (1 %, 5 %, 10 %)	DCM	r.t.

2.8.3. Properties of QMPs 2.1a and 2.1b

2.8.3.1. Determination of Extinction Coefficient of QMPs 2.1a and 2.1b

Determination of extinction coefficient of 2.1a. Three sets of solutions of **2.1a** at various concentrations in acetonitrile were prepared and their UV-spectra were recorded in 3 mL quartz cuvette. Several major absorption bands were found to have maximal absorbance at 230 nm, 275 nm, and 330 nm. Plotting absorbance values at certain wavelength vs. concentration (M) gave a slope that equaled to extinction coefficient (Figure 2.6).

$\log\varepsilon_{230} = 5.13$; $\log\varepsilon_{275} = 4.15$ and $\log\varepsilon_{330} = 3.76$.

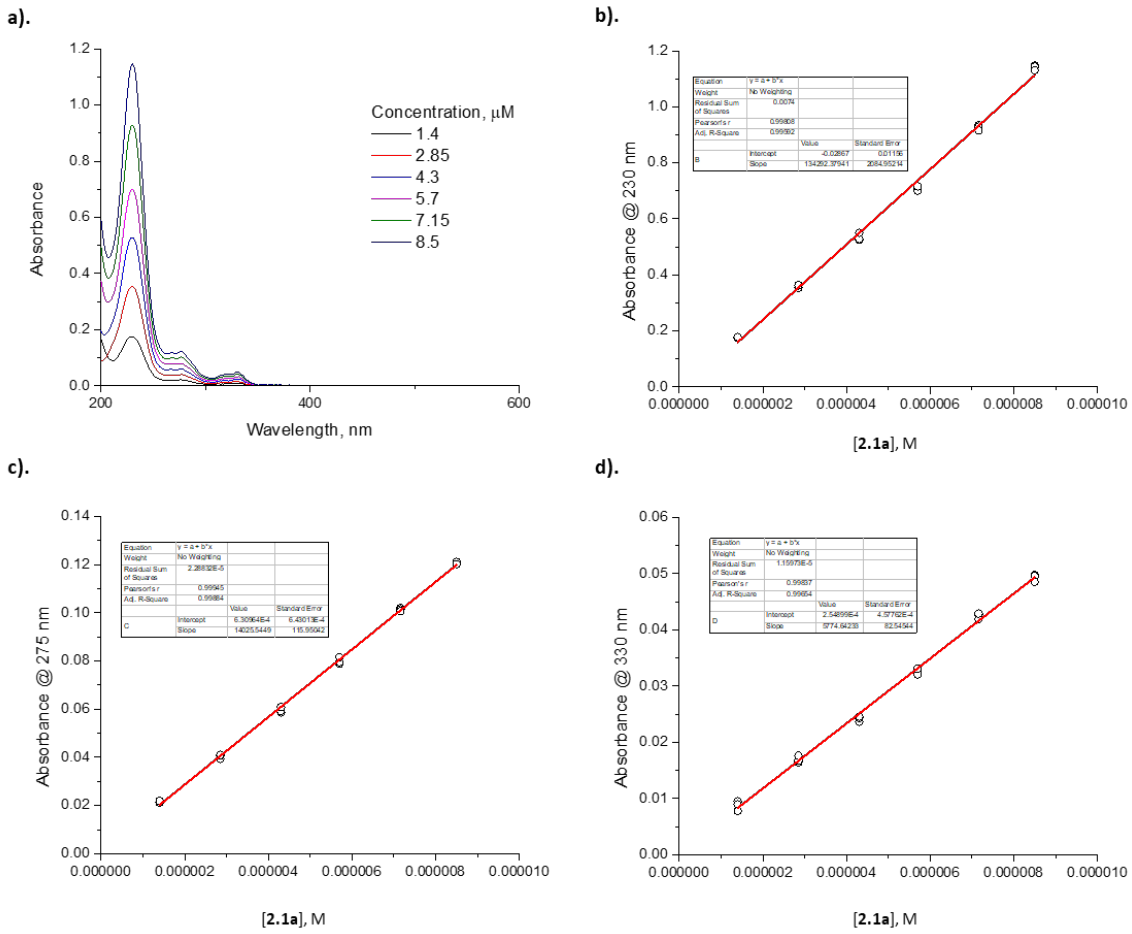

Figure 2.6. Determination of extinction coefficient of **2.1a**. **a).** UV-spectra of **2.1a** in acetonitrile at various concentrations. **b).** Absorbance values at 230 nm vs. concentration of **2.1a** (M). **c).** Absorbance values at 275 nm vs. concentration of **2.1a** (M). **d).** Absorbance values at 330 nm vs. concentration of **2.1a** (M).

Determination of extinction coefficient of 2.1b. Three sets of solutions of **2.1b** at various concentrations in acetonitrile were prepared and their UV-spectra were recorded in 3 mL quartz cuvette. Several major absorbance bands were found to have maximal absorbance at 220 nm, 248 nm, 280 nm, and 335 nm. Plotting absorbance values at certain wavelength vs. concentration (M) gave a slope that equaled to extinction coefficient (Figure 2.7).

$\log\varepsilon_{220} = 5.05$; $\log\varepsilon_{248} = 5.01$; $\log\varepsilon_{280} = 4.24$ and $\log\varepsilon_{335} = 3.82$.

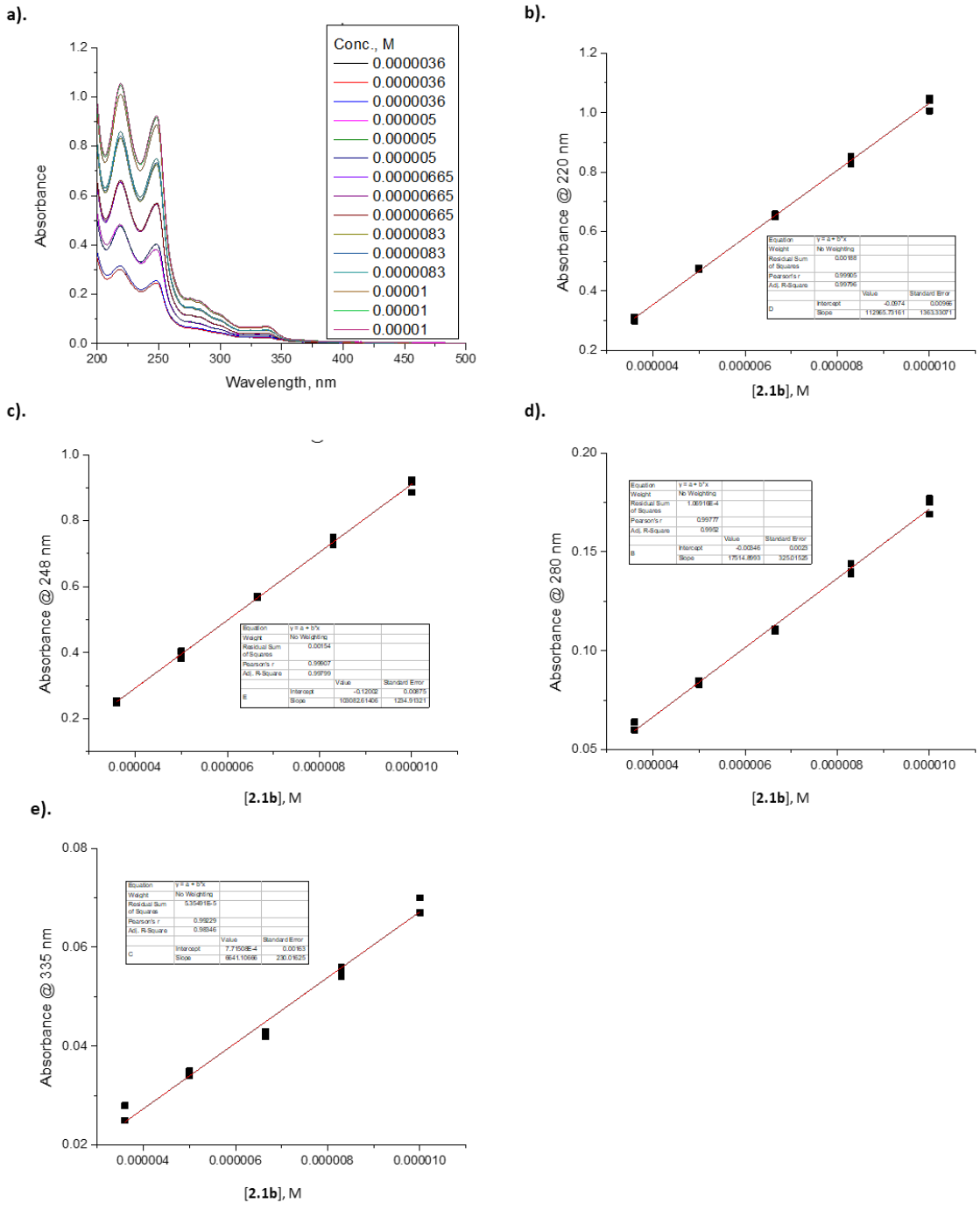

Figure 2.7. Determination of extinction coefficient of **2.1b**. **a).** UV-spectra of **2.1b** in acetonitrile at various concentrations. **b).** Absorbance values at 220 nm vs. concentration of **2.1b** (M). **c).** Absorbance values at 248 nm vs. concentration of **2.1b** (M). **d).** Absorbance values at 280 nm vs. concentration of **2.1b** (M). **e).** Absorbance values at 335 nm vs. concentration of **2.1b** (M).

2.8.3.2. Fluorescence Properties of 2.1a and 2.1b

Solutions of quinine sulfate (standard) in 0.5 M aq. H_2SO_4, **2.1a** in acetonitrile and **2.1b** in acetonitrile were prepared at various concentrations and their absorbance spectra were collected (Figure 2.). Absorbance values of all prepared solutions were below 0.1 a.u. at 305 nm.

Fluorescence spectra of obtained solutions were recorded in a range of 300-900 nm, excitation wavelength was 305 nm. Area of fluorescence intensity was recorded. Experiments were performed in triplicate (Figure 2.8). Plotting area of fluorescence intensity vs. absorbance value at 305 nm gave a slope – gradient of the plot *m* (Eq. 2.2).

Eq. 2.2

$$\Phi_{\mathbf{fl-sample}} = \Phi_{\mathbf{fl-standard}} \left(\frac{\mathbf{m_{sample}}}{\mathbf{m_{standard}}}\right)$$

Table 2.3. Calibration of quinine sulfate: absorbance vs. area of fluorescence intensity.

Quinine sulfate			
Abs. @ 305 nm	**Area of fluorescence intensity**		
0.003	23676.08	23152.13	23334.88
0.009	55340.25	56531.21	57290.05
0.019	129917.4	130489.5	131186.9
0.033	241730	249392.5	251808.6
0.048	368189.7	368949.2	370104.3
0.065	473827.8	476359	478426.4

$\Phi_{fl\text{-}standard}$=0.546±0.02

Table 2.4. Calibration of **2.1a**: absorbance vs. area of fluorescence intensity.

2.1a			
Abs. @ 305 nm	**Area of fluorescence intensity**		
0.005	23482.65	23407.54	23453.93
0.013	39132.31	39246.13	39298.74
0.024	66061.83	66201.93	66856.42
0.038	119966.3	119510.6	119660
0.051	160692.6	164307.3	165650.7
0.083	245569.9	246799.9	248529.3

Φ_{fl}=0.22±0.01, λ_{max}=358 nm

Table 2.5. Calibration of **2.1b**: absorbance vs. area of fluorescence intensity.

2.1b			
Abs. @ 305 nm	**Area of fluorescence intensity**		
0.009	36520.66	36706.97	36851.95
0.018	67829.8	67671.32	67021.02
0.028	124507.1	123786	124029.1
0.034	144183.6	142370.3	143884.9
0.048	193282.6	195110.2	195135.4
0.085	341525.9	339075	330461.4

Φ_{fl}=0.30±0.01, λ_{max}=371 nm

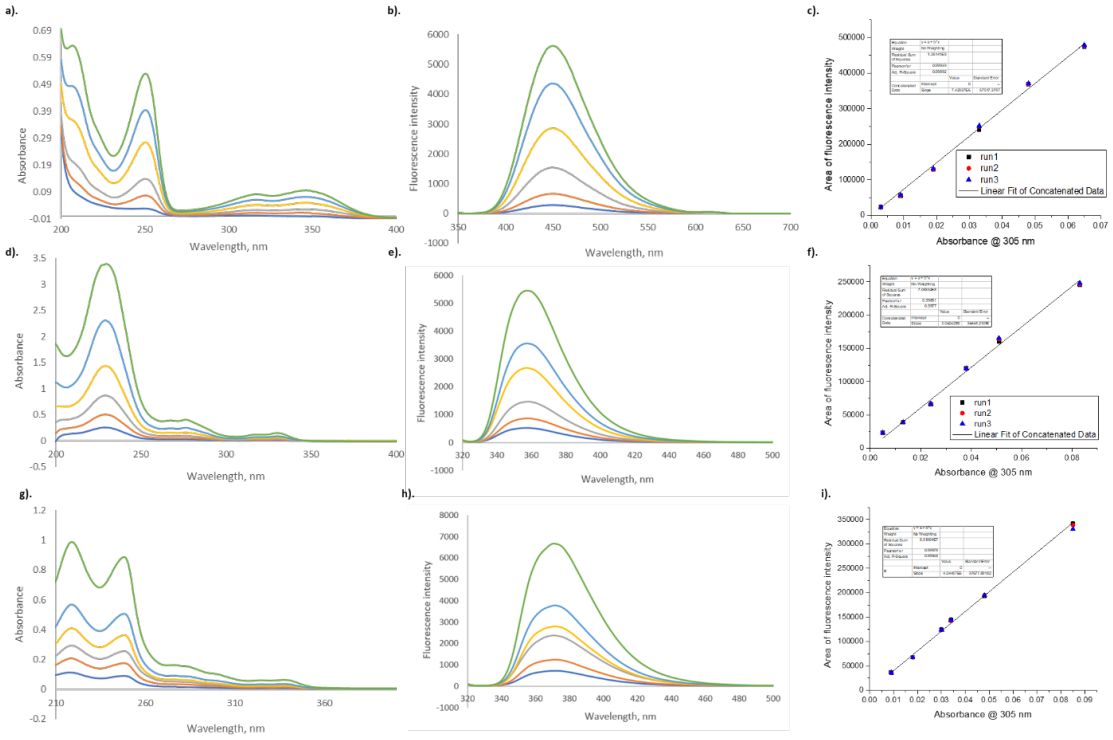

Figure 2.8. Determination of fluorescence quantum yield of QMPs. **a**). UV-spectra of quinine sulfate in 0.5 M aqueous sulfuric acid. **b).** Fluorescence spectra of quinine sulfate in o.5 M aqueous sulfuric acid at various concentrations. **c**). Calibration curve for quinine sulfate solutions. **d).** UV-spectra of **2.1a** in acetonitrile at various concentrations. **e).** Fluorescence spectra of **2.1a** in acetonitrile at various concentrations**. f).** Calibration curve for **2.1a** solutions. **g).** UV-spectra of **2.1b** in acetonitrile at various concentrations**. h).** Fluorescence spectra of **2.1b** in acetonitrile at various concentrations. **c).** Calibration curve for **2.1b** solutions.

2.8.3.3. Spectrophotometric Titration of 2.1a and 2.1b

Spectrophotometric titration of 2.1a. Solutions of **2.1a** (18 µM) of different pH were prepared by dilution of stock solution of **2.1a** in acetonitrile with 3 mL aqueous solutions of different pH (1.41, 2.97, 4.33, 5.31, 6.25, 7.41, 8.35, 9.4, 10.1, 10.8, 11.8, and 13.1). pH of solutions was monitored via pH-meter. IS of all solutions was 0.1M. The pKa was determined at three different wavelengths: 356 nm, 270 nm and 247 nm according to eq. 2.3:

Eq. 2.3

$$log_{10}\frac{(A_{HA}-A_i)}{(A_i-A_{A^-})} = pH_i - pK_a$$

where A_{HA} = absorbance value of fully protonated form, A_i = absorbance value at a givem pH_i and A_{A^-} = absorbance value of anionic form.

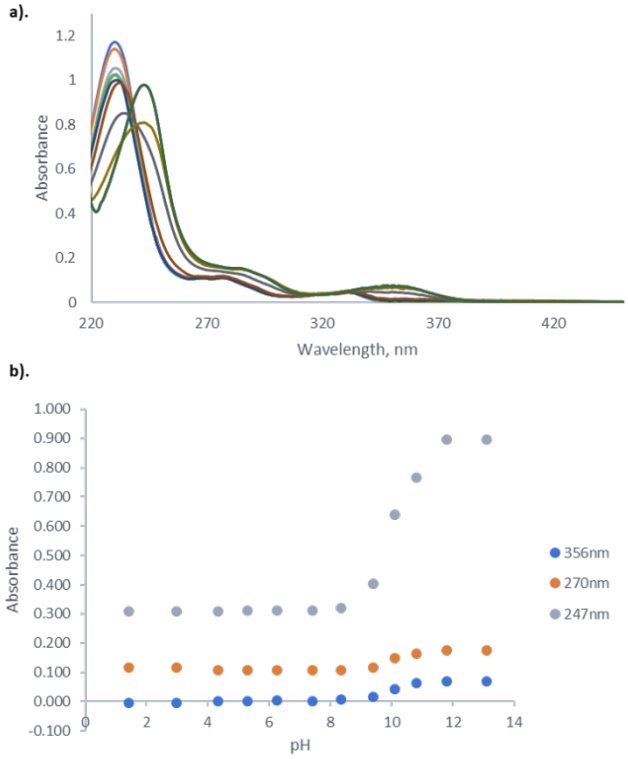

Figure 2.9 Spectrophotometric titration of **2.1a. a).** UV-spectra of **2.1a** at various pH. **b).** Spectrophotometric titration curves at 247 nm, 270 nm and 356 nm.

Table 2.6. Absorbance values at 356 nm, 270 nm and 247 nm at various pH.

pH	356nm	270nm	247nm
1.41	-0.004	0.118	0.308
2.97	-0.003	0.117	0.308
4.33	0.003	0.108	0.308
5.31	0.003	0.107	0.310
6.25	0.003	0.107	0.310
7.41	0.003	0.107	0.310
8.35	0.008	0.109	0.319
9.4	0.016	0.116	0.402
10.1	0.043	0.148	0.640
10.8	0.063	0.165	0.766
11.8	0.069	0.175	0.896
13.1	0.069	0.175	0.896

Table 2.7. Calculated $\log_{10}((A_{HA}-A_i)/(A_i-A_{A^-})$ values of **2.1a** at 356 nm, 270 nm and 247 nm at various pH.

	$\log_{10}((A_{HA}-A_i)/(A_i-A_{A^-})$		
pH	**356 nm**	**270 nm**	**247 nm**
7.41	-1.976	-1.772	-2.491
8.35	-1.023	-1.269	-1.725
9.4	-0.661	-0.776	-0.720
10.1	0.197	0.186	0.112
10.8	0.970	0.747	0.549
pKa	**9.818**	**9.982**	**10.133**

pKa = 9.977±0.015

Error calculated via Eq. 2.4

Eq. 2.4 $$\Delta pKa = \sqrt{\frac{\sum(\overline{pKa}-pKa_n)^2}{n-1}}$$

Spectrophotometric titration of 2.1b. Solutions of **2.1b** (8 µM) of different pH were prepared by dilution of stock solution of **2.1b** in acetonitrile with 3 mL aqueous solutions of different pH (1.41, 2.97, 4.33, 5.31, 6.25, 7.41, 8.35, 9.4, 10.1, 10.8, 11.8, and 13.1). pH of solutions was monitored via pH-meter. IS of all solutions was 0.1M. The pKa was determined at three different wavelengths: 248 nm, 265 nm and 365 nm according to eq. 2.3.

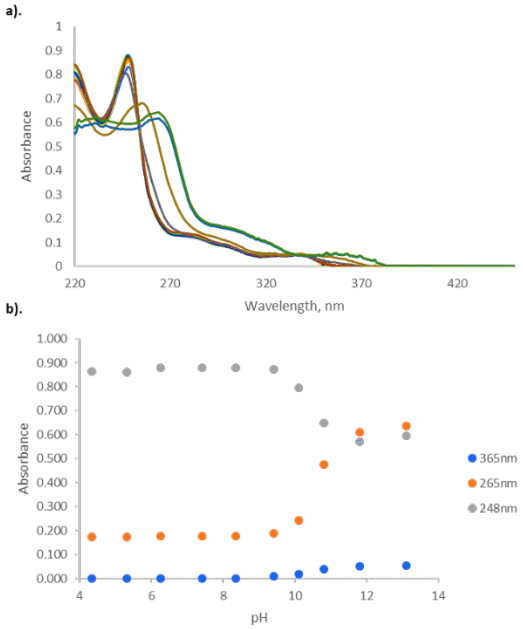

Figure 2.10. Spectrophotometric titration of **2.1b**. **a).** UV-spectra of **2.1b** at various pH. **b).** Spectrophotometric titration curves at 248 nm, 265 nm and 365nm.

Table 2.8. Absorbance values at 248 nm, 265 nm and 365 nm at various pH.

pH	365 nm	265 nm	248 nm
4.33	0.000	0.174	0.865
5.31	0.001	0.173	0.860
6.25	0.001	0.176	0.880
7.41	0.000	0.175	0.880
8.35	0.001	0.177	0.879
9.4	0.010	0.190	0.872
10.1	0.019	0.244	0.796
10.8	0.038	0.476	0.648
11.8	0.052	0.611	0.571
13.1	0.054	0.636	0.594

Table 2.9. Calculated $\log_{10}((A_{HA}-A_i)/(A_i-A_{A^-})$ values of **2.1b** at 248 nm, 265 nm and 365 nm at various pH.

	$\mathbf{Log_{10}((A_{HA}-A_i)/(A_i-A_{A^-})}$		
pH	**365 nm**	**265 nm**	**248 nm**
8.35	-1.877	-2.071	-2.676
9.4	-0.642	-1.416	-1.588
10.1	-0.265	-0.743	-0.426
10.8	0.376	0.277	0.480
11.8	1.415	1.254	2.811
pKa	**10.305**	**10.632**	**10.268**

pKa = 10.402±0.027

2.8.4. Reactivity of QMPs 2.1a and 2.1b

Quantum yield of photochemical generation of QM-2.1a. The efficiency of the photogeneration of **QM-2.1a** from **2.1a** in aqueous acetonitrile solution (1:1) was determined using 3,4-dimethoxynitrobenzene in 0.5 M aqueous KOH solution as an actinometer. Efficiency of formation of QM-2.1a was performed via photoirradiation of solution, that contained **2.1a** (0.8 mM), 2-aminoethylthiol hydrochloride (0.05 M) and phosphate buffer (pH = 7.41, 0.005 M, IS = 0.1 M) in acetonitrile/water (1:1). 2-Aminoethylthiol hydrochloride was used as fast and effective trapping agent for QMs. pH of the reaction mixture was determined to be 7.00. Irradiation was performed in a quartz cuvette (3 mL) in Rayonet photoreactor with 2 UV lamps of 300 nm light for 20 s. Absorbance of the actinometer solution, as well as of the **2.1a** solution was measured to be 1.04 a.u. at 300 nm. The composition of the irradiated solution of **2.1a** was analyzed by HPLC. System of methanol (50%), acetonitrile (1 %) and water (49%) was used as an eluent. Compound peak area on the chromatograms was determined at λ = 240 nm (Figure 2.11, Table 2.10, 2.11).

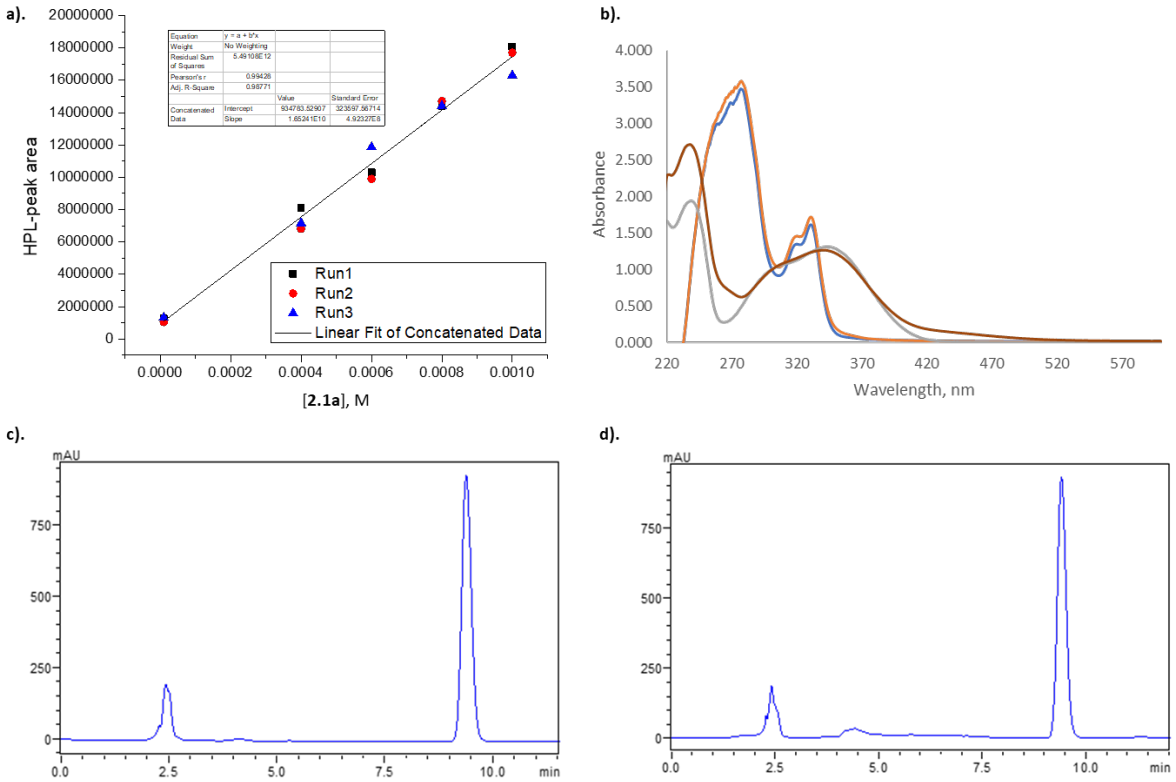

Figure 2.11. Quantum yield of photochemical generation of **QM-2.1a. a).** Calibration curve of compound **2.1a. b).** UV-spectra of **2.1a** prior irradiation (blue) and after irradiation (orange); UV-spectra of actinometer prior irradiation (grey) and after irradiation (brown). **c).** Representative chromatogram prior irradiation. **d).** Representative chromatogram after 20 s of irradiation at 300 nm.

Table 2.10. Calibration of **2.1a**: HPLC peak area and concentration.

Concentration, M	**Calibration of 2.1a – HPLC peak area**		
0.00001	1264816	1051527	1317772
0.0004	8093512	6814126	7156965
0.0006	10301224	9899406	11861194
0.0008	14382469	14705526	14398199
0.001	18071189	17705232	16296493

Table 2.11. Obtained data and calculations of actinometer and **2.1a**.

HPLC peak area of **2.1a**			
Time, s	run1	run2	run3
0	14705526	14398199	14622469
20	13925908	13443814	13526216
Absorbance change of actinometer at 450 nm			
Time, s	run1	run2	run3
0	0.014	0.009	0.003
20	0.121	0.139	0.151

Equations:

For the actinometer:

Eq. 2.5 $\Delta\text{Abs.} = \varepsilon\Delta c$ **Eq. 2.6** $\Delta\nu = \Delta cV$ Δν = amount converted (in moles)

Eq. 2.7 $F = \frac{\Delta\nu}{\Phi}$ F = number of photons absorbed

$\varepsilon(\text{Actinometer before irradiation})_{450\text{nm}} = 3\ \text{M}^{-1}\text{cm}^{-1} \approx 0$

$\varepsilon(\text{Actinometer after irradiation})_{450\text{nm}} = 3040\ \text{M}^{-1}\text{cm}^{-1}$

$V(\text{For irradiation}) = 3.0\ \text{mL}$ $\Phi(\text{Actinometer}) = 0.116 \pm 0.002$

For the compound:

From calibration curve: **Eq. 2.8** $\Delta\text{Area} = 16524068453\Delta c + 934783$

Eq. 2.6 $\Delta\nu = \Delta cV$ **Eq. 2.9** $\Phi = \frac{\Delta\nu}{F}$

1) Actinometer: $\Delta c = 3.52 \cdot 10^{-5} M$ $\Delta\nu = 1.06 \cdot 10^{-7} mol$ $F = 9.10 \cdot 10^{-7} Einsteins$

Compound: $\Delta c = 4.718 \cdot 10^{-5} M$ $\Delta\nu = 1.42 \cdot 10^{-7} mol$ $\Phi = \mathbf{0.156}$

2) Actinometer: $\Delta c = 4.28 \cdot 10^{-5} M$ $\Delta\nu = 1.28 \cdot 10^{-7} mol$ $F = 1.11 \cdot 10^{-6} Einsteins$

Compound: $\Delta c = 5.78 \cdot 10^{-5} M$ $\Delta\nu = 1.73 \cdot 10^{-7} mol$ $\Phi = \mathbf{0.156}$

3) Actinometer: $\Delta c = 4.87 \cdot 10^{-5} M$ $\Delta\nu = 1.46 \cdot 10^{-7} mol$ $F = 1.26 \cdot 10^{-6} Einsteins$

Compound: $\Delta c = 6.63 \cdot 10^{-5} M$ $\Delta\nu = 1.99 \cdot 10^{-7} mol$ $\Phi = \mathbf{0.158}$

Result: $\overline{\Phi} = 0.157$ **Eq. 2.10** $\sigma\Phi = \sqrt{\frac{\sum(\overline{\Phi} - \Phi_n)^2}{n-1}}$ = 0.001

$\Delta\Phi = 0.002$

$$\Phi = \mathbf{0.157 \pm 0.002}$$

Quantum yield of photochemical generation of QM-2.1b. The efficiency of the photogeneration of **QM-2.1b** from **2.1b** in aqueous acetonitrile solution (1:1) was determined using 3,4-dimethoxynitrobenzene in 0.5 M aqueous KOH solution as an actinometer. Efficiency of formation of QM-2.1a was performed via photoirradiation of solution, that contained **2.1b** (0.42 mM), 2-aminoethylthiol hydrochloride (0.05 M) and phosphate buffer (pH = 7.41, 0.005 M, IS = 0.1 M) in acetonitrile/water (1:1). 2-Aminoethylthiol hydrochloride was used as fast and effective trapping agent for QMs. pH of the reaction mixture was determined to be 7.00. Irradiation was performed in a quartz cuvette (3 mL) in Rayonet photoreactor with 2 UV lamps of 300 nm light for 20 s. Absorbance of the actinometer solution, as well as of the **2.1b** solution was measured to be 1.45 a.u. at 300 nm. The composition of the irradiated solution of **2.1b** was analyzed by HPLC. System of methanol (35%), acetonitrile (1 %) and water (64%) was used as an eluent. Compound peak area on the chromatograms was determined at λ = 240 nm (Figure 2.12, Table 2.12, 2.13).

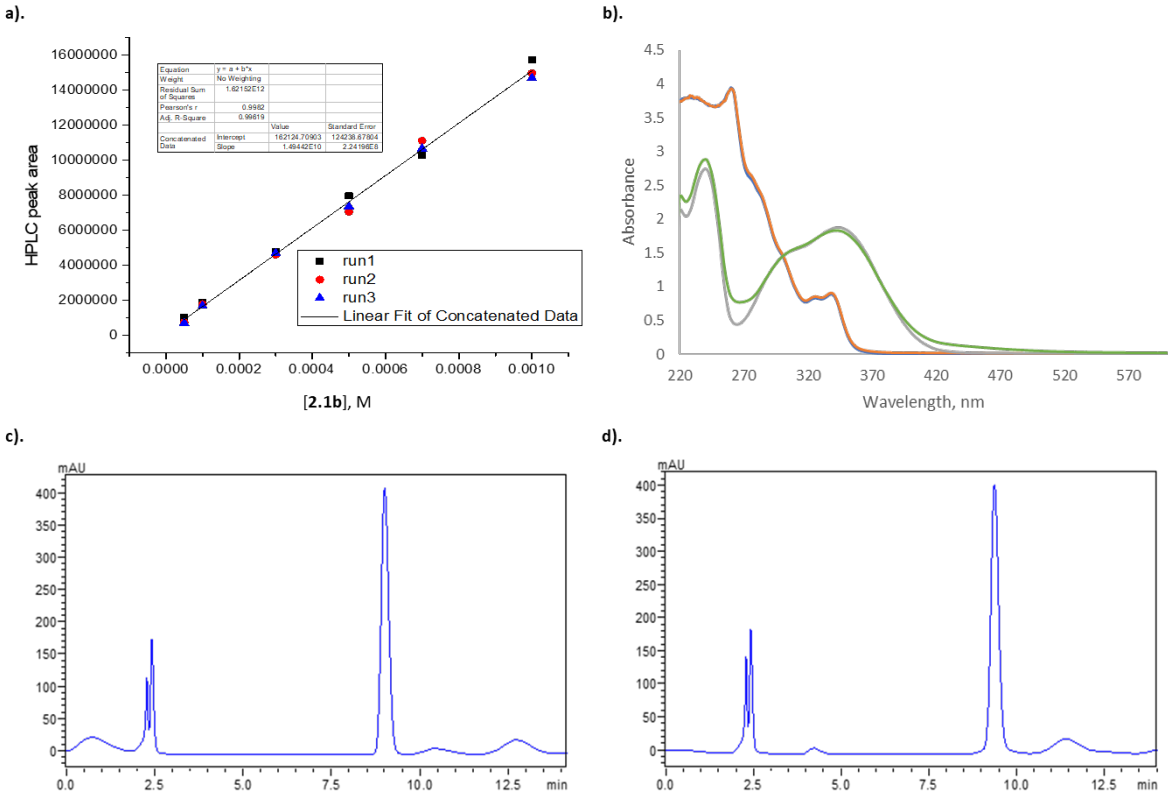

Figure 2.12. Quantum yield of photochemical generation of **QM-2.1b. a).** Calibration curve of compound **2.1b. b).** UV-spectra of **2.1b** prior irradiation (blue) and after irradiation (orange); UV-spectra of actinometer prior irradiation (grey) and after irradiation (green). **c).** Representative chromatogram prior irradiation. **d).** Representative chromatogram after 20 s of irradiation at 300 nm.

Table 2.12. Calibration of **2.1b**: HPLC peak area and concentration.

Concentration, M	**Calibration of 2.1b – HPLC peak area**		
0.00005	1030832	752194	699250
0.0001	1884940	1782162	1682454
0.0003	4758377	4604920	4693752
0.0005	7971515	7059852	7367908
0.0007	10283362	11113325	10667964
0.001	15724184	14963435	14684379

Table 2.13. Obtained data and calculations of actinometer and **2.1b**.

HPLC peak area of 2.1b			
Time, s	**run1**	**run2**	**run3**
0	6305295	6436407	6525736
20	6059148	6174422	6266152
Absorbance change of actinometer at 450 nm			
Time, s	**run1**	**run2**	**run3**
0	0.024	0.017	0.01
20	0.121	0.108	0.107

Equations:

For the compound: From calibration: **Eq. 2.12** $\Delta\text{Area} = 14944221413\Delta c + 162125$

1) Actinometer: $\Delta c = 3.20 \cdot 10^{-5} M$ $\Delta v = 9.57 \cdot 10^{-8} mol$ $F = 8.25 \cdot 10^{-7} Einsteins$

Compound: $\Delta c = 1.65 \cdot 10^{-5} M$ $\Delta v = 4.94 \cdot 10^{-8} mol$ $\Phi = \mathbf{0.060}$

2) Actinometer: $\Delta c = 2.99 \cdot 10^{-5} M$ $\Delta v = 8.98 \cdot 10^{-8} mol$ $F = 7.74 \cdot 10^{-7} Einsteins$

Compound: $\Delta c = 1.75 \cdot 10^{-5} M$ $\Delta v = 5.26 \cdot 10^{-8} mol$ $\Phi = \mathbf{0.068}$

3)Actinometer: $\Delta c = 3.19 \cdot 10^{-5} M$ $\Delta v = 9.57 \cdot 10^{-7} mol$ $F = 8.25 \cdot 10^{-7} Einsteins$

Compound: $\Delta c = 1.74 \cdot 10^{-5} M$ $\Delta v = 5.21 \cdot 10^{-8} mol$ $\Phi = \mathbf{0.063}$

Result:

$$\Phi = \mathbf{0.064 \pm 0.005}$$

2.8.5. Reactions of QMs

Rate measurements were conducted using LKS.60 kinetic spectrometer (Applied Photophysics) equipped with Brilliant B Nd:YAG laser (pulse width = 4 ns) fitted with 2nd and 4th harmonic generators. The signal from the spectrometer was digitized by Infiniium DSO8064A Oscilloscope (4 Gsamples / s, 600 MHz, by Agilent). Detector high voltage was set at 580 PM Volts. Wavelength of observation was 400 nm. Solutions of NQM precursors had OD ~ 0.4 at 254 nm. The measurements were conducted at 25 ± 0.05 ºC. Volume of solutions in the cuvette was 2.0 mL. First order rate constants were obtained by least-square fitting of

the observed data to a single exponential function. Second order rate constant with NQM trapping reagents were determine from the plot of the concentration of the trapping reagents Vs the observed first order rate constants. The observed first order rates are summarized below.

2.8.5.1. Hydration of QM-2.1a and QM-2.1b

2.8.5.1.1. Hydration in aqueous solutions of perchloric acid and sodium hydroxide

Table 2.14. Hydration of QM obtained from **2.1a** (0.033 mM) in dilute aqueous perchloric acid solutions at 25 ^{o}C.

Perchloric acid, M	k, s^{-1}	Error, s^{-1}
0.0001	0.432	0.005
0.0001	0.519	0.007
0.0001	0.513	0.006
0.0005	1.93	0.03
0.0005	2.19	0.03
0.0005	2.12	0.03
0.001	3.96	0.06
0.001	4.23	0.06
0.001	3.99	0.05
0.005	26.5	0.4
0.005	25.7	0.4
0.005	24.5	0.4
0.01	54.6	0.8
0.01	56.9	0.8
0.01	56.4	0.8
0.05	321	3
0.05	320	3
0.05	309	3
0.1	730	5
0.1	757	5
0.1	735	5
0.2	1773	13
0.35	3070	14
0.5	3572	18
0.5	3724	18
0.5	3880	18
0.75	8511	33
0.75	8222	32

Perchloric acid, M	k, s^{-1}	Error, s^{-1}
0.75	8073	30
0.875	12005	49
0.9	13612	60
1	18583	65
1	20172	72
1	20098	75

Table 2.15. Hydration of QM obtained from **2.1a** (0.033 mM) in dilute aqueous sodium hydroxide solutions at 25 ^{o}C.

Sodium hydroxide, M	k, s^{-1}	Error, s^{-1}
0.001	0.218	0.004
0.001	0.204	0.004
0.001	0.216	0.003
0.005	0.254	0.003
0.005	0.221	0.003
0.005	0.232	0.004
0.01	0.271	0.003
0.01	0.31	0.003
0.01	0.321	0.003
0.05	0.35	0.004
0.05	0.334	0.003
0.05	0.328	0.003
0.1	0.408	0.004
0.1	0.49	0.005
0.1	0.451	0.008

Table 2.16. Hydration of QM obtained from **2.1b** (0.033 mM) in dilute aqueous perchloric acid solutions at 25 ^{o}C. Two processes have been observed at pH 4 and 3.3. Fast process has not been observed at lower pH.

Perchloric acid, M	k, s^{-1}	Error, s^{-1}
Slow process		
0.0001	0.269	0.007
0.0001	0.273	0.007
0.0001	0.261	0.006
0.0005	2.13	0.06
0.0005	1.93	0.05
0.0005	2.16	0.06
0.001	3.4	0.1
0.001	3.24	0.09
0.001	3.7	0.1
0.01	48	1
0.01	52	1
0.01	53	2
0.05	456	4
0.05	474	4
0.05	458	4
0.1	812	5
0.1	853	5
0.1	873	5
Fast process		
0.0001	3832	10
0.0001	3778	10
0.0001	3776	10
0.0005	3811	10
0.0005	3843	10
0.0005	3838	10

Table 2.17. Hydration of QM obtained from **2.1b** (0.033 mM) in dilute aqueous sodium hydroxide solutions at 25°C. Only slow process has been observed.

Sodium hydroxide, M	k, s^{-1}	Error, s^{-1}
0.001	0.364	0.009
0.001	0.385	0.009
0.001	0.386	0.008
0.005	0.479	0.004
0.005	0.451	0.004
0.005	0.451	0.009
0.01	0.523	0.007
0.01	0.554	0.005
0.01	0.538	0.007
0.05	0.618	0.006
0.05	0.584	0.005
0.05	0.594	0.007
0.1	0.646	0.009
0.1	0.653	0.006
0.1	0.644	0.006

2.8.5.1.2. Buffer Catalyzed Hydration

Preparation of biphosphate buffer solutions

$$\underset{x}{NaH_2PO_4} + \underset{y}{Na_2HPO_4} \longrightarrow \underset{(x+2y)}{3Na^+} + \underset{x}{H_2PO_4^-} + \underset{y}{HPO_4^{2-}}$$

Eq. 2.12 $IS = 0.5*([Na_+] + [H_2PO_4^-] + 4*[HPO_4^{2-}]) = 0.5*(x+2y+x+4y)/V=(x+3y)/V$

Eq. 2.13 $BR = [H_2PO_4^-]/[HPO_4^{2-}]=x/y$

Eq. 2.14 $pH = pKa'-\log BR$

pKa_2 (thermodynamic) = 7.2

Stock buffer solutions:

1). BR = 0.3

pH = 6.73 - log 0.3 = 7.25 (measured 7.41)

IS = 0.0231+3*0.0769=0.2538 M

0.1 M buffer:

NaH_2PO_4 = 0.0231 mol

Na_2HPO_4 = 0.0769 mol

1000 mL water

2). BR = 1.8

pH = 6.76 - log 1.8 = 6.52 (measured 6.63)

IS = 0.0643+3*0.0357=0.1714 M

0.1 M buffer:

NaH_2PO_4 = 0.0643 mol

Na_2HPO_4 = 0.0357 mol

1000 mL water

3). BR = 1.2

pH = 6.75 - log 1.2 = 6.67 (measured 6.81)

IS = 0.0545+3*0.0455=0.191 M

0.1 M buffer:

NaH_2PO_4 = 0.0545 mol

Na_2HPO_4 = 0.0455 mol

1000 mL water

Total volume = 10 mL

$IS = (IS_{buffer}*V_{buffer}+0.1*V_{NaCl})/10$

Buffer catalyzed hydration of QM-2.1a

Table 2.18. Hydration of QM obtained from **2.1a** (0.033 mM) in dilute aqueous phosphate buffer solutions) at 25 ^{o}C.

Buffer 1, M	k, s^{-1}	Error, s^{-1}	Buffer 2, M	k, s^{-1}	Error, s^{-1}	Buffer 3, M	k, s^{-1}	Error, s^{-1}
$[H_2PO_4^-]/[HPO_4^{2-}]$ = 0.3			$[H_2PO_4^-]/[HPO_4^{2-}]$ = 1.8			$[H_2PO_4^-]/[HPO_4^{2-}]$ = 1.2		
0.001	0.0243	0.0003	0.001	0.057	0.001	0.003	0.052	0.001
0.001	0.0234	0.0004	0.001	0.051	0.002	0.003	0.049	0.001
0.001	0.025	0.0003	0.001	0.053	0.001	0.003	0.056	0.001
0.005	0.034	0.0004	0.005	0.089	0.002	0.005	0.061	0.001
0.005	0.0307	0.0004	0.005	0.096	0.002	0.005	0.067	0.001
0.005	0.0318	0.0004	0.005	0.086	0.002	0.005	0.056	0.001
0.0075	0.0362	0.0004	0.0075	0.108	0.002	0.0075	0.08	0.001
0.0075	0.0386	0.0005	0.0075	0.101	0.002	0.0075	0.076	0.001
0.0075	0.0353	0.0007	0.0075	0.115	0.002	0.0075	0.078	0.001
0.01	0.0481	0.0008	0.01	0.123	0.002	0.01	0.091	0.001
0.01	0.0489	0.0007	0.01	0.121	0.003	0.01	0.105	0.001
0.01	0.0431	0.0008	0.01	0.118	0.003	0.01	0.093	0.001

Table 2.19. Buffer catalytic coefficients ($M^{-1}s^{-1}$) of hydration of **QM-2.1a**.

	k, $M^{-1}s^{-1}$	Error, $M^{-1}s^{-1}$	Intercept, s^{-1}	Error
Buffer 1, M	2.4	0.2	0.021	0.001
Buffer 2, M	7.5	0.5	0.049	0.003
Buffer 3, M	6.4	0.5	0.031	0.004

To determine whether the reaction was catalyzed by general acid or general base, obtained observed rate constants were plotted vs. the concentration of general acid or general base, respectively. As a result, linear dependence of rate constant vs. general acid concentration was observed for hydration of **QM-2.1a** (Figure 2.13). Thus, reaction was catalyzed by general acid. On the other hand, presence of general base catalysis was not detected.

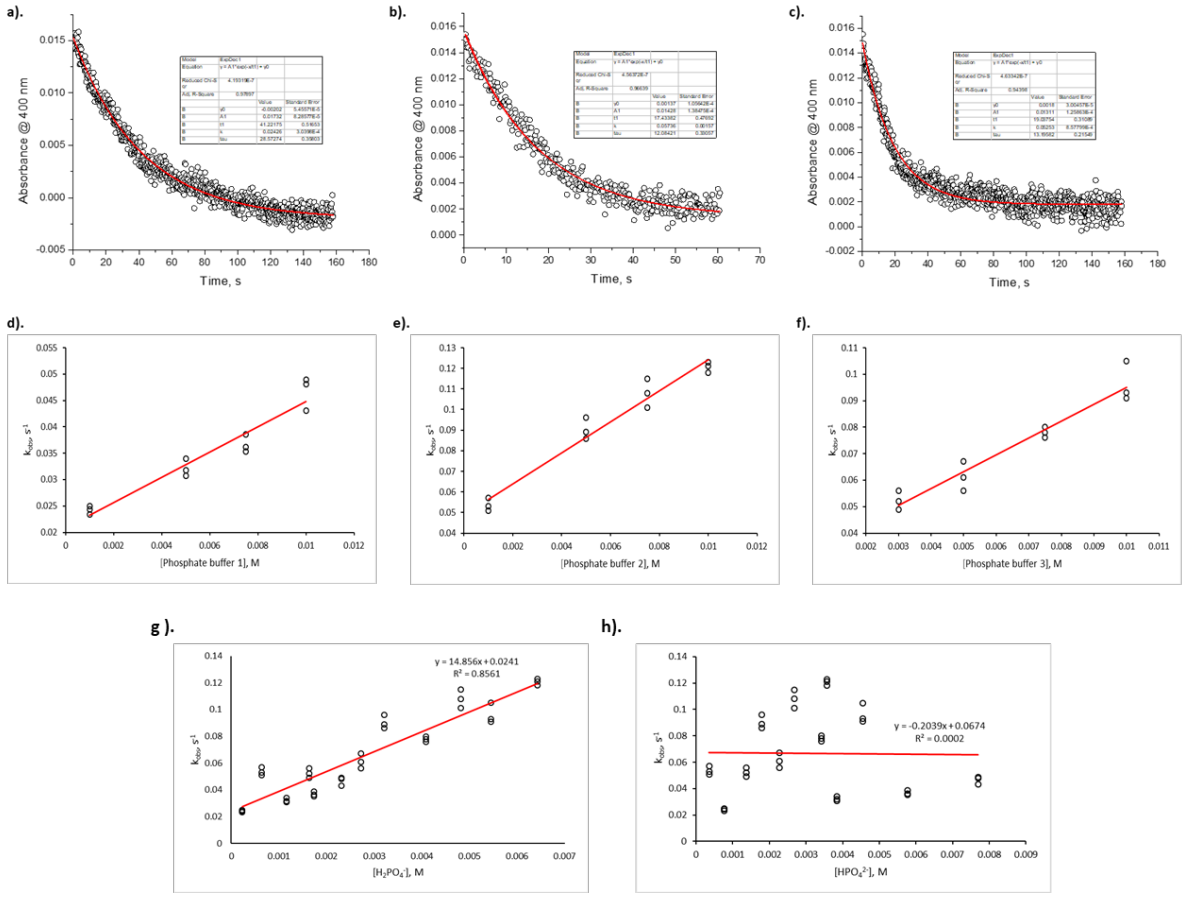

Figure 2.13. Buffer catalyzed hydrolysis**. a).** Decay of **QM-2.1a** (0.033 mM) in dilute phosphate buffer 1 (0.001 M). **b).** Decay of **QM-2.1a** (0.033 mM) in dilute phosphate buffer 2 (0.001 M). **c).** Decay of **QM-2.1a** (0.033 mM) in dilute phosphate buffer 3 (0.003 M). **d)**. Determination of buffer catalytic coefficients in phosphate buffer 1. **e)**. Determination of buffer catalytic coefficients in phosphate buffer 2. **f)**. Determination of buffer catalytic coefficients in phosphate buffer 3. **g).** Presence of general acid catalysis. **h).** Absence of general base catalysis.

Buffer catalyzed hydration of QM-2.1b

Hydration of QM obtained from **2.1b** (0.033 mM) in dilute aqueous phosphate buffer solutions at 25 ^{o}C. Two independent processes have been observed: slow and fast.

Table 2.20. Hydration of QM obtained from **2.1b** (0.033 mM) in dilute aqueous phosphate buffer solutions at 25 ^{o}C – slow process.

Buffer 1, M	k, s^{-1}	Error, s^{-1}	Buffer 2, M	k, s^{-1}	Error, s^{-1}	Buffer 3, M	k, s^{-1}	Error, s^{-1}
$[H_2PO_4^-]/[HPO_4^{2-}]$ = 0.3			**$[H_2PO_4^-]/[HPO_4^{2-}]$ = 1.8**			**$[H_2PO_4^-]/[HPO_4^{2-}]$ = 1.2**		
0.001	0.051	0.001	0.005	0.11	0.004	0.001	0.056	0.001
0.001	0.062	0.001	0.005	0.104	0.006	0.001	0.062	0.002
0.001	0.054	0.001	0.005	0.101	0.003	0.001	0.068	0.002
0.005	0.067	0.001	0.0065	0.118	0.004	0.005	0.075	0.002
0.005	0.069	0.002	0.0065	0.118	0.004	0.005	0.083	0.002
0.005	0.066	0.001	0.0065	0.119	0.003	0.005	0.089	0.003
0.0075	0.071	0.001	0.0075	0.127	0.004	0.0075	0.091	0.003
0.0075	0.075	0.002	0.0075	0.135	0.003	0.0075	0.104	0.003
0.0075	0.073	0.001	0.0075	0.125	0.005	0.0075	0.106	0.004
0.01	0.083	0.002	0.01	0.157	0.005	0.01	0.111	0.003
0.01	0.087	0.001	0.01	0.149	0.005	0.01	0.112	0.004
0.01	0.082	0.002	0.01	0.16	0.005	0.01	0.126	0.004

Table 2.21. Buffer catalytic coefficients ($M^{-1}s^{-1}$) of hydration of **QM-2.1b**.

	k, $M^{-1}s^{-1}$	Error, $M^{-1}s^{-1}$	Intercept, s^{-1}	Error
Buffer 1, M	3.05	0.29	0.052	0.002
Buffer 2, M	10.2	0.6	0.053	0.004
Buffer 3, M	6.08	0.6	0.055	0.004

To determine whether the reaction was catalyzed by general acid or general base, obtained observed rate constants were plotted vs. the concentration of general acid or general base, respectively. As a result, linear dependence of rate constant vs. general acid concentration[19] was observed for hydration (slow process) of **QM-2.1b**. Thus, reaction was catalyzed by general acid (Figure 2.14). On the other hand, presence of general base catalysis was not detected.

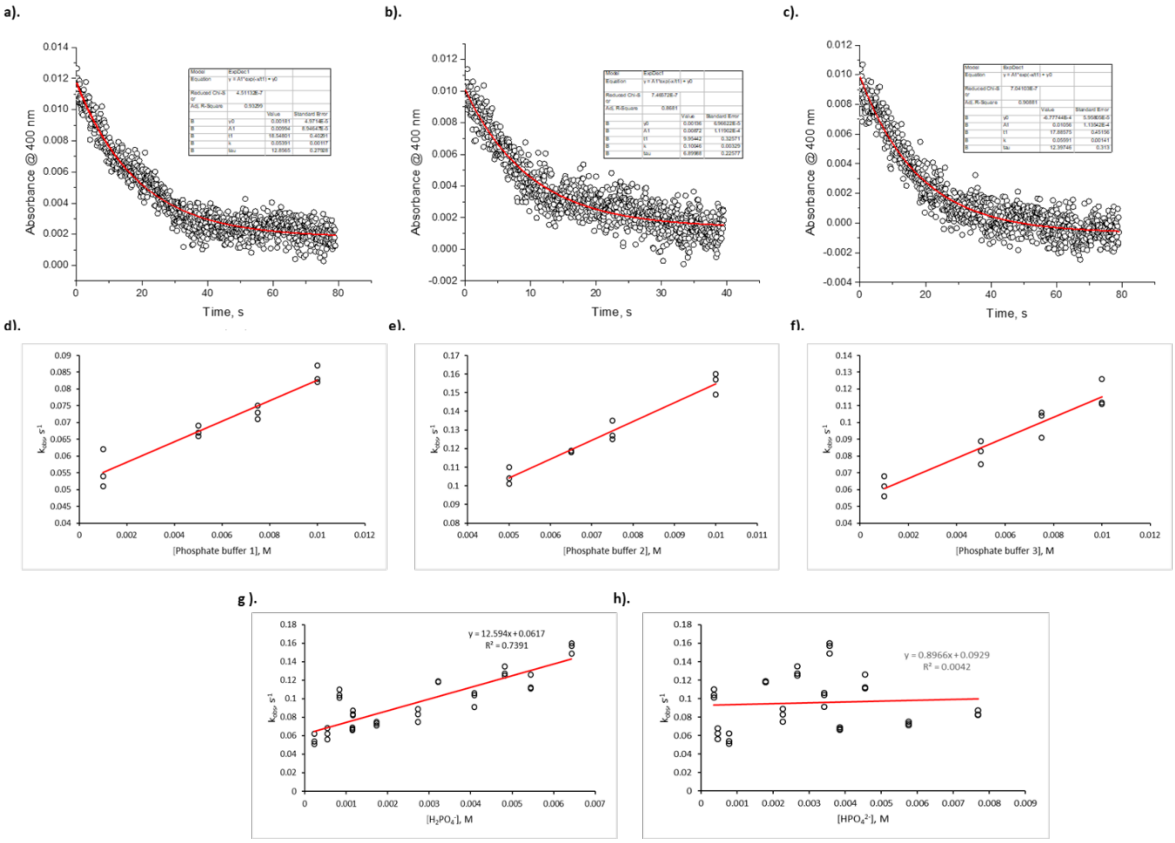

Figure 2.14. Buffer catalyzed hydrolysis – slow process. **a).** Decay of **QM-2.1b** (0.033 mM) in dilute phosphate buffer 1 (0.001 M). **b).** Decay of **QM-2.1b** (0.033 mM) in dilute phosphate buffer 2 (0.001 M). **c).** Decay of **QM-2.1b** (0.033 mM) in dilute phosphate buffer 3 (0.001 M). **d)**. Determination of buffer catalytic coefficients in phosphate buffer 1. **e)**. Determination of buffer catalytic coefficients in phosphate buffer 2. **f)**. Determination of buffer catalytic coefficients in phosphate buffer 3. **g).** Presence of general acid catalysis. **h).** Absence of general base catalysis.

Table 2.22. Hydration of QM obtained from **2.1b** (0.033 mM) in dilute aqueous phosphate buffer solutions at 25 ^{o}C – fast process.

Buffer 1, M	k, s^{-1}	Error, s^{-1}	Buffer 2, M	k, s^{-1}	Error, s^{-1}	Buffer 3, M	k, s^{-1}	Error, s^{-1}
$[H_2PO_4^-]/[HPO_4^{2-}]$ = 0.3			**$[H_2PO_4^-]/[HPO_4^{2-}]$ = 1.8**			**$[H_2PO_4^-]/[HPO_4^{2-}]$ = 1.2**		
0.001	3688	12	0.001	3731	11	0.001	3772	10
0.001	3640	12	0.001	3737	12	0.001	3785	10
0.001	3693	11	0.001	3726	11	0.001	3789	7
0.005	3792	7	0.005	3819	10	0.005	3844	7
0.005	3801	7	0.005	3825	7	0.005	3847	6
0.005	3796	7	0.005	3792	11	0.005	3841	7
0.0075	3832	8	0.0075	3828	10	0.0075	3886	7
0.0075	3827	7	0.0075	3852	11	0.0075	3869	6
0.0075	3818	7	0.0075	3840	7	0.0075	3919	7
0.01	3941	6	0.01	3945	6	0.01	3937	8
0.01	3975	6	0.01	3940	6	0.01	3971	8
0.01	3938	7	0.01	3940	6	0.01	3979	8

Observed rate constants of hydration in the fast process at different buffers and concentrations were very close and the difference in obtained numbers potentially could be assigned to the instrumental error. Thus, from these data we cannot conclude whether the process was catalyzed by geneal acid/base or no catalysis was present.

2.8.5.1.3. Hydration of QM-2.1b in the Presence of Air, Oxygen and Argon

Hydration of **QM-2.1b** obtained from **2.1b** (0.033 mM) in dilute aqueous phosphate buffer solution (pH = 7.41, IS = 0.1 M, 0.005 M) at 25 ^{o}C. Two independent processes have been observed: slow and fast. Slow process rate constants have been affected by saturation of solutions with oxygen and argon (bubbling gas for 15 minutes) compare to air. Fast process has not been affected by replacing air with oxygen and argon (Table 2.23).

Table 2.23. Pseudo-first order rate constants of hydration of **QM-2.1b** in the presence of air, oxygen and argon (slow process).

Buffer, 0.005 M	k, s^{-1}	Error, s^{-1}
$[H_2PO_4^-]/[HPO_4^{2-}]$ = 0.3		
Air	0.068	0.002
Air	0.067	0.001
Air	0.066	0.001
Argon	0.039	0.001
Argon	0.04	0.001
Argon	0.04	0.001
Oxygen	0.117	0.003
Oxygen	0.113	0.003
Oxygen	0.115	0.003

2.8.5.2. Reactivity of QM-2.1a and QM-2.1b towards Nucleophiles and Dienophiles

Photoreaction between QM-2.1a and 2-aminoethylthiol hydrochloride

Rate constant determination via LFP

Table 2.24. Decay of **QM-2.1a** obtained from **2.1a** (0.033 mM) in dilute phosphate buffer (pH = 7.41, IS = 0.1 M, 0.005 M) containing various concentration of 2-aminoethylthiol hydrochloride at 25ºC; pH = 7.00.

2-aminoethylthiol hydrochloride, M	k, s^{-1}	Error, s^{-1}
0.005	141	1
0.005	132	2
0.005	133	2
0.00575	208	3
0.00575	208	2
0.00575	197	2
0.0075	334	4
0.0075	326	4
0.0075	334	4
0.0085	364	4
0.0085	370	6
0.0085	380	5
0.01	485	7
0.01	477	7
0.01	479	7

HPLC analysis. Solution (3.0 mL, pH = 7.0)) that contained **2.1a** (0.5 mM), 2-aminoethylthiol hydrochloride (0.05 M), phosphate buffer (pH = 7.41, 0.005 M, IS=0.1 M) and acetonitrile/water (1:1) was irradiated with 2 UV-lamps at 300 nm in Rayonet reactor for 0, 1, 5, 10, 15, and 20 min. Reaction progress was monitored via HPLC. System of methanol (47%), acetonitrile (1%) and water (52%) was used as an eluent; ratio between starting material and product were analyzed at wavelength of 254 nm. According to chromatograms, maximum ratio between product and starting material was reached after 20 min of irradiation and was 82.6% and 17.4%, respectively. Prolonged irradiation resulted in decomposition of both compounds and formation of oligomers.

2.1a eluted at 12.356 min, **2.2a** eluted at 5.048 min.

HRMS (ESI), *m/z*: calcd. for **2.1a** $C_{17}H_{14}O_3$-H $[M-H]^-$ 265.0870, found 265.0867.

HRMS (ESI), *m/z*: calcd. for **2.2a** $C_{19}H_{20}ClNO_2S$-H $[M-H]^-$ 360.0831, found 360.0827.

Table 2.25. Photoreaction between **QM-2.1a** and 2-aminoethylthiol hydrochloride: HPLC analysis.

Time, min	**HPLC - peak area @ 254 nm**	
	2.1a	**2.2a**
0	1045270	0
1	991944	239162
5	778867	859891
10	579102	1232711
15	407531	1312110
20	263481	1249981
Time, min	**Percentage of QM in the mixture, %**	
	2.1a	**2.2a**
0	100.0	0.0
1	80.6	19.4
5	47.5	52.5
10	32.0	68.0
15	23.7	76.3
20	17.4	82.6

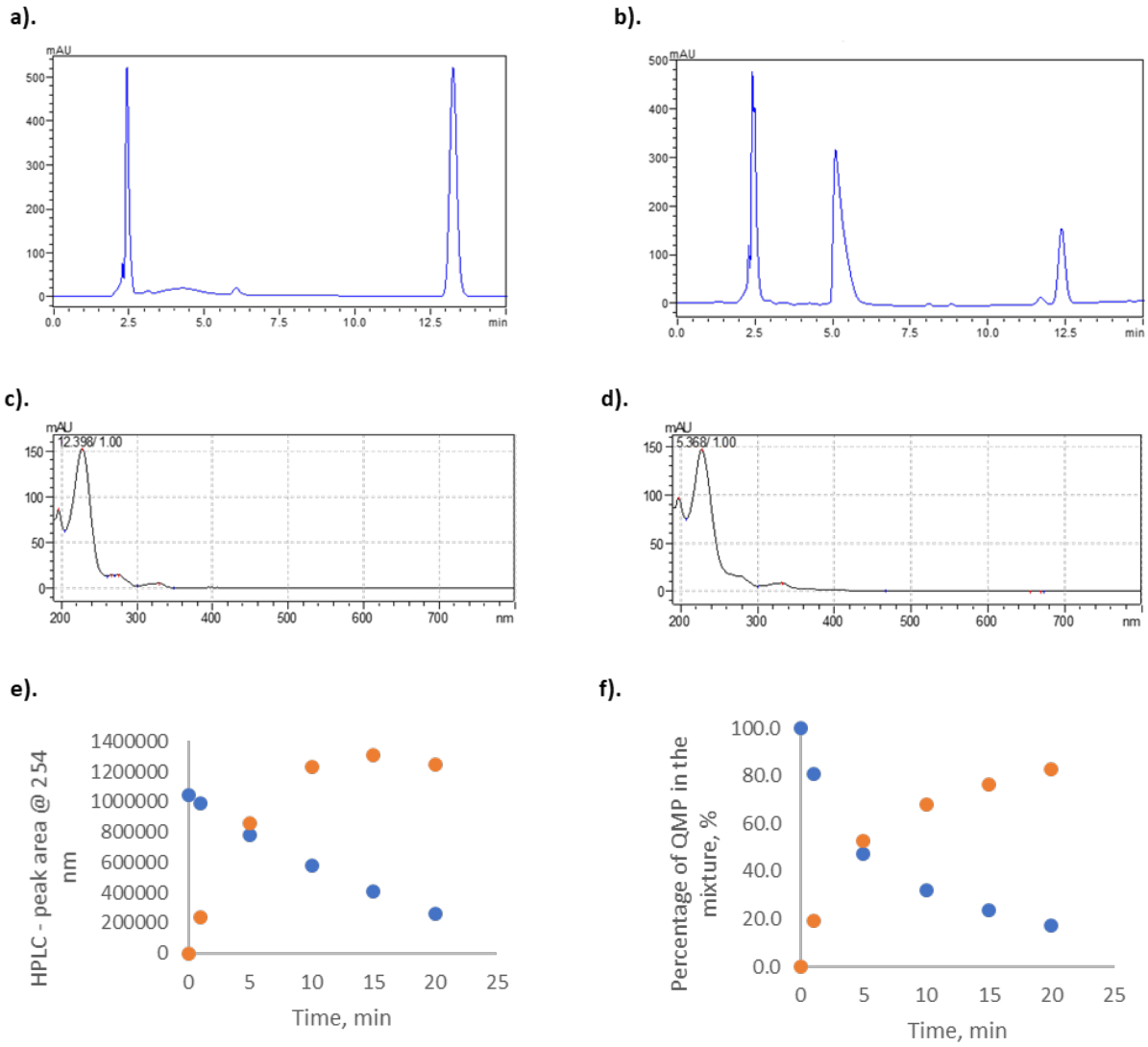

Figure 2.15. Photoreaction between **QM-2.1a** and 2-aminoethylthiol hydrochloride. **a).** HPLC chromatogram – reaction mixture prior irradiation. **b).** HPLC chromatogram – reaction mixture after 20 mins of irradiation at 300 nm. **c).** UV-spectrum of **2.1a**. **d).** UV-spectrum of **2.2a**. **e).** Change in peak areas over time. **f)**. Percentage of QMP in the mixture.

Photoreaction between QM-2.1b and 2-aminoethylthiol hydrochloride

Rate constant determination via LFP

Table 2.26. Decay of **QM-2.1b** obtained from **2.1b** (0.033 mM) in dilute phosphate buffer (pH = 7.41, IS = 0.1 M, 0.005 M) containing various concentration of 2-aminoethylthiol hydrochloride at 25 ºC; pH = 7.00.

2-aminoethylthiol hydrochloride, M	k, s^{-1}	Error, s^{-1}
0.01	2257	15
0.01	2283	15
0.01	2288	15
0.0075	2039	17
0.0075	2080	16
0.0075	2061	17
0.005	1909	19
0.005	1878	18
0.005	1994	18
0.0025	1710	19
0.0025	1765	18
0.0025	1787	18
0.001	1656	19
0.001	1600	19
0.001	1711	19

HPLC analysis. Solution (3.0 mL, pH = 7.0) that contained **2.1b** (0.5 mM), 2-aminoethylthiol hydrochloride (0.05 M), phosphate buffer (pH = 7.41, 0.005 M, IS=0.1 M) and acetonitrile/water (1:1) was irradiated with 2 lamps at 300 nm in Rayonet reactor for 0, 5, 10, 15, and 20 min. Reaction progress was monitored via HPLC. System of methanol (35%), acetonitrile (1%) and water (64%) was used as an eluent; ratio between 2.1b and 2.2b was analyzed at wavelength of 219 nm. According to chromatograms, maximal ratio between product and starting material was reached after 20 min of irradiation and was 81.2% and 17.8%, respectively. Prolonged irradiation resulted in decomposition of both compounds and formation of oligomers. **2.1b** eluted at 9.2 min, product **2.2b** eluted at 3.6 min.

HRMS (ESI), *m/z*: calcd. for **2.1b** $C_{17}H_{14}O_4$-H $[M-H]^-$ 281.0814, found 281.0817.

HRMS (ESI), *m/z*: calcd. for **2.2b** $C_{19}H_{20}ClNO_3S$-H $[M-H]^-$ 376.0780, found 376.0776.

Table 2.27. Photoreaction between **QM-2.1b** and 2-aminoethylthiol hydrochloride: HPLC analysis.

Time, min	HPLC - peak area @ 219 nm	
	2.1b	**2.2b**
0	8223435	0
5	6169328	3414985
10	3801270	4893270
15	1883565	6141796
20	1461468	6295471
Time, min	**Percentage of QMP in the mixture, %**	
	2.1b	**2.2b**
0	100.0	0.0
5	64.4	35.6
10	43.7	56.3
15	23.5	76.5
20	18.8	81.2

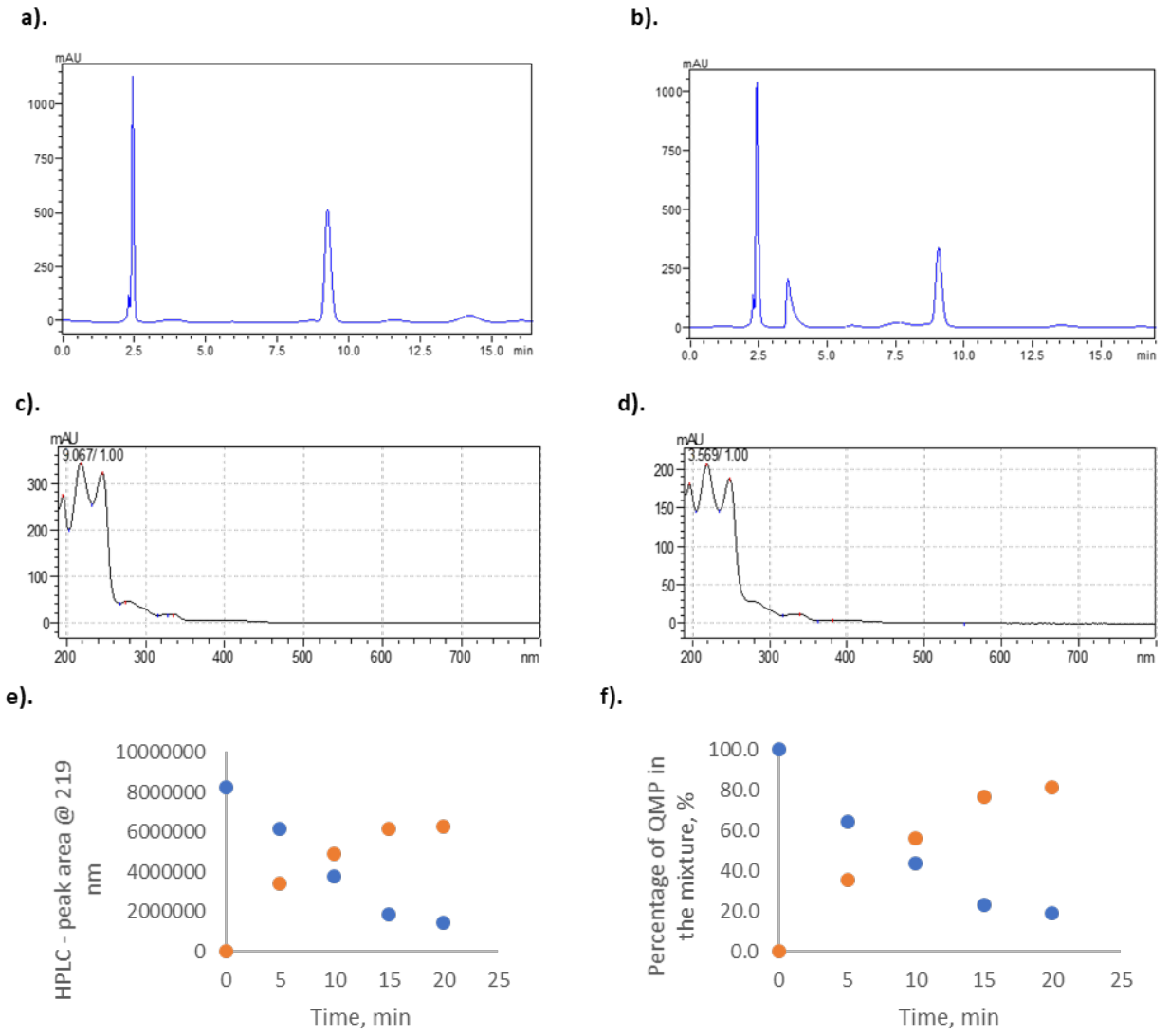

Figure 2.16. Photoreaction between **QM-2.1b** and 2-aminoethylthiol hydrochloride. **a).** HPLC chromatogram – reaction mixture prior irradiation. **b).** HPLC chromatogram – reaction mixture after 20 mins of irradiation at 300 nm. **c).** UV-spectrum of **2.1b**. **d).** UV-spectrum of **2.2b**. **e).** Change in peak areas over time. **f)**. Percentage of QMP in the mixture.

Photoreaction between QM-2.1a and methanol

HPLC analysis. Solution (3.0 mL) that contained **2.1a** (0.5 mM) and methanol/water (100:1) was irradiated with 6 lamps at 300 nm in Rayonet reactor for 0, 5, 10, 15, 20, 25, and 30 min. Reaction progress was monitored via HPLC. System of methanol (50%), acetonitrile (1%) and water (49%) was used as an eluent;

ratio between **2.1a** and **2.4a** were analyzed at wavelength of 227 nm. According to chromatograms, maximum ratio between product and starting material was reached after 30 min of irradiation and was 82.1% and 17.9%, respectively (Table 2.28). Prolonged irradiation resulted in decomposition of both compounds and formation of oligomers.

2.1a eluted at 8.9 min, **2.4a** eluted at 6.5 min.

Table 2.28. Photoreaction between **QM-2.1a** and methanol: HPLC analysis.

Time, min	HPLC - peak area @ 227 nm	
	2.1a	**2.4a**
0	9830760	0
5	6598387	3971949
10	4749442	5471000
15	3522729	7182012
20	2959267	7985778
25	1985696	8566131
30	1930590	8883468

Time, min	Percentage of QMP in the mixture %	
	2.1a	**2.4a**
0	100.0	0.0
5	62.4	37.6
10	46.5	53.5
15	32.9	67.1
20	27.0	73.0
25	18.8	81.2
30	17.9	82.1

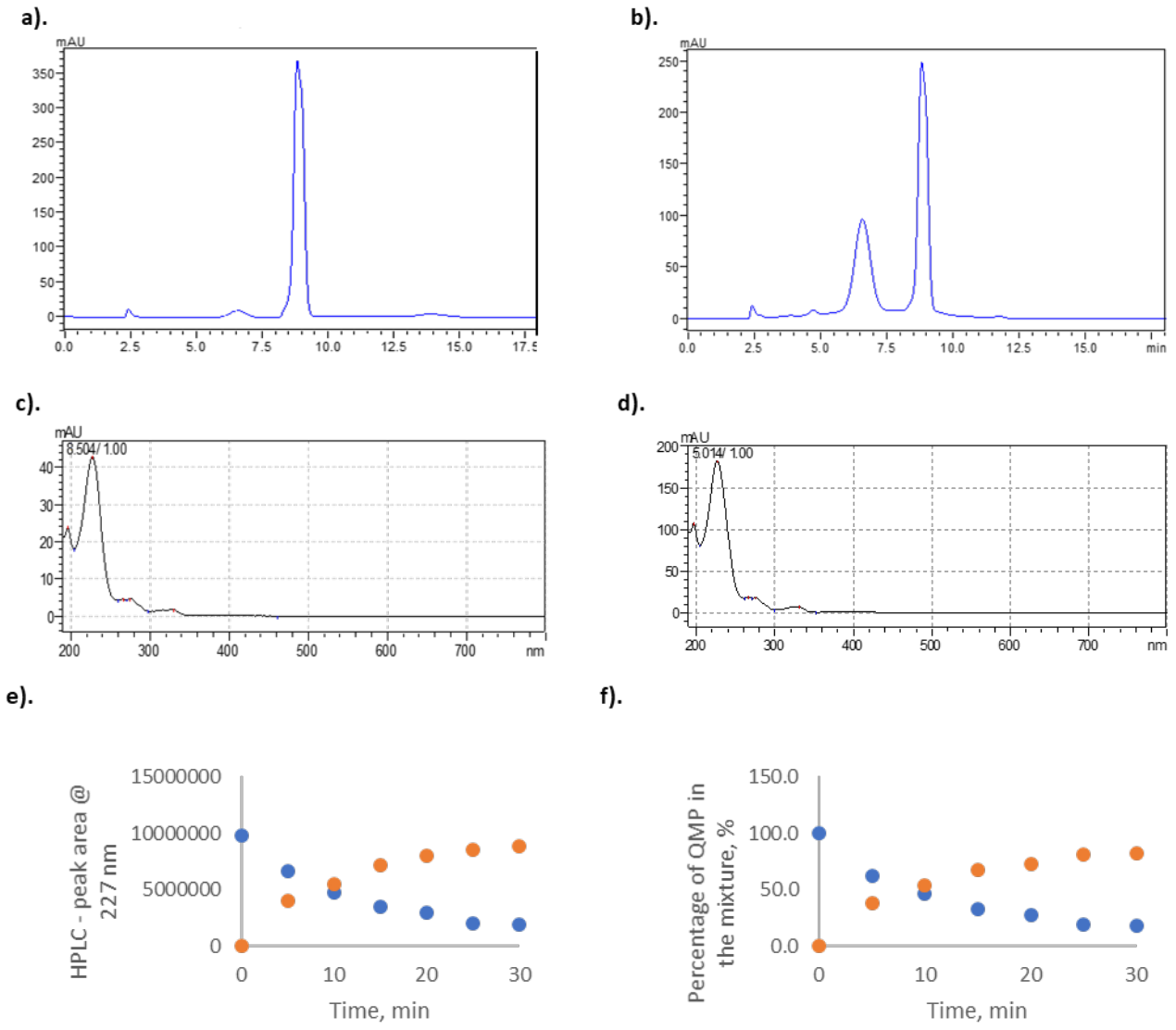

Figure 2.18. Photoreaction between **QM-2.1a** and methanol. **a).** HPLC chromatogram – reaction mixture prior irradiation. **b).** HPLC chromatogram – reaction mixture after 10 mins of irradiation at 300 nm. **c).** UV-spectrum of **2.1a**. **d).** UV-spectrum of **2.4a**. **e).** Change in peak areas over time. **f).** Percentage of QMP in the mixture.

Photoreaction between QM-2.1b and methanol

HPLC analysis. Solution (3.0 mL) that contained **2.1b** (0.5 mM) and methanol/water (100:1) was irradiated with 6 lamps at 300 nm in Rayonet reactor for 0, 10, 20, and 30 min. Reaction progress was monitored via HPLC. System of methanol (40%), acetonitrile (1%) and water (59%) was used as an eluent; ratio between

starting material and product were analyzed at wavelength of 219 nm. Prior irradiation four peaks, corresponding to QM-2.1b (QM-form and NQM form), **2.1b** and **2.4b** were present in ratio 79.1% (two overlapping peaks), 8% and 12.8 %, respectively. Irradiation at 300 nm resulted in disappearance of **2.1b** and partial conversion of **2.1b** and its **QM-2.1b** into **2.4b**. According to chromatograms, maximal ratio between product and starting materials was reached after 30 min of irradiation and was 83.2% and 16.8%, respectively (Table 2.29). Prolonged irradiation resulted in decomposition of both compounds and formation of oligomers.

QM-2.1b (QM and NQM forms) eluted at 6.2 min, **2.4b** eluted at 23.3 min, **2.1b** eluted at 23.8 min.

HRMS (ESI), *m/z*: calcd. for **2.1b** $C_{17}H_{14}O_4$-H $[M-H]^-$ 281.0814, found 281.0817.

HRMS (ESI), *m/z*: calcd. for **2.4b** $C_{18}H_{16}O_4$-H $[M-H]^-$ 295.0976, found 295.0972.

Table 2.29. Photoreaction between **QM-2.1b** and methanol: HPLC analysis.

Time, min	HPLC - peak area @ 219 nm		
	QM-2.1b	2.4b	2.1b
0	7120568	1153885	723934
10	3316551	4846520	0
20	1727826	5300230	0
30	1125877	5558892	0

Time, min	Percentage of QMP and QM in the mixture, %		
	QM-2.1b	2.4b	2.1b
0	79.1	12.8	8.0
10	40.6	59.4	0.0
20	24.6	75.4	0.0
30	16.8	83.2	0.0

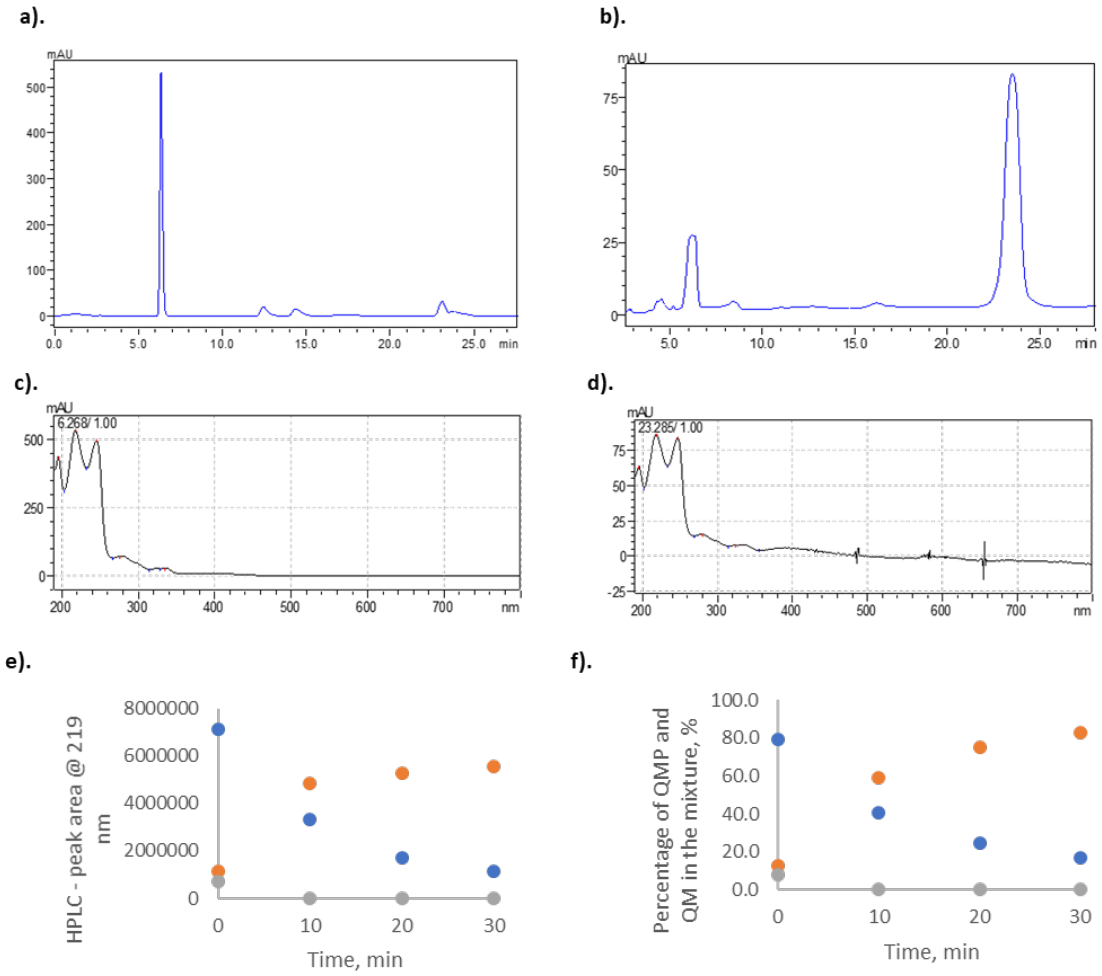

Figure 2.18. Photoreaction between **QM-2.1b** and methanol. **a).** HPLC chromatogram – reaction mixture prior irradiation. **b).** HPLC chromatogram – reaction mixture after 30 min of irradiation at 300 nm. **c).** UV-spectrum of **2.1b**. **d).** UV-spectrum of **2.4b**. **e).** Change in peak areas over time. **f)** Percentage of QMP in the mixture.

Photoirradiation of 2.1a in acetonitrile/water, 1:1

Solution (3.0 mL) that contained **2.1a** (0.0135 mM) and acetonitrile/water (1:1) was irradiated in a quartz cuvette with 2 lamps at 300 nm in Rayonet reactor for 0, 1, 11, 21, and 31 min. According to UV-spectra, short time irradiation (less than 1 min) resulted in formation of corresponding **QM-2.1a** (new absorbance band with maximum at 400 nm), however, prolonged irradiation caused formation of oligomers and resulted in broadening of absorbance bands and dramatic decrease of absorbance at 400 nm.

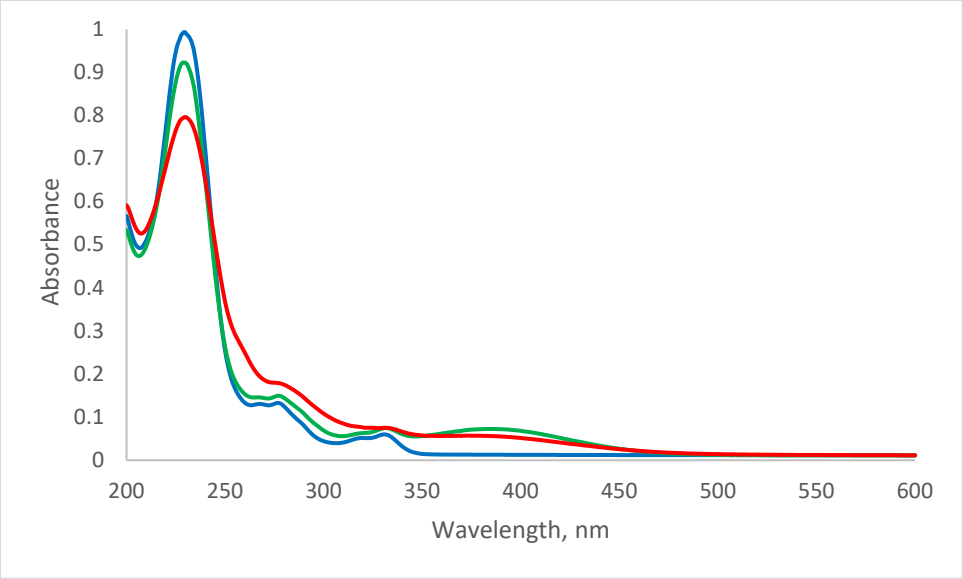

Figure 2.19. Photoirradiation of **2.1a** in acetonitrile/water, 1:1. UV-spectra of **2.1a** prior irradiation (blue), after 1 min of irradiation with 300 nm light (green) and after 30 mins of irradiation with 300 nm light (red).

HPLC analysis. Solution (3.0 mL) that contained **2.1a** (0.5 mM) and acetonitrile/water (1:1) was irradiated with 8 lamps at 300 nm in Rayonet reactor for 0, 5, 10, 15, 35, 55, and 70 min. Reaction progress was monitored via HPLC. System of methanol (50%), acetonitrile (1%) and water (49%) was used as an eluent. Conversion of **2.1a** into primary photoproduct was analyzed at wavelength of 220 nm. According to chromatograms, short time irradiation resulted in formation of one major product, however, prolonged irradiation resulted in decomposition of both compounds and formation of oligomers (Figure 2.19). Attempts to characterized the primary photo-product were unsuccessful due to low conversion and poor stability upon concentration of the reaction mixture.

2.1a eluted at 9.5 min, primary photoproduct eluted at 4.8 min.

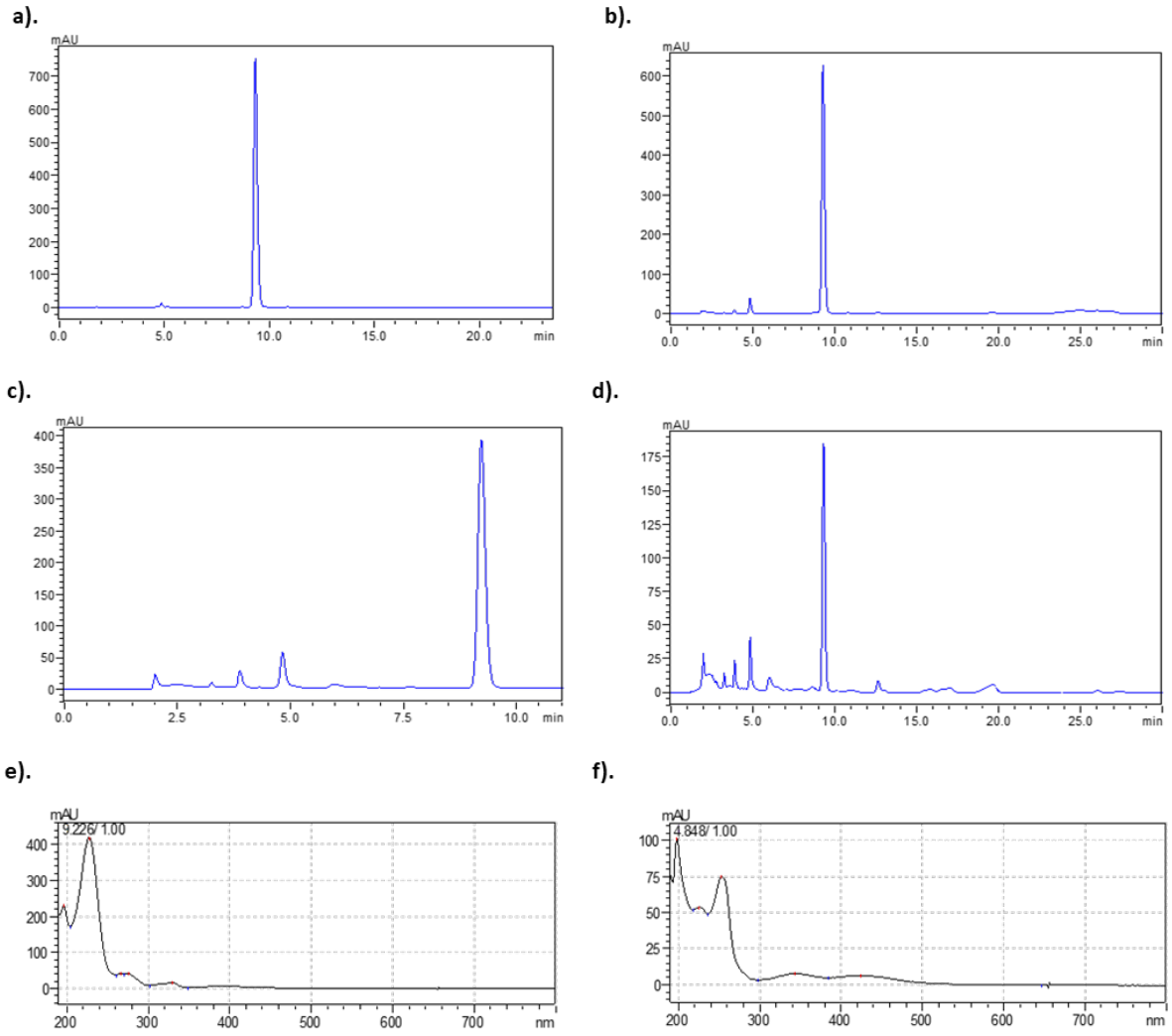

Figure 2.20. Photoirradiation of **2.1a** in aqueous acetonitrile, 1:1. **a).** HPLC chromatogram – reaction mixture prior irradiation. **b).** HPLC chromatogram – reaction mixture after 10 mins of irradiation at 300 nm. **c).** HPLC chromatogram – reaction mixture after 35 mins of irradiation at 300 nm. **d).** HPLC chromatogram – reaction mixture after 70 mins of irradiation at 300 nm. **e).** UV-spectrum of **2.1a**. **f)**. UV-spectrum of primary photoproduct.

In addition, fluorescence spectra of **2.1a** (0.5 mM solution, acetonitrile/water, 1:1) and corresponding NQM obtained after 1 min of irradiation in quartz cuvette (3 mL) in Rayonet reactor with 6 lamps of 300 nm were recorded. 400 nm was chosen as an excitation wavelength as only **QM-2.1** and primary photoproduct had absorption bands at that wavelength.

Photoirradiation of 2.1b in acetonitrile/water, 1:1

Solution (3.0 mL) that contained **2.1b** (0.0135 mM) and acetonitrile/water (1:1) was irradiated with 2 lamps at 300 nm in Rayonet reactor for 0, 1, 11, 21, and 31 min. According to UV-spectra, short time irradiation (less than 1 min) resulted in formation of corresponding NQM (new absorbance band with maximum at 400 nm; $\tau_{1/2}$ ~ 18 s), however, prolonged irradiation caused formation of oligomers and resulted in broadening of absorbance bands and dramatic decrease of absorbance at 400 nm.

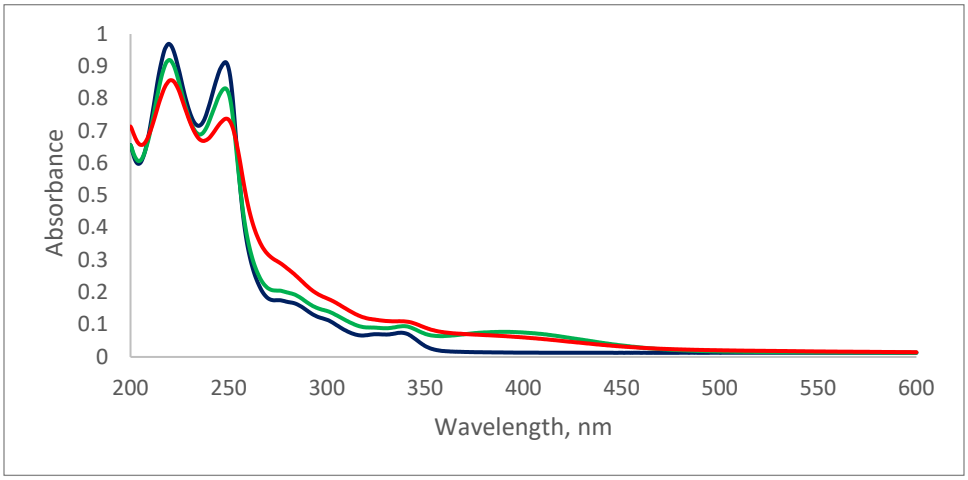

Figure 2.21. Photoirradiation of **2.1b** in acetonitrile/water, 1:1. UV-spectra of **2.1b** prior irradiation (blue), after 1 min of irradiation with 300 nm light (green) and after 30 mins of irradiation with 300 nm light (red).

Solution (3.0 mL) that contained **2.1b** (0.5 mM) and acetonitrile/water (1:1) was irradiated with 8 lamps at 300 nm in a quartz cuvette in Rayonet reactor for 0, 5, 10, 30 and 50 min. Reaction progress was monitored via HPLC. System of methanol (50%), acetonitrile (1%) and water (49%) was used as an eluent. Conversion of **QM-2.1b** (QM and NQM forms) and **2.1b** was analyzed at wavelength of 220 nm. According to chromatograms, irradiation resulted in decomposition of both compounds and formation of oligomers. **QM-2.1b** eluted at 4.5 min, **2.1b** eluted at 11.7 min.

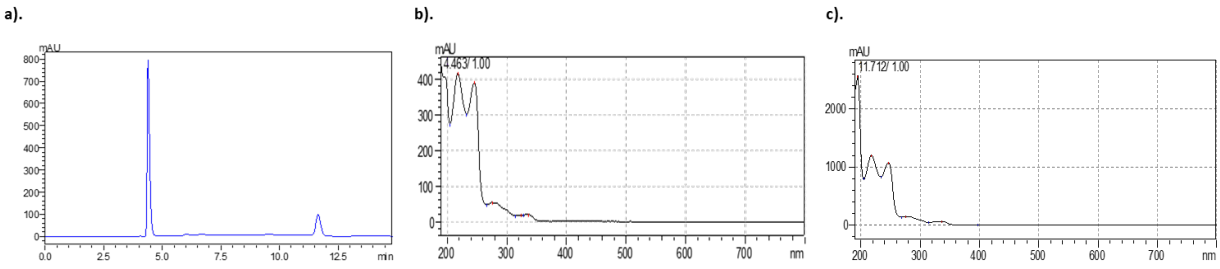

Figure 2.22. Photoirradiation of **QM-2.1b** in aqueous acetonitrile, 1:1. **a).** HPLC chromatogram – reaction mixture prior irradiation. **b).** UV-spectrum of **2.1b**. **c)**. UV-spectrum of primary photoproduct.

In addition, fluorescence spectra of **2.1b** (0.5 mM solution, acetonitrile/water, 1:1) and corresponding **QM-2.1b** obtained after 1 min of irradiation at 300 nm with 6 lamps in a quartz cuvette (3 mL) in Rayonet reactor were recorded. 400 nm was chosen as an excitation wavelength.

Photoreaction between 2.1a and sodium azide

Rate constant determination via LFP

Table 2.30. Decay of **QM-2.1a** obtained from **2.1a** (0.033 mM) in dilute phosphate buffer (pH = 7.41, IS = 0.1 M, 0.005 M) containing various concentration of sodium azide at 25ºC.

Sodium azide, M	k, s^{-1}	Error, s^{-1}
0.01	14.4	0.2
0.01	14.4	0.2
0.01	15.2	0.2
0.025	58.8	0.8
0.025	56	0.9
0.025	58	0.8
0.04	103	1
0.04	99	1
0.04	104	2
0.05	124	1
0.05	122	1
0.05	117	1
0.06	158	2
0.06	158	2
0.06	153	2
0.0675	170	2
0.0675	168	2
0.0675	174	2

HPLC analysis. Solution (3.0 mL) that contained **2.1a** (0.5 mM), sodium azide (0.1 M), phosphate buffer (pH = 7.41, 0.005 M, IS=0.1 M) and acetonitrile/water (1:1) was irradiated in a quartz cuvette with 6 lamps at 300 nm in Rayonet reactor for 0, 5, and 10 min. Reaction progress was monitored via HPLC. System of methanol (51%), acetonitrile (1%) and water (48%) was used as an eluent. "Disappearance" of starting material **2.1a** was observed, no new peaks were formed. Apparently, oligomers were formed and trapped in the column. Wavelength of observation was 220 nm.

2.1a eluted at 8.5 min.

Photoreaction between 2.1a and ethyl vinyl ether

Rate constant determination via LFP

Table 2.31. Decay of **QM-2.1a** obtained from **2.1a** (0.033 mM) in dilute phosphate buffer (pH = 7.41, IS = 0.1 M, 0.005 M) containing various concentration of ethyl vinyl ether at 25ºC.

Ethyl vinyl ether, M	k, s^{-1}	Error, s^{-1}
0.01	0.051	0.001
0.01	0.05	0.001
0.01	0.056	0.001
0.025	0.059	0.001
0.025	0.063	0.002
0.025	0.061	0.002
0.03	0.092	0.002
0.03	0.082	0.002
0.03	0.08	0.001
0.05	0.115	0.001
0.05	0.109	0.002
0.05	0.115	0.001
0.0725	0.138	0.002
0.0725	0.135	0.002
0.0725	0.144	0.002
0.09	0.165	0.004
0.09	0.174	0.004
0.09	0.188	0.003

HPLC analysis. Solution (3.0 mL) that contained **2.1a** (0.5 mM), ethyl vinyl ether (0.1 M), phosphate buffer (pH = 7.41, 0.005 M, IS=0.1 M) and acetonitrile/water (1:1) was irradiated in a quartz cuvette with 6 lamps at 300 nm in Rayonet reactor for 0, 5, 15, and 20 min. Reaction progress was monitored via HPLC. System of methanol (51%), acetonitrile (1%) and water (48%) was used as an eluent. "Disappearance" of starting material was observed, no new peaks were formed. Apparently, oligomers were formed and trapped in the column. Wavelength of observation was 220 nm.

2.1a eluted at 8.5 min.

Photoreaction between 2.1b and sodium azide

Rate constant determination via LFP

Table 2.32. Decay of **QM-2.1b** obtained from **2.1b** (0.033 mM) in dilute phosphate buffer (pH = 7.41, IS = 0.1 M, 0.005 M) containing various concentration of sodium azide at 25ºC. Only slow process has been observed.

Sodium azide, M	k, s^{-1}	Error, s^{-1}
0.01	11.3	0.2
0.01	10.8	0.2
0.01	11.4	0.2
0.025	43.8	0.9
0.025	41	0.9
0.025	43.1	1
0.04	81	1
0.04	75	2
0.04	71	1
0.05	92	1
0.05	87	1
0.05	89	1
0.0675	134	2
0.0675	133	3
0.0675	141	3

Photoreaction between 2.1b and ethyl vinyl ether

Rate constant determination via LFP

Table 2.33. Decay of **QM-2.1b** obtained from **2.1b** (0.033 mM) in dilute phosphate buffer (pH = 7.41, IS = 0.1 M, 0.005 M) containing various concentration of ethyl vinyl ether at 25ºC.

Ethyl vinyl ether, M	k, s^{-1}	Error, s^{-1}
0.01	3860	8
0.01	3859	8
0.01	3853	8
0.03	3878	8
0.03	3870	8
0.03	3888	8
0.06	3916	8
0.06	3903	8
0.06	3904	8
0.08	3918	8
0.08	3927	8
0.08	3920	8
0.095	3929	8
0.095	3933	8
0.095	3939	8

HPLC analysis. Analogous experiments with sodium azide and ethyl vinyl ether were performed with **2.1b**. Formation of new peaks was not observed on HPLC, only "disappearance" of starting material was observed. HPLC eluent systems tried: MeOH (35%), acetonitrile (1%), water (64%) and MeOH (90%), acetonitrile (1%), water (9%).

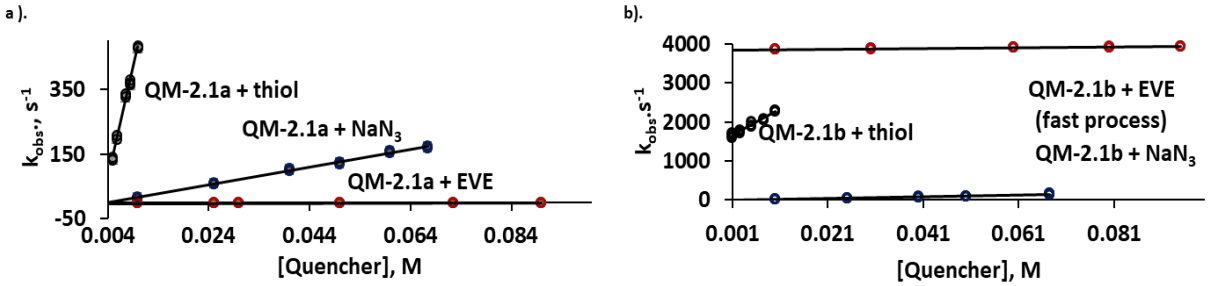

Figure 2.23. Quenching of **QM-2.1a** (**a**) and **QM-2.1b** (**b**) with nucleophiles and EVE.

2.9. References

1. Arumugam, S.; Popik, V. V. *J. Am. Chem. Soc.* **2009**, 131, 11892-11899.
2. Kulikov, A.; Arumugam, S.; Popik, V. V. *J. Org. Chem*. **2008**, 73, 7611-7615.
3. Arumugam, S.; Popik, V. V. *J. Am. Chem. Soc.* **2011**, 133, 5573-5579.
4. Nekongo, E. E.; Popik, V. V. *J. Org. Chem.* **2014**, 79 (16), 7665-7671.
5. Arumugam, S.; Popik, V. V. *Photochem. Photobiol. Sci.*, **2012**, 11, 518-521.
6. Arumugam, S.; Guo, J.; Mbua, N. E.; Friscourt, F.; Lin, N.; Nekongo, E.; Boons, G.-J.; Popik, V. V. *Chem. Sci*. **2014**, 5, 1591-1598.
7. Popik, V. V.; Boons, G.-J.; Guo, G.; Arumugam, S.; Nekongo, E.; Lin, N. *Methods for reacting cysteine residues in peptides and proteins*. US 2014/0054163 A1, Feb. 27, 2014.
8. Arumugam, S.; Popik, V. V. *J. Am. Chem. Soc.* **2012**, 134 (20), 8408-8411.
9. Popik, V. V.; Arumugam, S. *Methods for labeling a substrate having a plurality of thiol groups attached thereto*. US 2013/0281656 A1, Oct. 24, 2013.
10. Arumugam, S.; Orski, S. V.; Locklin, J.; Popik, V. V. *J. Am. Chem. Soc.* **2012**, 134 (1), 179-182.
11. Arumugam, S.; Popik, V. V. *J. Am. Chem. Soc.* **2011**, 133 (39), 15730-15736.
12. Diao, L.; Yang, C.; Wan, P. *J. Am. Chem. Soc.* **1995**, 117, 5369-5370.
13. Chiang, Y.; Kresge, A. J.; Zhu, Y. *J. Am. Chem. Soc.* **2003**, 125, 6349-6356.
14. Chang, J. A.; Kresge, A. J.; Zhan, H.-Q.; Zhu, Y. *J. Phys. Org. Chem.* **2004**, 17, 579-585.
15. Chiang, Y.; Kresge, A. J.; Zhu, Y. *J. Am. Chem. Soc.* **2000**, 122, 9854-9855.
16. Birks, J. B. *Photophysics of Aromatic Molecules*; Wiley Interscience: New York, 1970; 703 p.
17. Fletcher, A. N. *Photochem. Photobiol.* **1969**, 9 (5), 439-444.
18. Kuzmič, P.; Pavlíčková, L.; Velek, J.; Souček, M. *Collect. Czech. Chem. Commun*. **1986**, 51, 1665.
19. Girel, J. A. K., "Chemical Reaction Kinetics of the Kinetics of the Pictet-Spengler Reaction" (2016). College of Science and Health Theses and Dissertations. 142.

https://via.library.depaul.edu/sch_etd/142

20. Singh, M. S.; Nagaraju, A.; Anand, N., Chowdhuty, S. *RSD Adv.* **2014**, 4, 55924-55959.
21. Popik, V. V.; Arumugam, S. *Methods for labeling a substrate using a hetero-Diels-Alder reaction*. US 2011/0257047 A1, Oct. 20, 2011.
22. Padwa, A.; Dehm, D.; One, T.; Lee, G. A. *J. Am. Chem. Soc.* **1975**, 97 (7), 1837-1845.

CHAPTER 3

TOWARDS THE LIGHT-INDUCED "SMART" POLYMERIZATION BASED ON THE REACTION BETWEEN O-NAPHTHOQUINONE METHIDES AND THIOLS

3.1. Introduction

Chapter 1 has illustrated the unicity of reactivity of *o*-QMs towards nucleophiles and electron-rich dienophiles. Simple synthesis and long shelf life of o-QMPs, as well as catalyst free photogeneration of o-QMs make these reactive species great candidates for application in chemical biology and material science. *O*-hydroxybenzyl chromophore has little absorbance beyond 250 nm, and thus o-quinone methide precursors are not suitable for biological applications. However, extended conjugation system of 2-hydroxynaphthyl chromophore exhibit absorbance beyond 350 nm.[1-3] Thus, the research towards application of o-QMs is focused on QMs and their precursors with extended conjugation systems, such as naphthyl, binaphthyl, anthryl and phenanthryl. Our group has demonstrated multiple examples of the application of o-NQMs and their precursors is post-polymerization modification (PPM) of the surface.[4-8] The main advantage of given technique is an ability to immobilize multiple different chemical functionalities onto substrates of covalently grafted polymer films.

Surface modifications are based on the ability of *o*-NQMPs to generate *o*-NQMs upon light irradiation and the reactivity of the later ones to undergo irreversible Diels-Alder reaction and reversible reaction with nucleophiles, such as thiols. The nucleophilic addition of thiols to o-NQMs, as well as Diels−Alder photo-click reaction have been shown to be orthogonal to azide−alkyne click chemistry.[4-8] This feature enables us to perform surface derivatization followed by azide/alkyne click modification to create multifunction

surface. Additionally, photolithographic methods allow us to perform high-resolution surface patterning.[4-8]

In this project we were interested to investigate the ability of *o*-NQMPs **3.1** and **3.2** to form "smart" polymers in the solution, which potentially can be applied for hydrogel formation. The "smart" polymer could be generated on demand upon UV-light irradiation of (3,5-dihydroxynaphthalen-2-yl)methyl derivatives decorated with thiol moieties and undergo the photo-induced degradation upon light irradiation, when vinyl ethers were employed as *o*-NQM trapping agents (Scheme 2.1).

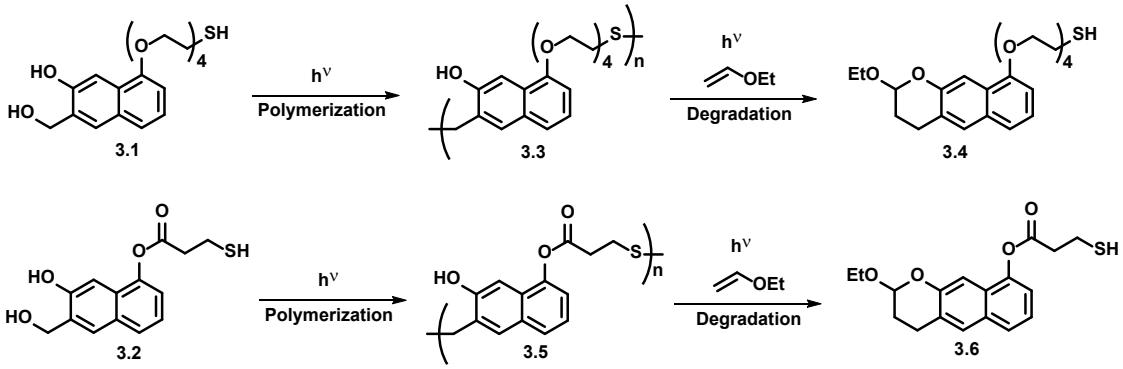

Scheme 3.1. "Smart" polymers from (3,5-dihydroxynaphthalen-2-yl)methyl derivatives decorated with thiol moieties.

3.2. Synthesis of Monomers 3-(Hydroxymethyl)-8-(2-(2-(2-(2-mercaptoethoxy)ethoxy)ethoxy)-ethoxy)-naphthalen-2-ol (3.1) and 7-Hydroxy-6-(hydroxymethyl)naphthalen-1-yl 3-mercaptopropanoate (3.2)

The synthesis of monomer **3.1** was started with esterification of commercially available 3,5-dihydroxy-2-naphthoic acid **3.7** and was followed by the reduction with lithium aluminum hydride to give alcohol **3.8**. The protection of phenolic hydroxyl in the position 2- of naphthalene moiety and of benzylic hydroxyl was performed with 2,2-dimethoxypropane and produced compound **3.9** in 95 % yield. The tetraethylene glycol (TEG) linker was incorporated into **3.9** via Williamson ether synthesis and resulted in formation of **3.10** in 65 %. Compound **3.10** thus obtained was converted in two steps into corresponding thioate **3.12**.

Deprotection of which under basic conditions resulted in the formation of the desired monomer **3.1** in 67 % yield (Scheme 3.3)

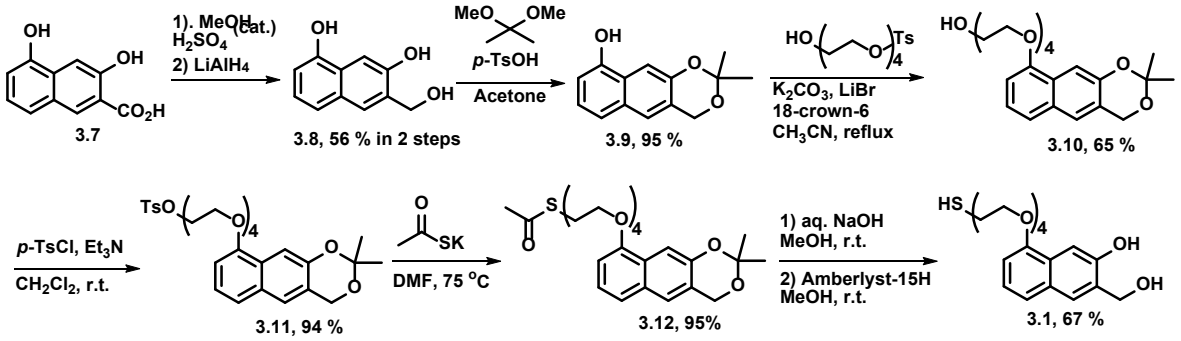

.

Scheme 3.2. Attempted synthesis of **3.1**.

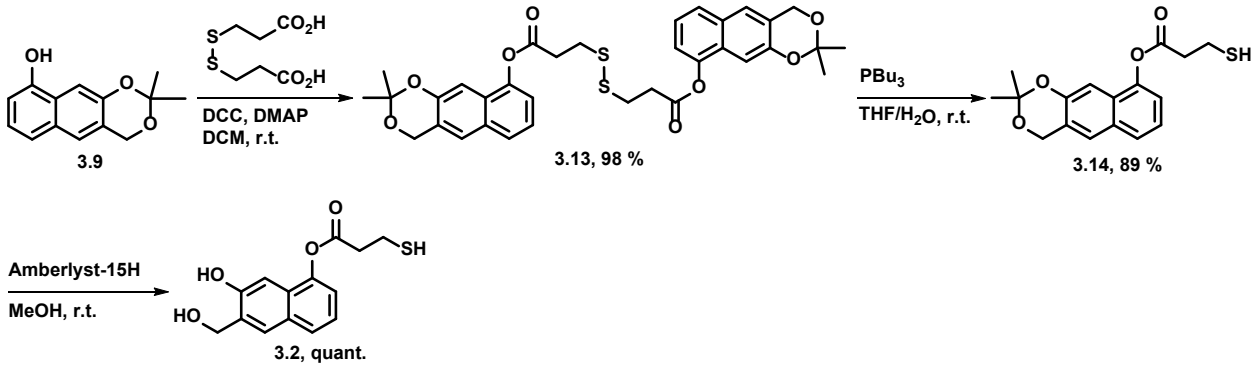

Scheme 3.3. Attempted synthesis of **3.2**.

Synthesis of the monomer **3.2** was started from the same precursors as the synthesis of **3.1**. DCC coupling between obtained 2,2-dimethyl-4H-naphtho[2,3-d][1,3]dioxin-9-ol **3.9** and commercially available 3,3'-dithiopropionic acid gave compound **3.13** in 98 % yield. Reduction of disulfide **3.13** with tri-*n*-butylphosphine, followed by deprotection of hydroxyl groups yielded the desired compound **3.2**. Even though, compound **3.2** was formed and isolated quantitatively, it was found to be very unstable towards acid promoted decomposition via cleavage of ester C-O bond and towards oxidation into corresponding disulfide by oxygen in the air. Unfortunately, since compound **3.2** appeared to be extremely unstable, its ability to form polymers was not studied.

3.3. Towards the synthesis of "smart" polymer

As it was mentioned earlier, Popik reported a novel approach of surface patterning, which was based on the reaction between 2-napthoquinone-3-methide (o-NQM1) and thiols ($k_{RSH} \approx 2.2 \times 10^5$ $M^{-1}s^{-1}$).[7,36] The example demonstrated the ability to perform photo-immobilization and further photo-replacement of NQMP-derivatized substrates on a thiol-functionalized surface.[36,46]

To the best of our knowledge, photoinduced polymerization of NQMP derivatives decorated with thiol moieties in the solution has not been studied. Herein, we investigate the ability of the synthesized monomer **3.1** to form oligomers and polymers under various conditions (Scheme 3.4). Our studies were started with observation of changes in the UV-spectrum of the argon-purged solution of compound **3.1** in acetonitrile/water (95:5) upon irradiation with 300 nm light in Rayonet reactor. We expected to observe broadening of the absorption bands due to polymer formation. And indeed, prolong irradiation resulted in broadening of the spectrum (Figure 3.1).

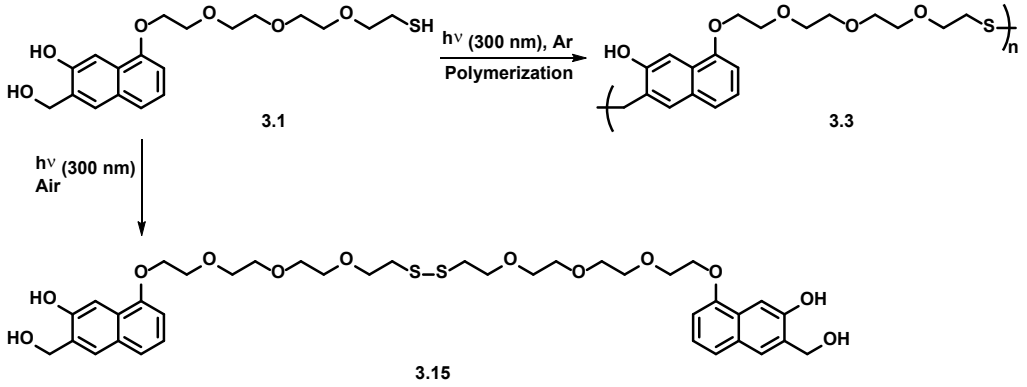

Scheme 3.4. Polymerization of compound **3.1**.

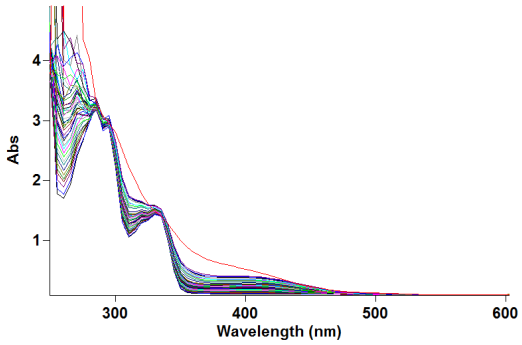

Figure 3.1. UV-spectra of the compound **3.1** (0.45 mM) in acetonitrile/water (95:5) in inert atmosphere prior UV-light irradiation and after irradiation with 300 nm light for 1-30 min.

Analysis of the reaction mixture via HPLC also confirmed that prolong irradiation with 300 nm light in the inert atmosphere resulted in the formation of short oligomers. Formation of relatively long oligomers and polymers could not be detected via HPLC as they were most likely trapped in the column (Figure 3.2).

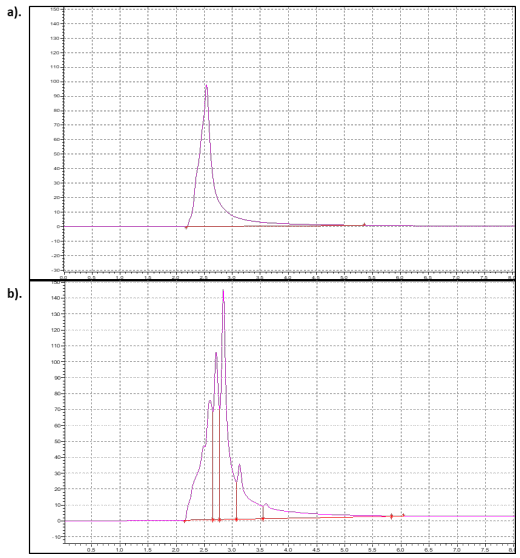

Figure 3.2. HPLC chromatograms of photoirradiation of the solution of **3.1** (0.45 mM). **a).** HPLC chromatogram prior UV-light irradiation. **b).** HPLC chromatogram after irradiation with 300 nm light for 30 mins.

Further analysis was conducted via GPC at various conditions. For instance, UV-light irradiation of argon-purged reaction mixture resulted in the formation of oligomers of up to 4 units. On the other hand,

conducting photoirradiation in the air saturated solution resulted in exclusive formation of disulfide **3.15**. Formation of disulfide was also confirmed with MALDI-TOF analysis. Since, presence of singlet oxygen prevented the polymerization, all other experiments were conducted in the inert atmosphere. One of the major problems, that we faced was the light penetration and the need in having relatively high concentration of monomer **3.1** in order to achieve oligomers with higher number of units. Upon irradiation the clear solution of a monomer had a tendency to become cloudy and, thus, prevented the light from penetration into the solution. Attempts to vary organic solvents, which would not absorb light at 300 nm and would be miscible with water, such acetonitrile and dioxane, did not show a significant difference. Varying the ratio between organic solvent and water in order to improve solubility of the oligomers and to prevent radical processes also did give a positive result. We also attempted to introduce sodium hydroxide and triethyl amine into the reaction mixture. We expected that increasing the pH of the solution would increase the nucleophilicity of the thiol, and thus, may improve the solubility of the compounds in aqueous solutions, as well as increase the rate of formation of the desired oligomers/polymers. Indeed, introduction of sodium hydroxide into the reaction mixture resulted in the increased formation of tetramers and trimers. Unfortunately, none of the attempted conditions produced oligomer of more than 4 units.

Potentially, current results could be explained via reversibility of the reactions between *o*-NQMs and nucleophiles. Since all the experiment were conducted in the presence of water, *o*-NQM generated upon light irradiation from thioethers **3.1** and **3.3** could react with water, causing formation of starting material **3.1** and depolymerization of **3.3**.

3.4. Conclusions and Future Directions

Herein, we attempted to synthesize “smart” polymers in the solution, that could undergo polymerization and degradation on demand upon UV-light irradiation. Unfortunately, one of the synthesized monomers

was unstable towards acid-promoted decomposition and oxidation, and thus its ability to form polymers was not tested. Monomer **3.2** was found to form oligomers of up to 4 units, however, formation of a polymer was not achieved. As potential problems were identified as poor solubility of oligomers and chance of depolymerization due to hydrolysis, polymerization between two monomers, such as 3-hydroxy-2-naphthalenemethanol and a linker with two ending thiol groups could be tested. In that case linker could be introduced into the reaction mixture in excess and, hopefully, prevent the hydrolysis of the formed oligomers.

3.5. Experimental Procedures and Compounds Data

3.5.1. General information

Column chromatography was performed using 40-63 μm silica gel. NMR spectra were recorded on a 400 MHz NMR spectrometer, unless otherwise noticed. Chemical shifts were referenced to residual solvent proton or carbon signals. Melting points were determined using a Fisher-Johns melting point apparatus. High resolution mass spectra were obtained using electron spray ionization and orbitrap mass analyzer. Solutions were prepared using HPLC grade water, methanol and acetonitrile. Photoreactions were conducted using a Rayonet photoreactor equipped with fifteen 4W 300 nm fluorescent lamps. GPC analysis of the samples were conducted using Shimadzu GPC.

3.5.2. Experimental Procedures and Compound Data

All reagents were obtained from commercial sources and were used without further purification unless otherwise noted. 2,2-Dimethyl-4H-naphtho[2,3-d][1,3]dioxin-9-ol **3.9** was prepared as reported previously.[9]

2-(2-(2-(2-hydroxyethoxy)ethoxy)ethyl 4-methylbenzenesulfonate (mono-Ts-TEG). Tetraethylene glycol (50 g, 262 mmol) was dissolved in DCM (30 mL). 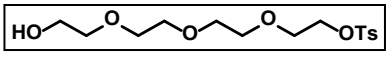

The solution was cooled to 0 °C and Et_3N (4 g, 39 mmol) was added. Subsequently tosylchloride (5 g, 26.2

mmol) was added in portions and the solution was allowed to reach r.t. The reaction mixture was stirred overnight. The next day DCM (30 mL) and water (30 mL) were added. Organic layer was separated and aq. layer was extracted with DCM (2 x 30 mL). Combined organic phases were washed with 5 % aq. HCl, then with saturated $NaHCO_3$ and brine, dried over Na_2SO_4. The product was purified via column chromatography (DCM/EtOAc, 1:4) and was isolated as colorless oil (8.81 g, 96.5 %).

^{1}H NMR (400 MHz, $CDCl_3$): 7.80-7.78 (2H, dd, *J* = 8.0 and 2.4 Hz), 7.33 (2H, d, *J* = 8.0 Hz), 4.16-4.14 (2H, dd, *J* = 4.4 and 1.6 Hz), 3.69-3.58 (14H, m), 2.44 (3H, s).

^{13}C NMR (100 MHz, $CDCl_3$): 144.78, 132.9, 129.8, 127.9, 72.4, 70.7, 70.6, 70.4, 70.3, 69.2, 68.7, 61.7, 21.6.

2-(2-(2-(2-((2,2-dimethyl-4H-naphtho[2,3-d][1,3]dioxin-9-yl)oxy)ethoxy)ethoxy)ethoxy)ethanol (3.10).

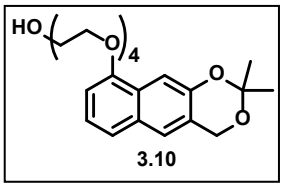

3.10

A mixture of **mono-Ts-TEG** (3.470 g, 10 mmol), compound **3.9** (2.300 g, 10 mmol), K_2CO_3 (2.760 g, 20 mmol), LiBr (10 mol %), and 18-crown-6 (10 mol %) in acetonitrile (300 mL) was refluxed for 24 h. The resulting suspension was filtered and the residue was washed with acetone. Combined organic solution was evaporated and the residue was purified via column chromatography (Hexanes/EtOAc, 1:6). The product **3.10** was isolated as a yellow oil (2.743 g, 65 %).

IR: 3268 (broad); 2900; 1604; 1448; 1263; 1076; 737 cm^{-1}.

^{1}H NMR (400 MHz, $CDCl_3$): 7.65 (1H, s), 7.42 (1H, s), 7.31-7.29 (1H, m), 7.22-7.18 (1H, m), 6.73 (1H, d, *J* = 8.0 Hz), 5.06 (2H, d, *J* = 1.6 Hz), 4.29-4.26 (2H, dd, *J* = 4.4 and 1.6 Hz), 3.99-3.96 (2H, dd, *J* = 4.4 and 1.6 Hz), 3.82-3.79 (2H, m), 3.73-3.67 (8H, m), 3.61-3.59 (2H, m), 1.60 (6H, s).

^{13}C NMR (100 MHz, $CDCl_3$): 153.6, 149.4, 129.4, 126.1, 123.7, 123.1, 121.4, 119.8, 107.1, 104.6, 99.8, 72.5, 71.0, 70.7, 70.6, 70.4, 69.9, 67.8, 61.8, 61.2, 25.0.

HRMS (ESI), *m/z*: calcd. for $C_{22}H_{30}O_7Na$ $[M+Na]^+$ 429.1884, found 429.1884.

2-(2-(2-(2-((2,2-dimethyl-4H-naphtho[2,3-d][1,3]dioxin-9-yl)oxy)ethoxy)ethoxy)ethoxy)ethyl 4-methyl-benzene-sulfonate (3.11). Compound **3.10** (2.743 g, 6.5 mmol) was dissolved in DCM (30 mL), then *para*- tosylchloride (1.5 g, 7.8 mmol) and Et_3N (2.3 mL, 31.4 mmol) were added. The mixture was stirred at r.t. for 48 h, then mixture was quenched with water and the product was extracted with DCM (3 x 50 mL) and concentrated. The residue was purified via column chromatography (Hexanes/EtOAc, 6:1). The product **3.11** was isolated as a brown oil (3.748 g, 94 %).

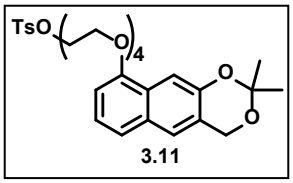

3.11

IR: 2988; 2901; 1604; 1447; 1354; 1093; 1055; 919 cm^{-1}.

^1H NMR (400 MHz, $CDCl_3$): 7.79-7.77 (2H, dd, *J* = 8.0 and 2.4 Hz), 7.64 (1H, s), 7.42 (1H, s), 7.32-7.29 (3H, m), 7.21-7.17 (1H, m), 6.72 (1H, d, *J* = 8.0 Hz), 5.06 (2H, s), 4.27-4.25 (2H, dd, *J* = 4.4 and 1.6 Hz), 4.14-4.12 (2H, dd, *J* = 4.4 and 1.6 Hz), 3.97-3.95 (2H, m), 3.78-3.76 (2H, m), 3.67-3.65 (4H, m), 3.60-3.57 (4H, m), 2.41 (3H, s), 1.59 (6H, s).

^{13}C NMR (100 MHz, $CDCl_3$): 153.6, 149.3, 144.7, 133.0, 129.8, 129.4, 128.5, 127.9, 126.1, 123.7, 123.1, 121.4, 119.8, 110.0, 107.0, 104.5, 99.7, 71.0, 70.7, 70.7, 70.6, 69.8, 69.2, 68.6, 61.2, 24.9, 21.6.

HRMS (ESI), *m/z*: calcd. for $C_{29}H_{36}O_9SNa$ $[M+Na]^+$ 583.1972, found 583.1971.

S-(2-(2-(2-(2-((2,2-dimethyl-4H-naphtho[2,3-d][1,3]dioxin-9-yl)oxy)ethoxy)ethoxy)ethoxy)ethyl) ethanethioate (3.12). Compound **3.11** (3.5 g, 6.1 mmol) was dissolved in anhydrous DMF (15 mL) under N_2, then potassium thioacetate (1.39 g, 12.2 mmol) was added. The reaction mixture was stirred at 75 ^oC overnight. The next day the solvent was removed, EtOAc (100 mL) and water (50 mL) were added. The layers were separated and aqueous layer was extracted with EtOAc. The combined organic layers were dried over Na_2SO_4. The residue was purified via column chromatography (EtOAc). The product **3.12** was isolated as a yellow oil (2.783 g, 95 %).

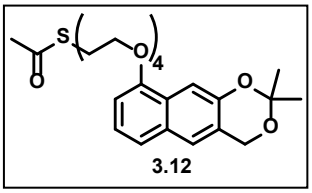

3.12

IR: 2987; 2901; 1688; 1508; 1447; 1091; 880 cm^{-1}.

^{1}H NMR (400 MHz, $CDCl_3$): 7.66 (1H, s), 7.42 (1H, s), 7.29-7.31 (1H, m), 7.22-7.18 (1H, m), 6.72 (1H, d, *J* = 8.0 Hz), 5.06 (2H, s), 4.28-4.26 (2H, dd, *J* = 4.4 and 1.6 Hz), 3.98-3.95 (2H, m), 3.78-3.76 (4H, m), 3.72-3.70 (2H, m), 3.66-3.57 (4H, m), 3.10-3.06 (2H, m), 2.32 (3H, s), 1.59 (6H, s).

^{13}C NMR (100 MHz, $CDCl_3$): 195.5, 153.6, 149.4, 129.4, 126.1, 123.7, 123.0, 121.4, 119.8, 107.1, 104.5, 99.7, 71.0, 70.7, 70.6, 70.3, 69.8, 69.9, 67.8, 61.2, 30.5, 28.8, 25.0.

HRMS (ESI), *m/z*: calcd. for $C_{24}H_{32}O_7SNa$ $[M+Na]^+$ 487.1761, found 487.1762.

3-(hydroxymethyl)-8-(2-(2-(2-(2-mercaptoethoxy)ethoxy)ethoxy)ethoxy)naphthalen-2-ol (3.1).

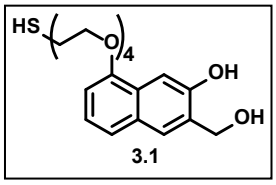

3.1

The thioester **3.12** (2.5 g, 5.2 mmol) was dissolved in methanol (20 mL), aq. NaOH solution (2M, 52 mmol, 26 mL) was added. The reaction mixture was stirred at r.t. overnight, then acidified by the addition of HCl (2M, 50 mL). The aqueous layer was extracted twice with EtOAc and combined organic fractions were dried over Na_2SO_4 and concentrated. The residue was dissolved in MeOH (10 mL) and Amberlyst-15H (1 g) was added. After 1 h the mixture was filtrated and purified via column chromatography (Hexanes/EtOAc, 1:6). The product **3.1** was isolated as a brown oil (1.50 g, 67 %).

IR: 3283 (broad); 2912; 2239 (S-H); 1604; 1448; 1263; 1078; 738 cm^{-1}.

^{1}H NMR (400 MHz, $CDCl_3$): 8.14 (1H, s), 7.65 (1H, s), 7.53 (1H, s), 7.30-7.28 (1H, m), 7.18-7.14 (1H, m), 6.73 (1H, d, *J* = 7.6 Hz); 4.87 (2H, d, *J* = 1.6 Hz); 4.24-4.22 (2H, dd, J = 4.4 and 1.6 Hz); 3.89-87 (2H, dd, J = 4.4 and 1.6 Hz); 3.77-3.68 (8H, m); 3.65-3.61 (2H, m), 3.32-3.29 (1H, m), 2.84-2.81 (2H, m); 2.01 (1H, s, SH).

^{13}C NMR (100 MHz, $CDCl_3$): 153.4, 153.3, 129.4, 128.9, 127.0, 126.9, 123.2, 120.6, 106.3, 105.1, 71.0, 70.7, 70.7, 70.4, 69.8, 69.6, 68.5, 63.4, 38.2.

HRMS (ESI), *m/z*: calcd. for $C_{19}H_{26}O_6S$-H $[M-H]^-$ 381.1377, found 381.1371.

Bis(2,2-dimethyl-4H-naphtho[2,3-d][1,3]dioxin-9-yl) 3,3'-disulfanediyldipropionate (3.13).

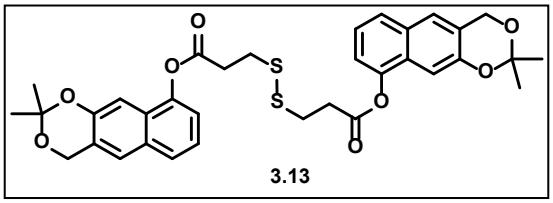

3.13

3,3'-Dithiopropionic acid (1.05 g, 5 mmol), compound **3.9** (2.3 g, 10 mmol) and DMAP (200 mg, 1.67 mmol) were dissolved in anhydrous DCM (100 mL), then DCC (2.3 g, 11.1 mmol) was added. Reaction mixture was stirred at r.t. under N_2 overnight. The next day mixture was filtered and the filtrate was washed with water, brine and dried over Na_2SO_4. The product **3.13** was purified via column chromatography (EtOAc/Hexanes, 1:6) and was isolated as white solid (3.126 g, 98 %).

M.p. = 123 ºC

^{1}H NMR (400 MHz, $CDCl_3$): 7.61 (2H, d, *J* = 8.0 Hz), 7.51 (2H, s), 7.31-7.27 (2H, m), 7.23 (2H, s), 7.18 (2H, d, *J* = 8.0 Hz), 5.06 (4H, s), 3.21-3.18 (8H, m), 1.59 (12H, s).

^{13}C NMR (100 MHz, $CDCl_3$): 170.3, 150.4, 145.4, 129.7, 127.2, 125.5, 123.8, 123.2, 121.9, 118.0, 105.8, 100.1, 61.1, 34.3, 33.0, 25.0.

HRMS (ESI), *m/z*: calcd. for $C_{34}H_{34}O_8S_2Na$ $[M+Na]^+$ 657.1587, found 657.1590.

2,2-Dimethyl-4H-naphtho[2,3-d][1,3]dioxin-9-yl 3-mercaptopropanoate (3.14). Compound **3.13** (1.076 g, 1.69 mmol) was dissolved in THF (17 mL) and tri-*n*-butylphosphine (485 µL, 1.89 mmol) was added at r.t. After several minutes H_2O (160 µL) was added and the mixture was stirred at r.t. overnight. On the next day solvent was evaporated and the product **3.14** was purified via column chromatography (DCM). The product **3.14** was isolated as white crystals (906 mg, 89 %).

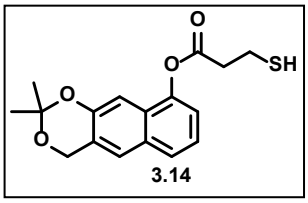

3.14

IR: 2991; 2560(S-H); 1748; 1506; 1448; 1070; 837 cm^{-1}.

^{1}H NMR (400 MHz, $CDCl_3$): 7.62 (1H, d, *J* = 8.0 Hz), 7.51 (1H, s), 7.32-7.28 (1H, m), 7.23 (1H, s), 7.19 (2H, d, *J* = 8.0 Hz), 5.06 (2H, s), 3.09-3.06 (2H, m), 2.99-2.93 (2H, m), 1.80 (1H, m), 1.60 (6H, s).

^{13}C NMR (100 MHz, $CDCl_3$): 170.2, 150.4, 145.4, 129.7, 127.2, 125.5, 123.8, 123.2, 121.9, 118.0, 105.8, 100.1, 61.1, 38.6, 25.0, 19.8.

HRMS (ESI), *m/z*: calcd. for $C_{17}H_{18}O_4SNa$ $[M+Na]^+$ 341.0818, found 341.0818.

7-Hydroxy-6-(hydroxymethyl)naphthalen-1-yl 3-mercaptopropanoate (3.2). Compound **3.14** (320 mg, 1 mmol) was dissolved in methanol (20 mL) and Amberlyst-15H (650 mg) was added. The mixture was stirred at r.t. for 2 h and then was filtrated and concentrated. The product **2** was obtained as white crystals (280 mg, quant.). Compound **3.2** underwent rapid decomposition. Attempts to collect ^{13}C NMR and HRMS (ESI) of the sample were unsuccessful.

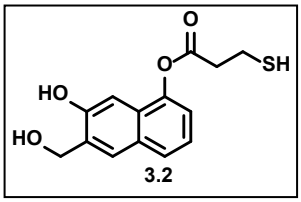

3.2

^1H NMR (400 MHz, $CDCl_3$): 7.59 (1H, d, *J* = 8.0 Hz), 7.51 (1H, s), 7.30-7.28 (1H, m), 7.19-7.18 (2H, m), 4.90 (2H, s), 3.47 (1H, s), 3.07-3.03 (2H, m), 2.97-2.91 (2H, m), 1.79 (1H, m).

DIP analysis in GC-MS gave peak of molecular ion 278, which corresponded to molecular weight of the product **3.2** ($C_{14}H_{14}O_4S^{\cdot+}$ 278) (Figure 3.2).

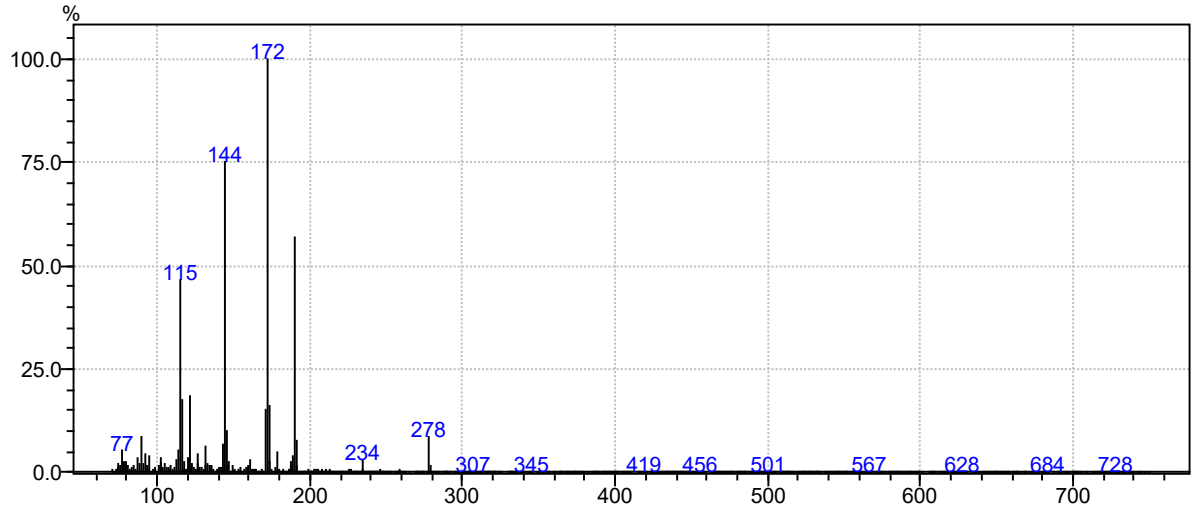

Figure 3.3. DIP analysis in GC-MS of **3.2**

3.5.3. Experiments toward Polymerization

Irradiation of 3-(hydroxymethyl)-8-(2-(2-(2-(2-mercaptoethoxy)ethoxy)ethoxy)ethoxy)naphthalen-2-ol (1) at 300 nm under various conditions

Solution (3.0 mL) of compound **3.1** (0.45 mM) in acetonitrile/water (95:5) saturated with Ar was irradiated with 15 UV-lamps at 300 nm in a quartz cuvette in Rayonet photoreactor for 0-30 min and UV-spectra were recorded. Broadening of absorbance bands and increase of absorbance at 280 nm, 320 nm and 400nm was observed. Current observation could indicate formation of oligomers/polymerization of starting material **3.1.**

HPLC ANALYSIS: Solution (3.0 mL) of compound **3.1** (0.45 mM) in acetonitrile/water (9:1) saturated with Ar was irradiated with 15 UV-lamps at 300 nm in a quartz cuvette in Rayonet photoreactor for 0, 1, 3, 10, 20, and 30 min. Reaction progress was monitored via HPLC. Methanol (100%) was used as an eluent, analysis was performed at wavelength of 220 nm. According to chromatograms, prolong irradiation resulted in formation of oligomers **3.3**.

Compound **3.1** eluted at 2.6 min, products **3.3** eluted at 2.7 min, 2.9 min, 3.2 min and 3.7 min.

GPC ANALYSIS: Experiments were performed with air saturated solutions.

Samples, containing compound **3.1** (10 mg, 26 μmol) in acetonitrile/water, 9:1 (35 mL), were irradiated at 300 nm for 0 min, 1 min, 7.5 min and 10 min. After irradiation the solvent was evaporated. Resulting mixtures were dissolved in chloroform and GPC Data were collected. For the samples of 1 min and 10 min of irradiation MALDI-tof Data were collected. According to GPC data and MALDI-tof data, only dimerization of compound **3.1** that resulted in formation of disulfide **3.15** occurred. Formation of desired oligomers/polymers **3.3** was not observed.

MALDI-tof: *m/z*: calcd. for compound **3.1** $C_{19}H_{26}O_6SNa$ $[M+Na]^+$ 405.1342, found 405.3; *m/z*: calcd. for compound **3.15** $C_{38}H_{50}O_{12}S_2Na$ $[M+Na]^+$ 785.2636, found 785.3. M/z: calcd. for compound **3.3,** n=2 $C_{38}H_{50}O_{11}S_2Na$ $[M+Na]^+$ 769.2687, was not detected.

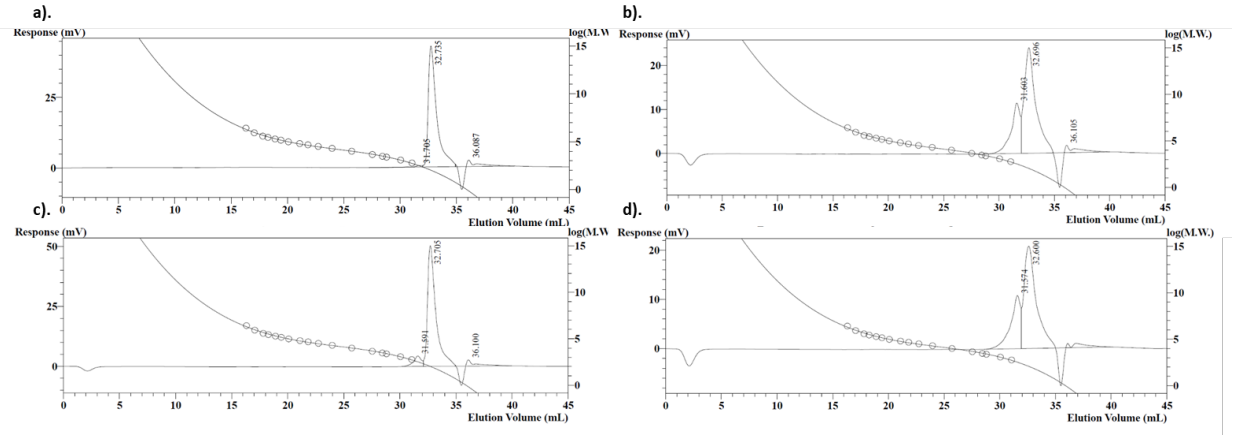

Figure 3.4. GPC data. Starting material **3.1** eluted at ~32.7 mL, disulfide **3.15** eluted at ~31.6 mL. Experiment was done in air saturated solution. **a).** Prior irradiation. **b).** 1 min irradiation at 300 nm. **c).** 7.5 min irradiation at 300 nm. **d).** 10 min irradiation at 300 nm.

GPC ANALYSIS: Experiments were performed in inert atmosphere (Ar). All solutions were prepared using freeze-pump-thaw technique and Schlenk flask.

Experiments in acetonitrile/water in the presence of Et_3N.

Sample, containing compound **3.1 (**10 mg, 26 µmol) in acetonitrile/water, 6:1 (35 mL) and Et_3N (3 µL, 26 µmol), was irradiated at 300 nm in the inert atmosphere for 40 minutes. After irradiation the solvent was evaporated. Resulting mixture were dissolved in chloroform and GPC Data was collected.

Compound **3.3**, n=2 (molecular weight ~747) eluted at ~31.6 mL, compound **3.3**, n=3 (molecular weight ~1110) eluted at ~30.4 mL.

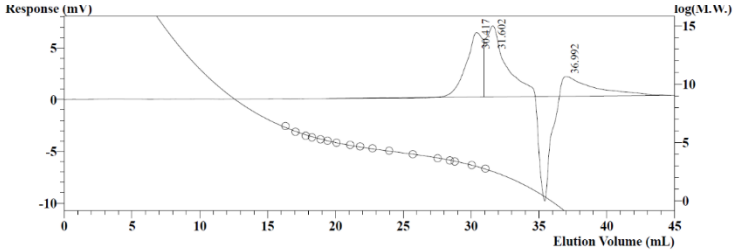

Figure 3.5. GPC data. 40 min irradiation at 300 nm in inert atmosphere.

Sample, containing compound **3.1 (**10 mg, 26 µmol) in acetonitrile/water, 1:1 (35 mL) and Et_3N (20 µL, 174 µmol), was irradiated at 300 nm in the inert atmosphere for 2 h. During irradiation the mixture became cloudy. After irradiation the solvent was evaporated. Resulting mixture were dissolved in chloroform and GPC Data was collected.

Compound **3.3**, n=3 (molecular weight ~1110) eluted at ~30.3 mL, compound **3.3**, n=4 (molecular weight ~1474) eluted at ~29.7 mL.

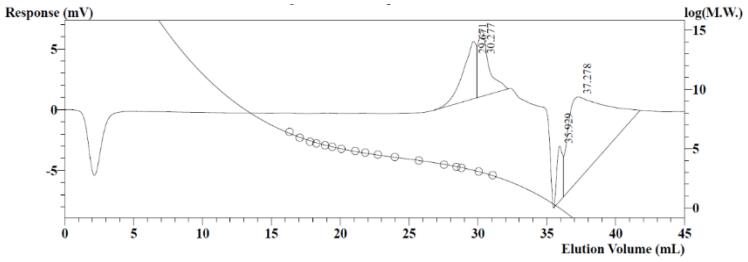

Figure 3.6. GPC data. 2 h irradiation at 300 nm in inert atmosphere.

Experiments in dioxane/water in the presence of Et_3N.

Sample, containing compound **3.1 (**10 mg, 26 µmol) in dioxane/water, 1:1 (35 mL) and Et_3N (20 µL, 174 µmol), was irradiated at 300 nm in the inert atmosphere for 2 h. During irradiation the mixture became cloudy. After irradiation the solvent was evaporated. Resulting mixture were dissolved in chloroform and GPC Data was collected.

Starting material **3.1** eluted at ~32.7 mL, compound **3.3**, n=2 (molecular weight ~747) eluted at ~31.4 mL, compound **3.3**, n=3 (molecular weight ~1110) eluted at ~30.4 mL, compound **3.3**, n=4 (molecular weight ~1474) eluted at ~29.7 mL.

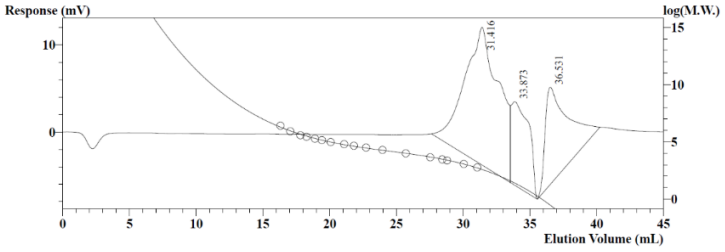

Figure 3.7. GPC data. 2 h irradiation at 300 nm in inert atmosphere in the presence of Et_3N.

Sample, containing compound **3.1 (**10 mg, 26 µmol) in dioxane/water, 2:1 (35 mL) and Et_3N (20 µL, 174 µmol), was irradiated at 300 nm in the inert atmosphere for 5 h. During irradiation the mixture became cloudy. After irradiation the solvent was evaporated. Resulting mixture were dissolved in chloroform and GPC Data was collected.

Compound **3.3**, n=3 (molecular weight ~1110) eluted at ~30.4 mL, compound **3.3**, n=4 (molecular weight ~1474) eluted at ~29.7 mL.

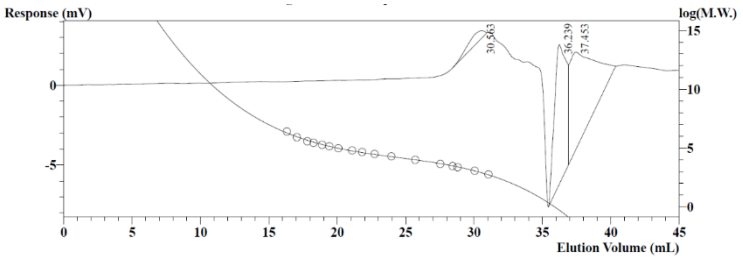

Figure 3.8. GPC data. 5 h irradiation at 300 nm in inert atmosphere in the presence of Et_3N.

Sample, containing compound **3.1** (50 mg, 130 µmol) in dioxane/water, 2:1 (35 mL) and Et_3N (100 µL, 870 µmol), was irradiated at 300 nm in the inert atmosphere for 5 h. During irradiation the mixture became cloudy. After irradiation the solvent was evaporated. Resulting mixture were dissolved in chloroform and GPC Data was collected.

Starting material **3.1** eluted at ~32.7 mL, compound **3.3**, n=2 (molecular weight ~747) eluted at ~31.3 mL, compound **3.3**, n=3 (molecular weight ~1110) eluted at ~30.4 mL.

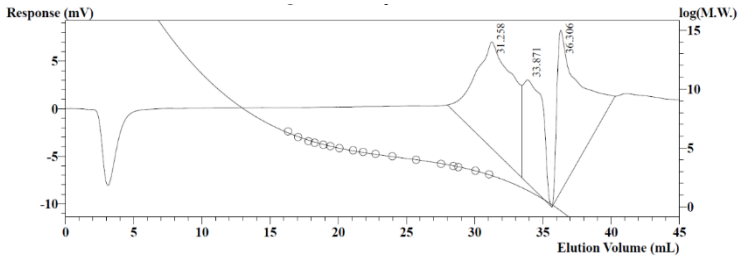

Figure 3.9. GPC data. 5 h irradiation at 300 nm in inert atmosphere in the presence of Et_3N (concentrated sample).

Sample, containing compound **3.1** (50 mg, 130 µmol) in dioxane/water, 2:1 (35 mL) and Et_3N (100 µL, 870 µmol), was irradiated at 300 nm in the inert atmosphere for 7.5 h. During irradiation the mixture became cloudy. After irradiation the solvent was evaporated. Resulting mixture were dissolved in chloroform and GPC Data was collected.

Starting material **3.1** eluted at ~32.7 mL, compound **3.3**, n=2 (molecular weight ~747) eluted at ~31.2 mL, compound **3.3**, n=3 (molecular weight ~1110) eluted at ~30.4 mL.

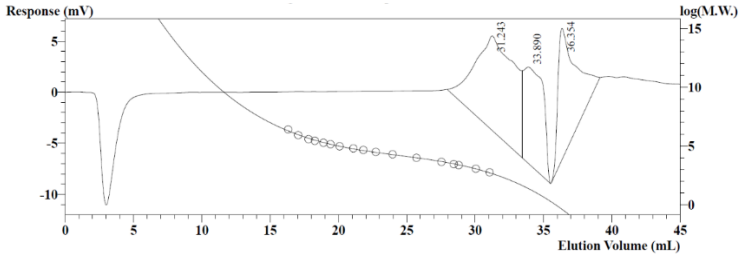

Figure 3.10. GPC data. 7.5 h irradiation at 300 nm in inert atmosphere in the presence of Et_3N (concentrated sample).

Sample, containing compound **3.1** (50 mg, 130 µmol) in dioxane/water, 2:1 (35 mL) and Et_3N (100 µL, 870 µmol), was irradiated at 300 nm in the inert atmosphere for 10 h. During irradiation the mixture became cloudy. After irradiation the solvent was evaporated. Resulting mixture were dissolved in chloroform and GPC Data was collected.

Starting material **3.1** eluted at ~32.7 mL, compound **3.3**, n=2 (molecular weight ~747) eluted at ~31.2 mL, compound **3.3**, n=3 (molecular weight ~1110) eluted at ~30.4 mL.

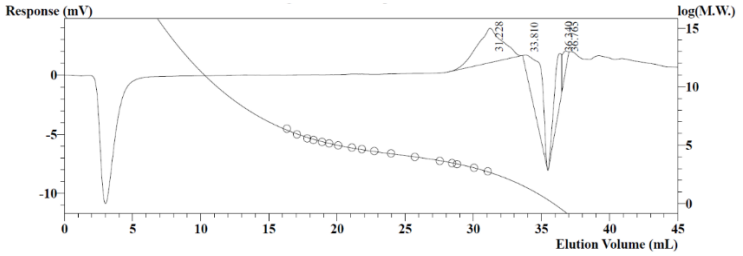

Figure 3.11. GPC data. 10 h irradiation at 300 nm in inert atmosphere in the presence of Et_3N (concentrated sample).

Experiment in acetonitrile/water in the presence of sodium hydroxide.

Sample, containing compound **3.1** (50 mg, 130 µmol) in acetonitrile/water, 1:1 (35 mL) and NaOH (26 µmol), was irradiated at 300 nm in the inert atmosphere for 1 h. After irradiation the solvent was evaporated. Resulting mixture were dissolved in chloroform and GPC Data was collected.

Starting material **3.1** eluted at ~32.5 mL, compound **3.3**, n=2 (molecular weight ~747) eluted at ~31.8 mL, compound **3.3**, n=3 (molecular weight ~1110) eluted at ~30.3 mL, compound **3.3**, n=4 (molecular weight ~1474) eluted at ~29.7 mL.

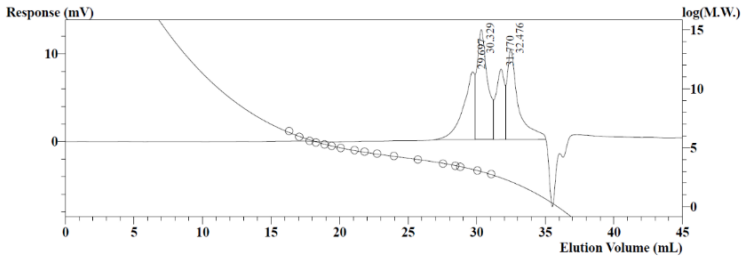

Figure 3.12. GPC data. 1 h irradiation at 300 nm in inert atmosphere in the presence of sodium hydroxide.

3.6. References

1. Arumugam, S.; Popik, V. V. *J. Am. Chem. Soc.* **2009**, 131, 11892-11899.
2. Skalamera, D.; Mlinaric-Majerski, K.; Martin-Kleiner, I.; Kralj, M.; Wan, P.; Basaric, N. *J. Org. Chem*. **2014**, 79, 4390-4397.
3. Verga, D.; Nadai, M.; Doria, F.; Percivalle, C.; Di Antonio, M.; Palumbo, M.; Richter, S. N.; Freccero, M. *J. Am. Chem. Soc*. **2010**, 132, 14625-14637.
4. Arnold, R. M.; Patton, D. L.; Popik V. V.; Locklin, J. *Acc. Chem. Res.* **2014**, 47 (10), 2999-3008.
5. Arumugam, S.; Popik, V. V. *J. Am. Chem. Soc.* **2012**, 134 (20), 8408-8411.
6. Popik, V. V.; Arumugam, S. *Methods for labeling a substrate having a plurality of thiol groups attached thereto*. US 2013/0281656 A1, Oct. 24, 2013.
7. Arumugam, S.; Orski, S. V.; Locklin, J.; Popik, V. V. *J. Am. Chem. Soc.* **2012**, 134 (1), 179-182.
8. Arumugam, S.; Popik, V. V. *J. Am. Chem. Soc.* **2011**, 133 (39), 15730-15736.

9. Arumugam, S.; Popik, V. V. *Photochem. Photobiol. Sci.*, **2012**, *11* (3), 518-521.

CHAPTER 4

PHOTO-CLEAVABLE ANALOG OF BAPTA FOR THE FAST AND EFFICIENT RELEASE OF Ca^{2+}*

4.1. Abstract

A new photocleavable analog of calcium-selective BAPTA chelating ligand has a high affinity towards Ca^{2+} ions (K= 2.5*10^6 M^{-1}). Upon 300 or 350 nm irradiation, one of the aminodicarboxylate "claws" is cleaved off reducing the calcium affinity by several orders of magnitude. The use of photolabile 3-(hydroxymethyl)-2-naphthol core for the photo-BAPTA design allows for the efficient (Φ=0. 63) and very fast (τ <12 μs) release of Ca^{2+} ions.

4.2. Introduction

Free calcium ions (Ca^{2+}) play an important role as a secondary messenger for a wide variety of regulatory functions in physiological and biological processes in cells.[1] The fluctuations of intracellular Ca^{2+} concentration regulate many cellular functions, such as neurotransmitter release,[2] operation of ion channels in the plasma membrane,[3] hormone secretion,[4] muscle contraction,[3] and many others. In recent years, the flash photolysis of photoresponsive calcium-ion chelators has become a common method in biochemical studies.[5]

The majority of photoresponsive calcium chelators are developed around polydentate ligands with high affinity to Ca^{2+}, such as ethylenediaminetetraacetic acid (EDTA),[6,7] ethylene glycol-*bis*(*o*-aminoethyl ether)-N,N,N',N'-tetraacetic acid (EGTA),[7,8] and 1,2-*bis*(*o*-aminophenoxy)ethane-*N,N,N',N*'-tetraacetic

*M. V. Sutton, M. McKinley, R. Kulasekharan and V. V. Popik, *Chem. Commun*., **2017**, 53, 5598-5601.

Reprinted with permission from The Royal Society of Chemistry

acid (BAPTA).[9,10] For biomedical applications, BAPTA-based ligands are preferable since BAPTA offers the highest selectivity towards calcium ions (versus magnesium and other divalent cations).

Two general strategies are commonly employed in the design of photo-responsive calcium chelators. In the first approach, a photoreactive moiety conjugated to the amino group can change the availability of the nitrogen atom lone pair, thus modulating the calcium binding constant upon irradiation.[10] Alternatively, a photolabile linker can be incorporated between two aminodicarboxylic acid fragments. The calcium affinity of tridentate ligands, produced upon photochemical cleavage, is many orders of magnitude lower than that of the octadentate precursor.[8] The latter strategy for calcium photorelease is preferable to the former, as it permits a much higher overall change in Ca^{2+} affinity of a ligand. However, photo-cleavable analogues of calcium-selective BAPTA chelators have not been reported so far. Additional consideration in the design of photolabile chelator is the rate of ion release.[11]

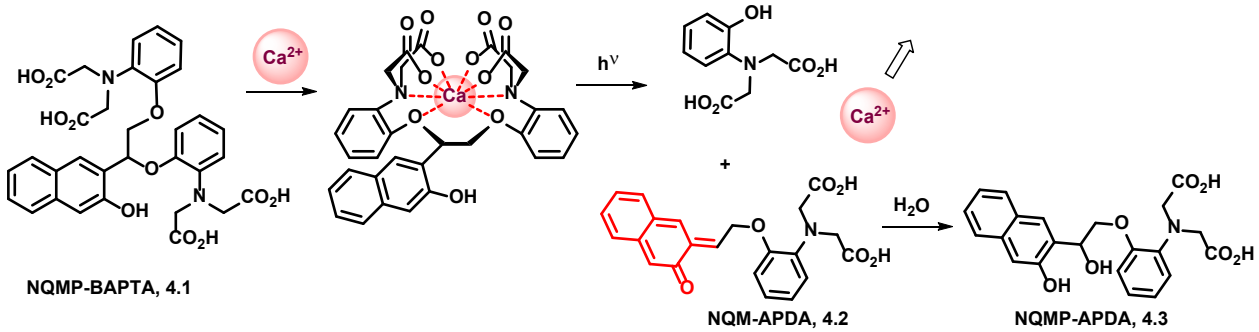

Scheme 4.1. Binding and release of calcium ions by NQMP-BAPTA.

Here, we report the synthesis, photochemical properties, and Ca^{2+} release kinetics of a novel photo-cleavable analogue of BAPTA (**4.1**, Scheme 4.1). 3-(Hydroxynaphth-2-yl)methyl ether servers as photolabile linker connecting two aminodicarboxyl ''claws''. Upon excitation, the former undergoes very fast (τ ~ 12 μs) scission of the benzylic ether bond to produce o-napthoquinone methide (*o*-NQM, structure highlighted in the intermediate **4.2**).[12] In neutral aqueous solutions, o-NQMs undergo rapid (τ ~

7 μs) hydration to produce 3-hydroxymethyl-2-naphthols (e.g., **4.3**, Scheme 4.1). NQMP derivatives show no dark- and photo-cytotoxicity below 100 mM.[13]

4.3. Synthesis of NQMP-BAPTA

The synthesis of NQMP-BAPTA starts from commercially available methyl 3-hydroxy-2-naphthanoate (**4.4**, Scheme 4.2). The protection of the phenolic hydroxyl with ethoxymethyl chloride (EOMCl), followed by LAH reduction of the ester produced 3-(hydroxymethyl)-2-naphthyl EOM ether (**4.6**).[14] The PCC oxidation of the latter gave naphthaldehyde **4.7**, which was converted to epoxide **4.8** under Corey–Chaykovsky conditions in an excellent yield.

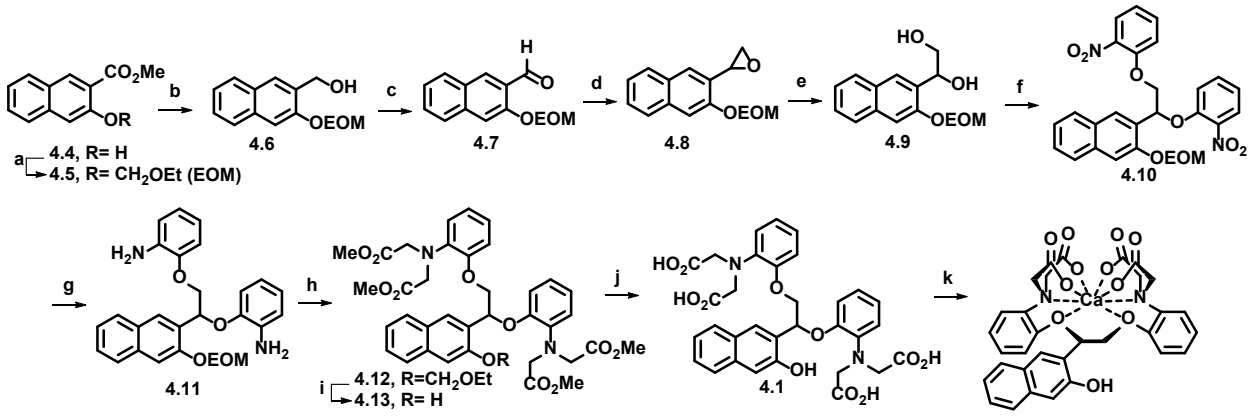

Scheme 4.2. Reagents and conditions: **a)** i) NaH, ii) chloromethyl ethyl ether, 99 %; **b)** $LiAlH_4$, 72 %; **c)** PCC, AcONa, molecular sieves, DCM, 89%; **d)** Trimethylsulfonium iodide, NaH, DMSO, THF, 99%; **e)** DMF-H_2O, 100 °C, 60%; **f)** 1-Fluoro-2-nitrobenzene , NaH, DMF, 120 °C, 78%; **g)** Zn, AcOH, MeOH, THF, 98%; **h)** Methyl bromoacetate, 1,8-bis(dimethylamino)naphthalene, NaI, 75%; **i)** Amberlyst-15(H), MeOH, 63%; **k)** KOH, MeOH, 1,4-dioxane, quant.; **l)** $CaCO_3$, HEPES/KCl.

Several attempts of the nucleophilic ring opening of epoxide **4.8** with 2-nitrophenolate produced only mediocre yields of *o*-nitrophenyl ether.[15] We, therefore, employed an alternative approach to the introduction of 2-nitrobenzyl moieties. First, the hydrolysis of **4.8** produced diol **4.9**, which, in turn, was treated with 2 equivalents of *o*-fluoronitrobenzene to give *bis*(*o*-nitrophenylether) **4.10**. The nitro groups

of the latter were quantitatively reduced by zinc in acetic acid. The alkylation of amino groups in resultingbis-aniline **4.11** with methyl bromoacetate, followed by the deprotection of naphthol with amberlyst-15(*H*), produced NQMP-BAPTA tetra-methyl ester (**4.13**). Finally, saponification of the latter gave a quantitative yield of the target **NQMP-BAPTA** chelator (**4.1**). Tetra-acid **4.1** in the neat form slowly decomposes on prolonged storage. Its potassium salt, however, is perfectly stable at room temperature.

4.4. Photochemical properties of NQMP-BAPTA

The photochemical behavior of **NQMP-BAPTA** was first studied on the example of its tetra-ester **4.13**. The irradiation of a solution of **4.13** in 50% aqueous acetonitrile with 300 nm fluorescent lamps resulted in the efficient cleavage of the starting material ($\Phi = 0.63 \pm 0.03$). After 5 min of irradiation, no traces of tetra-ester **4.13** could be detected in the photolysate. HPLC analysis of the reaction mixtures at low conversion (90 s of irradiation), allowed us to identify two initial photoproducts: ketone **4.14** and *o*-dicarbmethoxymethylamino-phenol **4.15**. Phenol **4.15** is rather unstable and undergoes rapid acid-catalyzed cyclization to lactone **4.16**. Exhaustive irradiation of the reaction mixture led to the formation of an additional photoproduct, 3-hydroxy-2-naphthaldehyde (**4.17**) (Scheme 4.3).[15]

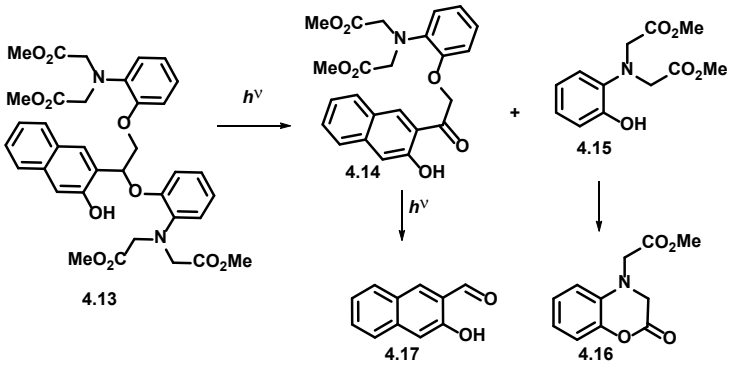

Scheme 4.3. Photochemical behavior of NQMP-BAPTA tetra-ester.

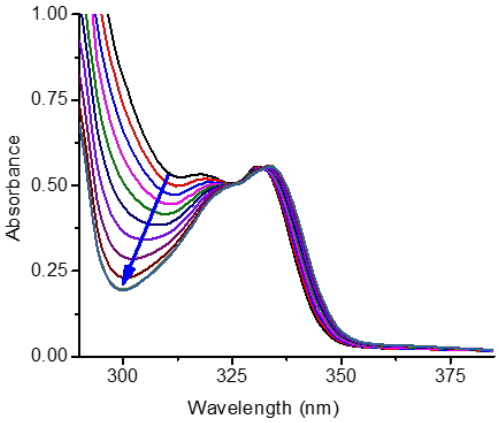

Figure 4.1

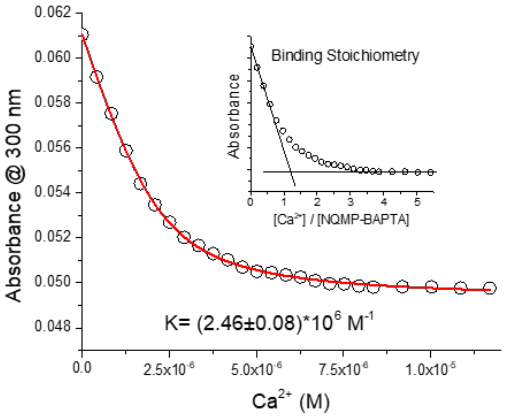

Figure 4.2

Figure 4.1. UV spectra of 0.2 mM aqueous solution of potassium salt of **4.1** at pH =7.4 at variable Ca^{2+} concentrations.

Figure 4.2. Spectrophotometric titration of 2.16 µM aqueous solution of NQMP-BAPTA with 0.25 mM of $CaCl_2$.

4.5. Ca^{2+} affinity of NQMP-BAPTA

The Ca^{2+} affinity of **NQMP-BAPTA (4.1)** was determined by spectrophotometric titration at pH = 7.4 in HEPES buffer. Due to the high calcium affinity of **NQMP-BAPTA**, the titration of **4.1** was conducted at 2.16 µM concentration of the substrate. The buffered solution of potassium salt of **4.1** (HEPES, pH = 7.4) was titrated with 0.25 mM of $CaCl_2$ following the changes in absorbance at 300 nm (Figures 4.1 and 4.2). The absorbance of the **NQMP-BAPTA** solution at 300 nm kept decreasing with successive addition of $CaCl_2$ until it levels off above 10 µM Ca^{2+} concentration (Figure 4.2). The calcium ion binding constant of **NQMP-BAPTA** was calculated using eq. (4.1):

Eq. 4.1
$$[LM] = \frac{([L]_0+[M]_0+\frac{1}{K})}{2} + \sqrt{\frac{([L]_0+[M]_0+\frac{1}{K})^2}{4} - [L]_0[M]_0}$$

Where [LM] is the equilibrium concentration of NQMP-BAPTA (4.1)–Ca^{2+} complex, $[L]_0$ and $[M]_0$ are stoichiometric concentrations of ligand **4.1** and Ca^{2+}, K is a binding constant. We assumed that the

difference in absorbance of the solution of **4.1** at [Ca^{2+}] = 0 (A_0) and at [Ca^{2+}] > 10 μM ($A\infty$) is mostly due to the differences in the extinction coefficients between the free and fully complexed ligand. The changes of the absorbance at 300 nm in the course of the titration is, therefore, represented by the eq. (4.2).

Eq. 4.2

$$A = A_0 - \frac{[LM]}{[L]_0}(A_\infty - A_0)$$

Fitting of the experimental data to the eq. (4.1) and (4.2) allowed us to calculate K_{bnd} = (2.46±0.08) x 10^6 M^{-1} (at pH = 7.4 and ionic strength of 0.1 M). This value is similar to the parent BAPTA ligand.[10a] The midpoint of titration, determined from the absorbance values vs. [Ca2+]/[1] ratio plot, indicates 1:1 binding stoichiometry (inset in Fig. 4.2).

4.6. Release of Calcium Ions from NQMP-BAPTA:Ca^{2+} complex

The release of calcium ions from NQMP-BAPTA:Ca^{2+} complex under irradiation was explored with the help of Calcein indicator. The binding constant of the latter is 3–4 orders of magnitude lower than that of **NQMP-BAPTA**,[17] thus calcein only forms the complex with free Ca^{2+} ions in solution. The concentration of free calcium in solution was calculated from the observed fluorescence intensity at 513 nm. As Figure 4.3 illustrates, the photorelease of calcium from **NQMP-BAPTA** occurs in a dose-dependent manner and is essentially complete after 6 min of irradiation. The increase of calcium concentration under given conditions can be approximated by a first-order rate law to give the apparent rate constant of (7.4±0.3) x 10^{-3} s^{-1}. It is important to note that Ca^{2+} is released quantitatively. This observation also indicates that the fragmentation of NQMP-BAPTA results in at least five orders of magnitude loss of calcium ion affinity (well below K_{bnd} of Calcein).

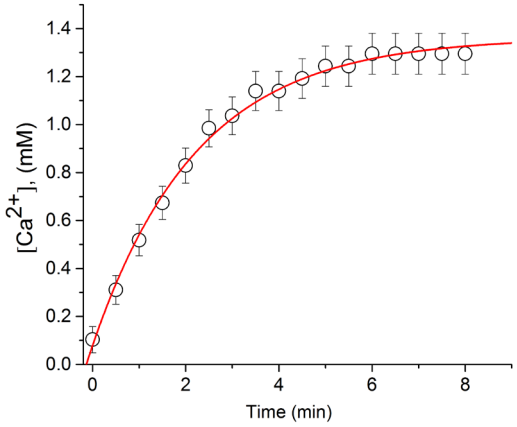

Figure 4.3. Photo-release of Ca^{2+} from the NQMP-BAPTA (**4.1**) - Ca^{2+} complex under 300 nm irradiation.

4.7. Conclusions and Future Directions

In summary, we have developed the first photo-cleavable analog of BAPTA Ca^4 chelator, NQMP-BAPTA (**4.1**), by incorporating photo-labile 3-(hydroxymethyl)-2-naphthol linker in the structure. NQMP-BAPTA possess very high calcium affinity (K_{bnd} = 2.46 x 10^6 M^{-1}), but upon irradiation, **4.1** loses one of its tridentate chelating arms resulting in the efficient calcium ion release. The high quantum yield (Φ = 0.63) of the NQMP-BAPTA cleavage makes it one of the most efficient of photosensitive calcium-ion chelators.[7,18] The NQMP linker photo-cleavage occurs on the microsecond time scale making NQMP-BAPTA suitable for time-resolved experiments.

4.8. Experimental Procedures

4.8.1. General Information

Column chromatography was performed using 40-63 μm silica gel. NMR spectra were recorded on a 400 MHz NMR spectrometer in $CDCl_3$, unless otherwise noticed. Chemical shifts were referenced to residual solvent proton or carbon signals. Melting points were determined using a Fisher-Johns melting point apparatus. High-resolution mass spectra were obtained using electron spray ionization and orbitrap mass analyzer. Solutions were prepared using HPLC grade water and acetonitrile. Photoreactions were

conducted using a Rayonet photoreactor equipped with fifteen 4W 300 nm fluorescent lamps. The quantum yield of photoreaction was measured against the 4-nitroveratrole actinometer.[19] Fluorescence spectra were recorded with excitation and emission slit widths of 5.0 and 2.0 nm respectively.

4.8.2. Experimental Procedures and Compound Data

All reagents were obtained from commercial sources and were used without further purification unless otherwise noted. (3-(Ethoxymethoxy)naphthalen-2-yl)methanol **4.6** was prepared as reported previously.[14]

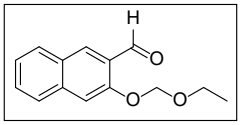

3-(Ethoxymethoxy)-2-naphthaldehyde (**4.7**). PCC (25.123 g, 97 mmol) was slowly added to a solution of **4.6** (15.1 g, 65 mmol), sodium acetate (7.95 g, 97 mmol), and molecular sieves Grade 564 8-12 mesh (2.5 g) in DCM (100 mL) at 0 °C. The reaction mixture was stirred at r.t. overnight and separated using short silica gel column (~ 15 cm, DCM) to produce 13.3 g (89%) of aldehyde 7 as colorless crystals.

M.p. = 48 ^{0}C. IR: 2977; 1682; 1623; 1594; 1068; 742 cm^{-1}.

^{1}H NMR: 10.60 (1H, s); 8.39 (1H, s); 7.89 (1H, dd, *J* = 8.6 and 1.2 Hz); 7.76 (1H, dd, *J* = 8.8 and 1.2 Hz); 7.55-7.52 (2H, m); 7.39 (1H, dd, *J* = 8.2 and 8.3 Hz); 5.47 (2H, s); 3.83 (2H, q, *J* = 7.2 Hz); 1.27 (3H, t, *J* = 7.2 Hz).

^{13}C NMR: 190.2; 155.2; 137.4; 130.6; 129.8; 129.1; 128.2; 126.9; 125.8; 125.0; 110.1; 93.5; 64.9; 15.1. HRMS (ESI), *m/z*: calcd. for $C_{14}H_{14}O_3Na$ $[M+Na]^+$ 253.0841, found 253.0836.

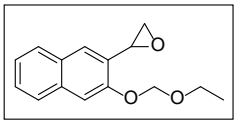

2-(3-(Ethoxymethoxy)naphthalen-2-yl)oxirane (**4.8**). NaH (4.52 g, 113 mmol) was added in small portions to a solution of trimethylsulfonium iodide (23 g, 113 mmol) in anhydrous DMSO (100 mL) and THF (65 mL) under Ar at 0 °C. Ice-bath was removed, and the reaction mixture was stirred for 30 minutes at r.t., cooled to 0 °C, and a solution of aldehyde **4.6** (13.0 g, 56.3 mmol)

in THF (30 mL) was added dropwise (over 1 h). The reaction mixture was allowed to reach r.t., stirred for 8 h, and quenched with water. The product was extracted with ether, organic layer washed water, brine, and dried over Na_2SO_4. Crude epoxide **4.8** (13.6 g, 99%, of pink oil) was used in the next step without purification.

IR: 2975; 2900; 1633; 1506; 1469; 1252; 1222; 1067; 991; 746 cm^{-1}.

HRMS (ESI), *m/z*: calcd. for $C_{15}H_{16}O_3Na$ $[M+Na]^+$ 267.0997, found 267.0992.

1-(3-(Ethoxymethoxy)naphthalen-2-yl)ethane-1,2-diol (**4.9**). Water (300 mL) was added under vigorous stirring to a solution of oxirane **4.8** (13 g, 53.3 mmol) in DMF (180 mL)and the resulting suspension was refluxed for 48 h. The reaction mixture was extracted with EtOAc, washed with water, brine, and dried over Na_2SO_4. The product was purified by column chromatography (EtOAc/Hexanes, 1:2) to give 8.38 g (60%) of diol **4.9** as yellowish powder.

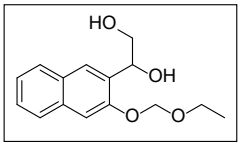

M.p. = 57 ºC.

IR: 3394 (broad); 2975; 1633; 1503; 1052; 985; 740 cm^{-1}.

^1H NMR: 7.90 (1H, s); 7.76-7.72 (2H, m); 7.45-7.41 (2H, m); 7.37-7.33 (1H, m); 5.35 (2H, s); 5.24 (1H, dd, *J* = 7.8 and 4.0 Hz); 3.95-3.91 (1H, m); 3.76-3.68 (3H, m); 3.30 (1H, d, *J* = 4.8 Hz); 2.64 (1H, dd, *J* = 7.8 and 4.0 Hz); 1.23 (3H, t, *J* = 7.2 Hz).

^{13}C NMR: 152.4; 133.8; 130.1; 129.0; 127.7; 126.7; 126.4; 126.3; 124.3; 108.8; 93.1; 70.9; 66.8; 64.7; 15.1.

HRMS (ESI), *m/z*: calcd. for $C_{15}H_{18}O_4Na$ $[M+Na]^+$ 285.1103, found 285.1098.

2-(1,2-bis(2-Nitrophenoxy)ethyl)-3-(ethoxymethoxy)naphthalene (**4.10**). NaH (1.52 g, 38 mmol) was added in small portions to a solution of diol **4.9** (5.0 g, 19 mmol) and 1-fluoro-2-nitrobenzene (5.4 g, 38 mmol) in anhydrous DMF (100 mL) and the reaction mixture was heated at 120 °C for 48 h. DMF was then evaporated in vacuum, the residue was dissolved in EtOAc, washed with water, brine, dried over

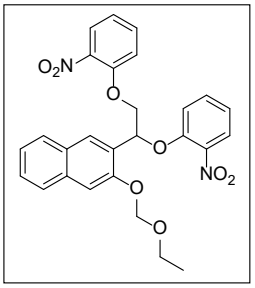

Na_2SO_4. The crude product was purified by column chromatography (EtOAc/Hexanes, 1:9) to give 8.1 g (78%) of compound **4.10** as orange crystals.

M.p. = 82 ºC.

IR: 2975; 1603; 1520; 1348; 1240; 974; 740 cm^{-1}.

^1H NMR: 8.04 (1H, s); 7.82-7.75 (4H, m); 7.57-7.53 (2H, m); 7.47-7.44 (1H, m); 7.38-7.34 (2H, m); 7.23 (1H. dd, *J* = 8.6 and 0.8 Hz); 7.09-7.04 (2H, m); 6.99-6.95 (1H, m); 6.31 (1H, dd, *J* = 7.8 and 2.8 Hz); 5.51 (2H, dd, *J* = 10.0 and 6.8 Hz); 4.56 (1H, dd, *J* = 10.8 and 2.8 Hz); 4.47 (1H, dd, *J* = 10.8 and 2.8 Hz); 3.86-3.80 (2H, m); 1.29 (3H, t, *J* = 7.2 Hz).

^{13}C NMR: 152.1; 151.9; 151.1; 140.4; 140.3; 134.3; 134.1; 133.9; 129.0; 128.1; 127.4; 127.0; 126.8; 125.6; 125.5; 125.4; 124.6; 121.3; 120.8; 116.1; 109.3; 93.5; 75.5; 73.3; 65.0; 15.2. HRMS (ESI), *m/z*: calcd. for $C_{27}H_{24}N_2O_8Na$ $[M+Na]^+$ 527.1430, found 527.1425.

2,2'-((1-(3-(Ethoxymethoxy)naphthalen-2-yl)ethane-1,2-diyl)bis(oxy))dianiline (**4.11**). Glacial acetic acid (13.9 g, 232 mmol) was added to a stirred suspension of zinc dust (15.2 g, 232 mmol) and **4.10** (8.10 g, 16.1 mmol) in the THF - methanol mixture (1:10, 0.5 L), and the reaction mixture was stirred at r.t. overnight. The reaction was quenched by the addition of saturated $NaHCO_3$ solution (250 mL); solids were removed by filtration, and aqueous layer was extracted with EtOAc. Organic layer was washed with water, brine, and dried over Na_2SO_4. Solvent was removed in vacuum to give 7.0 g (98%) of **4.11** as yellow crystals. Compound was used without further purification.

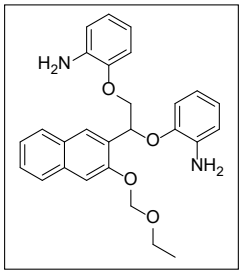

M.p. = 123 ºC.

IR: 3475; 3417; 3340; 2912; 1614; 1504; 1207; 981; 735 cm^{-1}.

^1H NMR: 8.02 (1H, s); 7.79-7.75 (2H, m); 7.52 (1H, s); 7.47-7.43 (1H, m); 7.38-7.34 (1H, m); 6.87 (1H, d, *J* = 7.9 Hz); 6.84-6.78 (1H,m); 6.75-6.73 (4H, m); 6.60 (1H, d, *J* = 7.9 Hz); 6.51-5.46 (1H, m); 6.00 (1H, dd, *J* =

8.0 and 2.8 Hz); 5.47 (2H, dd, *J* = 10.4 and 6.8 Hz); 4.43-4.32 (2H, m); 3.93 (4H, s); 3.78 (2H, q, *J* = 7.2 Hz); 1.27 (3H, t, *J* = 7.2 Hz).

^{13}C NMR: 152.0; 146.3; 145.9; 137.3; 136.8; 134.1; 129.1; 127.9; 127.6; 127.0; 126.8; 126.6; 124.3; 122.0; 121.7; 118.2; 118.2; 115.3; 115.3; 114.6; 112.3; 109.0; 93.2; 75.7; 71.6; 64.8; 15.2.

HRMS (ESI), *m/z*: calcd. for $C_{27}H_{29}N_2O_4$ $[M+H]^+$ 445.2127, found 445.2123.

Tetramethyl 2,2',2'',2'''-((((1-(3-(ethoxymethoxy)naphthalen-2-yl)ethane-1,2-diyl)bis(oxy))-bis(2,1-phenylene)) bis(azanetriyl))tetraacetate (**4.12**). Methyl bromoacetate (3.2 mL, 34 mmol) was added via syringe to a solution of aniline **4.11** (2.5 g, 5.6 mmol), 1,8-bis(dimethylamino)naphthalene (7.3 g, 34 mmol), NaI (450 mg, 3 mmol) in anhydrous CH_3CN (250 mL) under Ar and the reaction mixture was refluxed for 48 h. Toluene (200 mL) was added and precipitate of proton sponge was filtered of. The residue was washed with water, brine, and dried over Na_2SO_4. The product was purified by column chromatography (EtOAc/Hexanes, 1:6 to 1:2) to yield 3.1 g (75%) of tetraacetate as colorless crystals.

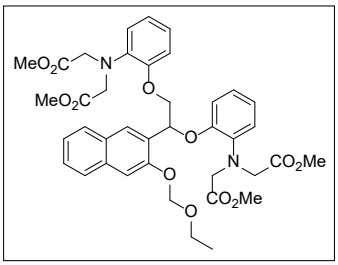

M.p. = 46 ºC.

IR: 2950; 1739; 1501; 1167; 984; 743 cm^{-1}.

^{1}H NMR: 8.05 (1H, s); 7.78 (1H, d, *J* = 8.0 Hz); 7.72 (1H, d, *J* = 8.4 Hz); 7.48 (1H, s); 7.43-7.39 (1H, m); 7.34-7.30 (1H, m); 6.87-6.86 (3H, m); 6.84-6.82 (2H, m); 6.73-6.71 (2H, m); 6.68-6.61 (1H, m); 6.22 (1H, t, *J* = 5.6 Hz); 5.47 (2H, dd, *J* = 11.2 and 7.2 Hz); 4.30 (4H, dd, *J* = 3.2 and 1.6 Hz); 4.24 (4H, dd, *J* = 3.2 and 1.6 Hz); 4.17 (1H, s); 4.12 (1H, s); 3.80 (2H, q, *J* = 7.2 Hz); 3.59 (6H, s); 3.44 (6H, s); 1.27 (3H, t, *J* = 7.2 Hz).

^{13}C NMR: 172.1; 171.6; 152.3; 150.4; 149.2; 139.8; 138.9; 134.0; 131.2; 128.0; 127.5; 126.8; 126.6; 124.1; 122.3; 122.0; 121.1; 121.0; 119.2; 114.0; 112.3; 108.7; 93.0; 73.1; 71.1; 64.6; 53.6; 52.9; 51.5; 51.3; 15.1.

HRMS (ESI), *m/z*: calcd. for $C_{39}H_{44}N_2O_{12}Na$ $[M+Na]^+$ 755.2792, found 755.2794.

Tetramethyl 2,2',2'',2'''-((((1-(3-hydroxynaphthalen-2-yl)ethane-1,2-diyl)bis-(oxy))bis(2,1-phenylene))bis(aza-netriyl))tetraacetate (**4.13**). A solution of compound **4.12** (3.0 g, 4 mmol) in MeOH (50 mL) was refluxed overnight with 1.4 g of Amberlyst 15(H) resin. The reaction mixture was filtered through a plug of celite (~ 2 cm), washed with MeOH, and the filtrate was concentrated.

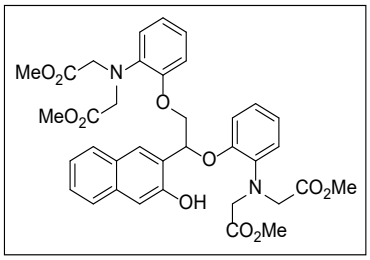

The product was purified by column chromatography (EtOAc/Hexanes, 1:8) to produce 1.7 g (63%) of tetraacetate **4.13** as yellowish crystals.

M.p. = 67 ºC.

IR: 3381 (broad); 2951; 1732; 1501; 1194; 1168; 743 cm^{-1}.

^{1}H NMR: 7.79 (1H, s); 7.73 (1H, d, *J* = 8.4 Hz); 7.62 (1H, d, *J* = 8.4 Hz); 7.52 (1H, s); 7.40-7.36 (1H, m); 7.31-7.27 (1H, m); 7.20 (1H, s); 6.92-6.87 (5H, m); 6.82-6.75 (3H, m); 6.05 (1H, dd, *J* = 8.8 and 3.2 Hz); 4.65 (1H, m); 4.21 (1H, dd, *J* = 10.0 and 3.2 Hz); 4.16 (4H, s); 4.14 (4H, s); 3.56 (6H, s); 3.49 (6H, s).

^{13}C NMR: 172.4; 171.8; 152.7; 150.4; 148.8; 140.0; 139.0; 134.6; 128.7; 128.3; 127.6; 126.6; 126.1; 124.5; 123.6; 122.8; 122.7; 121.7; 121.4; 120.1; 119.6; 114.7; 112.9; 112.3; 77.5; 70.6; 53.6; 53.0; 51.7; 51.5.

HRMS (ESI), *m/z*: calcd. for $C_{36}H_{39}N_2O_{11}$ $[M+H]^+$ 675.2554, found 675.2555.

2,2',2'',2'''-((((1-(3-hydroxynaphthalen-2-yl)ethane-1,2-diyl)bis(oxy))bis(2,10-phenylene))bis(azanetriyl))tetra-acetic acid (**NQMP-BAPTA**, **4.1**). 1 M aqueous potassium hydroxide (3 mL) was added to a solution of tetraacetate **4.13** (100 mg, 0.15 mmol) in MeOH - 1,4-dioxane mixture (1:1, 3 mL) and the reaction mixture was stirred at r.t. for 2 h. 1 M hydrochloric acid (20 mL) and brine (10 mL) were added to the reaction mixture, the resulted precipitate was separated, washed with water and dried under vacuum to give 92 mg (quant.) of tetra-acid **4.1** as colorless crystals.

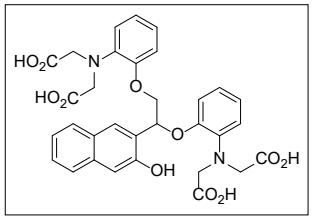

M.p. = 193 ºC.

IR: 3042 (broad); 2922 (broad); 1716; 1497; 1229; 746 cm^{-1}.

^{1}H NMR (CD_3OD, 500 MHz): 7.76 (1H, s); 7.68 (1H, d, *J* = 8.4 Hz); 7.64 (1H, d, *J* = 8.0 Hz); 7.39-7.36 (1H, m); 7.26-7.22 (2H, m); 7.15 (1H, d, *J* = 8.0 Hz); 7.07-7.04 (1H, m); 6.81-6.77 (3H, m); 6.14 (1H, dd, *J* = 8.8 and 2.4 Hz); 4.45 (1H, m); 4.35 (1H, dd, *J* = 10.4 and 2.4 Hz); 4.10 (2H, d, J = 17.6 Hz); 3.95 (2H, d, *J* = 17.6 Hz); 3.92 (2H, d, *J* = 17.6 Hz); 3.75 (2H, d, *J* = 17.6 Hz) ppm.

^{13}C NMR (CD_3OD, 125 MHz): 176.0; 175.5; 153.9; 152.3; 150.5; 140.3; 139.9; 136.4; 129.8; 128.9; 128.0; 127.1; 126.1; 126.1; 125.1; 124.7; 122.7; 122.4; 119.2; 115.0; 113.4; 110.9; 74.8; 71.1; 57.3; 56.5.

HRMS (ESI), *m/z*: calcd. for $C_{32}H_{30}N_2O_{11}Na$ $[M+Na]^+$ 641.1747, found 641.1743.

1-(3-(ethoxymethoxy)naphthalen-2-yl)-2-(2-nitrophenoxy)ethan-1-ol (**4.12**). A solution of epoxide **4.8** (500 mg, 2 mmol) and sodium 2-nitrophenolate (322 mg, 2 mmol) in anhydrous DMF (5 mL) was refluxed for 96 h. 1 M hydrochloric acid was added dropwise till the solution turned light yellow from red, product was extracted with EtOAc, washed with water, brine, and dried over Na_2SO_4. The product was purified by column chromatography (EtOAc/Hexanes, 1:6) to produce 411 mg (43%) of alcohol **4.12** as orange oil.

IR: 3587; 3386 (broad); 2903; 1603; 1522; 1355; 749 cm^{-1}.

^{1}H NMR: 7.88-7.85 (2H, m); 7.76 (1H, *J* = 8.4 Hz); 7.72 (1H, *J* = 8.0 Hz); 7.53 (1H, s); 7.46-7.43 (1H, m); 7.36-7.29 (2H, m); 7.00-6.96 (1H, m); 6.87 (1H, d, *J* = 8.4 Hz); 5.92 (1H, dd, *J* = 7.2 and 4.0 Hz); 5.50 (2H, dd, *J* = 10.8 and 6.8 Hz); 3.98 (2H, d, *J* = 6.8 Hz); 3.83 (2H, q, *J* = 7.2 Hz); 3.16 (1H, s); 1.30 (3H, t, *J* = 7.2 Hz).

^{13}C NMR: 151.6; 151.6; 140.0; 134.2; 134.1; 128.9; 127.8; 126.8; 126.7; 126.7; 126.0; 125.9; 125.7; 124.5; 120.8; 116.3; 109.1; 93.2; 79.4; 66.2; 64.8; 15.1.

HRMS (ESI), *m/z*: calcd. for $C_{21}H_{21}NO_6Na$ $[M+Na]^+$ 406.1267, found 406.1264.

4.8.3. Photochemical Studies

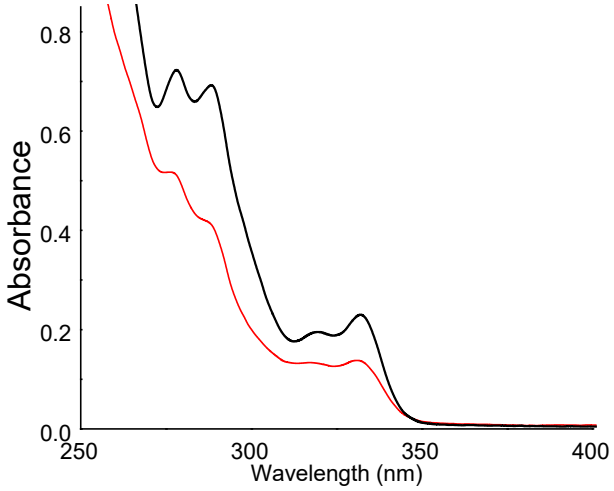

Figure 4.4. UV spectra of ca. 0.1 mM solutions of NQMP-BAPTA tetra-ester **4.13** (black line) and potassium salt of NQMP-BAPTA (**4.1**, red line) in HEPES buffer (pH= 7.4).

A solution of NQMP-BAPTA tetraacetate **4.13** (619 mg, 0.1 mmol) in 50% aqueous acetonitrile (1 L) was irradiated in a glass round-bottom flask under intensive stirring with 300 nm fluorescent lamps for 5 min. TLC of the reaction mixture showed complete consumption of the starting tetra-ester and the formation of four products. The HRMS-ESI analysis of the photolysate allowed to identify these products as diester **4.14**, phenol **4.15**, lactone **4.16,** and 3-hydroxy-2-naphthaldehyde **4.17** (Scheme 4.3). The products **4.14**, **4.16** and **4.17** were isolated by column chromatography (EtOAc/Hexanes, 1:8) and characterized by IR, ^{1}H NMR, ^{13}C NMR, and HRMS (ESI). Phenol **4.15** underwent rapid cyclization on silica gel to form lactone **4.16**.

Dimethyl 2,2'-((2-(2-(3-hydroxynaphthalen-2-yl)-2-oxoethoxy)phenyl)azanediyl)diacetate (**4.14**). Orange viscous oil, yield 23% (10 mg). IR: 3300 (broad); 2951; 1741; 1661; 1503; 1190; 1170; 746 cm^{-1}.

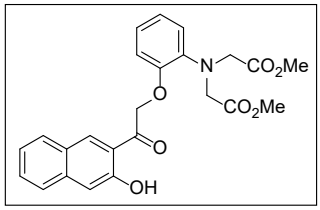

The compound **4.14** gives only one peak on HPLC and TLC, but two sets of ^{1}H NMR signals in the ratio of 1 : 10. We believe that it represents the presence of two rotamers, stabilized by intramolecular hydrogen bond.

^{1}H NMR (500 MHz): 11.17 (1H, s, major); 10.57 (0.1H, s, minor); 8.41 (1H, s, major); 8.40 (0.1H, s, minor); 7.90 (0.1H, d, *J* = 8.0 Hz, minor); 7.86-7.85 (0.1H, m, minor); 7.83 (1H, d, *J* = 8.5 Hz, major); 7.68 (1H, d, *J* = 8.5 Hz, major); 7.67-7.66 (0.1H, m, minor); 7.56-7.55 (0.1H, m, minor); 7.55-7.52 (1H, m, major); 7.45 (0.1H, *J* = 8.0 Hz, minor); 7.42 (0.1H, *J* = 8.0 Hz, minor); 7.36-7.32 (2H, m, major); 7.17 (0.1H, d, *J* = 8 Hz, minor); 7.05 (0.1H, s); 7.00-6.83 (4.0H, m, major); 6.88(0.1H, d, *J* = 8.0 Hz ,minor); 5.93(0.2H, s, minor); 5.60 (2H, s, major); 4.23 (4H, s, major); 4.18 (0.4H, s, minor); 3.73 (0.6H, s, minor); 3.70 (6H, s, major) ppm. ^{13}C NMR (125 MHz) 200.2; 171.7; 156.7; 149.9; 140.0; 138.3; 131.8; 130.0; 129.4; 126.9; 126.3; 124.3; 123.4; 122.9; 120.1; 119.0; 116.9; 112.6; 71.5; 53.6; 51.8. HRMS (ESI), *m/z*: calcd. for $C_{24}H_{24}NO_7$ $[M+H]^+$ 438.1553, found 438.1550.

Methyl 2-(2-oxo-2,3-dihydro-4H-benzo[b][1,4]oxazin-4-yl)acetate (**4.16**). Yellowish crystals, yield 72% (32 mg), m.p.= 84 ºC. IR: 3066; 2958; 1771; 1735; 1505; 1198; 742 cm^{-1}. ^{1}H NMR: 7.07-7.02 (2H, m); 6.90-6.85 (1H, m); 6.60 (1H, dd, *J* = 8.0 and 1.6 Hz); 4.10 (2H, s); 4.01 (2H, s); 3.76 (3H, s) ppm. ^{13}C NMR: 169.6; 164.2; 141.6; 133.2; 125.2; 120.5; 117.1; 112.4; 52.2; 50.9; 50.5. HRMS (EI), *m/z*: calcd. for $C_{11}H_{11}NO_4$ $[M]^{+\cdot}$ 221.0688, found 221.0682.

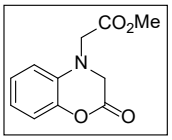

3-Hydroxy-2-naphthaldehyde 4.17. Yellow crystals, yield 64% (11 mg), M.P. = 94 ºC [lit. 95-96 ºC].[3]

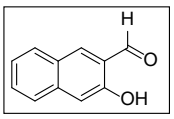

IR: 3289 (broad); 2918; 1659; 1503; 1456; 743 cm^{-1}.

^{1}H NMR: 10.33 (1H, s); 10.10 (1H, s); 8.17 (1H, s); 7.88 (1H, d, *J* = 8.4 Hz); 7.72 (1H, d, *J* = 8.4 Hz); 7.59-7.55 (1H, m); 7.40-7.36 (1H, m); 7.29 (1H, s).

^{13}C NMR: 196.7; 155.8; 138.2; 137.9; 130.3; 129.4; 127.4; 126.7; 124.4; 122.3; 111.9.

HRMS (ESI), *m/z*: calcd. for $C_{11}H_7O_2$ $[M-H]^-$ 171.0446, found 171.0441.

4.8.4. Independent Syntheses of Photoproducts

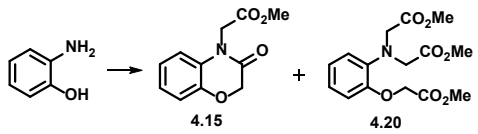

Scheme 4.4. Preparation of lactam **4.15** (an isomer of lactone **4.16**).

1,8-bis(Dimethylamino)naphthalene (980 mg, 4.58 mmol), methyl bromoacetate (1.051 g, 6.87 mmol) and NaI (7 mg, 46 µmol) were added to a solution of 2-aminophenol (250 mg, 2.29 mmol) in anhydrous CH_3CN (50 mL). The reaction mixture was heated at 70 ºC under Ar for 48 h, extracted with EtOAc, washed with water, brine, and dried over Na_2SO_4. Products were isolated by column chromatography (EtOAc/Hexanes, 1:8).

Methyl 3-oxo-2,3-dihydro-4H-benzo[b][1,4]oxazine-4-carboxylate (**4.15**). Yield 53% (268 mg), yellow crystals, M.p. = 78 ºC. IR: 2953; 1747; 1684; 1502; 1392; 1211; 749 cm^{-1}. ^1H NMR: 7.04-7.01 (3H, m); 6.76 (1H, dd, *J* = 8.00 and 2.0 Hz); 4.68 (2H, s); 4.67 (2H, s); 3.79 (3H, s). ^{13}C NMR: 168.3; 164.9; 145.1; 128.6; 124.3; 122.9; 117.2; 114.3; 67.5; 52.7; 42.8 ppm. HRMS (EI), *m/z*: calcd. for $C_{11}H_{11}NO_4$ $[M]^{+\cdot}$ 221.0688, found 221.0683.

Dimethyl 2,2'-((2-(2-methoxy-2-oxoethoxy)phenyl)azanediyl)diacetate (**4.20**). Yield 17% (127 mg), yellowish crystals, M.P. = 74 ºC [lit. 75 ºC][4]. ^1H NMR: 6.95-6.87 (3H, m); 6.80-6.78 (1H, m); 4.66 (2H, s); 4.20 (4H, s); 3.77 (3H, s); 3.71 (6H, s). ^{13}C NMR: 171.7; 169.4; 149.6; 139.4; 122.7; 122.6; 119.8; 114.7; 75.8; 66.1; 53.5; 52.1; 51.7.

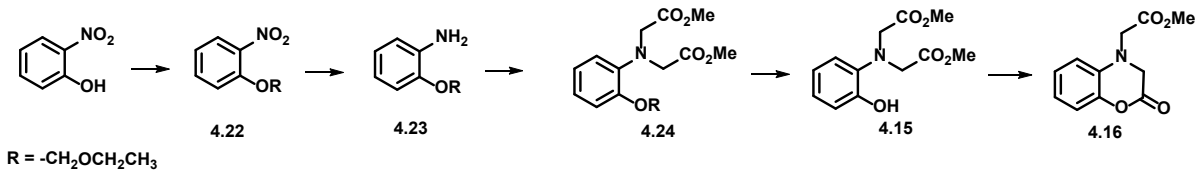

Scheme 4.5. Independent synthesis of lactone **4.16**.

1-(Ethoxymethoxy)-2-nitrobenzene (**4.22**). Sodium hydride (346 mg, 8.64 mmol) was added to an ice-cold solution of 2-nitrophenol (1 g, 7.2 mmol) in anhydrous THF (100 mL). The reaction mixture was stirred at 0 °C for 30 minutes, then chloromethyl ethyl ether (1.79 g, 14.4 mmol) was added dropwise (over 30 min), and the solution was stirred at 0 °C for 2 h. The reaction was quenched by slow addition of cold water, the product was extracted with EtOAc, washed with water, brine, and dried over Na_2SO_4. The product was purified by column chromatography (EtOAc/Hexanes, 1:6) to provide 1.4 g (99%) of **4.22** as orange oil.

IR: 2978; 1606; 1523; 1485; 1351; 1239; 962; 745 cm^{-1}.

^1H NMR: 7.80 (1H, dd, *J* = 8.0 and 1.6 Hz); 7.53-7.48 (1H, m); 7.35-7.33 (1H, m); 7.10-7.05 (1H, m); 5.34 (2H, s); 3.77 (2H, q, *J* = 7.2 Hz); 1.22 (3H, *J* = 7.2 Hz).

^{13}C NMR: 150.5; 133.8; 125.2; 121.4; 117.2; 94.0; 65.1; 15.0 ppm.

HRMS (ESI), *m/z*: calcd. for $C_9H_{11}NO_4NNa$ $[M+Na]^+$ 220.0586, found 220.0580.

2-(Ethoxymethoxy)aniline (**4.23**). Acetic acid (6.0 g, 101 mmol) was added dropwise to a stirred suspension of **4.22** (1.4 g, 7 mmol) and zinc dust (6.6 g, 101 mmol) in THF - methanol mixture (1:10, 275 mL), the reaction mixture was stirred overnight at r.t, and quenched with saturated $NaHCO_3$ solution (50 mL). Solids we removed by filtration and filtrate was extracted with EtOAc. Organic layer was washed with water, brine, and dried over Na_2SO_4. The solvent was removed in vacuum to give 981 mg (84%) of aniline **4.23** as orange oil.

IR: 3460; 3369; 2975; 2985; 1614; 1502; 1204; 988; 739 cm^{-1}.

^1H NMR: 7.05 (1H, dd, *J* = 8.0 and 1.2 Hz); 6.87-6.83 (1H, m); 6.75-6.69 (1H, m); 5.25 (2H, s); 3.82 (2H, s); 3.75 (2H, q, *J* = 7.2 Hz); 1.25 (3H, t, *J* = 7.2 Hz).

^{13}C NMR: 144.9; 136.7; 122.3; 118.3; 115.3; 114.7; 93.7; 64.2; 15.0. HRMS (ESI), *m/z*: calcd. for $C_9H_{14}NO_2$ $[M+H]^+$ 168.1025, found 168.1019.

Dimethyl 2,2'-((2-(ethoxymethoxy)phenyl)azanediyl)diacetate 4.24. A solution of aniline **4.23** (770 mg, 4.61 mmol), methyl bromoacetate (1.94 g, 12.7 mmol), anhydrous Na_2HPO_4 (1.80 g, 12.7 mmol), and NaI

(347 mg, 2.3 mmol) in acetonitrile (35 mL) were stirred and refluxed under Ar for 18 h. The cooled reaction mixture was diluted with water until dissolution of inorganic salts. Then the mixture was extracted with toluene (4x50 mL). The combined organic extracts were dried with Na_2SO_4, filtered and evaporated. The product was purified by column chromatography (EtOAc/Hexanes. 1:8) to give 1.0 g (72%) of diacetate **4.24** as a colorless oil.

IR: 2952; 1739; 1502; 1167; 988; 746 cm^{-1}.

^{1}H NMR: 7.10-7.07 (1H, m); 6.90-6.88 (2H, m); 6.86-6.81 (1H, m); 5.18 (2H, s); 4.14 (4H, s); 3.74-3.69 (8H, m); 1.22 (3H, t, *J* = 7.2 Hz).

^{13}C NMR: 171.8; 149.0; 139.4; 122.3; 122.2; 119.1; 116.3; 93.7; 64.3; 53.8; 51.6; 15.0.

HRMS (ESI), *m/z*: calcd. for $C_{15}H_{22}NO_6$ $[M+H]^+$ 312.1447, found 312.1444.

Dimethyl 2,2'-((2-hydroxyphenyl)azanediyl)diacetate 4.15. A solution of **4.24** (1 g, 3.2 mmol) in MeOH (15 mL) with 1 g of Amberlyst 15(*H*) resin was refluxed overnight, filtered through a plug of celite (~ 2 cm), washed with MeOH, and the solvent removed in vacuum. The ^{1}H NMR and HRMS (ESI) spectra of the crude product indicate the presence of compounds **4.15** and **4.16** in the ratio 1:2. ^{1}H NMR: 7.88 (1H, s, **4.15**); 7.31 (1H, dd, *J* = 8.0 and 1.6Hz, **4.15**); 7.11-7.02 (5H, m, 1H of **4.15** and 4H of **4.16**); 6.94 (1H, dd, *J* = 8.0 and 1.6 Hz, **4.15**); 6.90-6.86 (2H, m, **4.16**); 6.83-6.79 (1H, m, **4.15**); 6.60 (2H, dd, *J* = 8.0 and 1.2 Hz, **4.16**); 4.11 (4H, s, **4.16**); 4.01 (4H, s, **4.16**); 3.89 (4H, s, **4.15**); 3.76 (6H, s, **4.16**); 3.72 (6H, s, **4.15**).

HRMS (ESI) of **4.15**, *m/z*: calcd. for $C_{12}H_{16}NO_5$ $[M+H]^+$ 254.1028, found 254.1023. Phenol **4.15** could not be isolated in a pure form as it underwent rapid cyclization to lactone **4.15** on silica gel.

4.8.5. HPLC analysis of photolysate of 4.13

A solution tetraester **4.13** (100 μM) in 50% aqueous acetonitrile was irradiated in a quartz cuvette with 300 nm fluorescent lamps for 0, 90, 120, and 180 s. The composition of the photolysate after each period was analyzed by HPLC (eluent: MeOH (75%), CH_3CN (1%), water (24%)). After 90s of exposure, the formation of three products, namely **4.14**, **4.15**, and **4.16** are observed (Figure 4.5). Prolonged irradiation

of the reaction mixture (>180 s) led to formation of a secondary photochemical product, which was found to be 3-hydroxy-2-naphthaldehyde **4.17**.

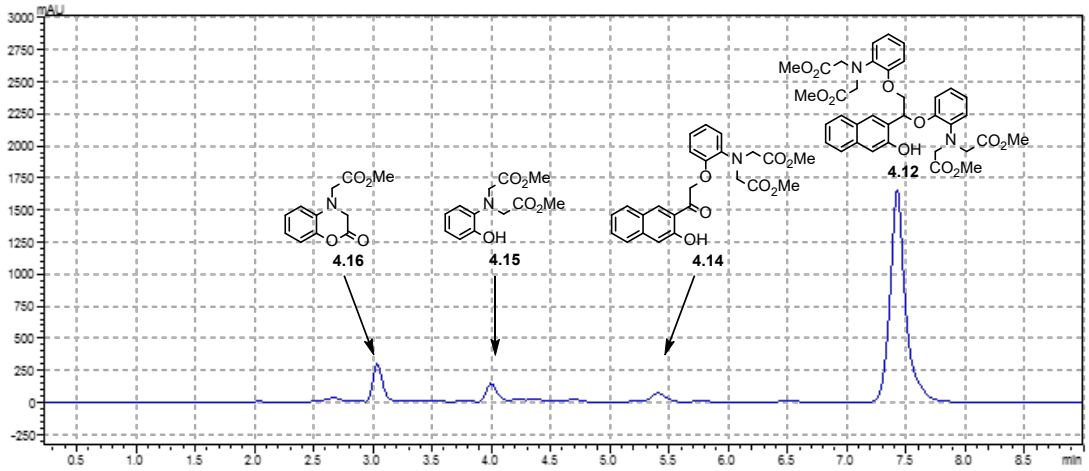

Figure 4.5. HPLC trace of the reaction mixture after 90 s of 300 nm irradiation of NQMP-BAPTA tetra-ester **4.13** in HEPES buffer at pH= 7.4.

4.8.6. Determination of Calcium Ca^{2+} Affinity of NQMP-BAPTA (**4.1**).

A 2.16 µM solution of the NQMP-BAPTA (**4.1**) potassium salt in HEPES buffer (30 mM, pH= 7.20, [KCl] = 0.1 M) was titrated with 0.25 µM aqueous solution of $CaCl_2$ (in 5 µL aliquoutes) following the absorbance changes at 300 nm at 25.0±0.1 °C (Figure 4.1). Triplicate measurements were conducted at each Ca^{2+} concentration and the average absorption value was used for the analysis (Table 4.1). Titration was performed to achieve full saturation of the chelation.

Table 4.1. Observed absorbance at 300 nm at different concentrations of Ca^{2+}.

[Ca^{2+}] (μM)	**Absorbance @ 300 nm, a.u.**
0.0000	0.061057
0.4175	0.059175
0.8350	0.057540
1.2525	0.055895
1.6700	0.054422
2.0875	0.053480
2.5050	0.052702
2.9225	0.052028
3.3400	0.051667
3.7575	0.051303
4.1750	0.051030
4.5925	0.050700
5.0100	0.050521
5.4275	0.050458
5.8450	0.050352
6.2625	0.050265
6.6800	0.050101
7.0975	0.049963
7.5150	0.049957
7.9325	0.049869
8.3500	0.049817
9.1850	0.049827
10.0200	0.049828
10.8550	0.049773
11.6900	0.049769

Determination of Calcium Photo-Release Efficiency was conducted using calcein indicator at pH 7.40. Calibration plot (Figure S4) has been constructed by measuring the 513 nm emission of 0.7 nM calcein solution in HEPES (30 mM)/KCl (100 mM) buffer in the presence of variable concentrations of Ca^{2+} (Figure 4.6, Table 4.2).

Table 4.2. Observed intensity of fluorescence at 513 nm at different concentrations of Ca^{2+}.

Concentration of Ca^{2+}, M x 10^3	Intensity @ 513 nm, a. u.
0.00	1.28 x 10^6
0.25	1.23 x 10^6
0.50	1.16 x 10^6
0.75	1.11 x 10^6
1.00	1.08 x 10^6
1.25	1.04 x 10^6
1.50	986627
1.75	927507
2.00	886686

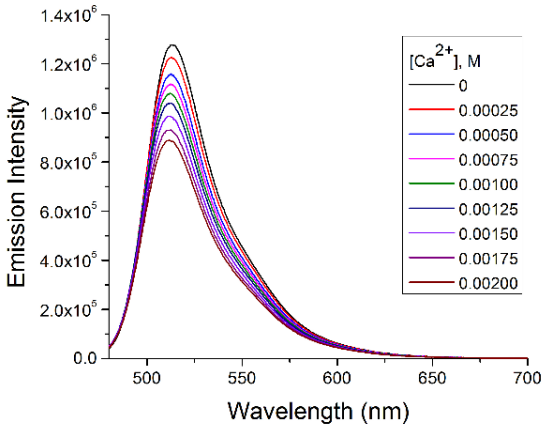

Figure 4.6. Emission spectra of calcein at different concentration of Ca^{2+}.

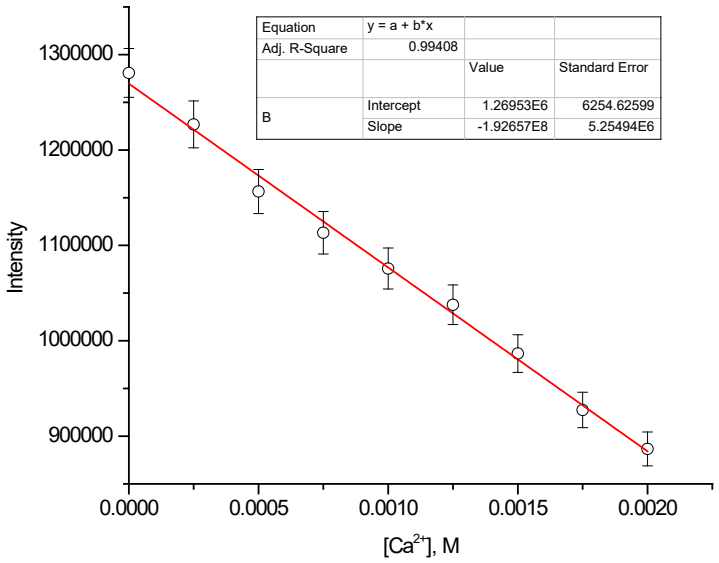

Figure 4.7. The intensity of 513 nm emission of 0.7 nM calcein solution in HEPES buffer versus [Ca^{2+}].

4.8.7. Determination of Ca^{2+} release

Glass vials contained solutions of **4.1** (1.135 mM) and Ca^{2+} (1.25 mM) in HEPES (30 mM)/KCl (100 mM) buffer at pH 7.40 were irradiated for 0, 0.5, 1.5, 2, 2.5, 3, 3.5, 4, 4.5, 5, 5.5, 6, 6.5, 7, 7.5, and 8 min with 300 nm fluorescent lamps. Then 0.5 µL of calcein solution was added into each vial. Emission spectra were

collected in 480-700 nm range at 25 ºC (Table 4.3, Figure 4.8). Intensity of emission at 513 nm was used for determination of concentration of calcium, which was released. The intensity of fluorescence of calcein were plotted to determine efficiency of Ca^{2+} release (Figure 4.7).

Table 4.3. Intensity of calcein fluorescence at 513 nm at different duration of irradiation at 300 nm.

Time of irradiation, min	Emission Intensity @ 513 nm
0	1.25 x 10^6
0.5	1.21 x 10^6
1	1.17 x 10^6
1.5	1.14 x 10^6
2	1.11 x 10^6
2.5	1.08 x 10^6
3	1.07 x 10^6
3.5	1.05 x 10^6
4	1.05 x 10^6
4.5	1.04 x 10^6
5	1.03 x 10^6
5.5	1.03 x 10^6
6	1.02 x 10^6
6.5	1.02 x 10^6
7	1.02 x 10^6
7.5	1.02 x1 0^6
8	1.02 x 10^6

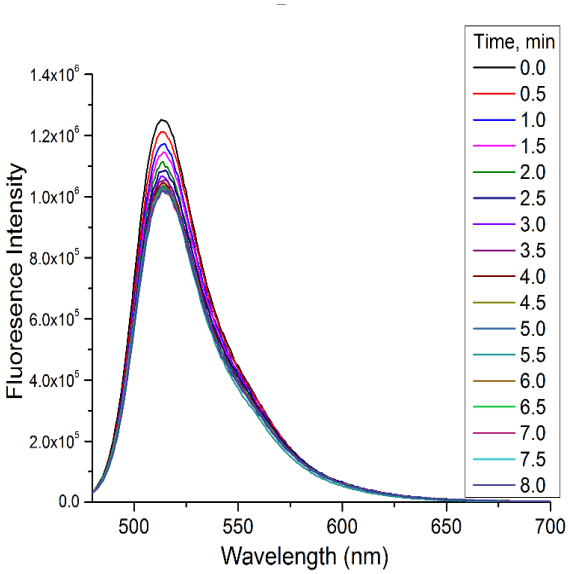

Figure 4.8. Emission spectra of calcein at different duration of exposure of NQMP-BAPTA:Ca^{2+} complex to 300 nm light.

4.9. References

1. G. C. R. Ellis-Davies and J. H. Kaplan, *Proc. Natl. Acad. Sci. U. S. A.,* **1994**, 91, 187; G. C. R. Ellis-Davies, J. H. Kaplan and R. J. Barsotti, *Biophys. J.*, **1996**, 70, 1006.

2. E. M. Alder, G. J. Augustine, S. N. Duffy and M. P. Charlton, *J. Neurosci.*, **1991**, 11, 1496; E. Neher and T. Sakaba, *Neuron*, **2008**, 59, 861; M. Stavermann, P. Meuth, M. Doengi, A. Thyssen, J. W. Deitmer and C. Lohr, *Cell Calcium*, **2015**, 58, 215.

3. D. Terentyev, S. Viatchenko-Karpinski, H. H. Valdivia, A. L. Escobar and S. Gyorke, *Circ. Res.*, **2002**, 91, 414.

4. A. T. Harootunian, J. P. Y. Kao, S. Paranjape and R. Y. Tsien, *Science*, **1991**, 251, 75.

5. For example: D. M. O'Malley, B. J. Burbach and P. R. Adams, Fluorescent Calcium Indicators: Subcellular Behavior and Use in Confocal Imaging, Humana Press, Totowa, NJ, 1999; E. Decrock, M. De Bock, N. Wang, M. Bol, A. K. Gadicherla and L. Leybaert, *Cold Spring Harb. Protoc*., **2013**, 239; K. R. Delaney and V. Shahrezaei, *Cold Spring Harb. Protoc*., **2013**, 1115; J. Almassy and D. I. Yule, *Cold Spring Harb. Protoc*., **2013**, 8; A. Burgalossi, S. Jung, K. M. Man, R. Nair, W. J. Jockusch, S. M. Wojcik, N. Brose and J.-S. Rhee, *Nat. Protoc*., **2012**, 1351.

6. J. H. Kaplan and G. C. R. Ellis-Davies, Proc. Natl. Acad. Sci. U. S. A., 1988, 85, 6571; G. C. R. Ellis-Davies and J. H. Kaplan, *J. Org. Chem*., **1988**, 53, 1966.

7. A. Barth, S. R. Martin and J. E. T. Corrie, *Photochem. Photobiol. Sci*., **2006**, 5, 107; T. D. Parsons, G. C. R. Ellis-Davies and W. Almers, *Cell Calcium*, **1996**, 19, 185.

8. G. C. R. Ellis-Davies and R. J. Barsotti, *Cell Calcium*, **2006**, 39, 75; A. Momotake, N. Lindegger,E. Niggli, R. J. Barsotti and G. C. R. Ellis Davies, *Nat. Methods*, **2006**, 3, 35; E. Sobie, J. Kao and W. Lederer, *Eur. J. Appl. Physiol*., **2007**, 454, 663; A. Burgalossi, S. Jung, K. N. M. Man, R. Nair, W. J. Jockusch, S. M. Wojcik, N. Brose and J. S. Rhee*, Nat. Protoc*., **2012**, 7, 1351; H. K. Agarwal, R. Janicek, S.-H. Chi, J. W. Perry, E. Niggli and G. C. R. Ellis-Davies, *J. Am. Chem. Soc*., **2016**, 138, 3687.

9. S. R. Adams, J. P. Y. Kao, G. Grynkiewicz, A. Minta and R. Y. Tsien, *J. Am. Chem. Soc*., **1988**, 110, 3212.

10. (a) R. Y. Tsien, *Biochemistry*, **1980**, 19, 2396; (b) R. Pethig, M. Kuhn, R. Payne, E. Adler, T.-H. Chen and L. Jaffe, *Cell Calcium*, **1989**, 10, 491; (c) L. Wu, Y. Dai and G. Marriott, *Org. Lett*., **2011**, 13, 2018; (d) S. R. Adams, V. Lev-Ram and R. Y. Tsien, *Chem. Biol*., 1997, 4, 867; (e) J. Cui, R. A. Gropeanu, D. R. Stevens, J. Rettig and A. D. Campo, *J. Am. Chem. Soc*., **2012**, 134, 7733.

11. Y. V. Il'ichev, M. A. Schworer and J. Wirz*, J. Am. Chem. Soc*., **2004**, 126, 4581.

12. S. Arumuqam and V. V. Popik*, J. Am. Chem. Soc*., **2012**, 134, 8408.

13. S. Arumugam and V. V. Popik, *J. Am. Chem. Soc.*, **2011**, 133, 5573.

14. E. E. Nekongo and V. V. Popik, *J. Org. Chem*., **2014**, 79, 7665.

15. M. V. Sutton, M. McKinley, R. Kulasekharan and V. V. Popik, *Chem. Commun*., **2017**, 53, 5598.

16. E. Cielen, A. Stobiecka, A. Tahri, G. J. Hoornaert, F. C. De Schryver, J. Gallay, M. Vincent and N. Boens, *J. Chem. Soc., Perkin Trans. 2*, **2002**, 1197.

17. V. C. Chiu and D. H. Haynes, *Biophys. J*., 1977, 18, 3.

18. S. R. Adams, V. Lev-Ram and R. Y. Tsien, *Chem. Biol.*, **1997**, 4, 867.

19. P. Kuzmič, L. Pavlíčková, J. Velek, and M. Souček, *Collect. Czech. Chem. Commun.* **1986**, *51*, 1665.

CHAPTER 5

DESIGN OF A NOVEL FLUOROGENIC PHOTOLABILE PROTECTING GROUP WITH ABILITY TO SERVE AS INTRACELLULAR pH INDICATOR

5.1. Introduction

5.1.1. Importance of Measuring of Intracellular pH

Intracellular pH (pH_i) is a crucial property of the cell environment. Alternations in pH_i are known to affect the majotiry of cellular processes, such ion transport,[1] endocytosis,[2] membrane potential,[3] cell growth,[3] state of polymerization of cytoskeleton,[4] muscle contraction[5] and enzyme secretion.[6] Change of intracellular hydronium ion concentration is often a primary response of the cell to external stimuli, including hormones and neurotransmitters.[7] Some organelles maintain pH, which is different form cytoplasmic pH (pHi 6.80-7.40),[8] for instance, lysosomes and mitochondria have pH 4.50-6.50.[9] Abnormal fluctuations in cytosolic and vesicular hydronium ion concentration have been linked to cancer,[10] mucolipidosis type IV,[11] chronic granulomatous disease[12] and Alzheimer's disease.[13] The size of individual cell and sensitivity to pH alternations requires sensitive and non-destructive approaches. Techniques to measure cellular pH include H^+ permeable microelectrodes, nuclear magnetic resonance (NMR) analysis of affected metabolites, absorbance spectroscopy and fluorescent spectroscopy of weak acid fluorescent dyes.[14] In comparison to other pHi measuring techniques, fluorescent spectroscopy is characterized by great spatial and temporal resolution, high analytical sensitivity and specificity.[15] Finally, fluorescence gives opportunity to study individual cell and population of cells at the same time by combining cell imagine with fluorescent spectroscopy.[14]

The prime interest of development of novel fluorescent pH_i indicators can be explained by advantages provided by fluorescent spectroscopy. Existent collection of fluorescent pH probes has been developed

using a small set of scaffolds, the majority of which can be represented by coumarin, boron dipyrromethene difluoride (BODIPY), fluorescein, rhodamine, phenoxazine and cyanine core structures (Scheme 5.1).[16] Modification of the core structure, such as introduction of electron-donating and electron-withdrawing substituents and extending conjugation system, has been shown as a useful method to shift the spectral properties of the indicator.[17] The majority of pHi indicators is based on the acid/base sensitivity of phenolic hydroxyl (-OH), carboxylic acid (-CO_2H) and amino (-NH_2) groups. Thus, introduction of electron-donating and electron-withdrawing substituents into the scaffold can alter pH response range of the indicator.[18-19]

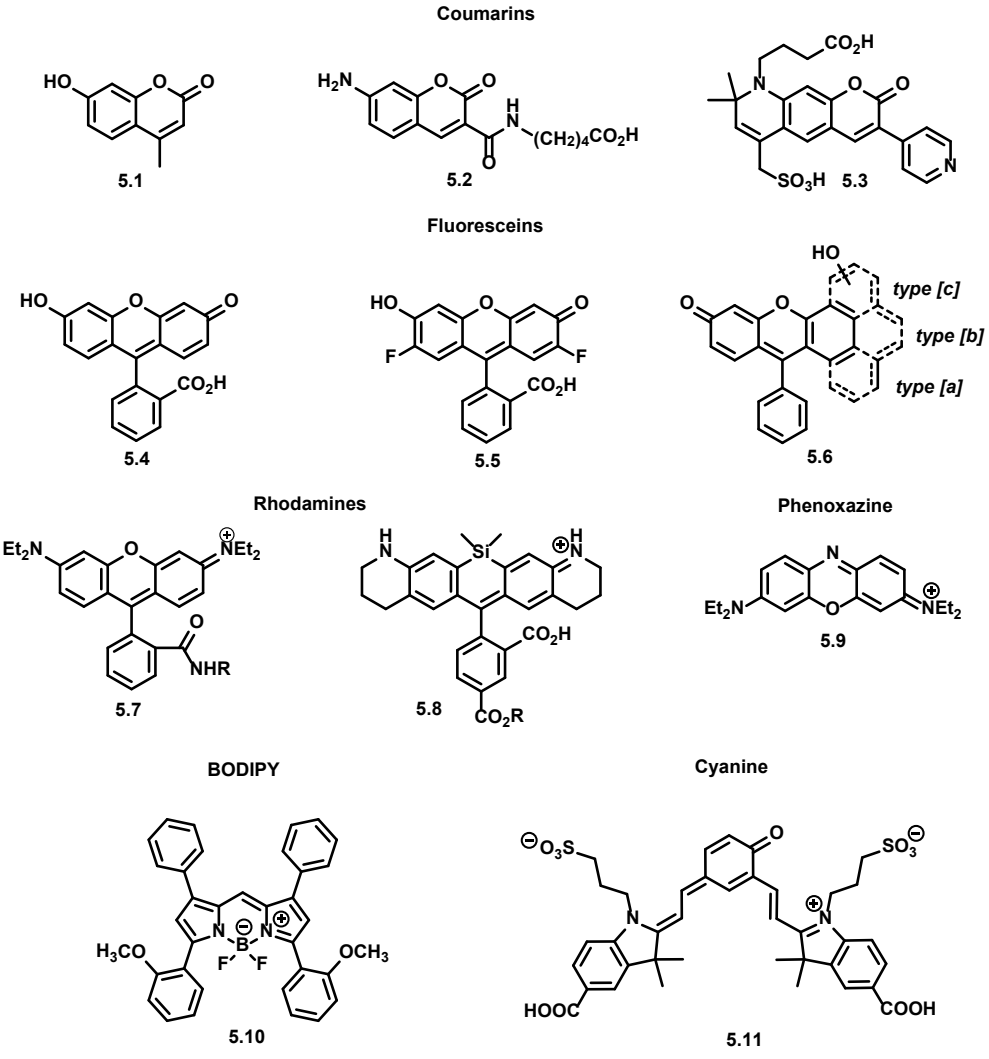

Scheme 5.1. Examples of common fluorescent pH_i indicators.

Xanthene-based pH indicators can be mostly represented by fluorescein and rhodamine derivatives. Hydronium ion sensitivity of fluorescein is based on the pH dependent equilibrium between an "open" fluorescent quinoid form **5.15** and a "closed' nonfluorescent lactone **5.12**: below pH 5 fluorescein exists in an equilibrium between weakly fluorescent charge-neutral open form **5.13** and nonfluorescent spirolactone **5.12**, in pH range of 5-6.5 it exists in monoanionic form **5.14** with fluorescence quantum yield 0.37, and at pH above 6.5 fluorescein exhibits strong green fluorescence (fluorescence quantum yield 0.93) (Scheme 5.2a).[20] Similarly, pH sensitivity of rhodamine-based pH indicators is based on the equilibrium between highly fluorescent open-ring form **5.17** and nonfluorescent spirolactam **5.16** (Scheme 5.2b).[21-23]

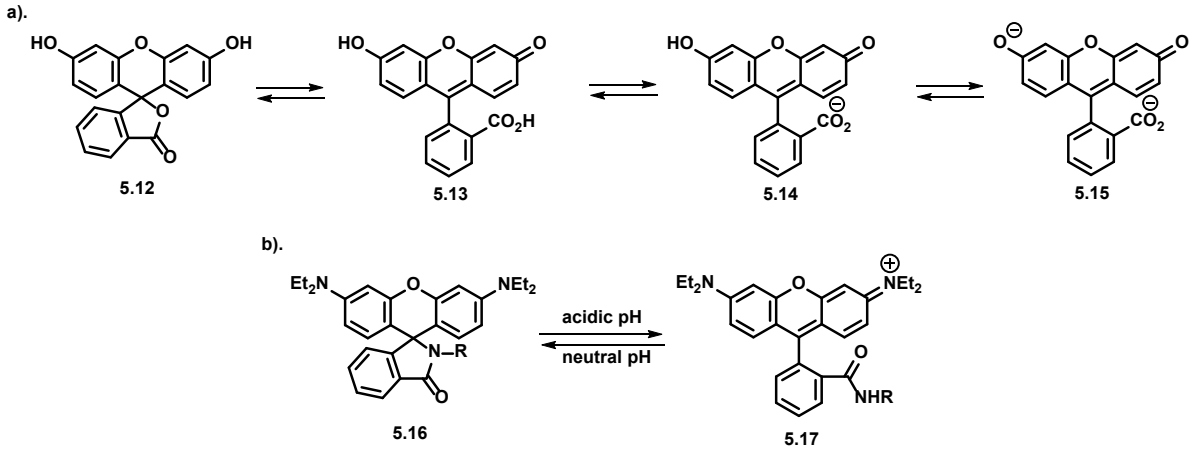

Scheme 5.2. a). Acid/base equilibrium of fluorescein. **b).** Acid/base equilibrium of rhodamine.

Recently, 9-aryl-9*H*-xanthene-9-ol **5.18** has been presented by Popik as a new platform for the design of fluorescent pH probes. pH sensitivity in given case is based on hydronium-ion mediated reversible dehydroxylation of 9-aryl-9*H*-xanthene-9-ol **5.18** (Scheme 5.3). The equilibrium between highly fluorescent green 9-arylxanthilium cation **5.19** and colorless nonfluorescent 9-aryl-9*H*-xanthene-9-ol has been shown to depend only on H^+ concentration and has not been affected by general acids. Additionally, new pH indicator demonstrated fluorescence enhancement of more than 1300-folds and ability to vary pH response range depending on substituents introduced into the core structure. [24]

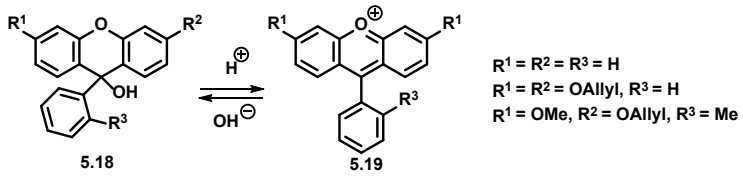

Scheme 5.3. Acid/base equilibrium of 9-aryl-9*H*-xanthen-9-ol.

5.1.2. Photolabile protecting groups (PPGs)

Incorporation of blocking groups that are removable by external stimuli, such as light, enzymatic catalysis and changes in chemical environment, into the core structure of the fluorescent compound can widely expend their application. Photoactivatable (caged) fluorescent dyes, which are generally colorless and nonfluorescent until photoirradiation with UV-light, have received significant attention in multicolor fluorescent microscopy,[25] protein dynamics[26] and cell lineage studies.[27] Nonfluorescent state of the dye is achieved by incorporation of photolabile protecting groups (PPGs), such as *o*-nitrobenzyl,[28] *o*-nitroveratryl (ONV),[29] diethylaminocoumarin-4-yl (DEACM),[30] 2-diethylamino-5-nitrophenyl (DANP),[31] 8-bromo-7-hydroxyquinoline (BHQ)[32] and 9-phenylxanthen-9-yl (pixyl),[33] photocleavage of which results in the release of the fluorescent dye (Scheme 5.4a). As caged fluorescent probes are mainly used in biological studies on living cells, it creates certain limitations for the selection of PPGs. For instance, PPGs, as well as their photoproducts, should be hydrophilic, small, non-toxic, preferably colorless and simple in synthesis. For example, small 2-diazoketone caging group incorporated into a spiro-9*H*-xanthene fragment was found to be a promising candidate (Scheme 5.4b).[34] Even though, the PPGs with desirable properties are known, the majority of them are rather lipophilic, bulky, produce toxic compounds upon irradiation and require complex synthesis. Thus, the prime interest is to develop a novel PPG, that would respond to all desired properties.

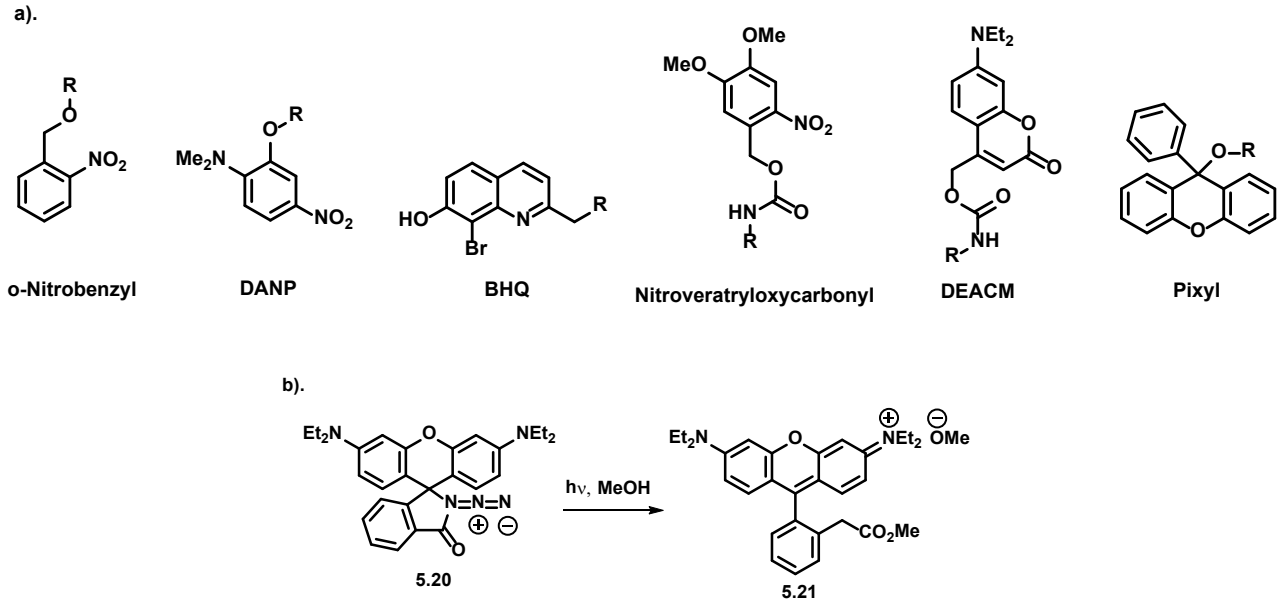

Scheme 5.4. a). Examples of common PPGs. **b).** 2-Diazoketone caging group for rhodamine-based pH indicator.

Even fewer examples of fluorogenic PPGs are known. In 2008 the first example of 3-arylthiochromone derivatives were proposed as new PPGs for alcohols, amines and carboxylic acids.[34] Later it was shown that the same PPGs can successfully protect phosphate derivatives,[35] oligonucleotides,[36] amino acids and sulfonic acids (Scheme 5.5a).[37] Deprotection in all reported cases occurred almost quantitatively under UV-light in neutral condition and the photoproduct **5.23** showed high fluorescence intensity (fluorescence quantum yield Φ_{Fl} = 0.85, λ_{em} ~450 nm).[34-37] Another example of fluorogenic PPG for carboxylic acids was based on the oxazine dye precursors. They were found to undergo photochemical reaction upon irradiation with UV-light that resulted in the generation of oxazine dye derivatives **5.26** (fluorescence quantum yields Φ_{Fl} = 0.001-0.24). Dye precursors **5.25** were reported to be nonfluorescent, while photogenerated oxazine dyes emitted strong fluorescence (Scheme 5.5b).[38]

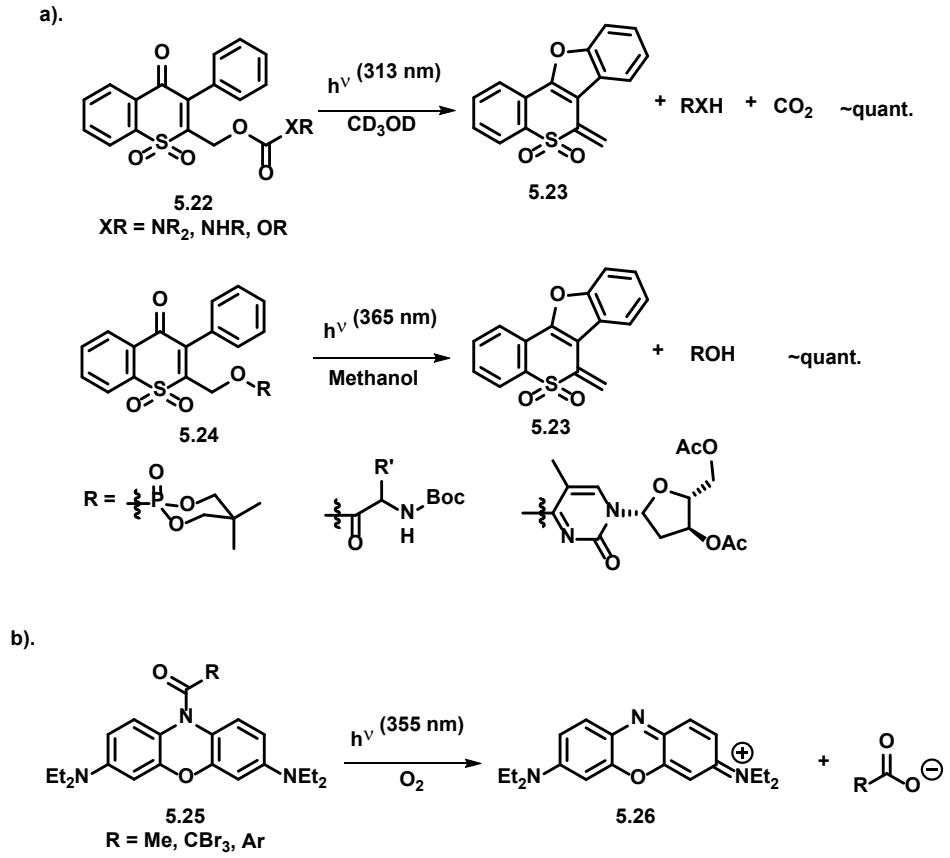

Scheme 5.5. a). 3-Arylthiochromone as a fluorogenic PPG. **b).** Oxazine dye as a fluorogenic PPG.

5.2. Goals of the Project and Experimental Design

As it was mentioned earlier, existent collection of fluorescent pH probes has been developed on a small set of scaffolds. In particular, all fluorescein derivatives share a core structure of 6-hydroxy-3*H*-xanthen-3-one, and their spectroscopic properties and pH response range are varied by introduction of substituents and extending conjugation system in the molecule.[16] However, to the best of our knowledge, examples of 8-hydroxy-1*H*-xanthen-1-one derivatives are unknown. We expected 9*H*-xanthen-1,8,9-triols **5.27** to undergo hydronium-ion mediated reversible dehydroxylation which would yield highly fluorescent 8-hydroxy-1*H*-xanthen-1-one derivatives **5.28**. Additionally, 9*H*-xanthene-1,8,9-triol derivatives can be considered as photoactivatable fluorophores and fluorogenic PPGs, as 9*H*-xanthen-1,8,9-triols **5.27** are expected to generate relatively stable quinone methide (QM) **5.28** upon UV-light irradiation, one of the

resonance structures of which is fully aromatic **5.28'** (Scheme 5.6). Due to its structural similarity with fluorescein derivatives, we expected 8-hydroxy-1*H*-xanthen-1-one to be highly fluorescent.

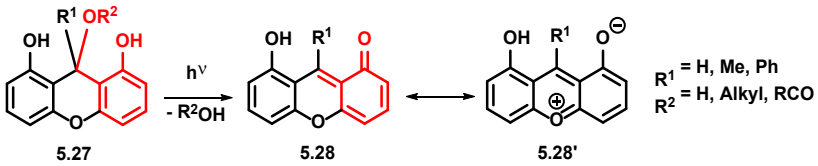

Scheme 5.6. Proposed mechanism of action of a new fluorogenic PPG.

5.3. Toward the Synthesis of 9*H*-xanthen-1,8,9-triols and 8-Hydroxy-1*H*-xanthen-1-ones

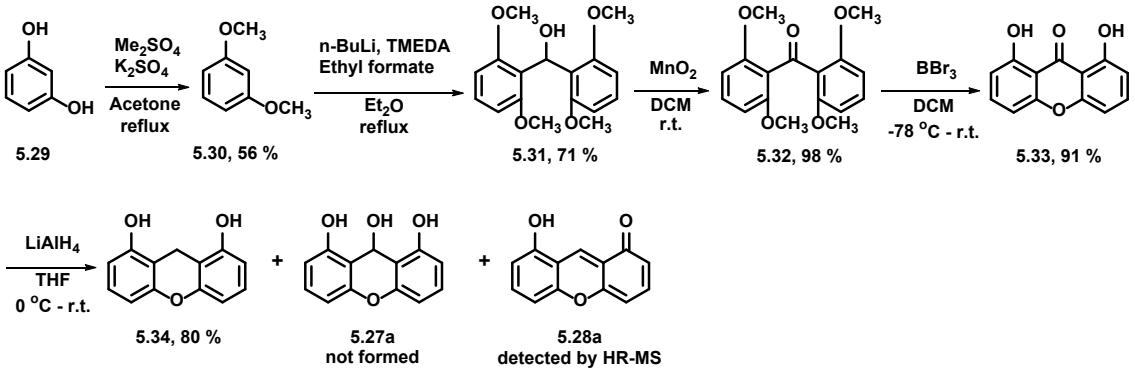

Scheme 5.7. Attempted synthesis of 9*H*-xanthen-1,8,9-triol and 8-hydroxy-1*H*-xanthen-1-one.

The synthesis of 9*H*-xanthen-1,8,9-triol **5.27a** started with methylation of commercially available 1,3-dihydroxybenzene **5.29** and was followed by condensation of obtained veratrole **5.30** with ethyl formate. Attempts to deprotect methyl-protected hydroxyls in compound **5.31** under acidic conditions (excess of BBr_3 in DCM) and under nucleophilic conditions (excess of 2-aminoethanethiol and sodium *t*-butylate in anhydrous DMF) were unsuccessful. Thus, deprotection was conducted in two steps: oxidation of the compound **5.31** into corresponding ketone **5.32** with manganese (IV) oxide was followed by demethylation with BBr_3 and resulted in the formation of the compound **5.33**. Reduction of the **5.33** with excess of lithium aluminum hydride resulted in the formation of unexpected over-reduced compound **5.34** with 80 % yield (Scheme 5.7). Unfortunately, expected 9*H*-xanthene-1,8,9-triol **5.27a** or 8-hydroxy-1*H*-xanthen-1-one **5.28a** have not been observed via GC-MS, TLC and NMR analysis of the crude mixture.

However, HR-MS data of the reaction mixture and isolated compound **5.34** suggested the presence of molecular ion corresponding to the desired compound **5.28a** in the system. We believe that oxidation of the benzylic position of compound **5.34** happened during electron-spray ionization and caused the formation of the molecular ion of compound **5.28a**.

Additionally, we observed that the yellowish solution of the compound **5.34** in organic solvents was slowly (over 24 h) turning into bright green solution when exposed to air. This fact could indicate the formation of highly fluorescent compound **5.28a** due to the oxidation by the oxygen in the air. Attempted bubbling of oxygen into the solution for 1 h also resulted in the formation of green-colored solution. However, in both experiments no noticeable changes of ^{1}H NMR spectra of the solutions were observed.

Interestingly, addition of aqueous basic solution, such as sodium bicarbonate, into the obtained green solution resulted in the discoloration of the solution. On the other hand, acidification of the colorless solution with concentrated HCl regenerated bright green color.

These observations support the obtained HR-MS data and indicate the formation of the **5.28a**, however, the desired compound was formed in undetectable by NMR amount.

Thus, in order to synthesize desired 9*H*-xanthen-1,8,9-triol **5.27a**, reduction of carbonyl group of the compound **5.33** was attempted with milder reducing agents, such as borane dimethylsulfide in THF at low temperature, sodium borohydride in methanol and DIBAL-H in toluene. However, no reaction happened under attempted conditions and only starting material was recovered. Additionally, introduction of alkyl and aryl substituents into the carbonyl group of the compound **5.33** was attempted via Grignard reaction with excess of methylmagnesium iodide and phenylmagnesium iodide, however, only starting material **5.33** was found in the reaction mixture. Attempted alkylation of carbonyl with excess of *n*-BuLi did not result in the formation of desired compounds **5.27d** and **5.28d**, and no reaction occurred (Scheme 5.8). Current observations potentially can be explained by the fact that two anionic oxygens hinder the attack of a nucleophilic reagent.

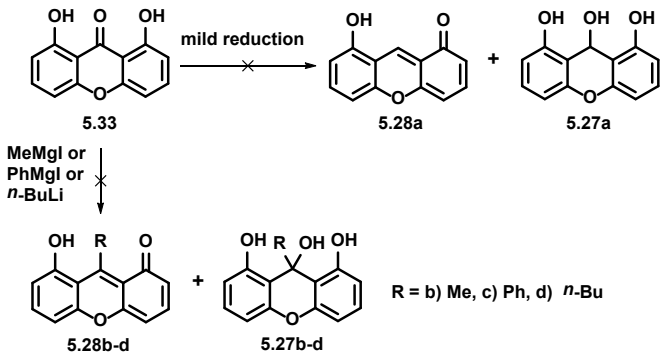

Scheme 5.8. Alternative synthesis of 9*H*-xanthen-1,8,9-triols and 8-hydroxy-1*H*-xanthen-1-ones.

Concurrently with the previous experiments, we attempted the synthesis of 9-phenyl-9*H*-xanthene-1,8,9-triol **5.27c** stating with condensation of veratrole with benzoyl chloride (Scheme 5.9). *Bis*(2,6-dimethoxyphenyl)(phenyl)methanol **5.35** was obtained as a minor product of the reaction in 15 % yield. Demethylation was attempted under acidic conditions and under nucleophilic conditions, however, the first conditions resulted in decomposition of the starting material and the formation of a complex, while under the second conditions no reaction occurred.

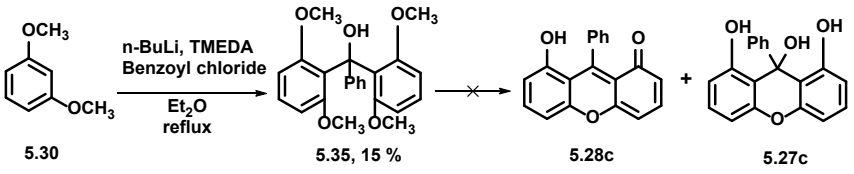

Scheme 5.9. Alternative synthesis 9-phenyl-9*H*-xanthene-1,8,9-triol and 8-hydroxy-9-phenyl-1*H*-xanthen-1-one.

5.4. Discussion of Unexpected Results

Observed phenomenon of over-reduction of xanthone derivatives is very uncommon. Majority of reported examples of reduction of xanthone derivatives resulted in the formation of corresponding 9*H*-xanthen-9-ols. The most commonly used reducing agents and conditions for the transformation were reduction with lithium aluminum hydride in THF at low temperatures,[39,40] reflux with potassium

borohydride[39] or sodium borohydride in methanol,[41,42] and reflux with sodium amalgam[43,44] or sodium hydroxide, zinc in ethanol (Scheme 5.10).[45,46]

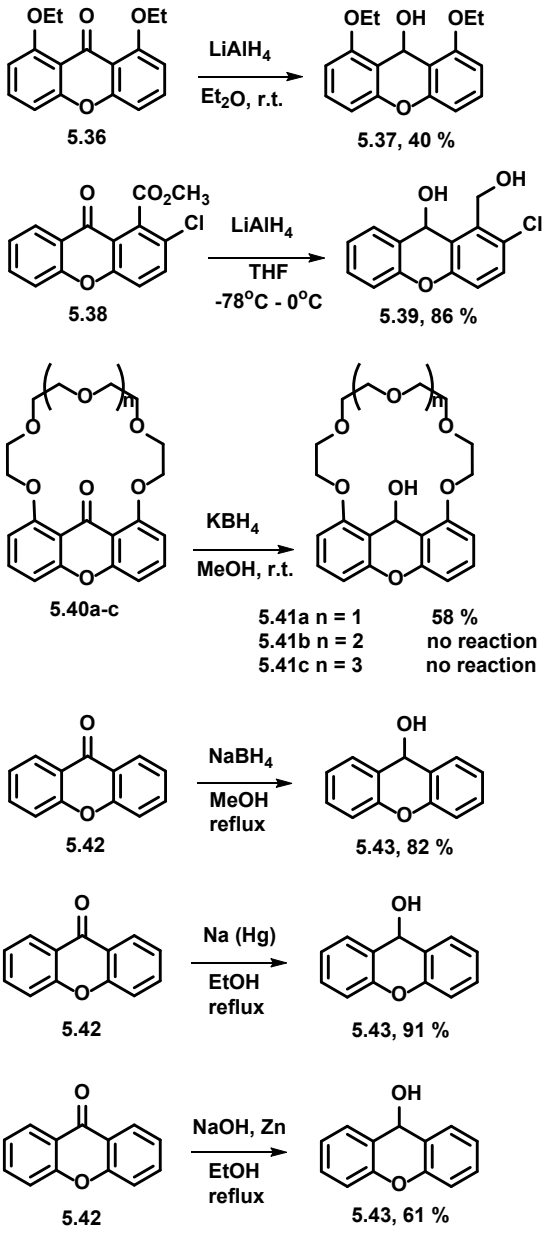

Scheme 5.10. Reduction of xanthone derivatives under various conditions that resulted in the formation of corresponding 9*H*-xanthen-9-ols.

Several examples of over-reduction of xanthone derivatives into xanthenes have been reported previously. In 1986 Borras has published a reduction of methyl 1,3-dimethoxy-9-oxo-9*H*-xanthen-2-

carboxylate **5.44** conducted with $LiAlH_4$, that led to formation of 1,3-Dimethoxy-2-(hydroxymethyl)-9*H*-xanthene **5.45** in 28 % yield.[47] Formation of other products in the reaction has not been mentioned. Discussion of the experiment or mechanism of the transformation have not been provided. Another example of formation of secondary reduction products was reported by Box in 1995.[39] In described experiment reduction of the crown ketones of 1,8-dihydroxyxanthone **5.40** was performed with lithium aluminum hydride in THF, and the resulting 9*H*-xanthen-9-ols **5.41** were found to be unstable to the reaction conditions and were converted to secondary reduction products identified as the xanthenes **5.46**. The most recent example of formation of secondary reduction product was reported in 2012 by Yamamoto: reduction of 3,6-bis(dimethylamino)-9*H*-xanthen-9-one **5.47** performed with lithium aluminum hydride in THF at r.t. yielded corresponding xanthene **5.48** (Scheme 5.11).[48] All secondary reduction products had characteristic NMR peaks in ^{1}H and ^{13}C NMR spectra. In ^{1}H NMR signal corresponding to hydrogens in position 9 of 9H-xanthenes was found to have chemical shift of ~3.7-3.96 ppm and was presented as singlet of integral equaled 2. In ^{13}C NMR spectra characteristic signal of carbon in position 9 could be found at ~17.9-18.6 ppm.[39,47,48] Alternatively, products of primary reduction (9*H*-xanthen-9-ols) have been characterized by presence of broad singlet at ~ 2.8 ppm corresponding to hydrogen of hydroxyl group and by singlet of integral 1 at ~6.06-6.40 ppm, corresponding to a hydrogen in position 9 of 9*H*-xanthen-9-ol. In ^{13}C NMR spectra characteristic signal of carbon in position 9 could be found at ~64.7-65.5 ppm.[39-46] ^{1}H and ^{13}C NMR data obtained for 9*H*-xanthen-1,8-diol **5.34** agreed with previously reported chemical shifts of analogous 9*H*-xanthenes, and characteristic peaks of hydrogens and carbon in position 9 had chemical shifts of 3.73 ppm and 18.7 ppm, respectively.

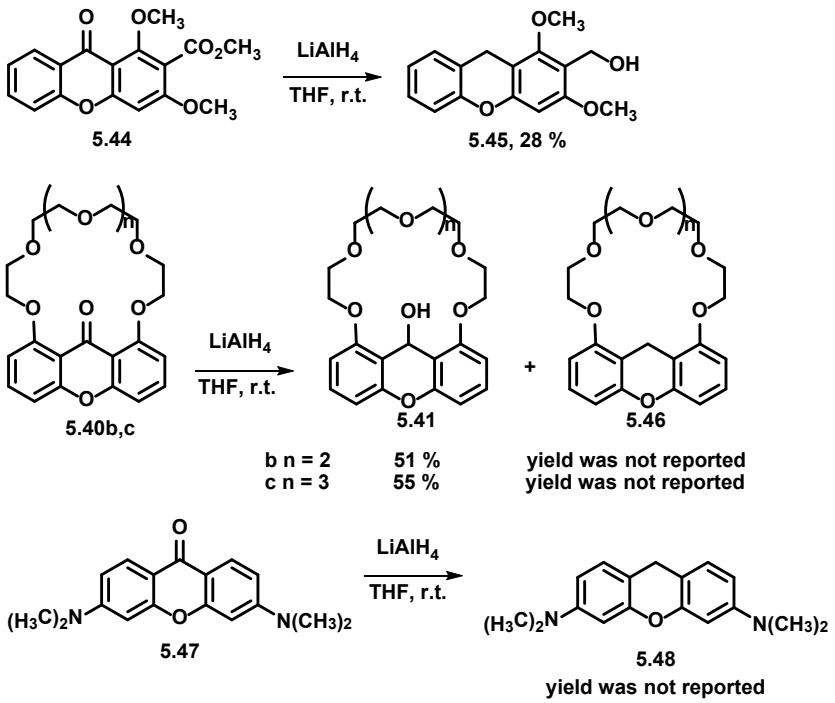

Scheme 5.11. Reduction of xanthone derivatives with lithium aluminum hydride that resulted in the formation of secondary reduction products.

There is no clear explanation why reduction of xanthones with lithium aluminum hydride in THF resulted in some cases in the formation of 9*H*-xanthen-9-ols and in others proceeded further and yielded xanthenes. According to experimental procedures, that resulted in formation of secondary reduction products, reduction was less straightforward, proceeded significantly slower, required higher temperatures and primary products (9*H*-xanthen-9-ols) were found to be unstable to the reaction conditions.

5.5. Conclusions and Future Directions

We have attempted the synthesis of novel fluorescent pH_i indicators and photoactivatable fluorogenic PPGs, which would be based on 9H-xanthene-1,8,9-triol scaffold. However, standard reduction method applied to 1,8-dihydroxy-9H-xanthen-9-one resulted in the formation of unexpected secondary reduction product. Due to the instability of the primary reduction product in the reaction conditions and the fact of

formation of the desired 8-hydroxy-1*H*-xanthen-1-one from corresponding xanthene under electron-spray ionization conditions, future synthetic efforts should be focused on oxidation of 9H-xanthene-1,8-diol. Additionally, it would be interesting to measure the redox potential for 9*H*-xanthene-1,8-diol and 1,8-dihydroxy-9*H*-xanthen-9-one and to study the influence of different substituents on the redox potential.

5.6. Experimental Procedures

5.6.1. General Information

Column chromatography was performed using 40-63 μm silica gel. NMR spectra were recorded on a 400 MHz NMR spectrometer, unless otherwise noticed. Chemical shifts were referenced to residual solvent proton or carbon signals. Melting points were determined using a Fisher-Johns melting point apparatus. High resolution mass spectra were obtained using electron spray ionization and orbitrap mass analyzer.

5.6.2. Experimental Procedures and Compound Data

All reagents were obtained from commercial sources and were used without further purification unless otherwise noted.

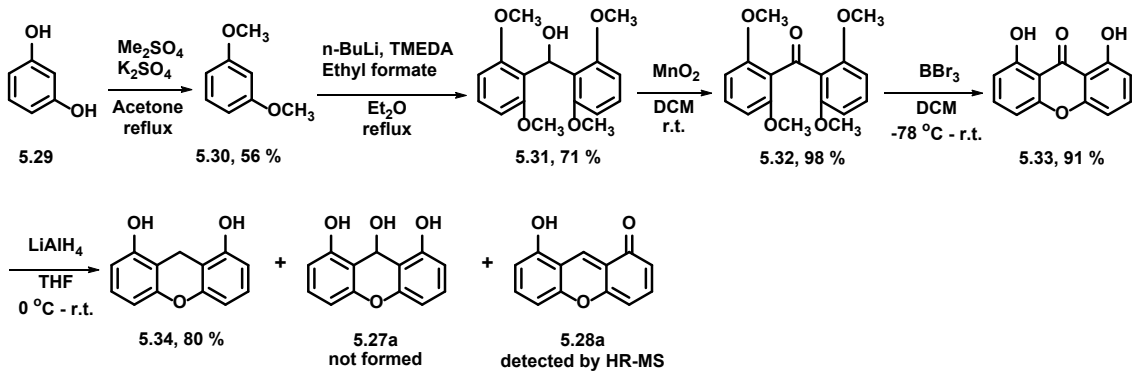

Scheme 5.7. Attempted synthesis of 9*H*-xanthen-1,8,9-triol and 8-hydroxy-1*H*-xanthen-1-one.

1,3-dimethoxybenzene (5.30). 1,3-Dihydroxybenzene **5.29** (20 g, 182 mmol) and K_2CO_3 (85 g, 637 mmol) were mixed with acetone (500 mL). Me_2SO_4 (30 mL, 319 mmol) was added dropwise, then reaction mixture was refluxed for 12 h. The reaction mixture was filtrated from salt, acetone was evaporated and the residue was dissolved in DCM. Obtained solution was washed with water, 1M NaOH, brine and dried over Na_2SO_4. The product was obtained as a yellow oil (14.06 g, 56 %). No purification was required.

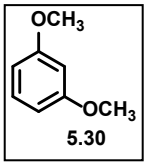

5.30

^{1}H NMR ($CDCl_3$, 400 MHz): 7.21-7.17 (1H, m), 6.53-6.50 (2H, m), 6.49-6.47 (1H, m), 3.79 (6H, s).[49]

Bis(2,6-dimethoxyphenyl)methanol (5.31). *n*-BuLi (2.5 M, 27 mL, 67.5 mmol) and TMEDA (1 mL, 6.7 mmol) were added to a solution of 1,3-dimethoxybenzene (8.7 g, 63 mmol) in diethyl ether (100 mL) at -78 ºC. The mixture was warmed up gradually to r.t. over 2 h, and then re-cooled to -78 ºC. Ethyl formate (2.8mL, 34 mmol) was added slowly via syringe, after which the solution was warmed up to r.t. and left overnight. The reaction was quenched by addition of water (40 mL) and 10 % aq. HCl. Products were extracted with EtOAc, washed with water, BRINE and dried over Na_2SO_4. The product **3** was isolated via column chromatography (EtOAc/Hexanes) as white crystals (6.8 g, 71 %).

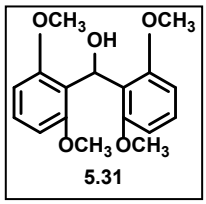

5.31

M.p. = 179 ºC

^{1}H NMR ($CDCl_3$, 500 MHz): 7.14-7.12 (2H, m), 6.68 (1H, d, *J* = 8.2 Hz), 6.52 (4H, d, *J* = 10.0 Hz), 5.63 (1H, d, *J* = 10.0 Hz), 3.76 (12H, s).[39]

Bis(2,6-dimethoxyphenyl)methanone (5.32). Alcohol **5.31** (4.195 g, 13.8 mmol) was dissolved in DCM (250 mL), activated MnO_2 (24.6 g, 184 mmol) was added to the solution. The mixture was stirred at r.t. for 12 h, then precipitate was filtered off. The solvent was evaporated. The product **5.32** was obtained as white crystals (4.084 g, 98 %). No purification was required.

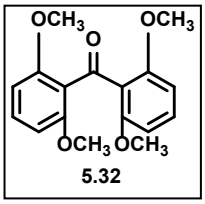

5.32

M.p. = 204 ºC[3]

^{1}H NMR ($CDCl_3$, 400 MHz): 7.29 (2H, d, *J* = 8.4 Hz), 6.57 (4H, d, *J* = 8.4 Hz), 3.73 (12H, s).

^{13}C NMR ($CDCl_3$, 100 MHz): 193.8, 158.4, 130.9, 121.9, 104.5, 56.2.[39]

1,8-dihydroxy-9*H*-xanthen-9-one (5.33). A solution of ketone **5.32** (580 mg, 1.92 mmol) in DCM (30 mL) was cooled to – 10 ºC, then BBr_3 (9.62 g, 3.7 mL, 39.1 mmol) was added dropwise. The reaction mixture was allowed to reach r.t. overnight. Water (40 mL) was added to the obtained solution, and obtained precipitate was filtered off. Solution was extracted with EtOAc, washed with water, brine and dried over Na_2SO_4. The product **5** was obtained as yellow crystals (400 mg, 91 %).

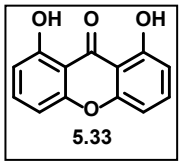

5.33

M.p. = 185 ºC.

IR: 3232 (broad); 1716; 1629; 1455; 1004; 763 cm^{-1}.

^{1}H NMR ($CDCl_3$, 400 MHz): 11.83 (2H, s), 7.63-7.59 (2H, m), 6.93-6.91 (2H, m), 6.81-6.79 (2H, m).[39]

^{13}C NMR ($CDCl_3$, 100 MHz): 186.2, 161.3, 156.3, 137.5, 110.8, 107.8, 107.2.

HRMS (ESI), *m/z*: calcd. for $C_{13}H_8O_4H$ $[M+H]^+$ 229.0495, found 229.0497.

9*H*-xanthen-1,8-diol (5.34) and **8-hydroxy-1*H*-xanthen-1-one (5.28a).** Xanthone **5.33** (425 mg, 1.87 mmol), was dissolved in anhydrous THF (30 mL). $LiAlH_4$ (800 mg, 18.7 mmol) was added in small portions at 0 ºC. The mixture was allowed to reach r.t. and was stirred at r.t. for 4 h, then water (20 mL) and concentrated HCl (10 mL) were added. Solution started to have bright green color. The reaction mixture was extracted with EtOAc, washed with water, brine and dried over Na_2SO_4. Sample of the solution was submitted to HR-MS analysis. According to TLC and GC-MS, two compounds were present in the reaction mixture: starting material **5.33** (molecular ion observed via GC-MS had a mass of 228) and product **5.34** (molecular ion observed via GC-MS had a mass of 213). Two compounds were separated via column chromatography, EtOAc/Hexanes, 1:3 then 3:1. Starting material **5.33** was isolated as yellow crystals (82.8 mg, 19.5 %) and product **5.34** was isolated as pale greenish crystals (320 mg, 80 %).

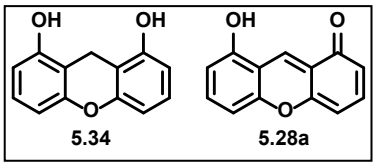

5.34 5.28a

M.p. = 204 ºC.

IR: 2922 (broad); 1653; 1597; 1479; 1454; 1212; 817; 724 cm^{-1}.

^{1}H NMR (CD_3OD, 400 MHz): 6.98-6.94 (2H, m), 6.48-6.43 (4H, m), 4.65 (1H, broad), 3.73 (2H, s).

^{13}C NMR (CD_3OD, 100 MHz): 156.9, 153.6, 128.3, 109.6, 109.0, 108.1, 18.7

HRMS (ESI) of **5.34**, *m/z*: calcd. for $C_{13}H_{10}O_3H$ $[M+H]^+$ 215.0703, found 215.0704.

Expected compound **5.28a** has not been observed via GC-MS, TLC and NMR of the crude mixture. However, HR-MS data of the reaction mixture and isolated compound **5.34** suggested the presence of molecular ion corresponding to the compound **5.28a** in the system. Thus, oxidation of the benzylic position of compound **5.34** happened during electron-spray ionization and caused the formation of the molecular ion of compound **5.28a**.

HRMS (ESI) of **5.28a**, *m/z*: calcd. for $C_{13}H_8O_3H$ $[M+H]^+$ 213.0546, found 213.0550.

HRMS (ESI) of **5.28a**, *m/z*: calcd. for $C_{13}H_8O_3Na$ $[M+Na]^+$ 235.0366, found 235.0366.

HRMS (ESI) of **5.28a**, *m/z*: calcd. for $C_{13}H_8O_3$-H $[M-H]^-$ 211.0401, found 211.0401.

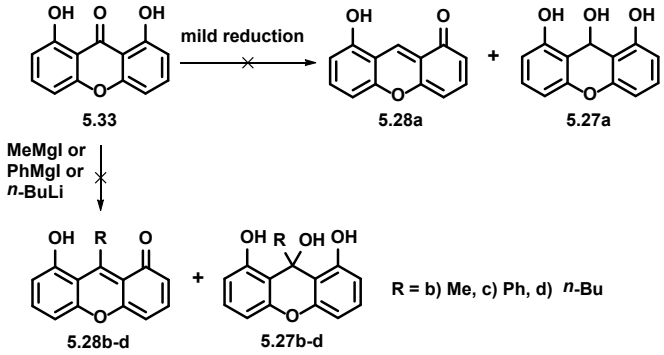

Scheme 5.8. Alternative synthesis of 9*H*-xanthen-1,8,9-triols and 8-hydroxy-1*H*-xanthen-1-ones.

In order to synthesize compound **5.27a**, reduction of carbonyl group of the compound **5.33** was attempted with milder reducing agents, such as borane dimethylsulfide in THF, sodium borohydride in methanol and DIBAL-H in toluene. No reaction happened under attempted conditions and only starting material was present.

Additionally, introduction of alkyl and aryl substituents into the carbonyl group of the compound **5.33** was attempted via Grignard reaction with excess of methylmagnesium iodide and phenylmagnesium iodide, however, only starting material **5.33** was present. Attempted alkylation with excess of *n*-BuLi did not result in the formation of desired compounds **5.27d** and **5.28d**, and no reaction occurred.

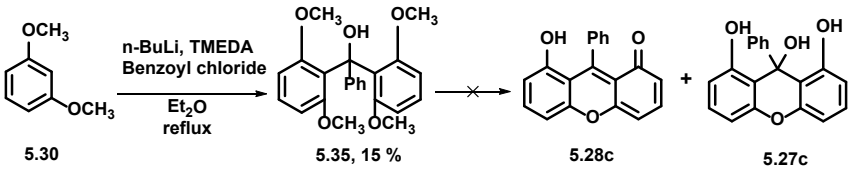

Scheme 5.9. Alternative synthesis 9-phenyl-9*H*-xanthene-1,8,9-triol and 8-hydroxy-9-phenyl-1*H*-xanthen-1-one.

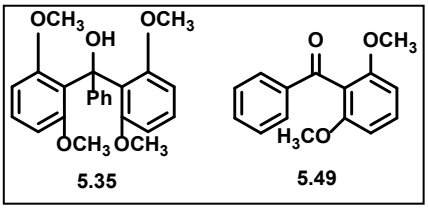

Bis(2,6-dimethoxyphenyl)(phenyl)methanol (5.35). n-BuLi (2.5 M, 16 mL, 39.5 mmol) and TMEDA (0.6 mL, 3.985 mmol) were added to a solution of 1,3- dimethoxybenzene (5.0 g, 36.23 mmol) in diethyl ether (100 mL) at -78 ºC. The mixture was warmed up gradually to r.t. over 2 h, and then re-cooled to -78 ºC. Benzoyl chloride (2.536 g, 2.1 mL, 18.1 mmol) was added slowly via syringe, after which the solution was warmed up to r.t. and left overnight. The reaction was quenched by addition of water (40 mL) and 10 % aq. HCl. Products were extracted with EtOAc, washed with water, BRINE and dried over Na_2SO_4. Two products were isolated via column chromatography, (EtOac/Hexanes): desired compound **5.35** as white crystals (1.03 g, 15 %) and by-product **5.49** ((2,6-dimethoxyphenyl)(phenyl)methanone) as white crystals (3.3 g, 75 %).

Physical properties of **5.35**:

M.p. = 93 ºC.[50]

IR: 3466; 2935 (broad); 1578; 1468; 1243; 1103; 732 cm^{-1}.

^1H NMR ($CDCl_3$, 400 MHz): 7.46 (2H, d, *J* = 7.6 Hz), 7.24-7.20 (2H, m), 7.15-7.11 (3H, m), 6.55 (4H, d, *J* = 8.4 Hz), 6.45 (1H, d, *J* = 1.2 Hz), 3.40 (12H, s).

^{13}C NMR ($CDCl_3$, 100 MHz): 158.0, 149.3, 127.3, 126.6, 126.5, 126.4, 125.4, 106.8, 79.4, 56.4 ppm.

HRMS (ESI), *m/z*: calcd. for $C_{23}H_{24}O_5Na$ $[M+Na]^+$ 403.1516, found 403.1516.

Attempts to deprotect methyl-protected hydroxyls in compounds **5.31** and **5.35** under acidic conditions (excess of BBr_3 in DCM) and under nucleophilic conditions (excess of 2-aminoethanethiol and sodium *t*-butylate in anhydrous DMF) were unsuccessful. Decomposition of starting materials was observed under acidic conditions, however, no reaction happened under nucleophilic conditions in a course of a week. Desired compounds **5.27c** and **5.28c** could not be obtained via given pathway of synthesis.

5.7. References

1. Willumsen, N. J.; Boucher, R. C. *J. Physiol*. **1992**, 455, 247-269.
2. Sakai, H.; Li, G.; Hino, Y.; Moriura, Y.; Kawawaki, J.; Sawada, M.; Kuno, M. *J. Physiol*. **2013**, 591, 5851-5866.
3. Zilberstin, D.; Agmon, V., Schuldiner, S.; Padan, E. *J. Bacteriol*. **1984**, 158 (1), 246-252.
4. Naccache, P. H.; Therrien, S.; Caon, A. C.; Liao, N.; Gilbert, C.; McColl, S. R. *J. Immunol*. **1989**, 142 (7), 2438-2444.
5. Westerblad, H.; Allen, D. G. *J. Physiol*. **1993**, 466, 611-628.
6. Gottlieb, R. A.; Dosanjh, A. *Proc. Natl. Acad. Sci. U. S. A*. **1996**, 93, 3587–3591.
7. Putnam, R. W. *Cell Physiology Source Book*, Sperelakis, N., 4th edn, 2011.
8. Nelson, D. L.; Cox, M. M. *Lehninger Principles of Biochemistry*, W. H. Freeman, 4th edn, 2004.
9. Vieira, O. V.; Botelho, R. J.; Grinstein, S. *Biochem. J.* **2002**, 366, 689–704.
10. Schindler, M.; Grabski, S.; Hoff, E.; Simon, S. M. *Biochemistry* **1996**, 35, 2811–2817.
11. Bach, G.; Chen, C. S.; Pagano, R. E. *Clin. Chim. Acta* **1999**, 280, 173–179.
12. Granzotto, M.; Leone, V.; Lepore, L.; Zerial, M., Tommasini, A.; Ciambra, R.; Gombac, F.; Ventura, A. *Pediatr. Hematol. Oncol*. **2005**, 22, 147–151.

13. Davies, T. A.; Fine, R. E.; Johnson, R. J.; Levesque, C. A.; Rathbun, W. H.; Seetoo, K. F.; Smith, S. J.; Strohmeier, G.; Volicer, L.; Delva, L.; Simons, E. R. *Biochem. Biophys. Res. Commun*. **1993**, 194, 537–543.
14. Loiselle, F. B., Casey, J. R. *Methods Mol. Biol*. **2010**, 637, 311-331.
15. Burgess, K.; Han, J. Y. *Chem. Rev*. **2010**, 110, 2709–2728.
16. Lavis, L. D.; Raines, R. T. *ACS Chem. Biol*. **2014**, 9, 855−866.
17. Ipuy, M.; Billon, C.; Micouin, G.; Samarut, J.; Andraud, C.; Bretonnière, Y. *Org. Biomol. Chem*. **2014**, 12, 3641-3648.
18. Su, M.; Liu, Y.; Ma, H.; Ma, Q.; Wang, Z.; Yang, J.; Wang, M. *Chem. Commun*. **2001**, 960-961.
19. Li, X.; Gao, X.; Shi, W.; Ma, H. *Chem. Rev.* **2014**, 114, 590−659.
20. Leonhard, H.; Gordon, L.; Livingst, R. *J. Phys. Chem*. **1971**, 75, 245-249.
21. Hasegawa, T.; Kondo, Y.; Koizumi, Y.; Sugiyama, T.; Takeda, A.; Ito, S.; Hamada, F. *Bioorg. Med. Chem*. **2009**, 17, 6015-6019.
22. Zhu, H.; Fan, J.; Xu, Q.; Li, H.; Wang, J.; Gao, P.; Peng, X. *Chem. Commun*. **2012**, 48, 11766-11768.
23. Li, Z.; Wu, S.; Han, J.; Han, S. *Analyst* **2011**, 136, 3698-3706.
24. Nekongo, E. E.; Bagchi, P.; Fahrnib, C. J.; Popik, V. V. *Org. Biomol. Chem*. **2012**, 10, 9214-9218.
25. Lord, S. J.; Lee, H. D.; Samuel, R.; Weber, R.; Liu, N.; Conley, N. R.; Thompson, M. A.; Twieg, R. J.; Moerner, W. E. *J. Phys. Chem. B* **2010**, 114 (45), 14157-14167.
26. Lidke, D. S.; Wilson, B. S. *Trends Cell Biol*. **2009**, 19, 566-574.
27. Kozlowski, D. J.; Weinberg, E. S. *Methods Mol. Biol*. **2000**, 135, 349-355.
28. Pelliccioli, A. P.; Wirz, J. *Photochem. Photobiol. Sci*. **2002**, 1, 441-458.
29. Stegmaier, P.; Alonso, J. M.; Campo, A. *Langmuir* **2008**, 24 (20), 11872-11879.

30. Banerjee, A.; Grewer, C.; Ramakrishnan, L., Jager, J.; Gameiro, A.; Breitinger, H.-G. A.; Gee, K. R.; Carpenter, B. K.; Hess, G. P. *J. Org. Chem*. **2003**, 68, 8361-8367.
31. Fedoryak, O. D.; Dore, T. M. *Org. Lett*. **2002**, 4, 3419-3422.
32. Misetic, A.; Boyd, M. K. *Tetrahedron Lett*. **1998**, 39, 1653-1656.
33. Belov, V. N.; Wurm, C. A.; Boyarskiy, V. P.; Jakobs, S.; Hell, S. W. *Angew. Chem. Int. Ed*. **2010**, 49, 3520-3523.
34. Kitani, S.; Sugawara, K.; Tsutsumi, K.; Morimoto, T.; Kakiuchi, K. *Chem. Commun*. **2008**, 2103–2105.
35. Zhang, Y.; Tanimoto, H.; Nishiyama, Y., Morimoto, T.; Kakiuchi, K. *Synlett* **2012**, 23, 367–370.
36. Hikage, S.; Sasaki, Y.; Hisai. T.; Tanimoto, H.; Morimoto, T.; Nishiyama, Y.; Kakiuchi, K. *J. Photochem. Photobiol. A: Chem*. **2016**, 331, 175–183.
37. Zhang, Y.; Zhang, H.; Ma, C.; Li, J.; Nishiyama, Y.; Tanimoto, H.; Morimoto, T.; Kakiuchi, K. *Tetrahedron Lett*. **2016**, 57, 5179–5184.
38. Akiba, M.; Dvornikov, A. S.; Rentzepis, P. M. *Chemistry* **2007**, 190, 69-76.
39. Mills, O. S.; Mooney, N. J.; Robinson,P. M.; Watt, C. I. F.; Box, B. J. *J. Chem. Soc. Perkin Trans. 2* **1995**, 697-706.
40. Greco, M. N.; Rasmussen, C. R. *J. Org. Chem*. **1992**, 57, 5532-5535.
41. Hammann, B.; Razzaghi, M.; Kashefolgheta, S.; Lu, Y. *Chem. Commun*. **2012**, 48 (92), 11337-11339.
42. Long, J. Z.; Jin, X.; Adibekian, A.; Li, W.; Cravatt, B. F. *J. Med. Chem*. **2010**, 53 (4), 1830-1842.
43. Holleman, A. F. *Org. Synth*. **1927**, 7, 88-89.
44. Goldberg, A. A.; Wragg, A. H. *J. Chem. Soc*. **1957**, 4823-4829.
45. Bo, X. *Anhui Huagong* **2012**, 38 (3), 29-32.
46. Zhang, S. *Method for synthesizing xanthene alcohol*. CN 107698551, Feb. 16, 2018.

47. Pillai, r. K. M.; Naiksatam, P.; Johnson, F.; Rajagopalan, R.; Watts, P. C., Cricchio, R.; Borras, S. *J. Org. Chem*. **1986**, 51 (5), 717-723.

48. Sugawara, S.; Kojima, S.; Yamamoto, Y. *Chem. Commun*. **2012**, 48, 9735-9737.

49. Tobisu, M.; Yamakawa, K.; Shimasaki, T.; Chatani, N. *Chem. Commun.* **2011**, 47 (10), 2946-2948.

50. Wada, M.; Mishima, H.; Watanabe, T.; Natsume, S.; Konishi, H.; Kirishima, K.; Hayase, S.; Erabi, T. *Bull. Chem. Soc. Jpn*. **1995**, 68 (1), 243-249.

CHAPTER 6

CONCLUSIONS

o-QMs and *p*-QMs demonstrate different chemical properties and different reactivity. However, to the best of our knowledge, the molecules containing competing *o*-NQM and *p*-QM moieties, have not been studied. Thus, the major goal of the first project was to develop and synthesize novel QMPs with ability to generate *o*-NQM and *p*-QM under light irradiation. According to obtained rate constants of hydration and reactions between photochemically generated QMs and nucleophiles, it may be concluded that novel QM systems exhibit predominantly properties of *p*-QMs than *o*-NQMs. The extremely small rate constants of intermolecular Diels-Alder reaction also supported the predomination of the *p*-QM form over o-NQM tautomer.

We have also attempted to synthesize "smart" polymers in the solution, that could undergo polymerization and degradation on demand upon UV-light irradiation. Unfortunately, one of the synthesized monomers was unstable towards acid-promoted decomposition and oxidation, and thus its ability to form polymers has not been tested. Another monomer was found to form oligomers of up to 4 units, however, formation of a polymer was not achieved. As potential problems were identified as poor solubility of oligomers and chance of depolymerization due to hydrolysis, polymerization between two monomers, such as 3-hydroxy-2-naphthalenemethanol and a linker with two ending thiol groups should be tested.

We have developed the first photo-cleavable analog of BAPTA Ca^{2+} chelator, NQMP-BAPTA, by incorporating photo-labile 3-(hydroxymethyl)-2-naphthol linker in the structure. NQMP-BAPTA possess very high calcium affinity (K_{bnd} = 2.46 x 10^6 M^{-1}), but upon irradiation, the ligand loses one of its tridentate chelating arms resulting in the efficient calcium ion release. The high quantum yield (Φ = 0.63) of the

NQMP-BAPTA cleavage makes it one of the most efficient of photosensitive calcium-ion chelators. The NQMP linker photo-cleavage occurs on the microsecond time scale making NQMP-BAPTA suitable for time-resolved experiments.

Finally, we have attempted the synthesis of novel fluorescent pH_i indicators and photoactivatable fluorogenic PPGs, which would be based on 9H-xanthene-1,8,9-triol scaffold. However, standard reduction method applied to 1,8-dihydroxy-9H-xanthen-9-one resulted in the formation of unexpected secondary reduction product. Due to the instability of the primary reduction product in the reaction conditions and the fact of formation of the desired 8-hydroxy-1*H*-xanthen-1-one from corresponding xanthene under electron-spray ionization conditions, future synthetic efforts should be focused on oxidation of 9H-xanthene-1,8-diol.

APPENDIX A

^{1}H AND ^{13}C NMR SPECTRA

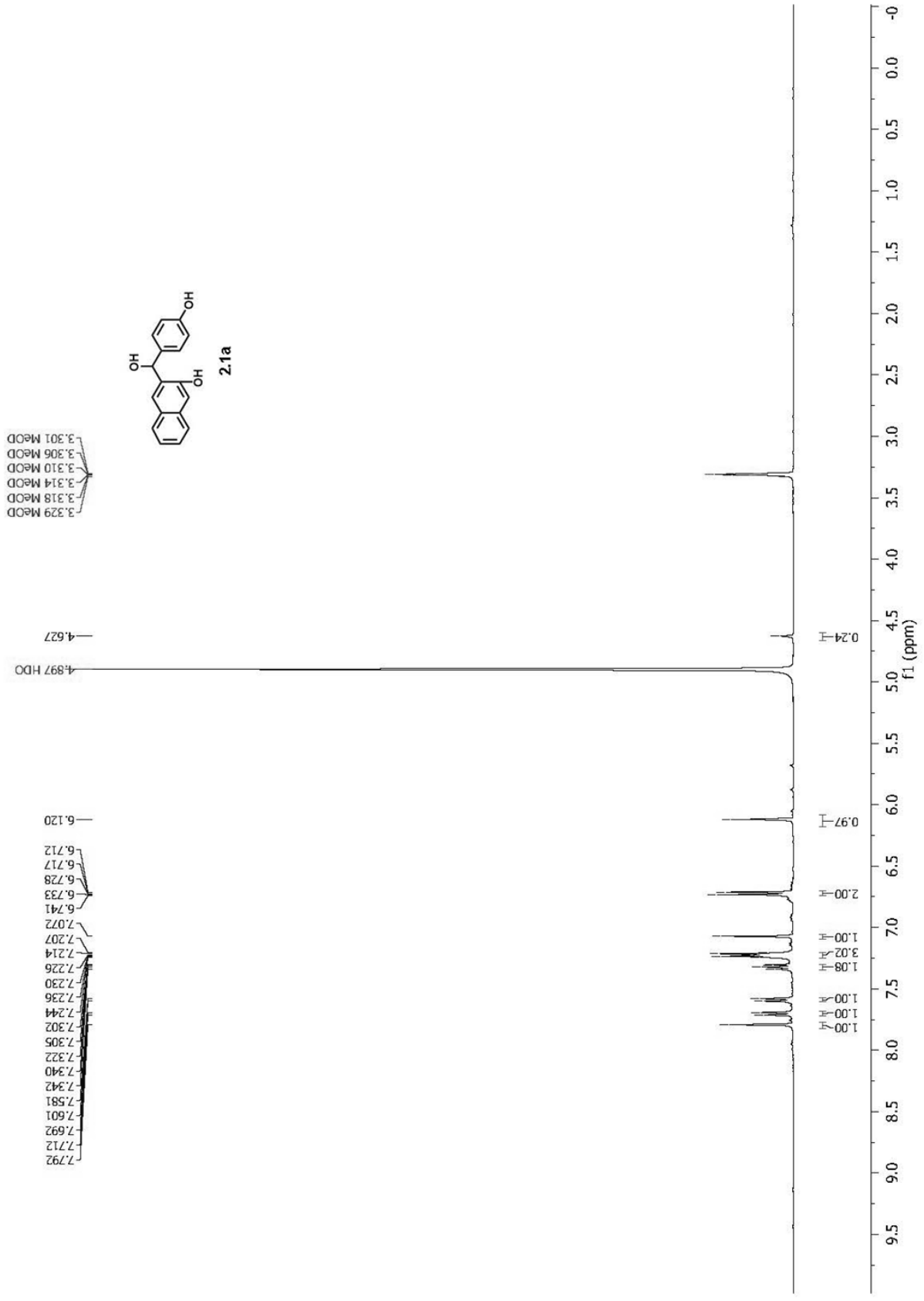
2.1a
OH
OH
OH
3.301 MeOD
3.306 MeOD
3.310 MeOD
3.314 MeOD
3.318 MeOD
3.329 MeOD
4.627
4.897 HDO
6.120
6.712
6.717
6.728
6.733
6.741
7.072
7.207
7.214
7.226
7.230
7.236
7.244
7.302
7.305
7.322
7.340
7.342
7.581
7.601
7.692
7.712
7.792
0.24
0.97
2.00
1.00
3.02
1.08
1.00
1.00
1.00
1.00
f1 (ppm)

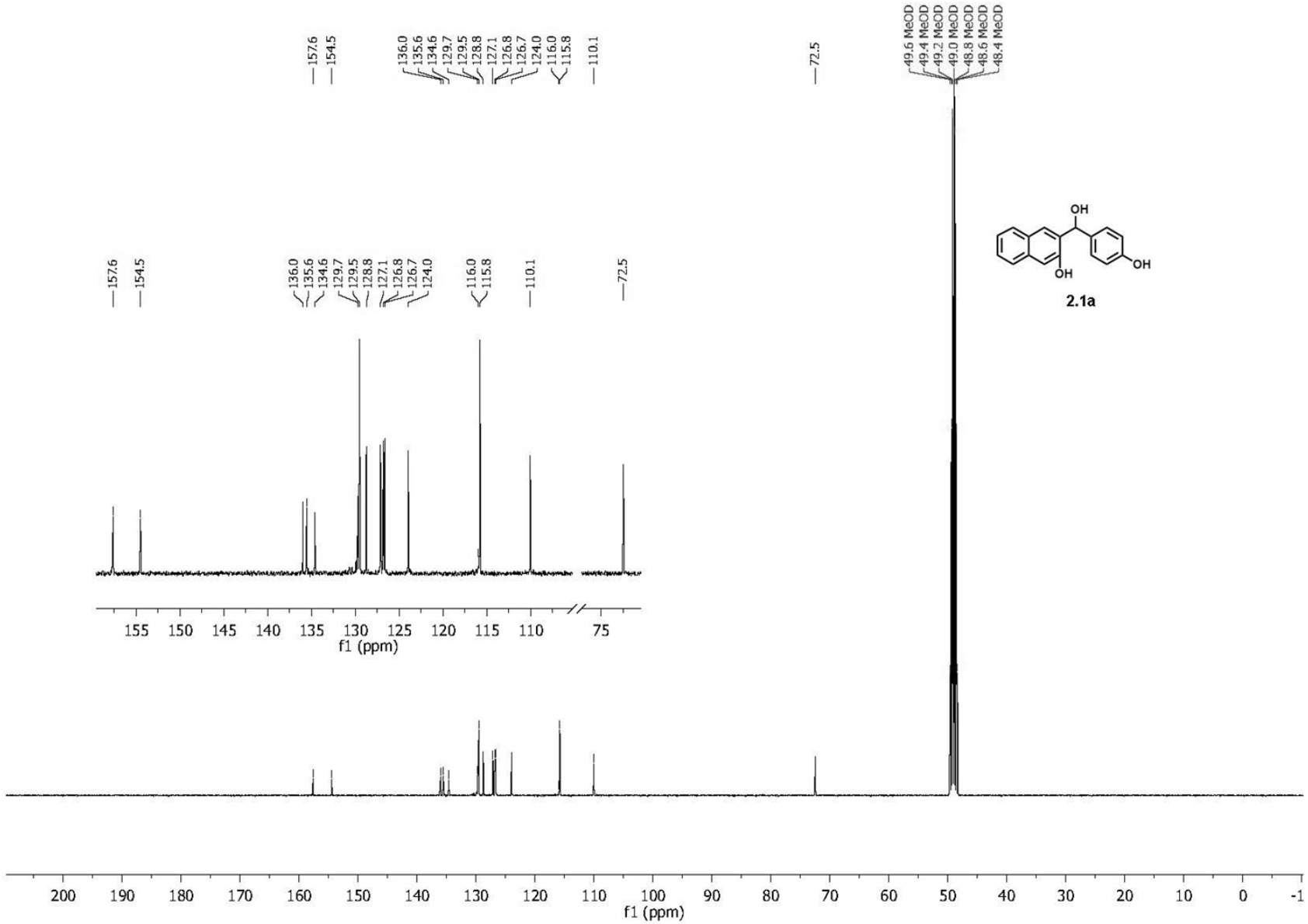
157.6
154.5
136.0
135.6
134.6
129.7
129.5
128.8
127.1
126.8
126.7
124.0
116.0
115.8
110.1
72.5
49.6 MeOD
49.4 MeOD
49.2 MeOD
49.0 MeOD
48.8 MeOD
48.6 MeOD
48.4 MeOD
OH
OH
OH
2.1a
f1 (ppm)
f1 (ppm)

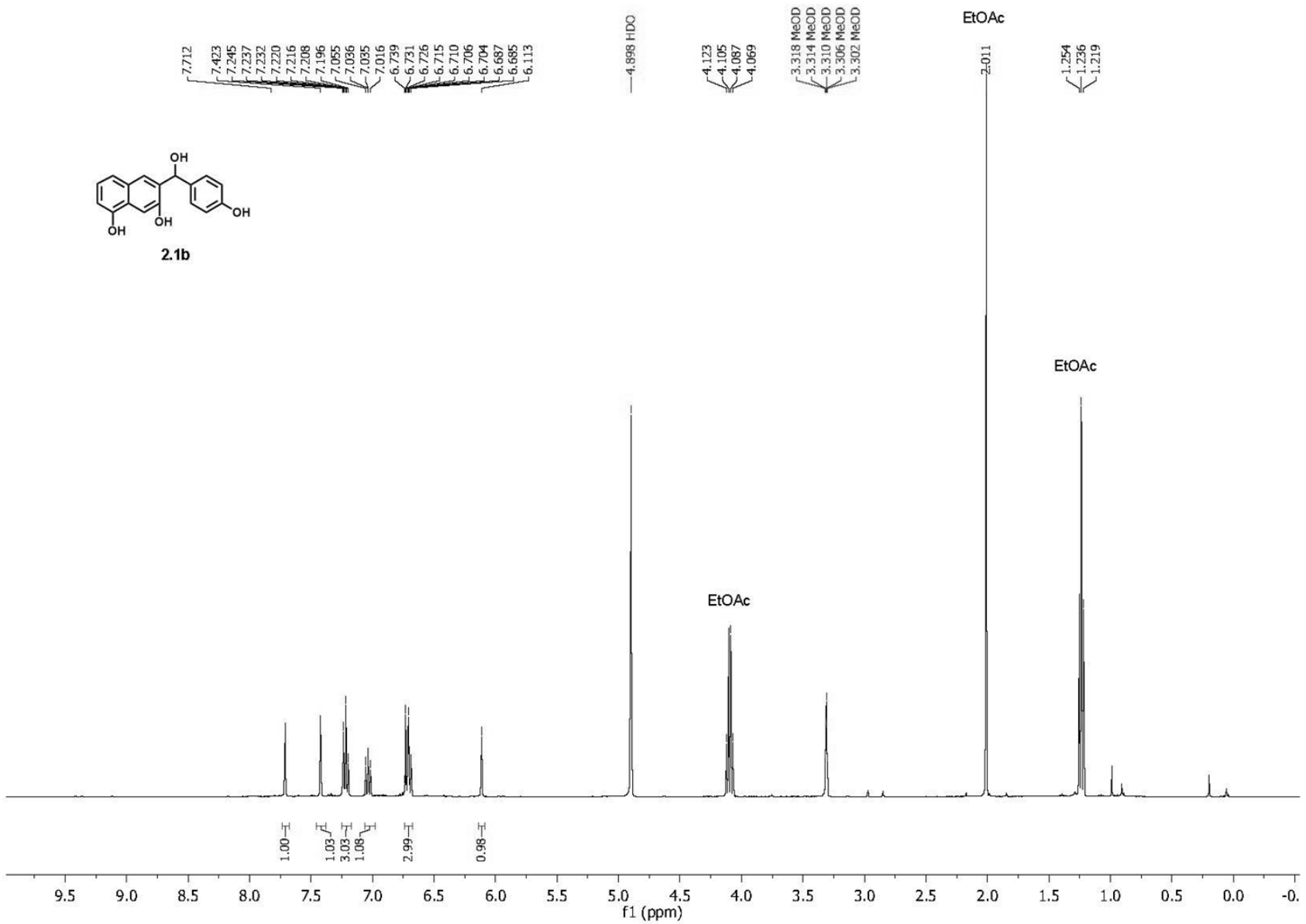
7.712
7.423
7.245
7.237
7.232
7.220
7.216
7.208
7.196
7.055
7.036
7.035
7.016
6.739
6.731
6.726
6.715
6.710
6.706
6.704
6.687
6.685
6.113
4.898 HDO
4.123
4.105
4.087
4.069
3.318 MeOD
3.314 MeOD
3.310 MeOD
3.306 MeOD
3.302 MeOD
2.011
1.254
1.236
1.219
EtOAc
EtOAc
EtOAc
OH
OH
OH
OH
2.1b
1.00
1.03
3.03
1.08
2.99
0.98
f1 (ppm)

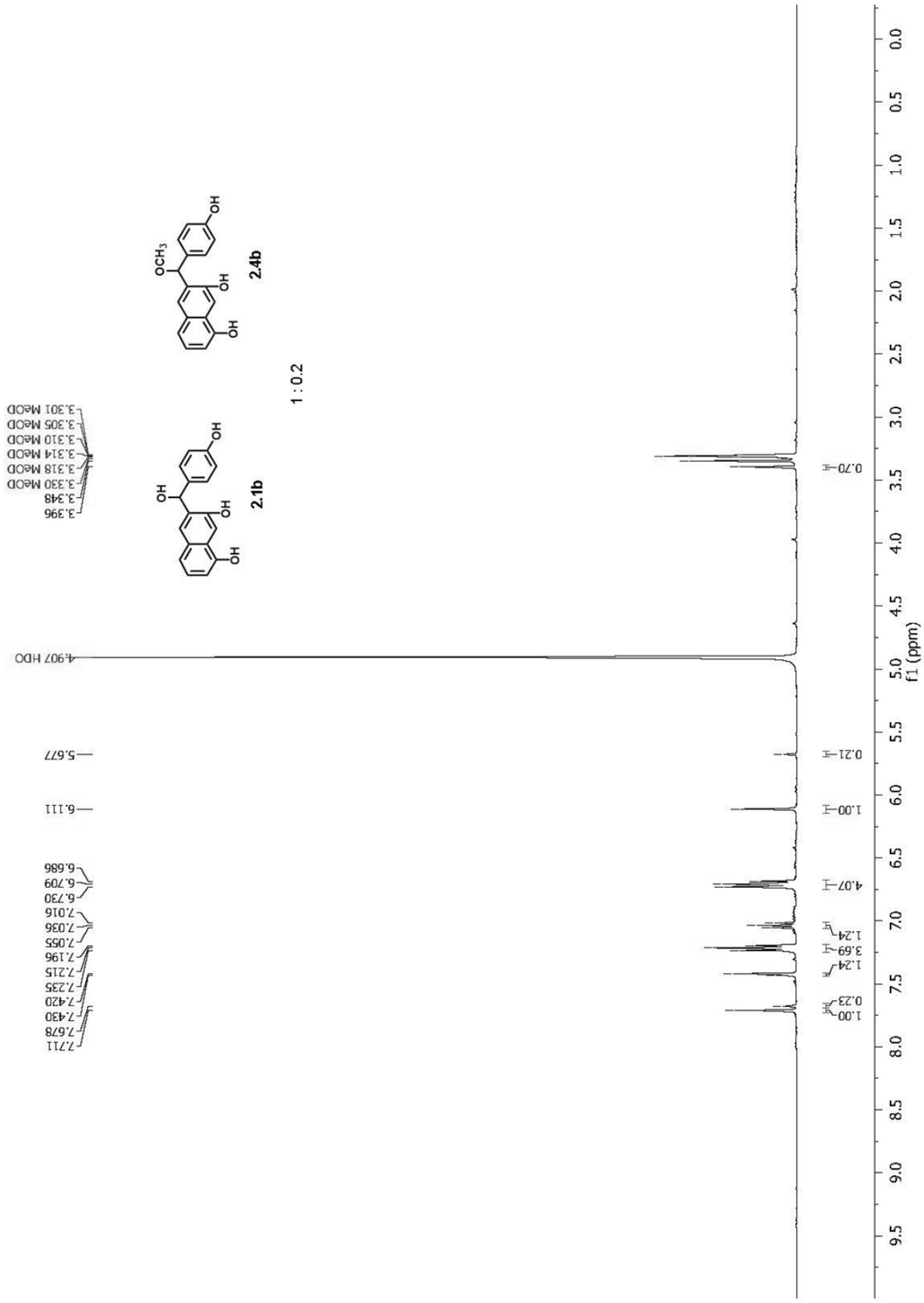
2.4b
1 : 0.2
2.1b
f1 (ppm)

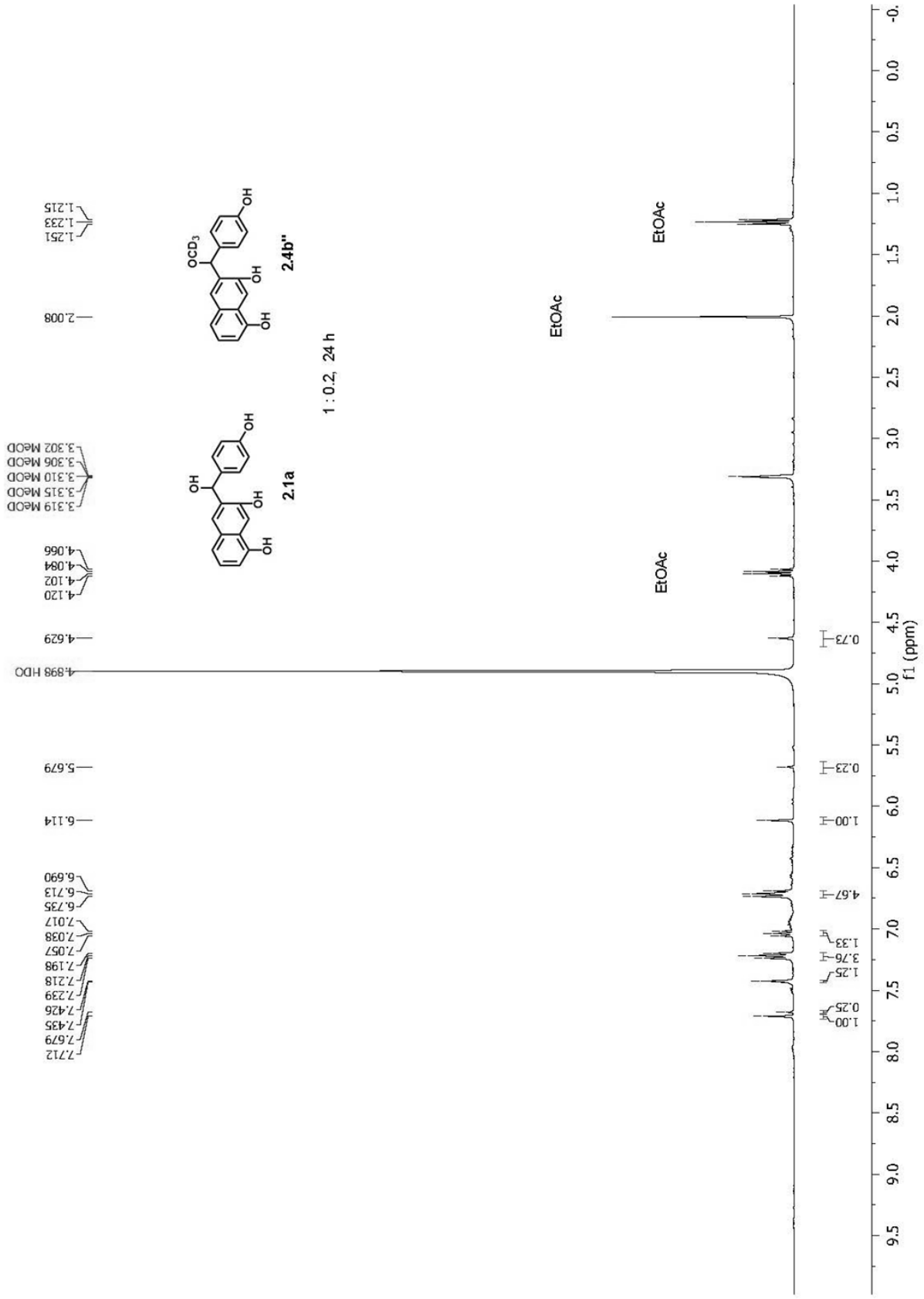
EtOAc
EtOAc
EtOAc
1 : 0.2, 24 h
2.4b"
2.1a
f1 (ppm)

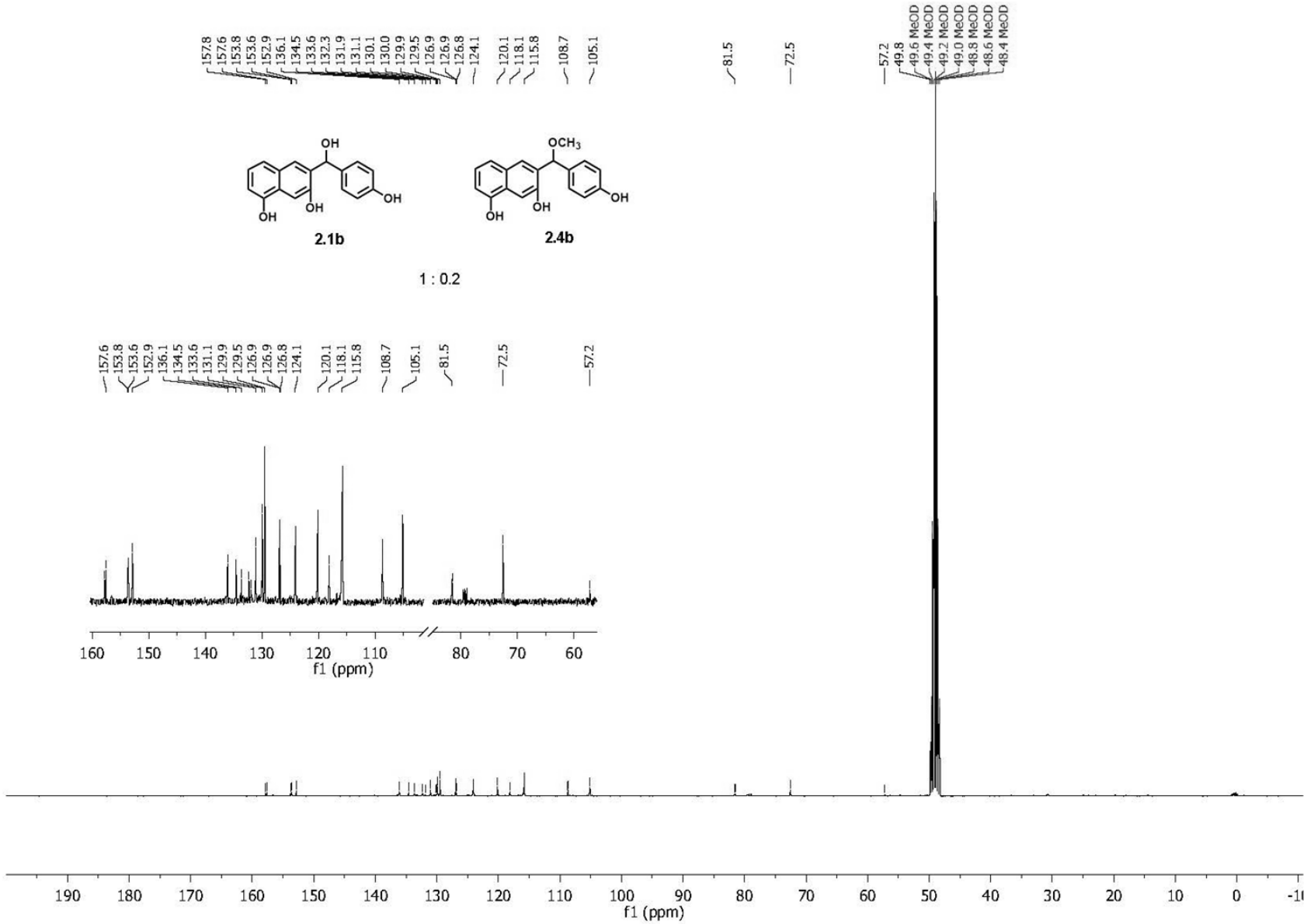
157.8
157.6
153.8
153.6
152.9
136.1
134.5
133.6
132.3
131.9
131.1
130.1
130.0
129.9
129.5
126.9
126.9
126.8
124.1
120.1
118.1
115.8
108.7
105.1
81.5
72.5
57.2
49.8
49.6 MeOD
49.4 MeOD
49.2 MeOD
49.0 MeOD
48.8 MeOD
48.6 MeOD
48.4 MeOD
OH
OH
OH
OH
2.1b
OCH3
OH
OH
OH
2.4b
1 : 0.2
157.6
153.8
153.6
152.9
136.1
134.5
133.6
131.1
129.9
129.5
126.9
126.9
126.8
124.1
120.1
118.1
115.8
108.7
105.1
81.5
72.5
57.2
160
150
140
130
120
110
80
70
60
f1 (ppm)
190
180
170
160
150
140
130
120
110
100
90
80
70
60
50
40
30
20
10
0
f1 (ppm)

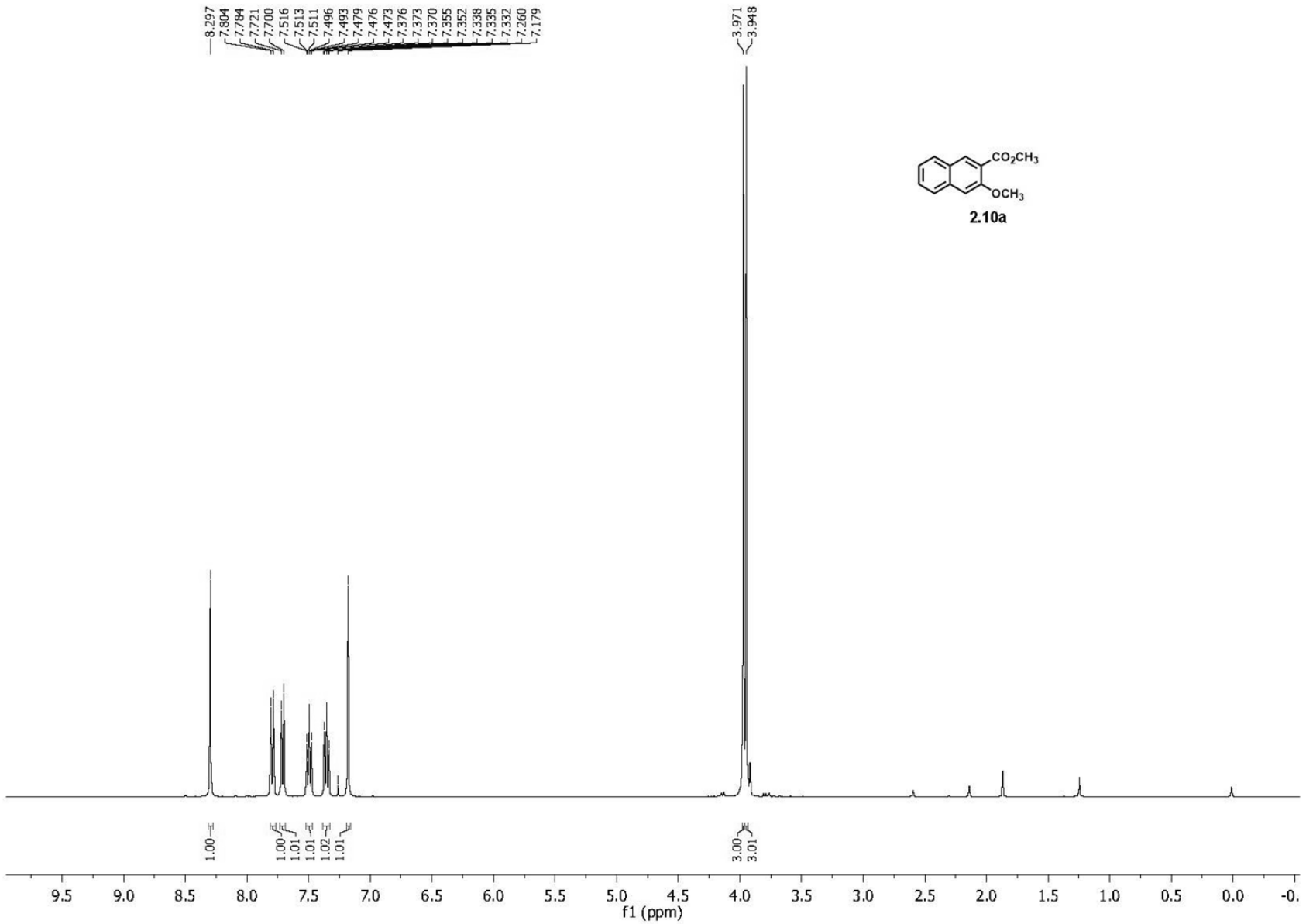
8.297
7.804
7.784
7.721
7.700
7.516
7.513
7.511
7.496
7.493
7.479
7.476
7.473
7.376
7.373
7.370
7.355
7.352
7.338
7.335
7.332
7.260
7.179
3.971
3.948
CO2CH3
OCH3
2.10a
1.00
1.00
1.01
1.01
1.02
1.01
3.00
3.01
9.5
9.0
8.5
8.0
7.5
7.0
6.5
6.0
5.5
5.0
4.5
4.0
3.5
3.0
2.5
2.0
1.5
1.0
0.5
0.0
-0.
f1 (ppm)

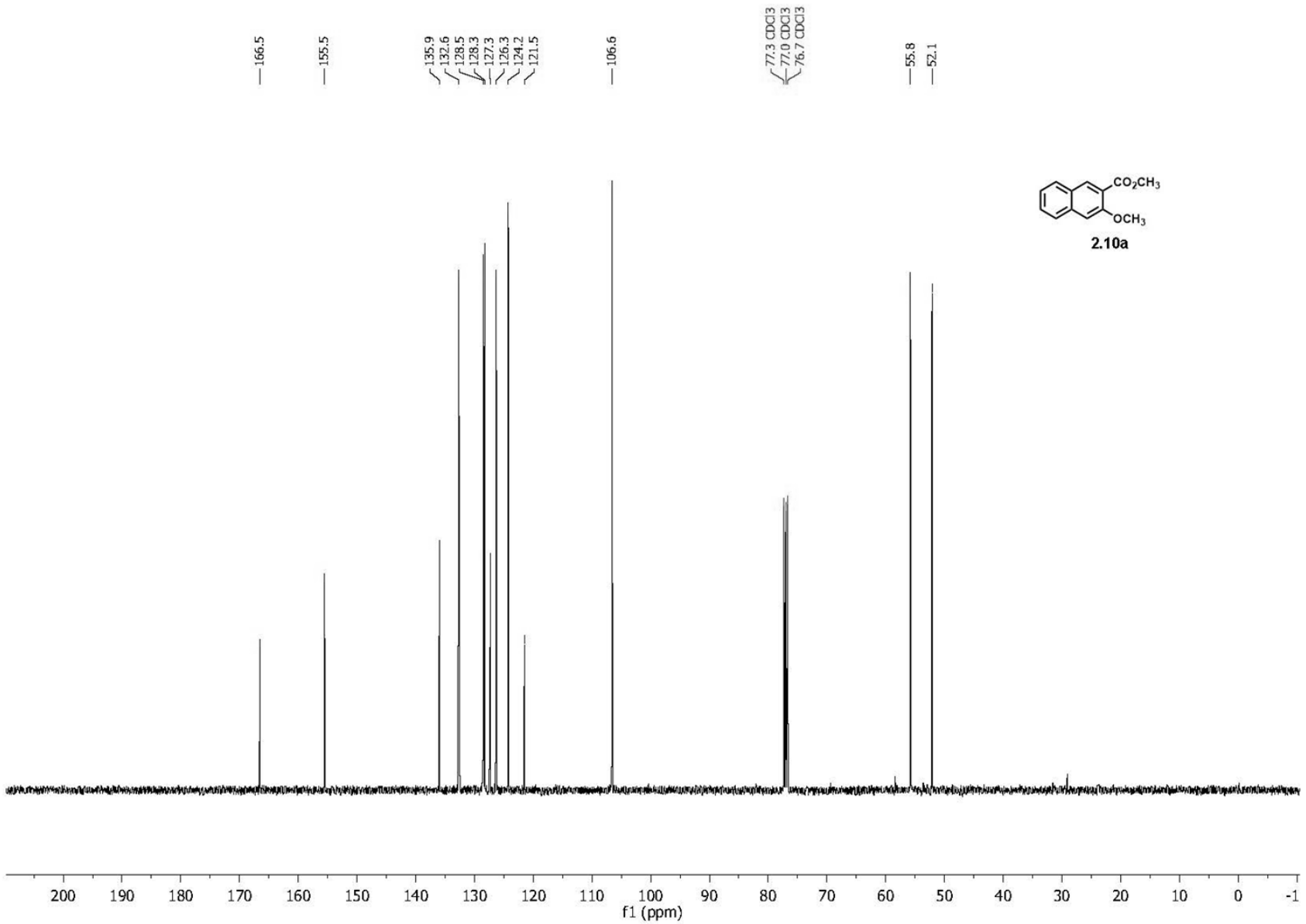
166.5
155.5
135.9
132.6
128.5
128.3
127.3
126.3
124.2
121.5
106.6
77.3 CDCl3
77.0 CDCl3
76.7 CDCl3
55.8
52.1
CO2CH3
OCH3
2.10a
200
190
180
170
160
150
140
130
120
110
100
90
80
70
60
50
40
30
20
10
0
-1
f1 (ppm)

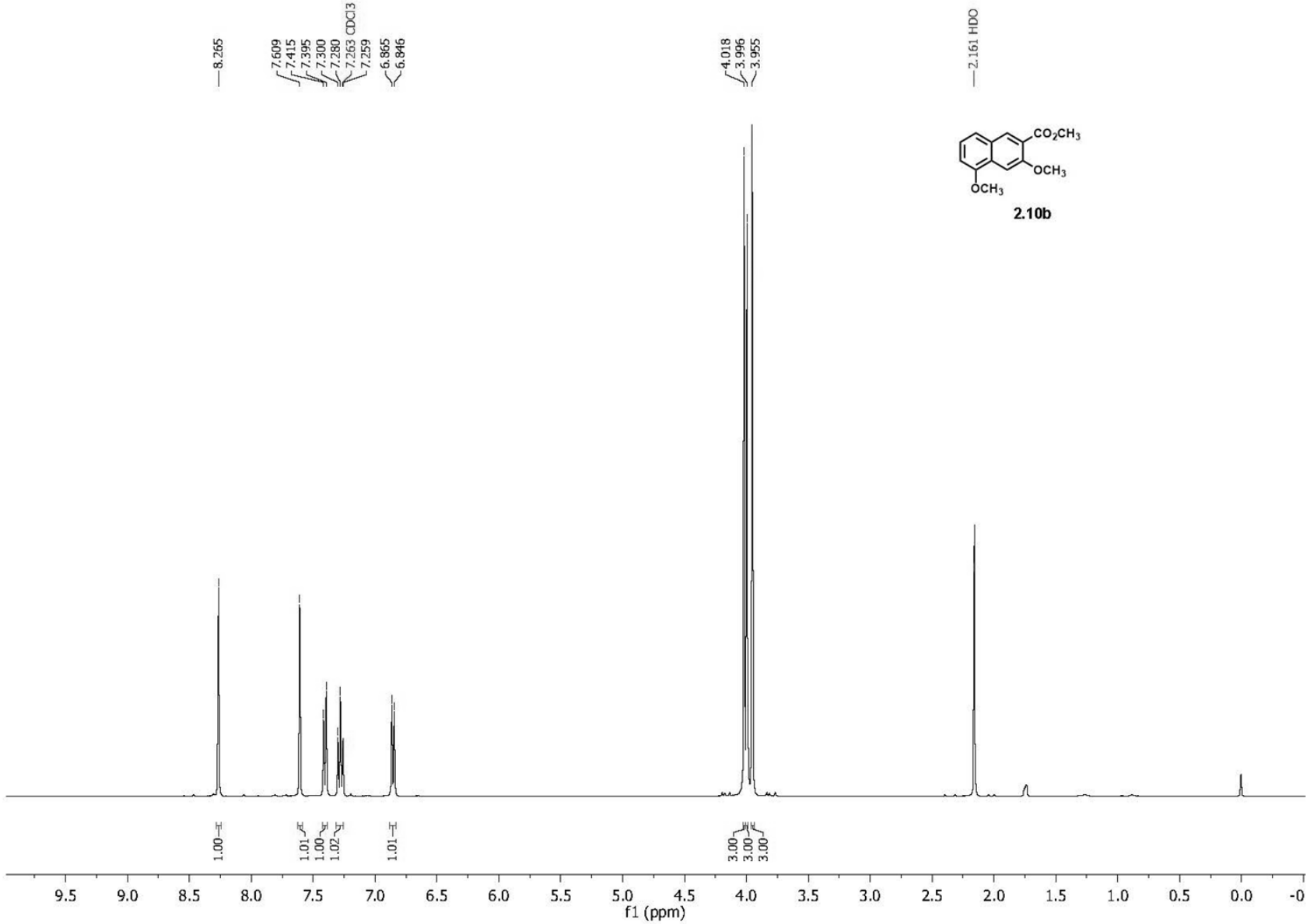
8.265
7.609
7.415
7.395
7.300
7.280
7.263 CDCl3
7.259
6.865
6.846
4.018
3.996
3.955
2.161 HDO
CO2CH3
OCH3
OCH3
2.10b
1.00
1.01
1.00
1.02
1.01
3.00
3.00
3.00
9.5
9.0
8.5
8.0
7.5
7.0
6.5
6.0
5.5
5.0
4.5
4.0
3.5
3.0
2.5
2.0
1.5
1.0
0.5
0.0
-0
f1 (ppm)

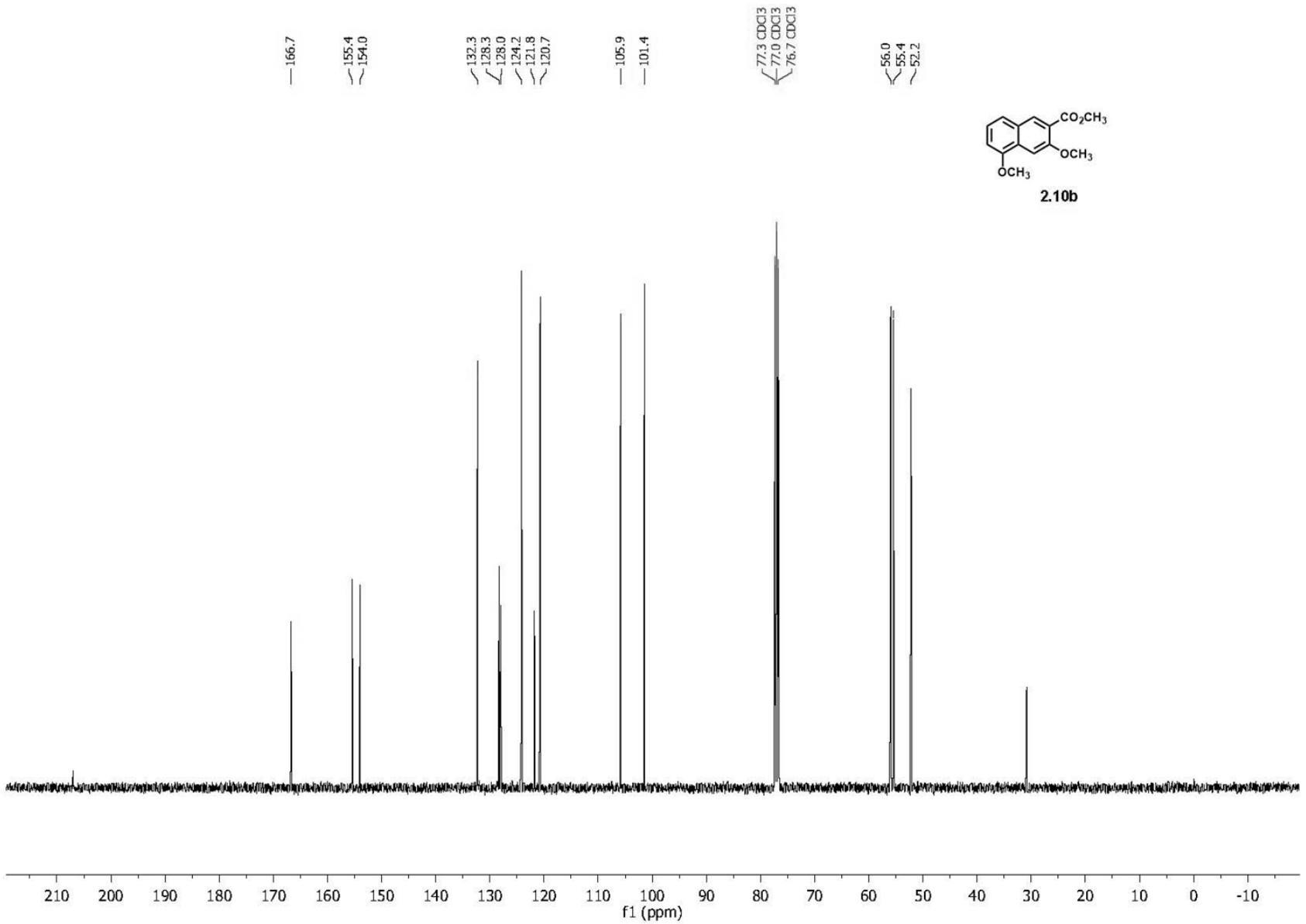
166.7
155.4
154.0
132.3
128.3
128.0
124.2
121.8
120.7
105.9
101.4
77.3 CDCl3
77.0 CDCl3
76.7 CDCl3
56.0
55.4
52.2
CO2CH3
OCH3
OCH3
2.10b
210 200 190 180 170 160 150 140 130 120 110 100 90 80 70 60 50 40 30 20 10 0 -10
f1 (ppm)

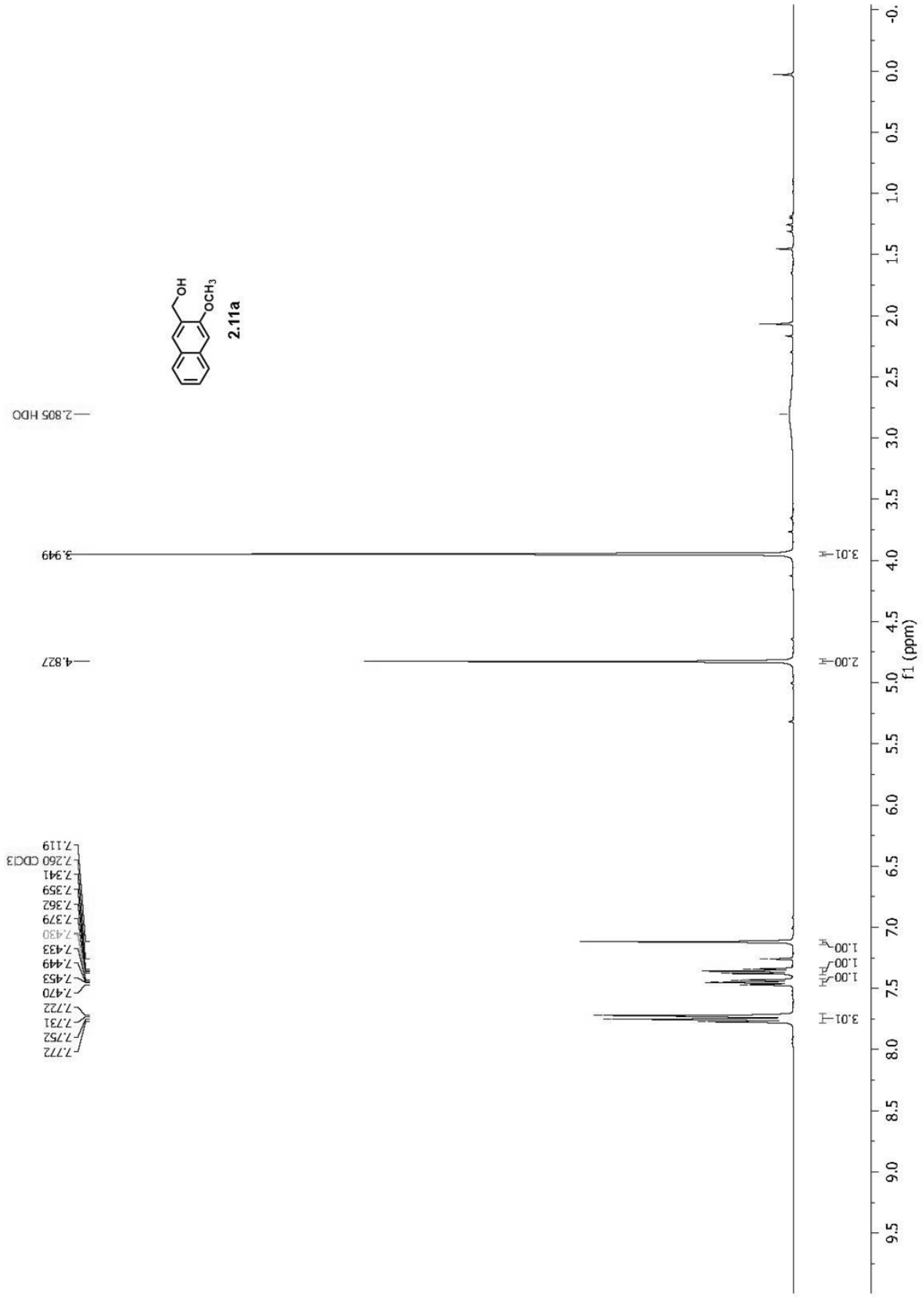
OH
OCH3
2.11a
2.805 HDO
3.949
4.827
7.119
7.260 CDCl3
7.341
7.359
7.362
7.379
7.430
7.433
7.449
7.453
7.470
7.722
7.731
7.752
7.772
3.01
2.00
1.00
1.00
1.00
3.01
f1 (ppm)

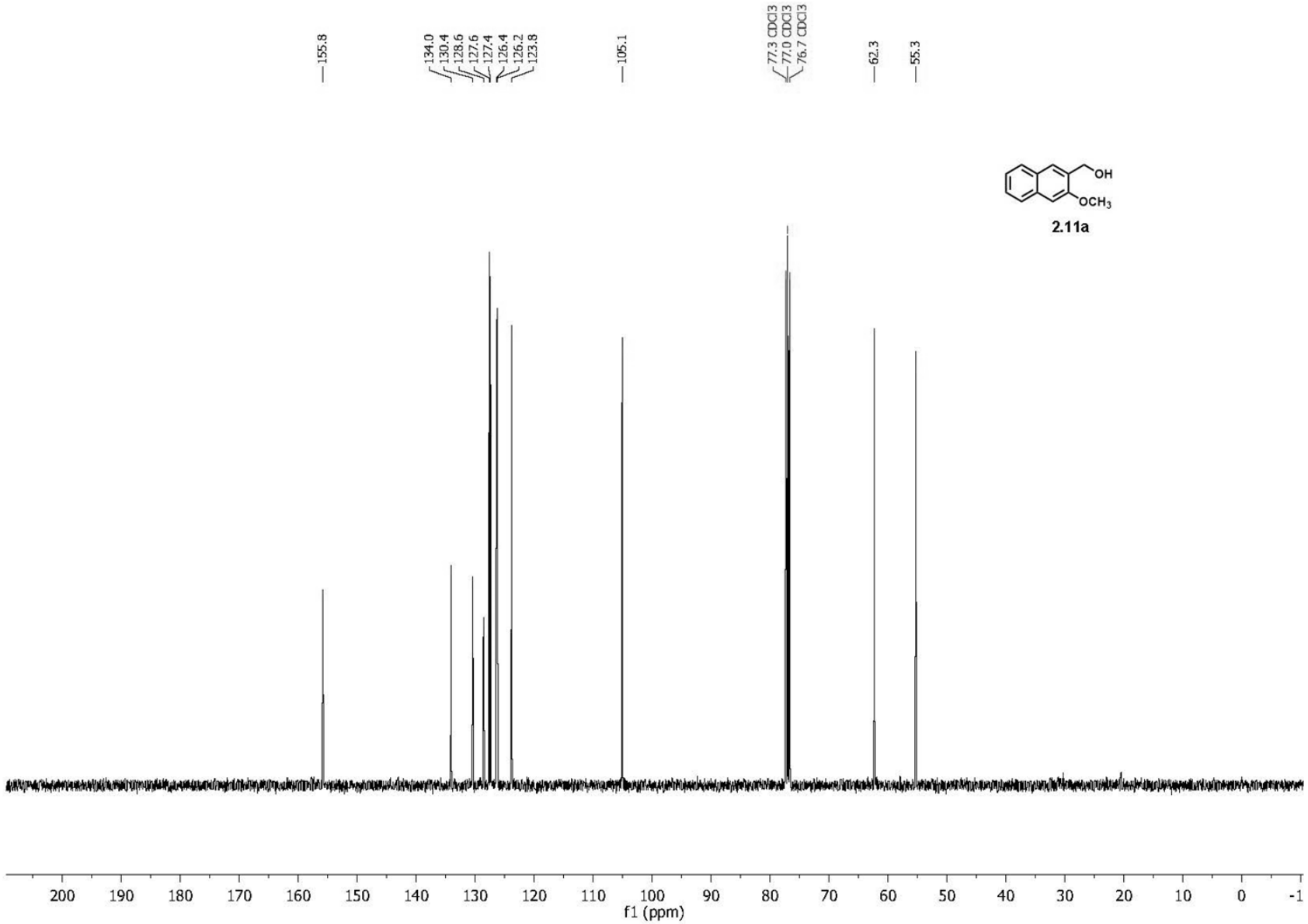
155.8
134.0
130.4
128.6
127.6
127.4
126.4
126.2
123.8
105.1
77.3 CDCl3
77.0 CDCl3
76.7 CDCl3
62.3
55.3
OH
OCH3
2.11a
200
190
180
170
160
150
140
130
120
110
100
90
80
70
60
50
40
30
20
10
0
-1
f1 (ppm)

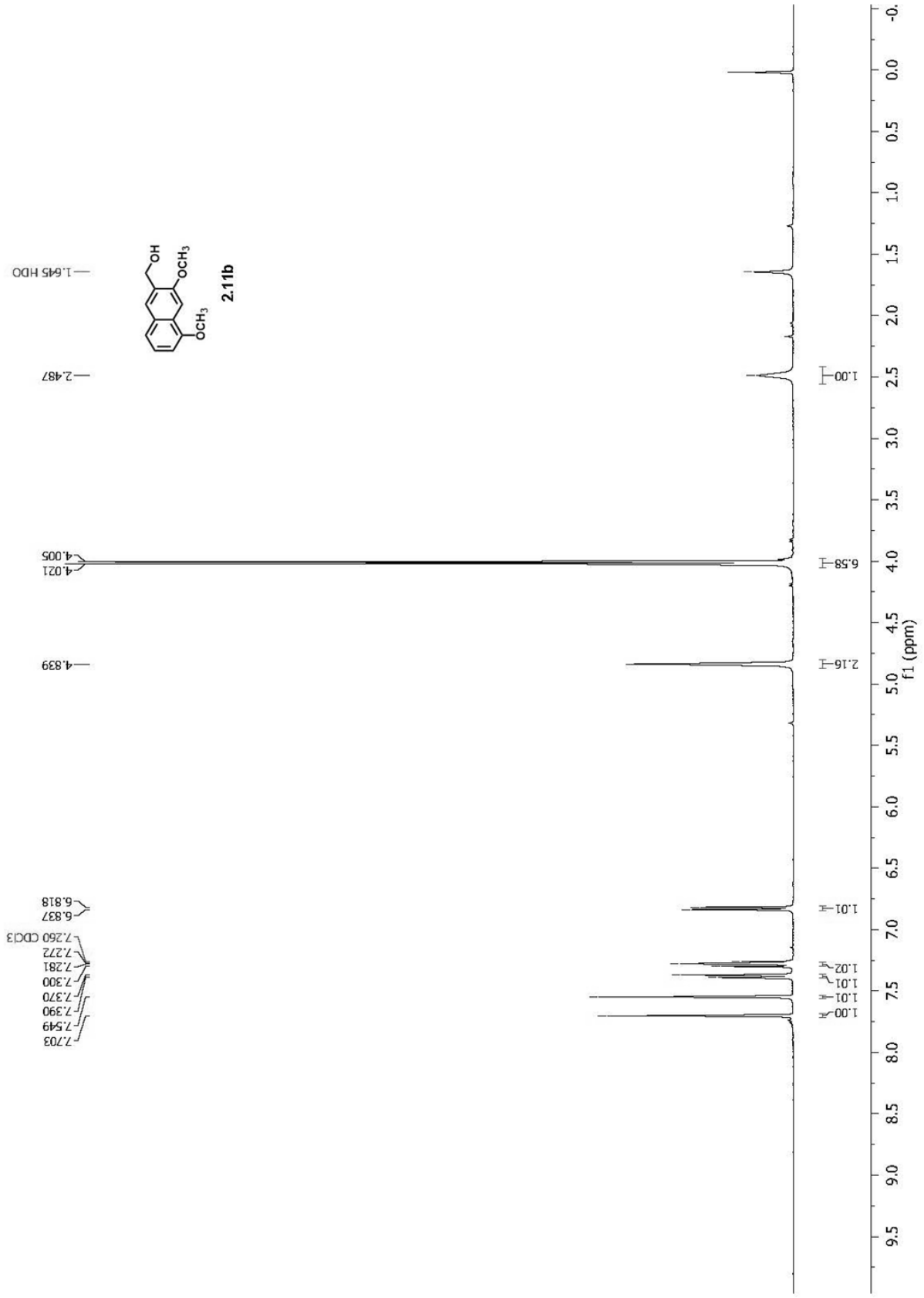
OH
OCH3
OCH3
2.11b
1.645 HDO
2.487
4.005
4.021
4.839
6.818
6.837
7.260 CDCl3
7.272
7.281
7.300
7.370
7.390
7.549
7.703
1.00
6.58
2.16
1.01
1.02
1.01
1.01
1.00
f1 (ppm)

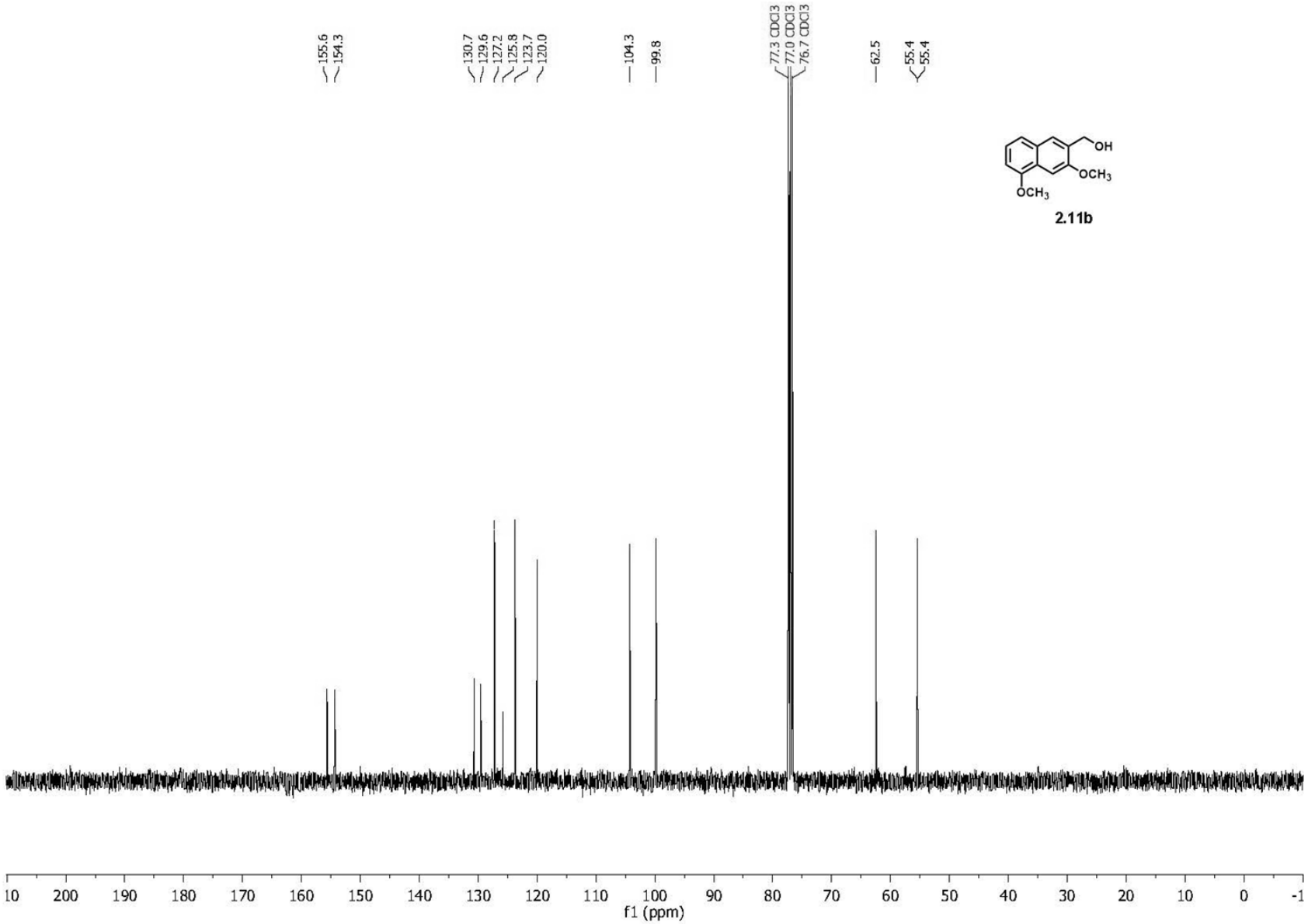
155.6
154.3
130.7
129.6
127.2
125.8
123.7
120.0
104.3
99.8
77.3 CDCl3
77.0 CDCl3
76.7 CDCl3
62.5
55.4
55.4
OH
OCH3
OCH3
2.11b
f1 (ppm)

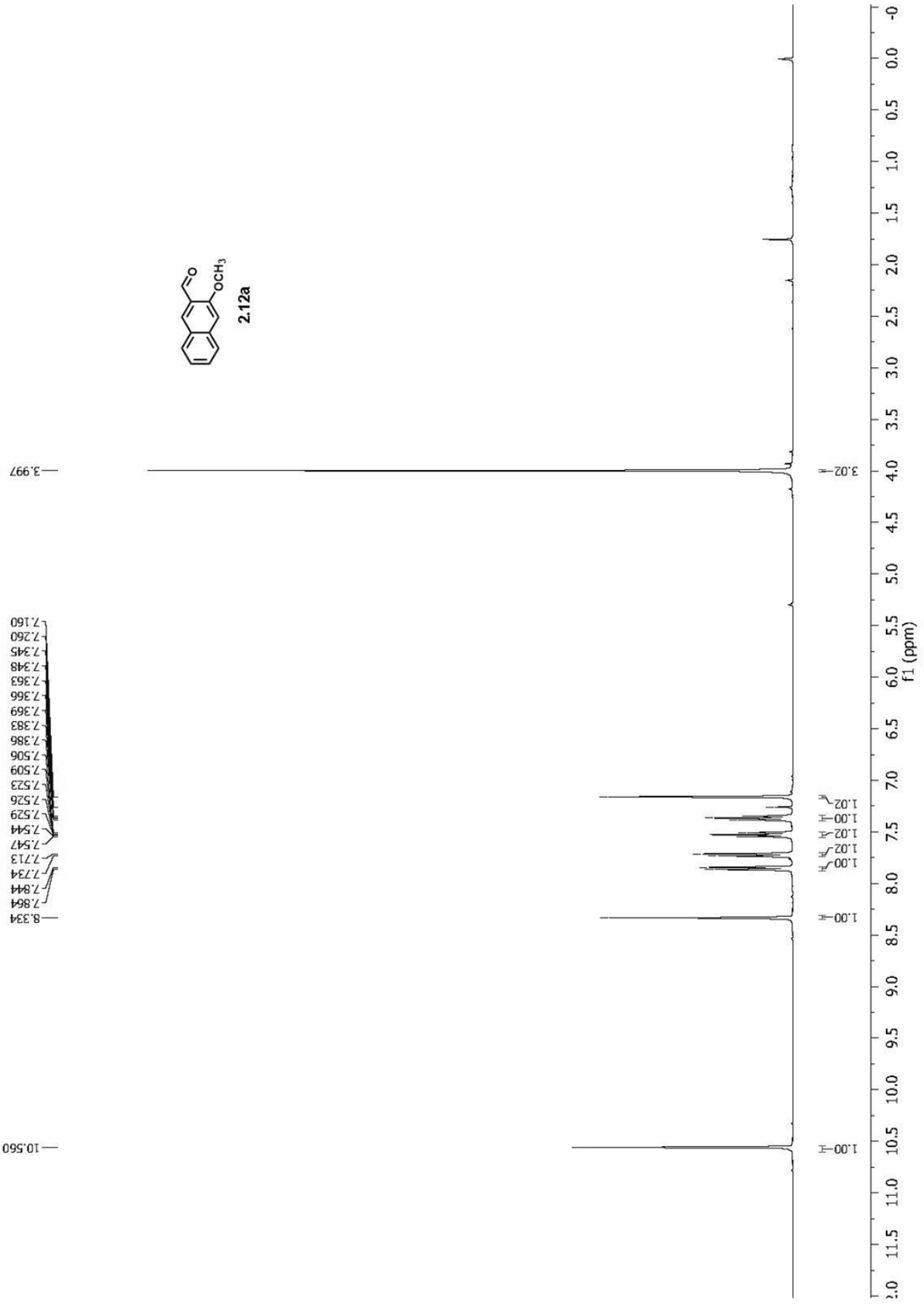
2.12a
OCH3
O
10.560
8.334
7.864
7.844
7.734
7.713
7.547
7.544
7.529
7.526
7.523
7.509
7.506
7.386
7.383
7.369
7.366
7.363
7.348
7.345
7.260
7.160
3.997
1.00
1.00
1.02
1.00
1.02
1.00
1.02
3.02
1.00
f1 (ppm)

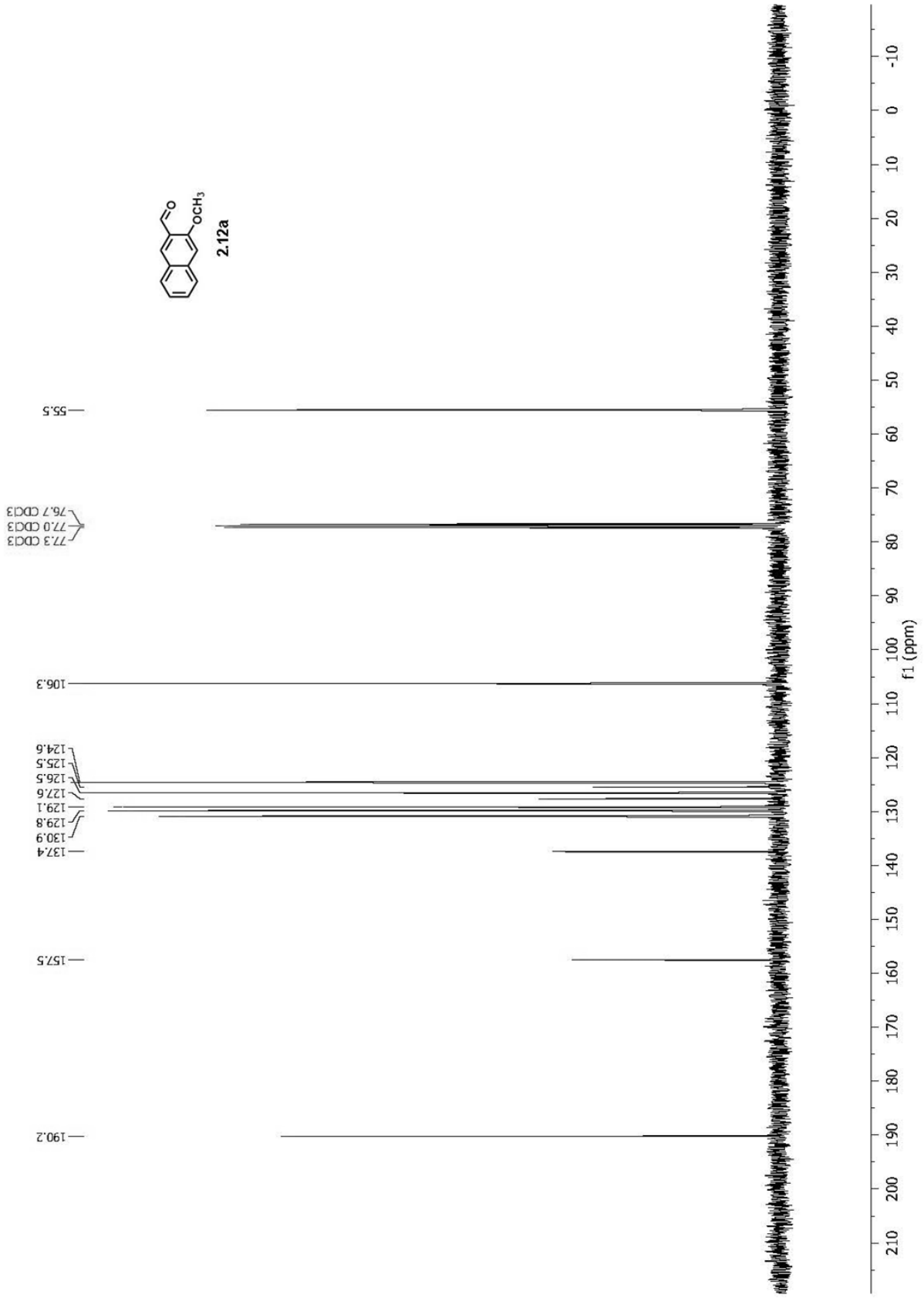
2.12a
190.2
157.5
137.4
130.9
129.8
129.1
127.6
126.5
125.5
124.6
106.3
77.3 CDCl3
77.0 CDCl3
76.7 CDCl3
55.5
f1 (ppm)

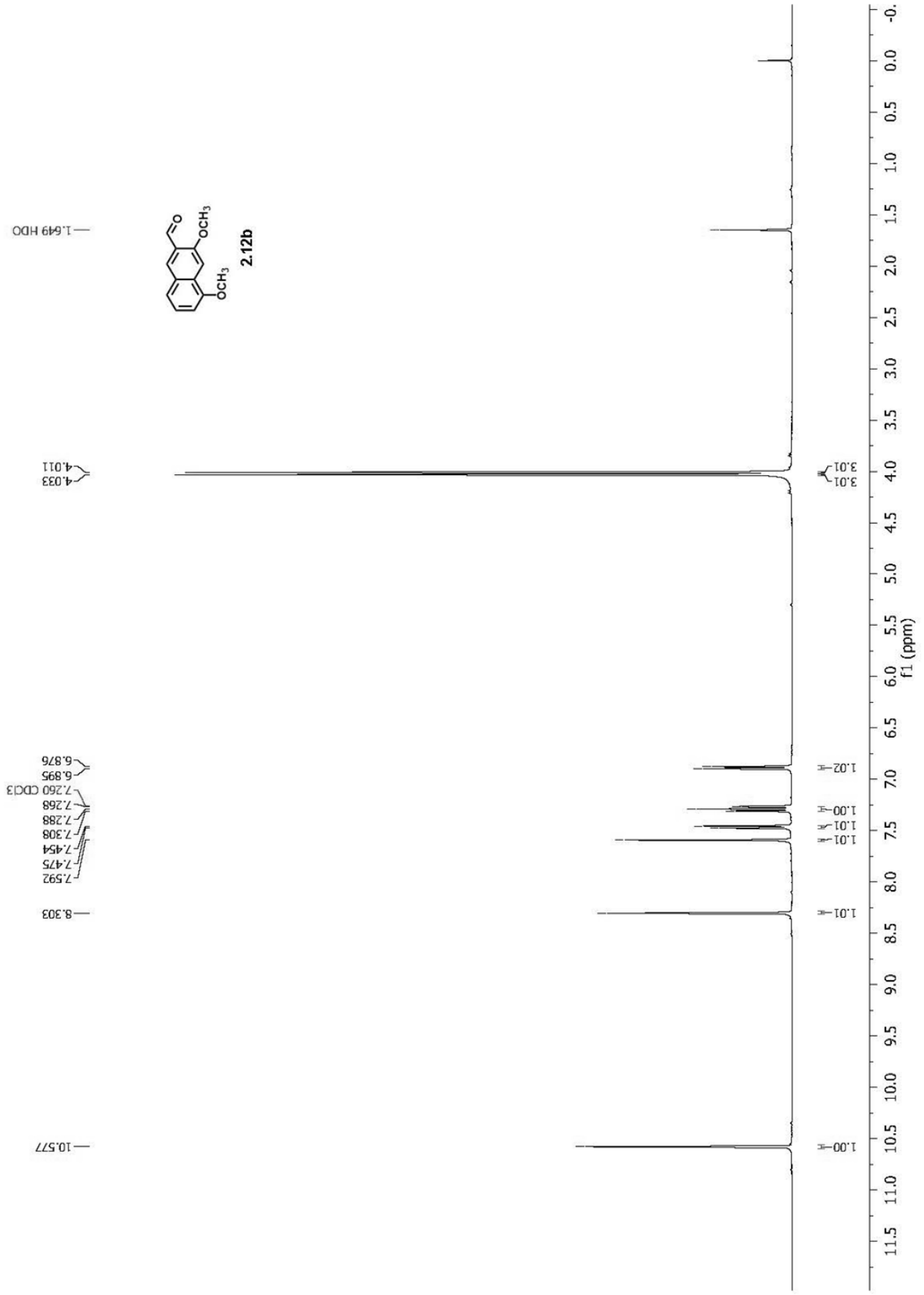
10.577
8.303
7.592
7.475
7.454
7.308
7.288
7.268
7.260 CDCl3
6.895
6.876
4.033
4.011
1.649 HDO
2.12b
1.00
1.02
1.01
1.01
1.00
1.01
3.01
3.01
f1 (ppm)

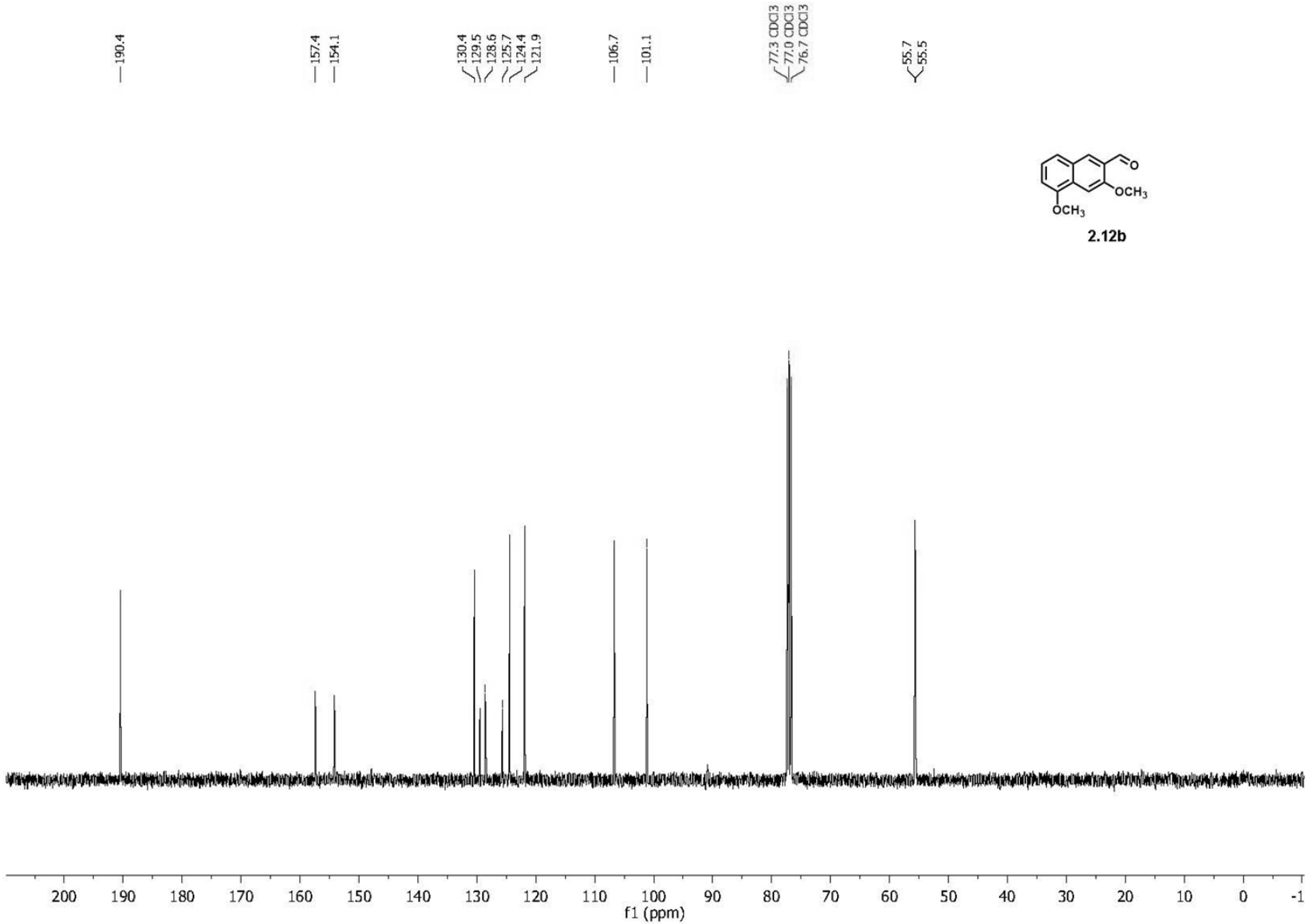
190.4
157.4
154.1
130.4
129.5
128.6
125.7
124.4
121.9
106.7
101.1
77.3 CDCl3
77.0 CDCl3
76.7 CDCl3
55.7
55.5
OCH3
OCH3
2.12b
200
190
180
170
160
150
140
130
120
110
100
90
80
70
60
50
40
30
20
10
0
-1
f1 (ppm)

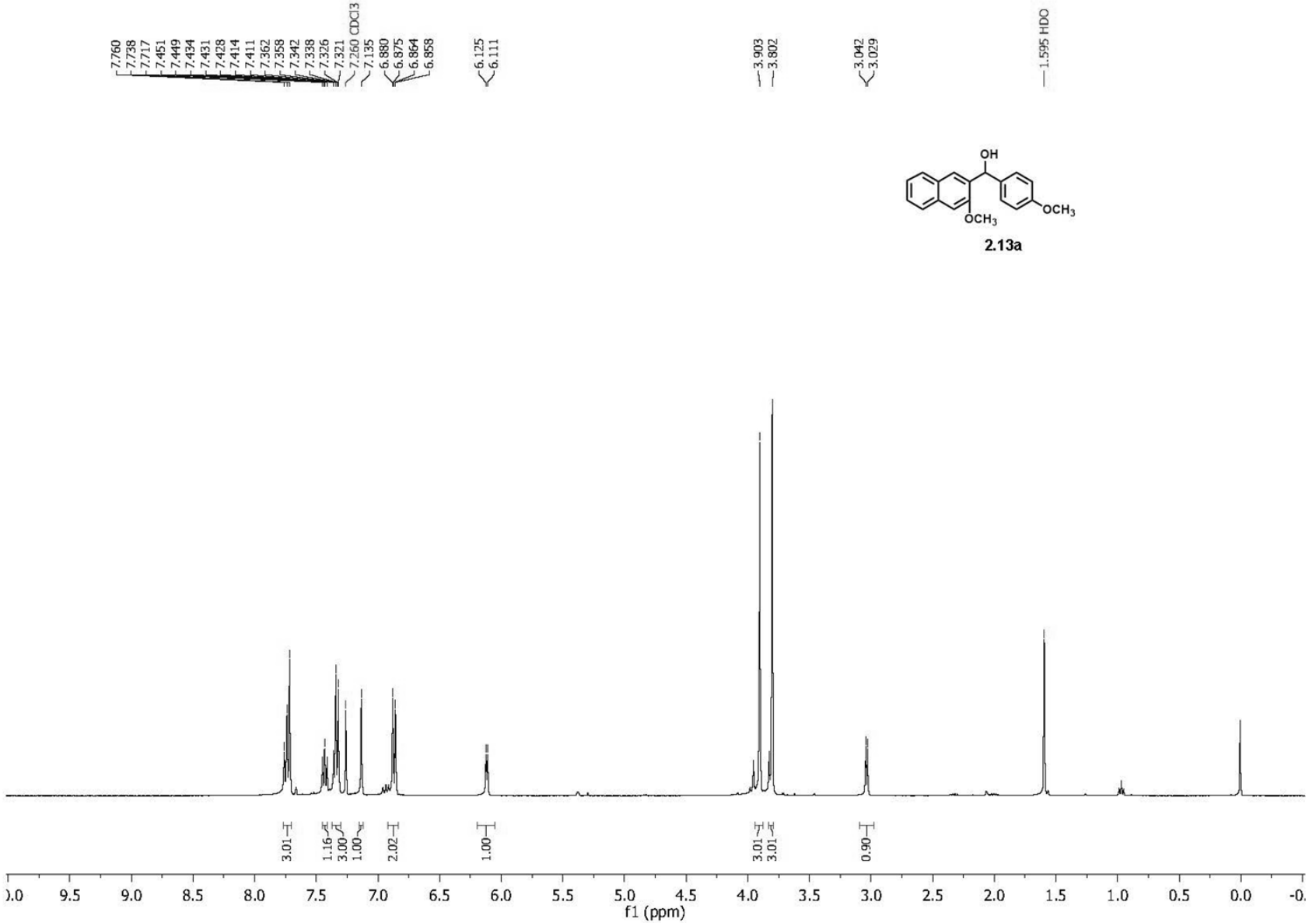
7.760
7.738
7.717
7.451
7.449
7.434
7.431
7.428
7.414
7.411
7.362
7.358
7.342
7.338
7.326
7.321
7.260 CDCl3
7.135
6.880
6.875
6.864
6.858
6.125
6.111
3.903
3.802
3.042
3.029
1.595 HDO
OH
OCH3
OCH3
2.13a
3.01
1.16
3.00
1.00
2.02
1.00
3.01
3.01
0.90
f1 (ppm)

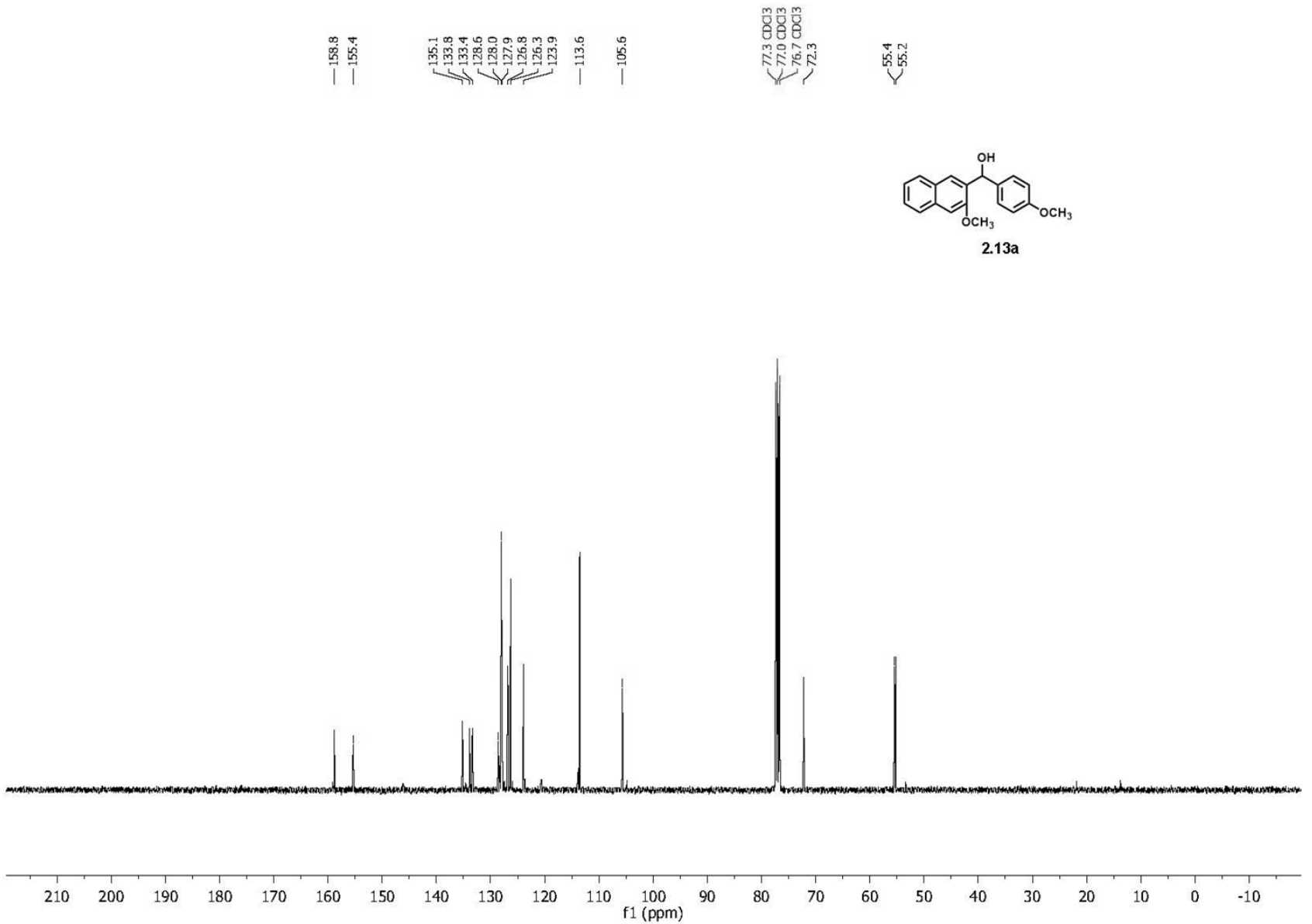
158.8
155.4
135.1
133.8
133.4
128.6
128.0
127.9
126.8
126.3
123.9
113.6
105.6
77.3 CDCl3
77.0 CDCl3
76.7 CDCl3
72.3
55.4
55.2
OH
OCH3
OCH3
2.13a
f1 (ppm)

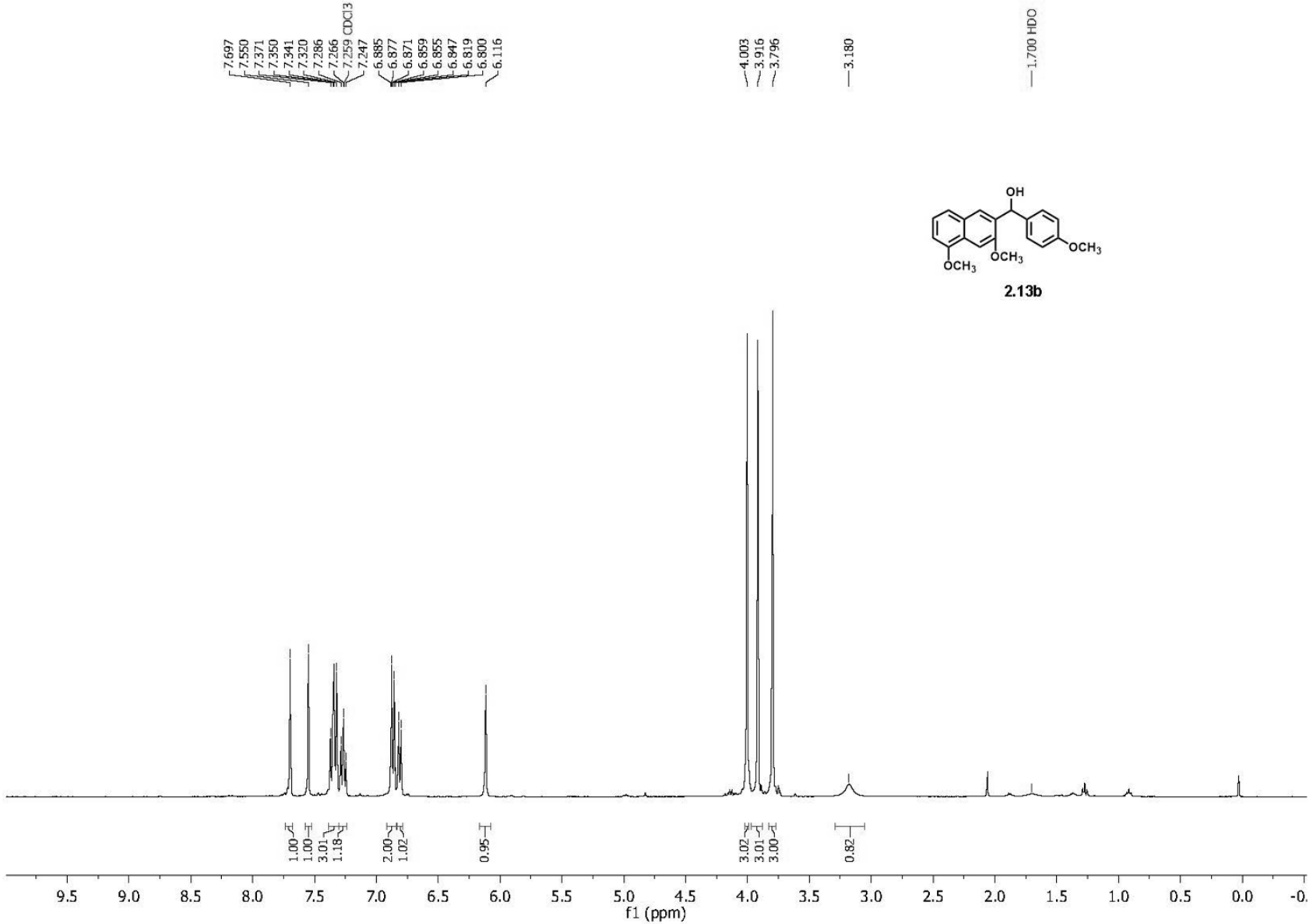
7.697
7.550
7.371
7.350
7.341
7.320
7.286
7.266
7.259 CDCl3
7.247
6.885
6.877
6.871
6.859
6.855
6.847
6.819
6.800
6.116
4.003
3.916
3.796
3.180
1.700 HDO
OH
OCH3
OCH3
OCH3
2.13b
1.00
1.00
3.01
1.18
2.00
1.02
0.95
3.02
3.01
3.00
0.82
f1 (ppm)

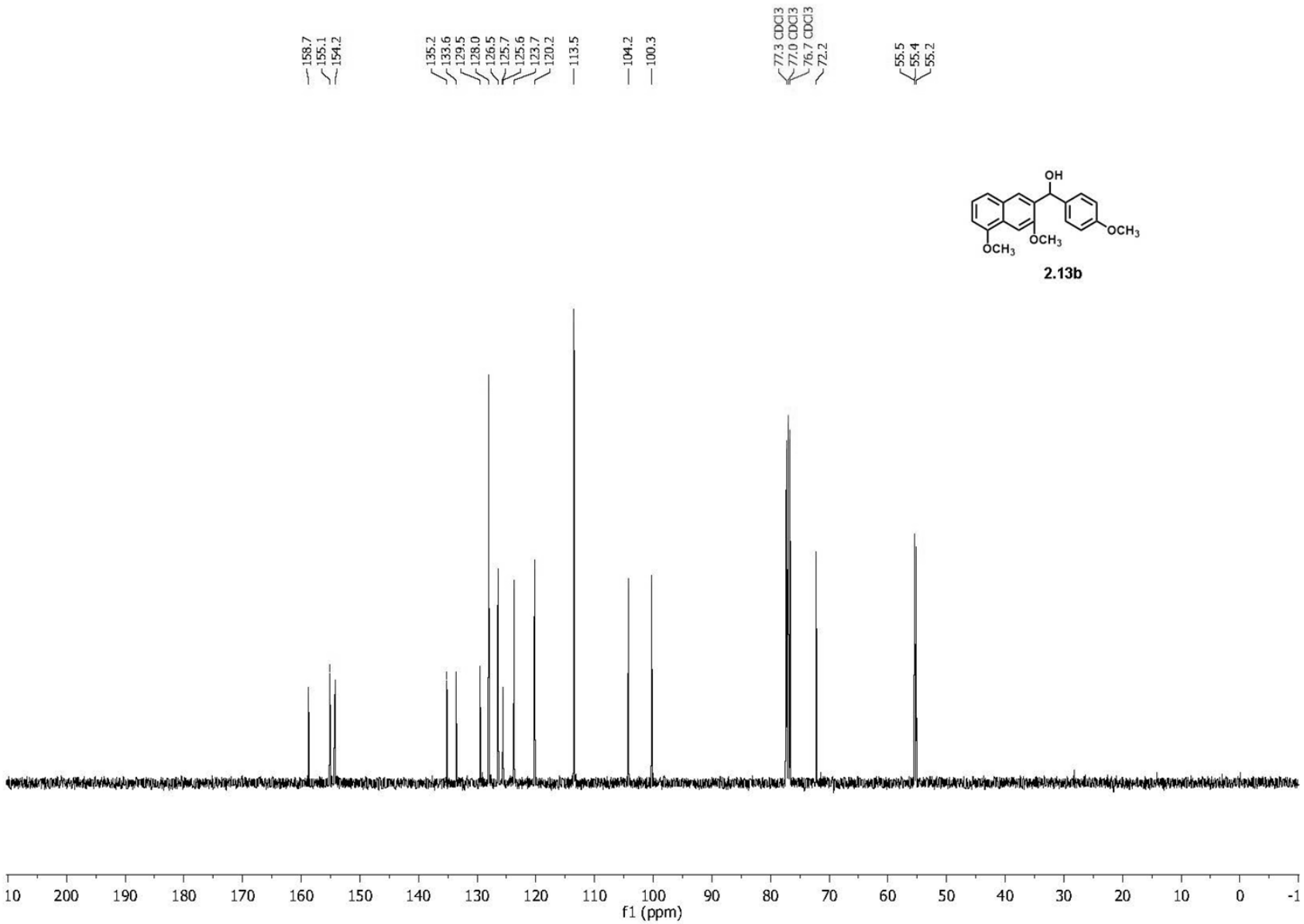
158.7
155.1
154.2
135.2
133.6
129.5
128.0
126.5
125.7
125.6
123.7
120.2
113.5
104.2
100.3
77.3 CDCl3
77.0 CDCl3
76.7 CDCl3
72.2
55.5
55.4
55.2
OH
OCH3
OCH3
OCH3
2.13b
f1 (ppm)

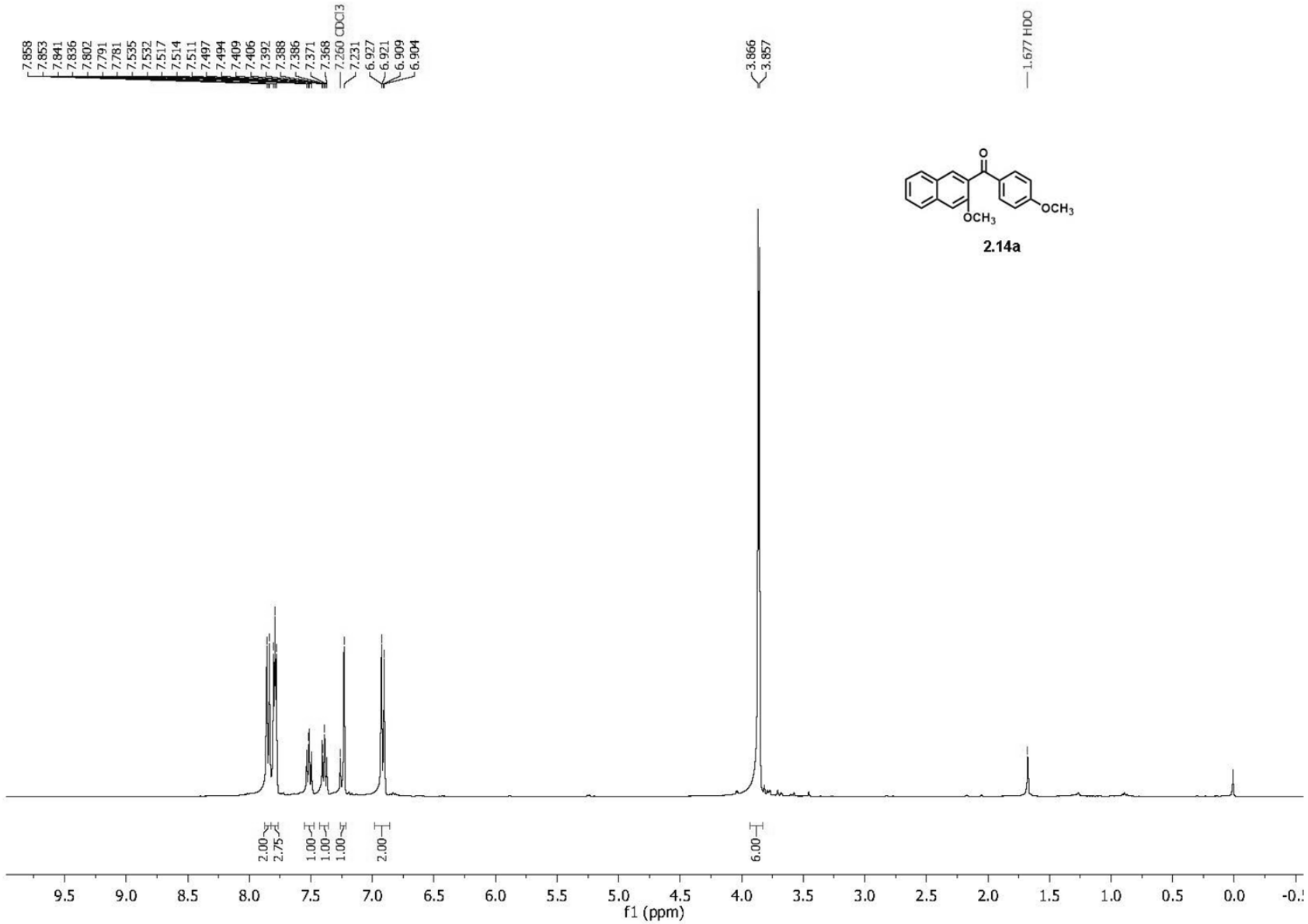
7.858
7.853
7.841
7.836
7.802
7.791
7.781
7.535
7.532
7.517
7.514
7.511
7.497
7.494
7.409
7.406
7.392
7.388
7.386
7.371
7.368
7.260 CDCl3
7.231
6.927
6.921
6.909
6.904
3.866
3.857
1.677 HDO
OCH3
OCH3
2.14a
2.00
2.75
1.00
1.00
1.00
2.00
6.00
f1 (ppm)

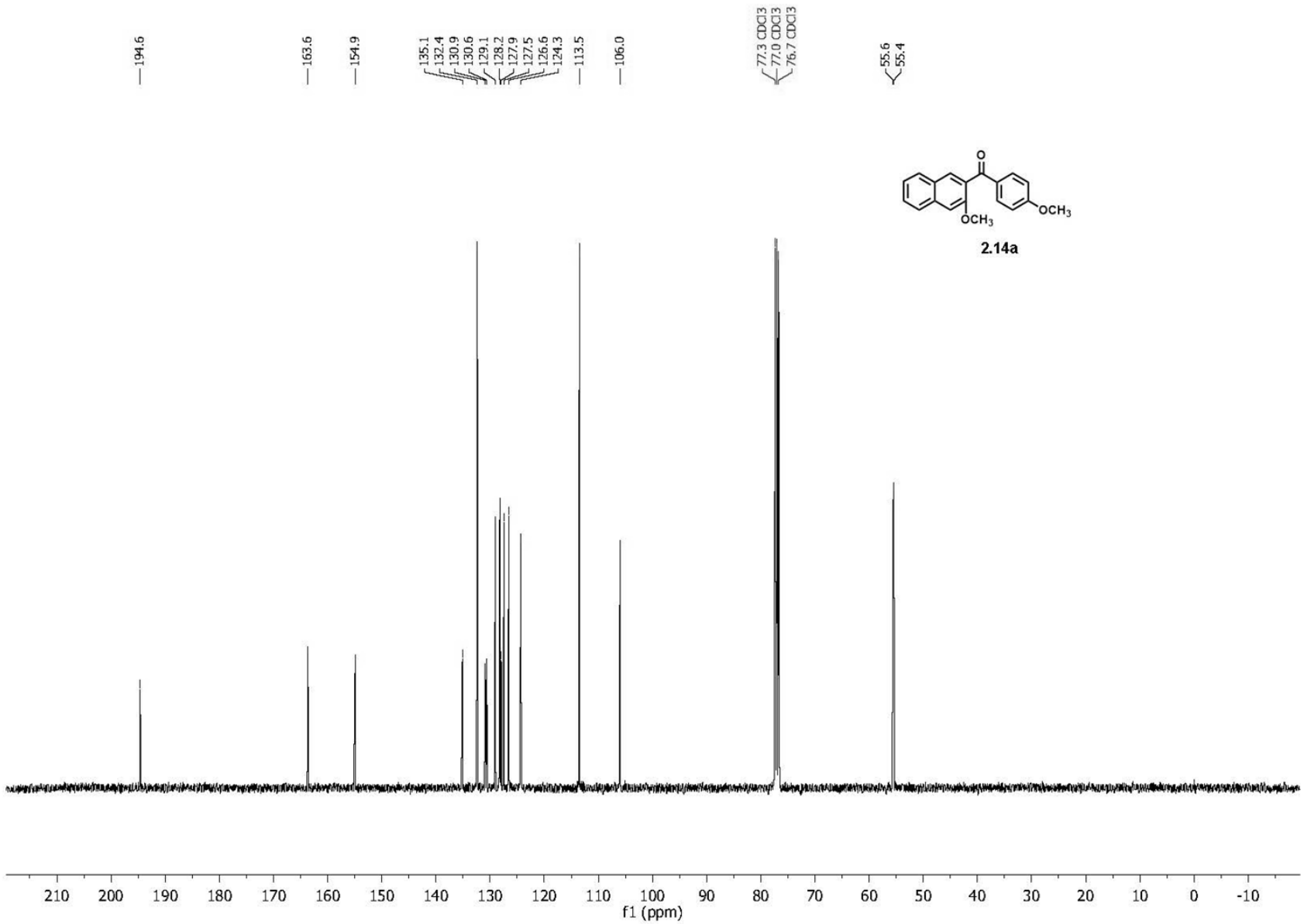
194.6
163.6
154.9
135.1
132.4
130.9
130.6
129.1
128.2
127.9
127.5
126.6
124.3
113.5
106.0
77.3 CDCl3
77.0 CDCl3
76.7 CDCl3
55.6
55.4
OCH3
OCH3
2.14a
210 200 190 180 170 160 150 140 130 120 110 100 90 80 70 60 50 40 30 20 10 0 -10
f1 (ppm)

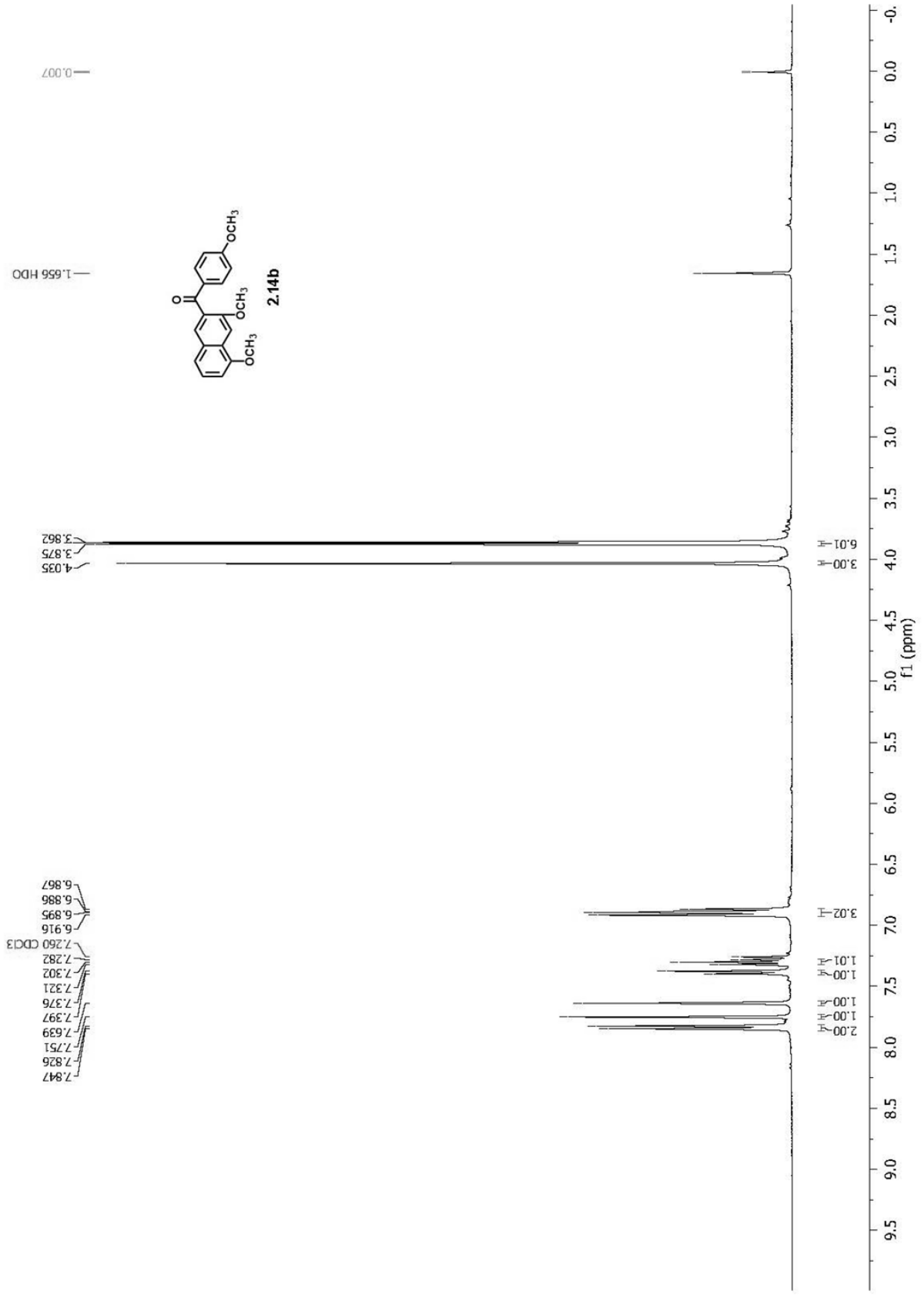
2.14b
f1 (ppm)

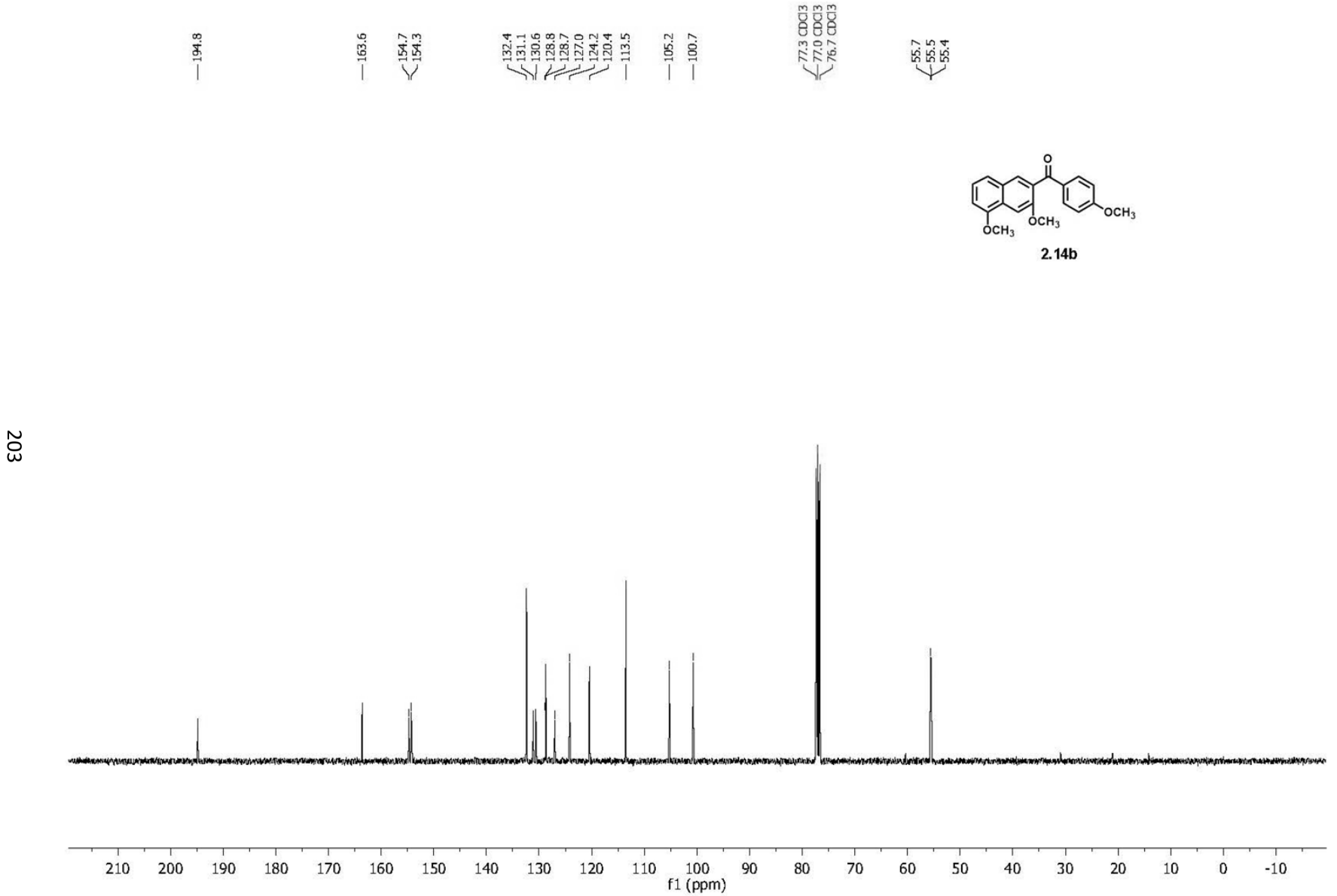
194.8
163.6
154.7
154.3
132.4
131.1
130.6
128.8
128.7
127.0
124.2
120.4
113.5
105.2
100.7
77.3 CDCl3
77.0 CDCl3
76.7 CDCl3
55.7
55.5
55.4
OCH3
OCH3
OCH3
2.14b
210 200 190 180 170 160 150 140 130 120 110 100 90 80 70 60 50 40 30 20 10 0 -10
f1 (ppm)

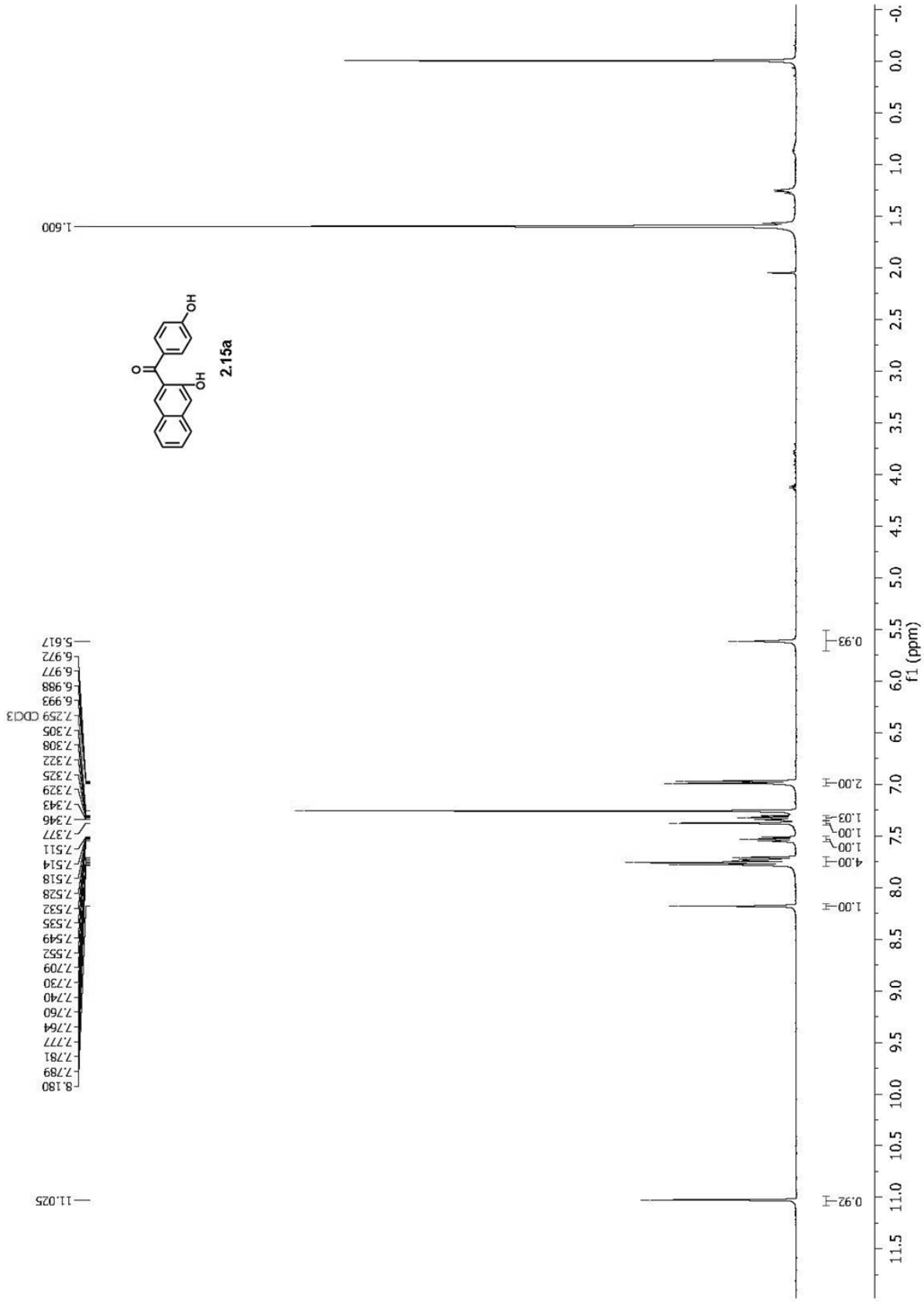
2.15a
OH
O
OH
11.025
8.180
7.789
7.781
7.777
7.764
7.760
7.740
7.730
7.709
7.552
7.549
7.535
7.532
7.528
7.518
7.514
7.511
7.377
7.346
7.343
7.329
7.325
7.322
7.308
7.305
7.259 CDCl3
6.993
6.988
6.977
6.972
5.617
1.600
0.92
4.00
1.00
1.00
1.00
1.03
2.00
0.93
f1 (ppm)

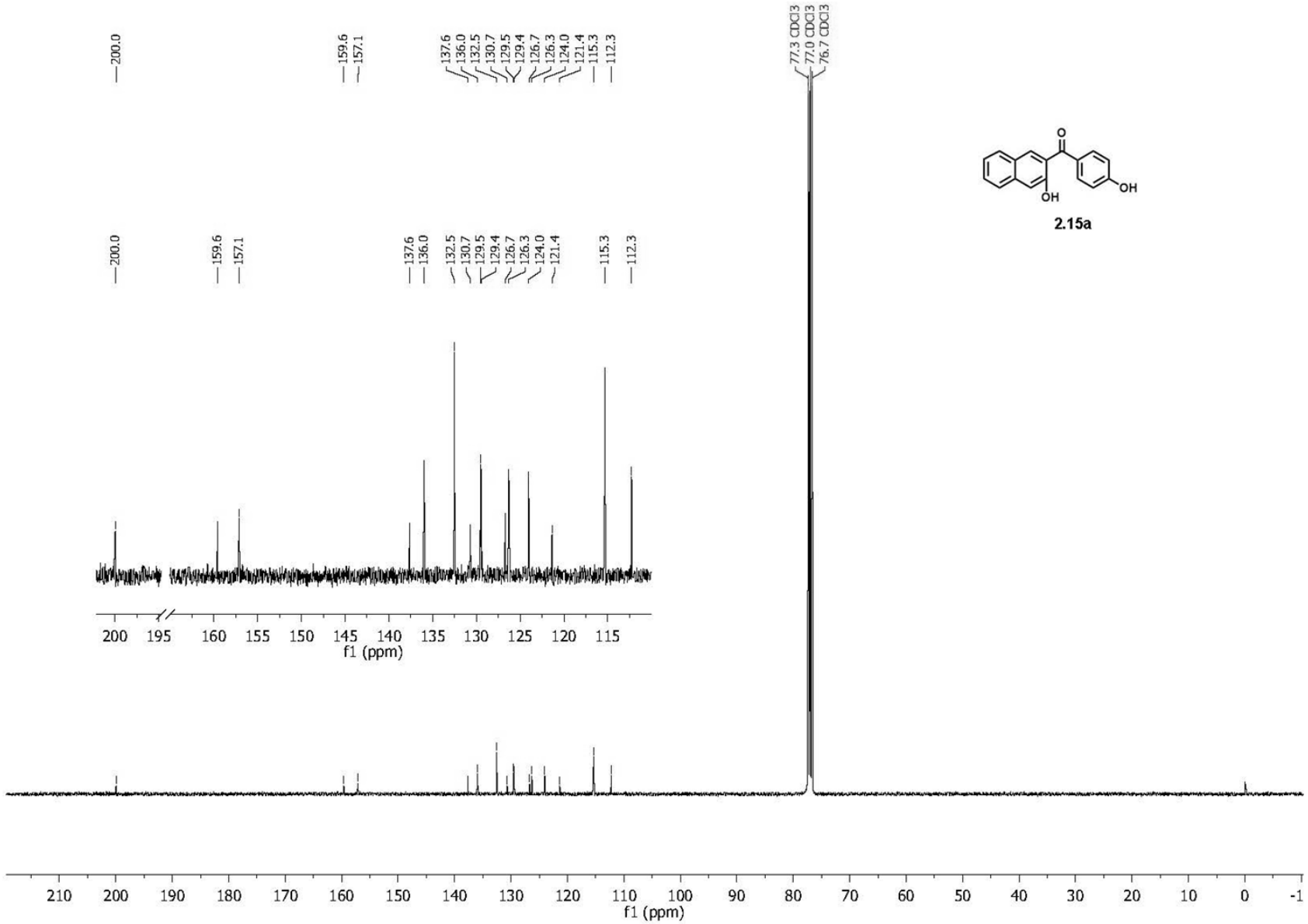
200.0
159.6
157.1
137.6
136.0
132.5
130.7
129.5
129.4
126.7
126.3
124.0
121.4
115.3
112.3
77.3 CDCl3
77.0 CDCl3
76.7 CDCl3
OH
OH
2.15a
f1 (ppm)
f1 (ppm)

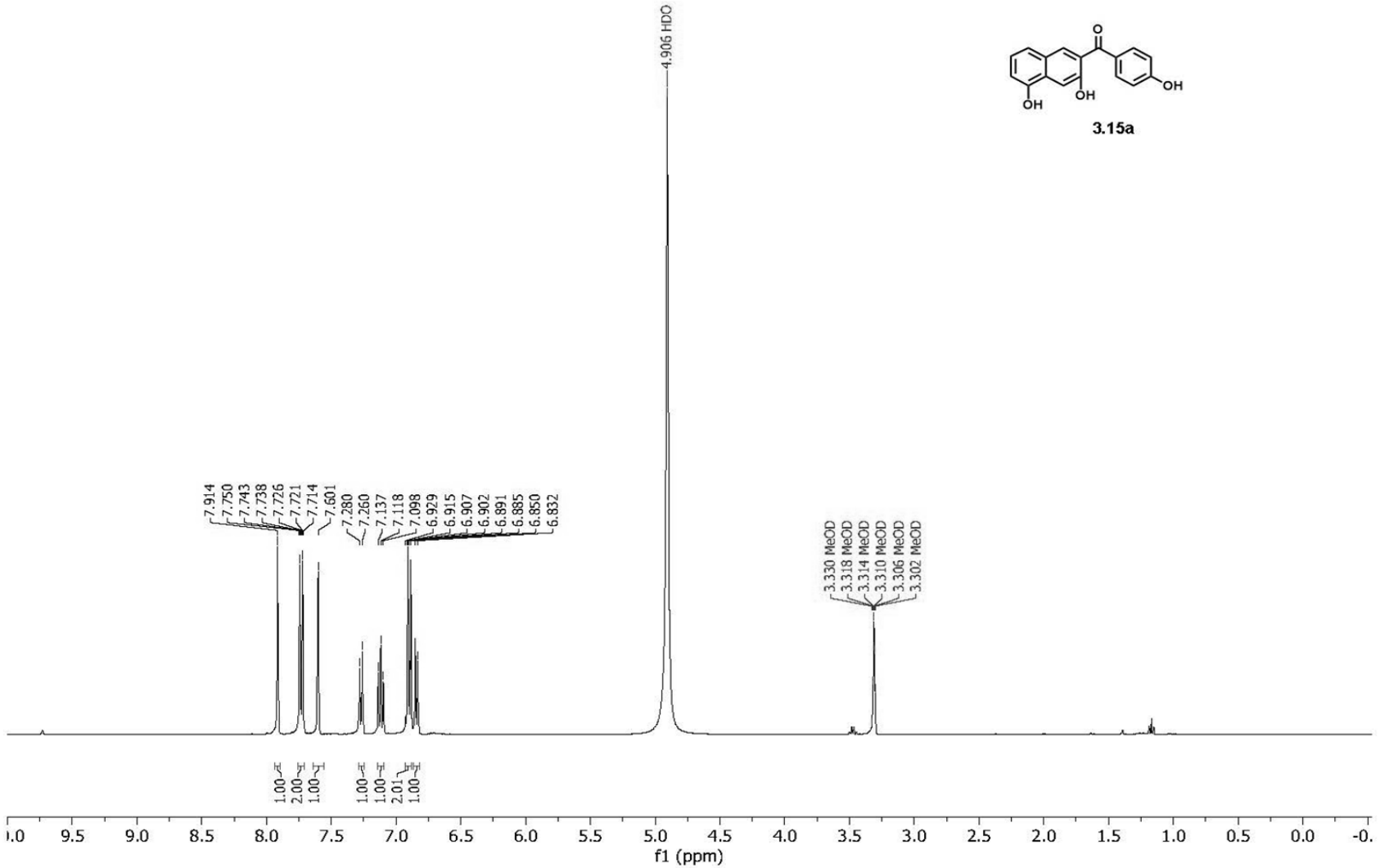
4.906 HDO
7.914
7.750
7.743
7.738
7.726
7.721
7.714
7.601
7.280
7.260
7.137
7.118
7.098
6.929
6.915
6.907
6.902
6.891
6.885
6.850
6.832
3.330 MeOD
3.318 MeOD
3.314 MeOD
3.310 MeOD
3.306 MeOD
3.302 MeOD
1.00
2.00
1.00
1.00
1.00
2.01
1.00
f1 (ppm)

O
OH
OH
OH

3.15a

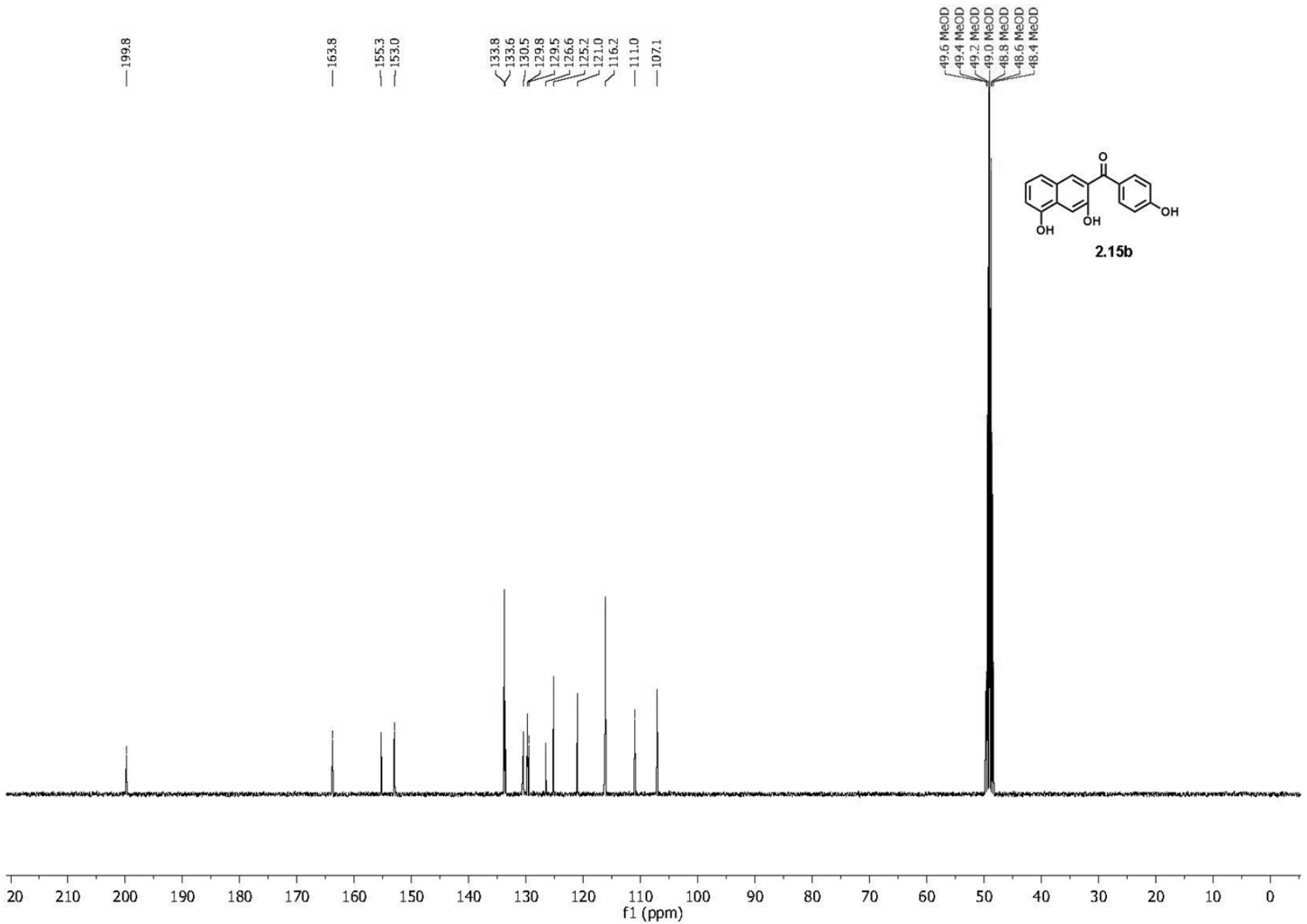
199.8
163.8
155.3
153.0
133.8
133.6
130.5
129.8
129.5
126.6
125.2
121.0
116.2
111.0
107.1
49.6 MeOD
49.4 MeOD
49.2 MeOD
49.0 MeOD
48.8 MeOD
48.6 MeOD
48.4 MeOD
O
OH
OH
OH
2.15b
f1 (ppm)

OCH3
OCH3
OCH3
OCH3
2.21b
3.518
3.794
3.954
4.018
5.800
6.822
6.841
6.893
6.913
7.259 CDCl3
7.303
7.323
7.343
7.412
7.432
7.501
7.521
7.596
8.061
3.00
3.00
6.01
1.00
1.01
2.01
1.01
1.01
2.00
1.00
1.01
1.00
f1 (ppm)

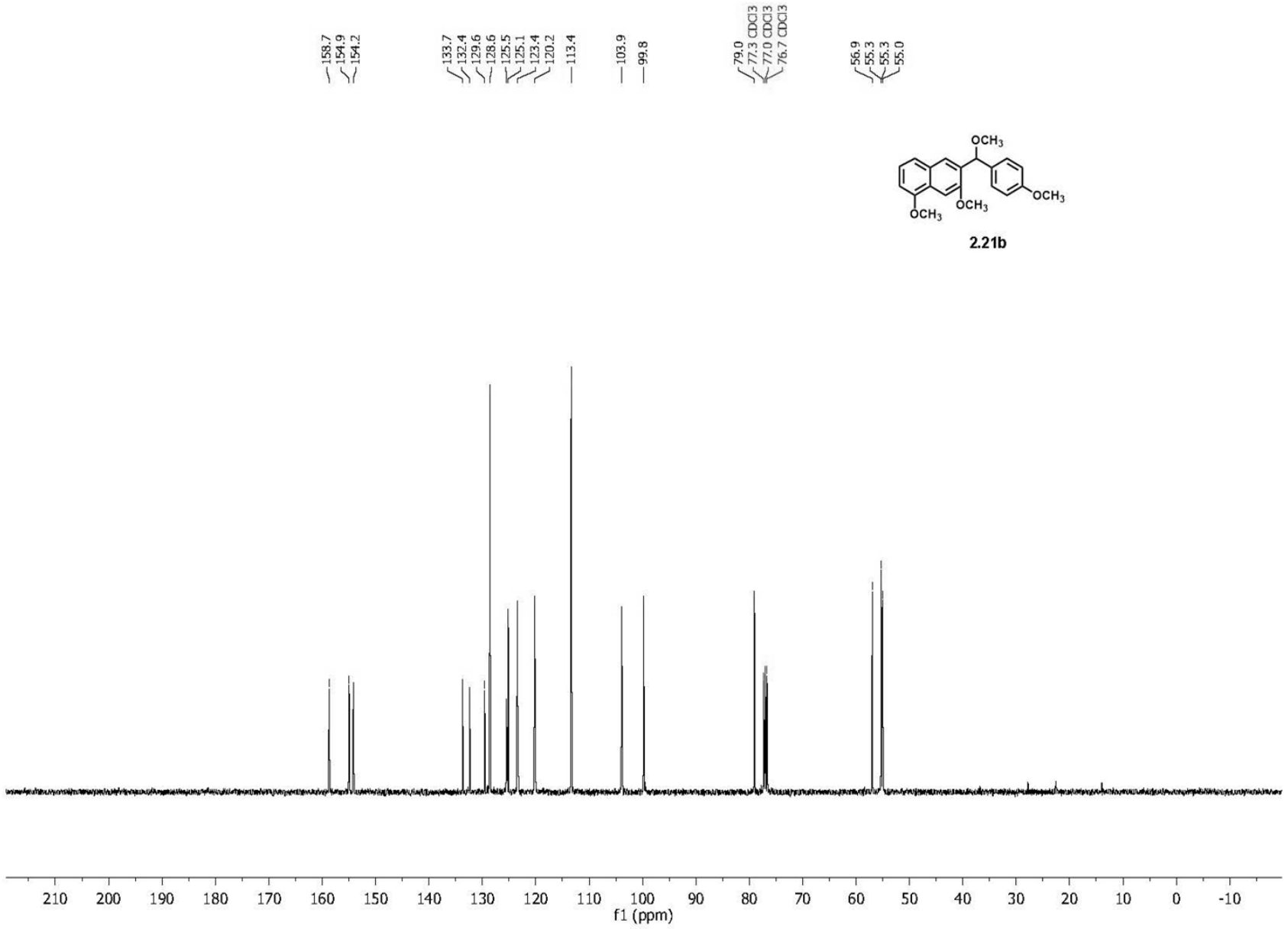
158.7
154.9
154.2
133.7
132.4
129.6
128.6
125.5
125.1
123.4
120.2
113.4
103.9
99.8
79.0
77.3 CDCl3
77.0 CDCl3
76.7 CDCl3
56.9
55.3
55.3
55.0
OCH3
OCH3
OCH3
OCH3
2.21b
f1 (ppm)

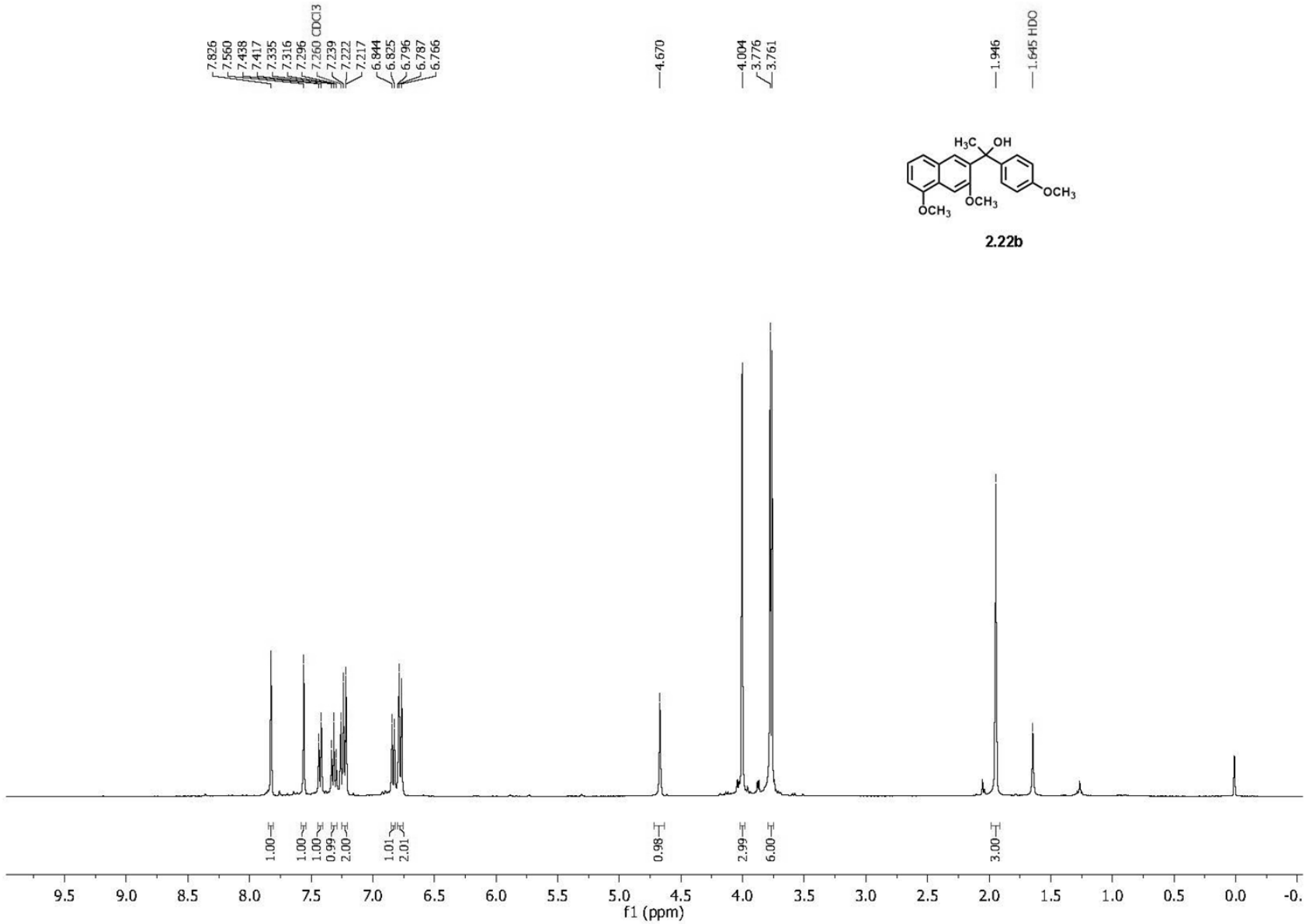
7.826
7.560
7.438
7.417
7.335
7.316
7.296
7.260 CDCl3
7.239
7.222
7.217
6.844
6.825
6.796
6.787
6.766
4.670
4.004
3.776
3.761
1.946
1.645 HDO
H3C
OH
OCH3
OCH3
OCH3
2.22b
1.00
1.00
1.00
0.99
2.00
1.01
2.01
0.98
2.99
6.00
3.00
9.5
9.0
8.5
8.0
7.5
7.0
6.5
6.0
5.5
5.0
4.5
4.0
3.5
3.0
2.5
2.0
1.5
1.0
0.5
0.0
f1 (ppm)

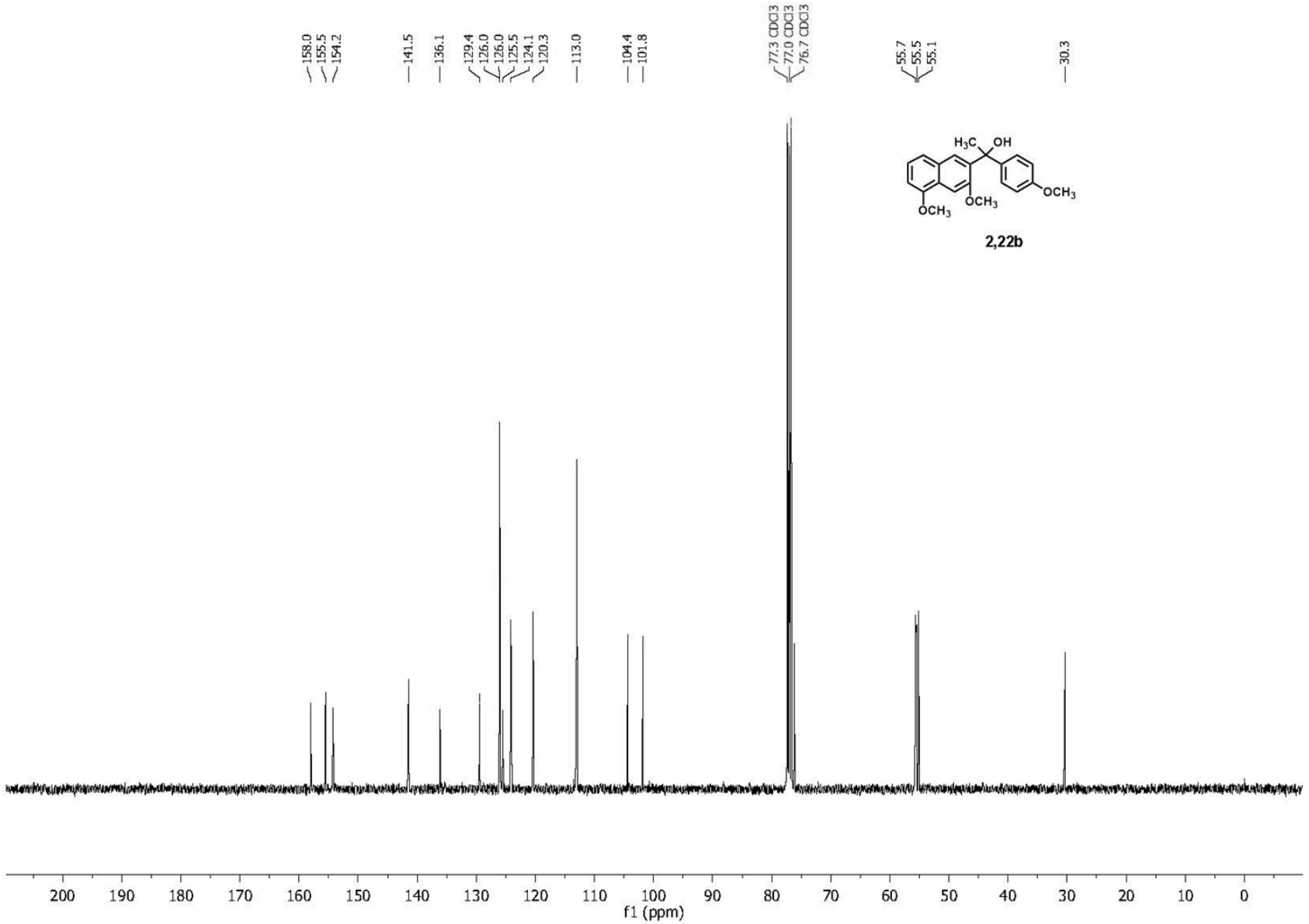
158.0
155.5
154.2
141.5
136.1
129.4
126.0
126.0
125.5
124.1
120.3
113.0
104.4
101.8
77.3 CDCl3
77.0 CDCl3
76.7 CDCl3
55.7
55.5
55.1
30.3
H3C
OH
OCH3
OCH3
OCH3
2,22b
200
190
180
170
160
150
140
130
120
110
100
90
80
70
60
50
40
30
20
10
0
f1 (ppm)

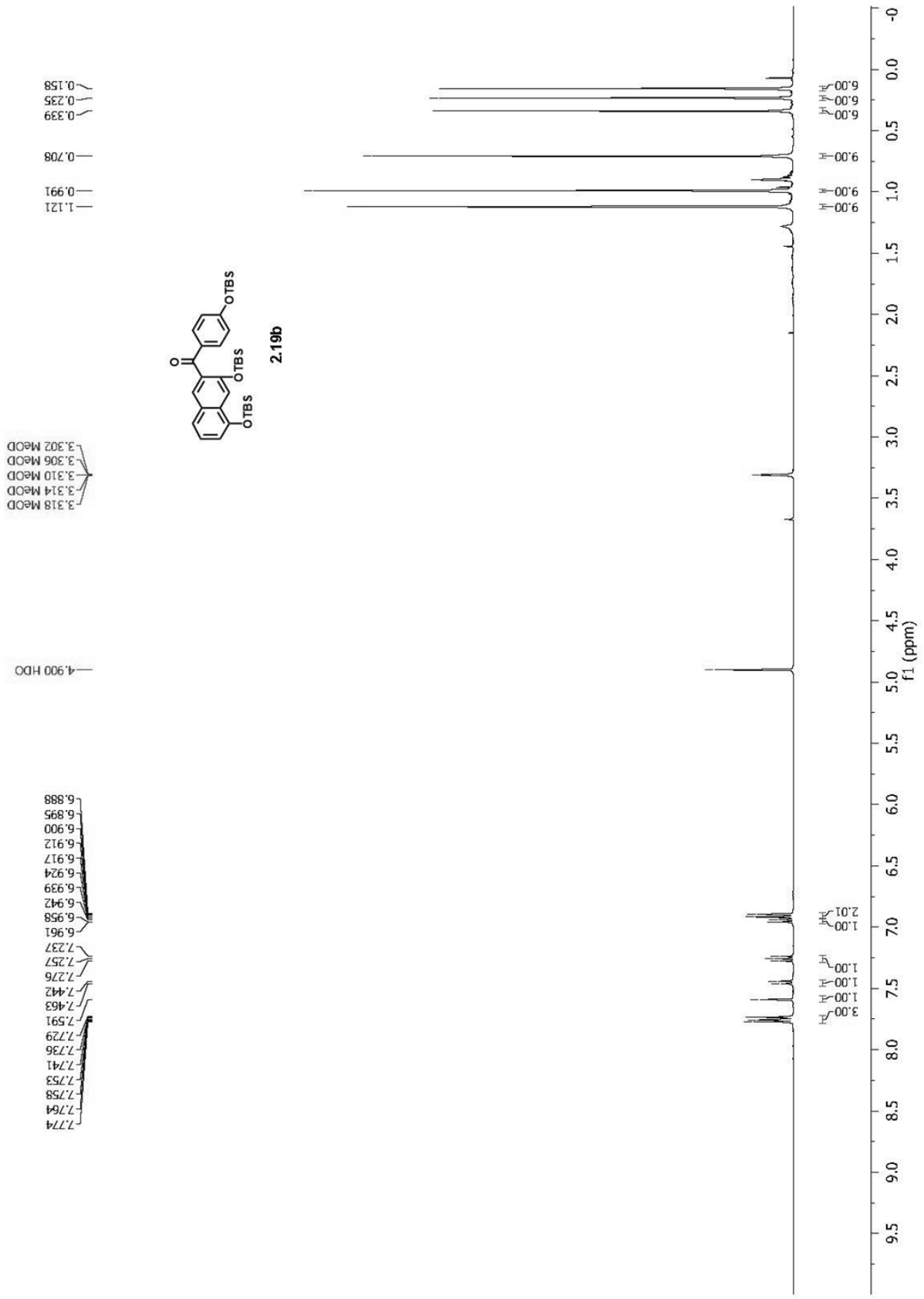
OTBS
OTBS
OTBS
2.19b
f1 (ppm)

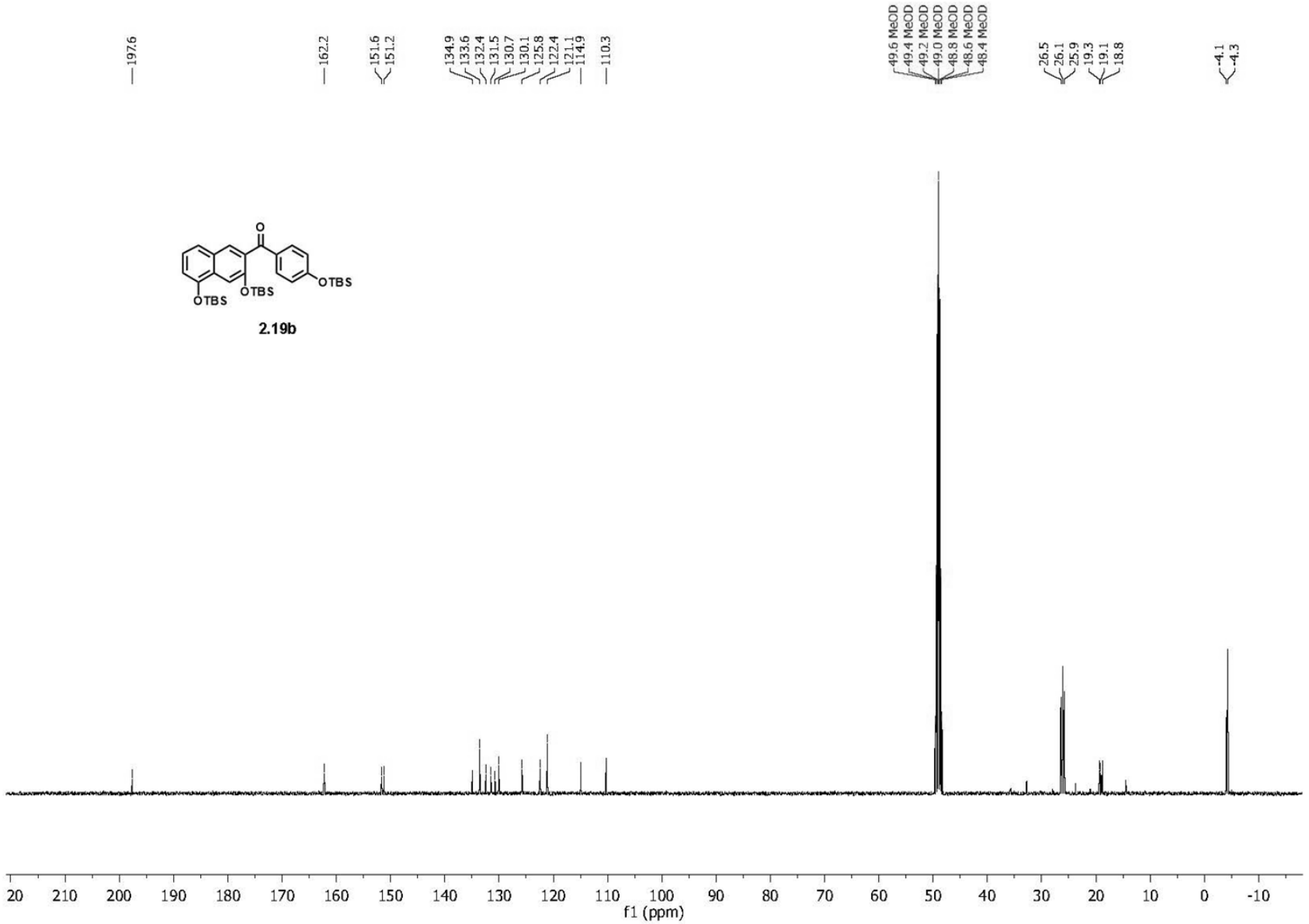
197.6
162.2
151.6
151.2
134.9
133.6
132.4
131.5
130.7
130.1
125.8
122.4
121.1
114.9
110.3
49.6 MeOD
49.4 MeOD
49.2 MeOD
49.0 MeOD
48.8 MeOD
48.6 MeOD
48.4 MeOD
26.5
26.1
25.9
19.3
19.1
18.8
-4.1
-4.3
OTBS
OTBS
OTBS
2.19b
f1 (ppm)

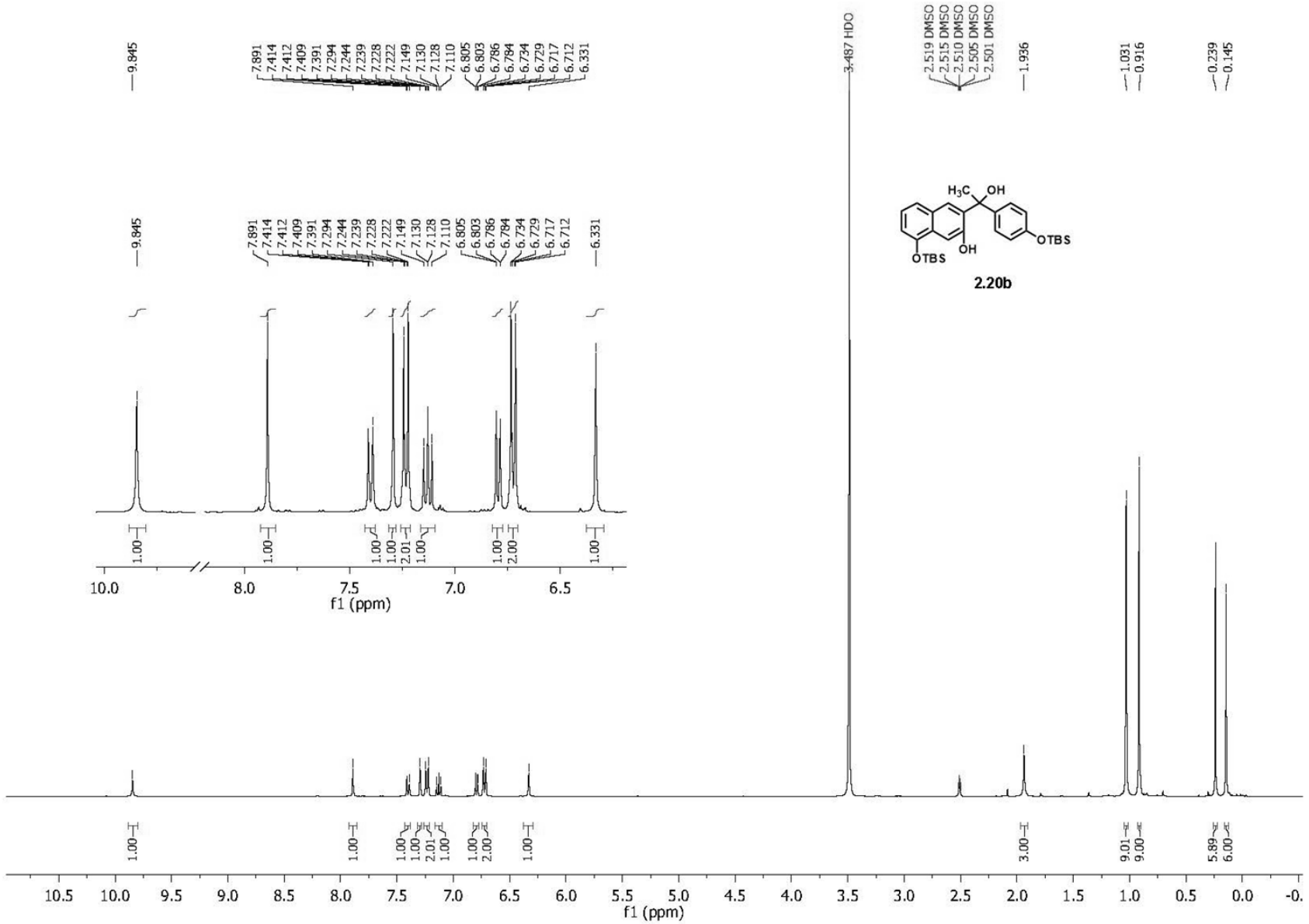
9.845
7.891
7.414
7.412
7.409
7.391
7.294
7.244
7.239
7.228
7.222
7.149
7.130
7.128
7.110
6.805
6.803
6.786
6.784
6.734
6.729
6.717
6.712
6.331
3.487 HDO
2.519 DMSO
2.515 DMSO
2.510 DMSO
2.505 DMSO
2.501 DMSO
1.936
1.031
0.916
0.239
0.145
H3C
OH
OTBS
OH
OTBS
2.20b
f1 (ppm)

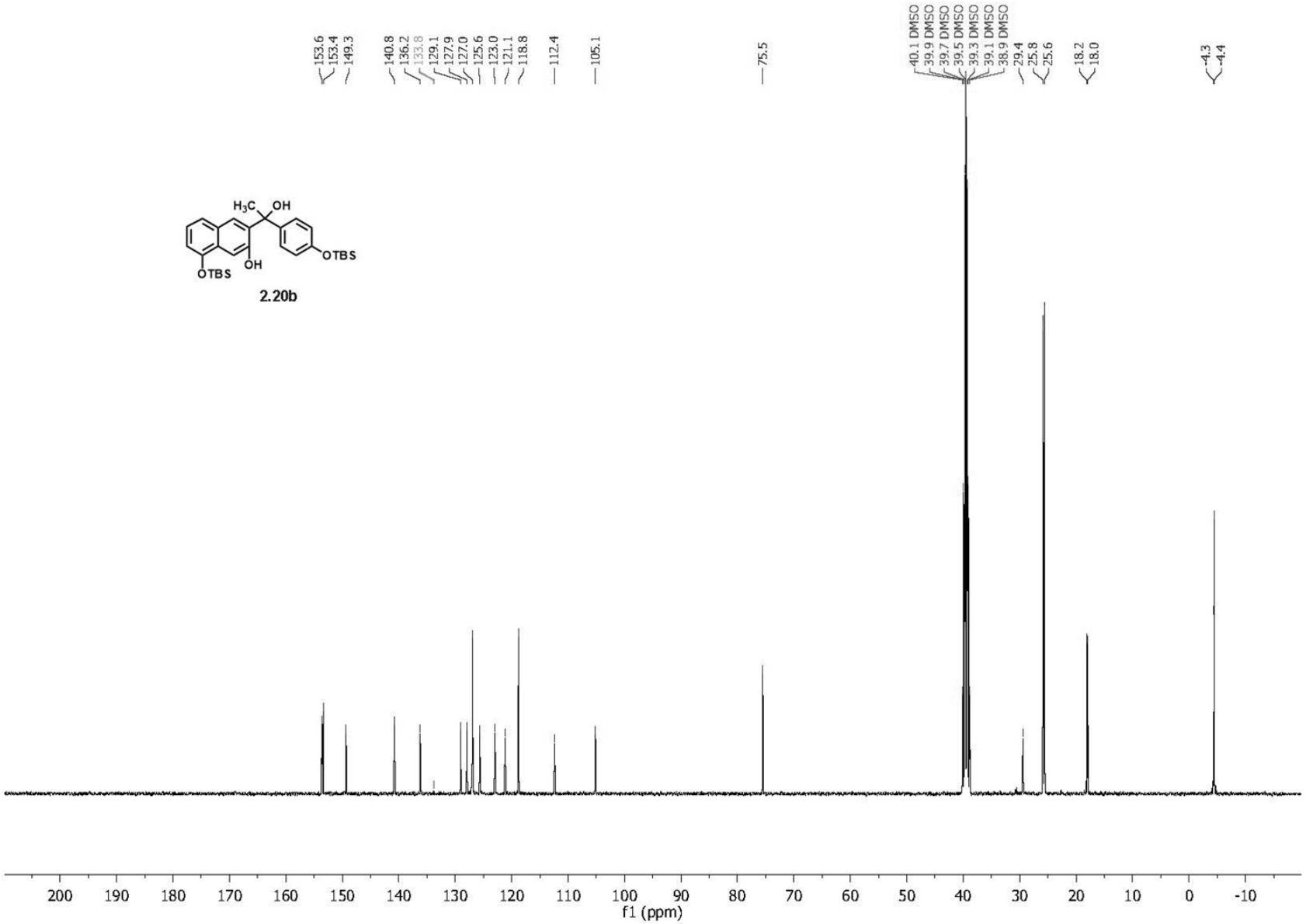
153.6
153.4
149.3
140.8
136.2
133.8
129.1
127.9
127.0
125.6
123.0
121.1
118.8
112.4
105.1
75.5
40.1 DMSO
39.9 DMSO
39.7 DMSO
39.5 DMSO
39.3 DMSO
39.1 DMSO
38.9 DMSO
29.4
25.8
25.6
18.2
18.0
-4.3
-4.4
H3C
OH
OTBS
OH
OTBS
2.20b
200
190
180
170
160
150
140
130
120
110
100
90
80
70
60
50
40
30
20
10
0
-10
f1 (ppm)

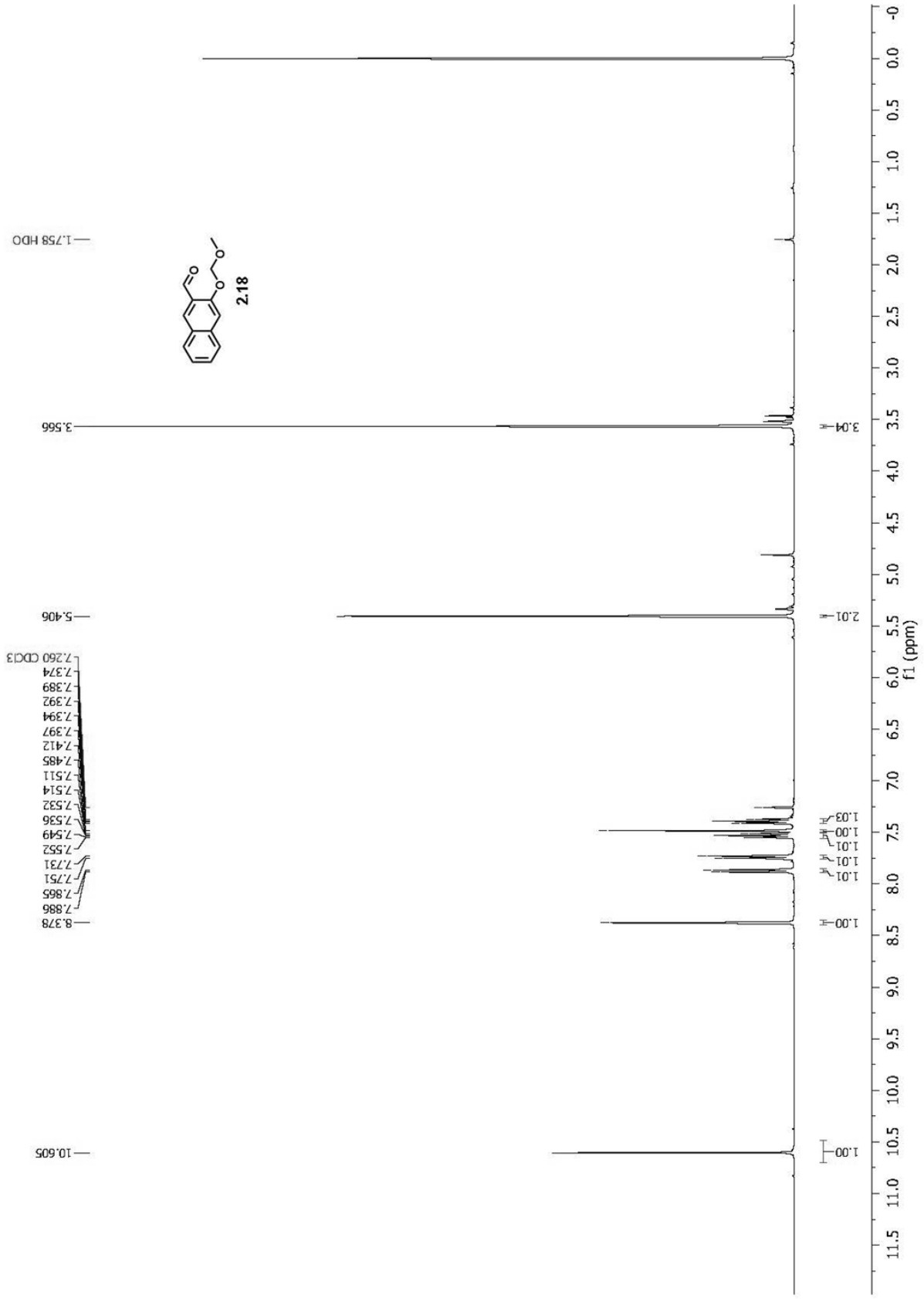
10.605
8.378
7.886
7.865
7.751
7.731
7.552
7.549
7.536
7.532
7.514
7.511
7.485
7.412
7.397
7.394
7.392
7.389
7.374
7.260 CDCl3
5.406
3.566
1.758 HDO
2.18
1.00
2.01
3.04
1.00
1.01
1.01
1.01
1.00
1.03
f1 (ppm)

2.18
190.1
155.0
137.3
130.6
129.8
129.1
128.2
126.9
125.7
125.0
110.1
94.7
77.3 CDCl3
77.0 CDCl3
76.7 CDCl3
56.4
f1 (ppm)

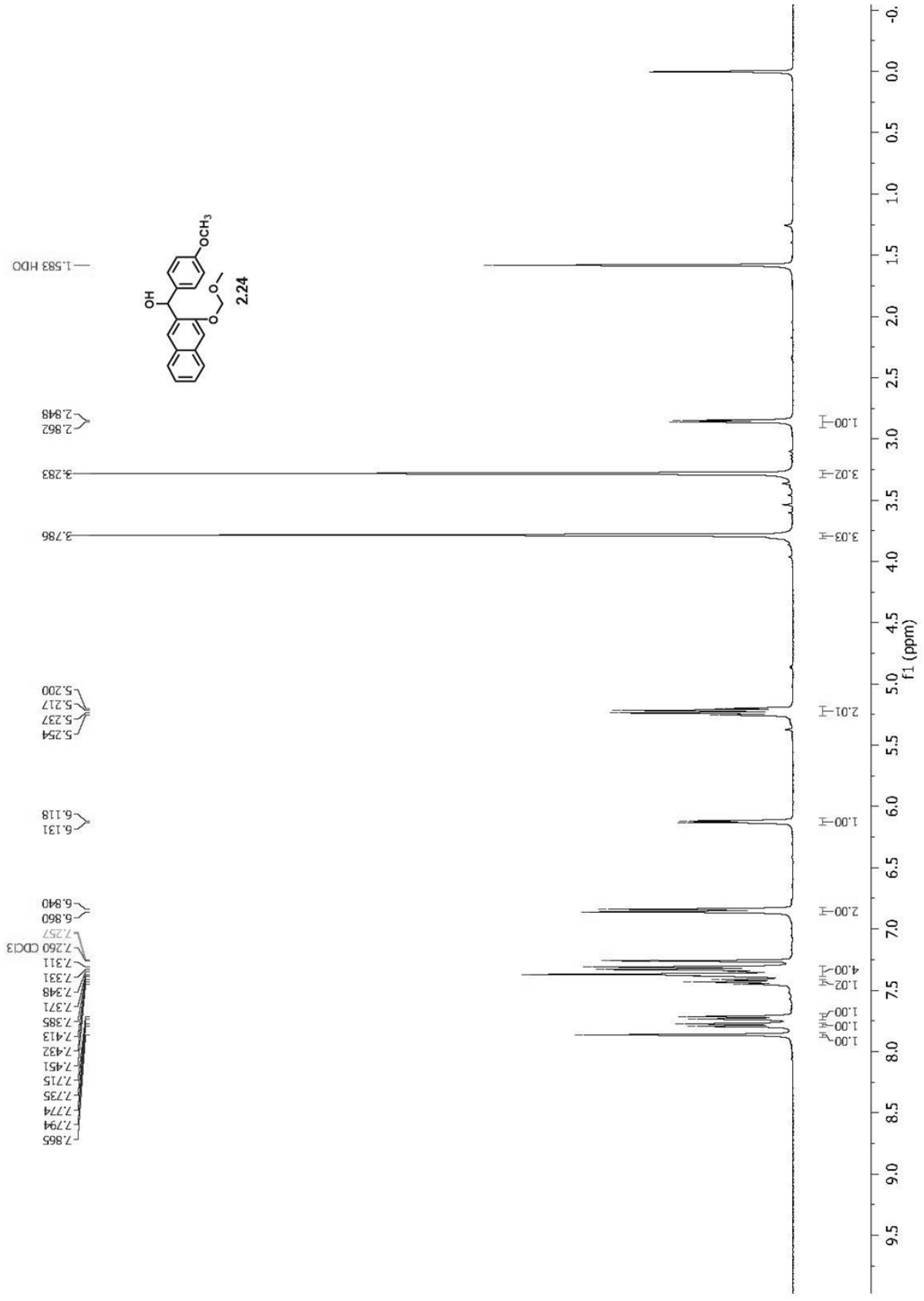
OCH3
OH
O
O
2.24
1.583 HDO
2.862
2.848
3.783
3.786
5.254
5.237
5.217
5.200
6.131
6.118
6.860
6.840
7.260 CDCl3
7.257
7.311
7.331
7.348
7.371
7.385
7.413
7.432
7.451
7.715
7.735
7.774
7.794
7.865
1.00
3.02
3.03
2.01
1.00
2.00
4.00
1.02
1.00
1.00
1.00
f1 (ppm)

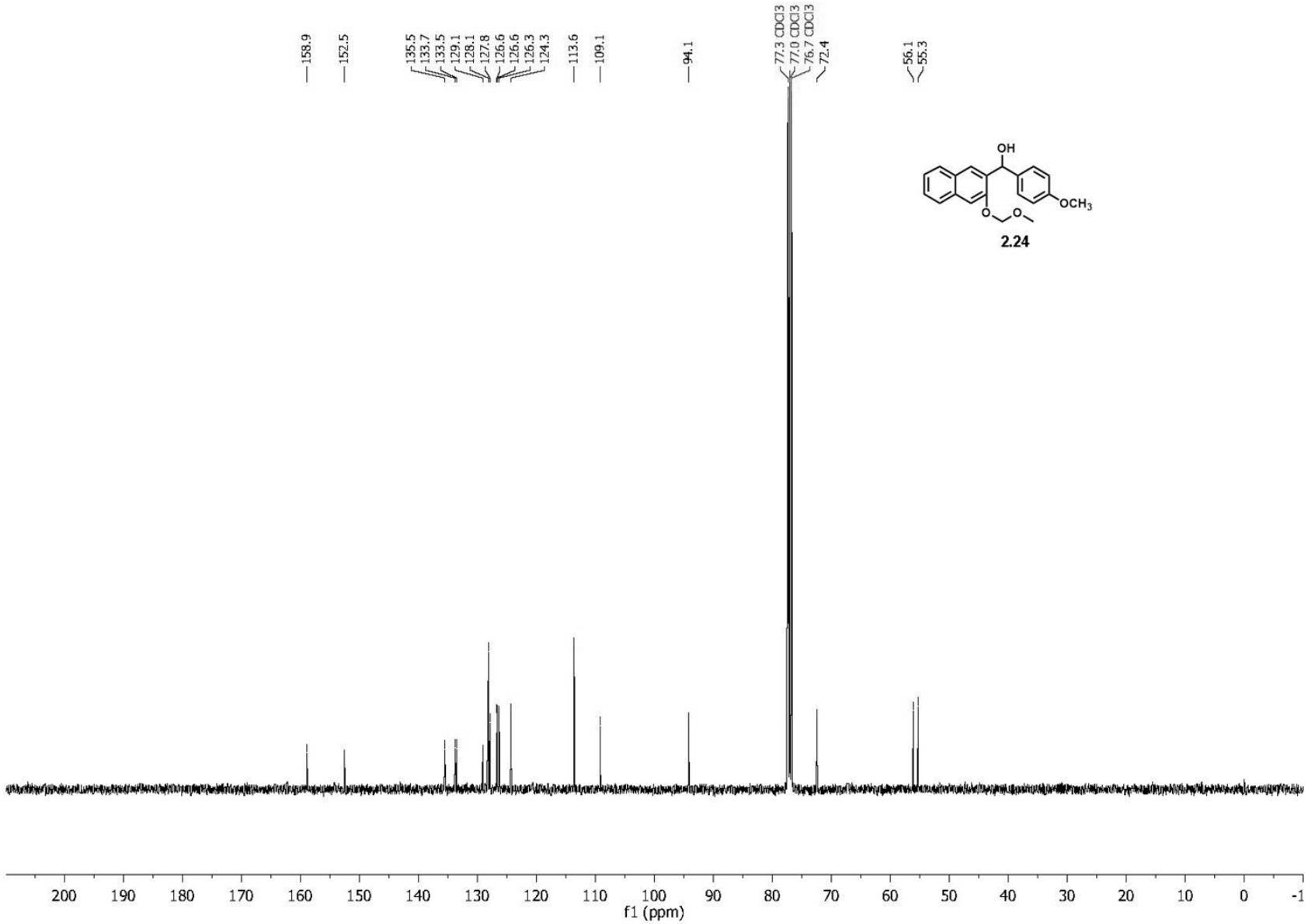
158.9
152.5
135.5
133.7
133.5
129.1
128.1
127.8
126.6
126.6
126.3
124.3
113.6
109.1
94.1
77.3 CDCl3
77.0 CDCl3
76.7 CDCl3
72.4
56.1
55.3
OH
OCH3
O
O
2.24
200
190
180
170
160
150
140
130
120
110
100
90
80
70
60
50
40
30
20
10
0
-1
f1 (ppm)

HS
O
4
OH
OH
3.1
f1 (ppm)

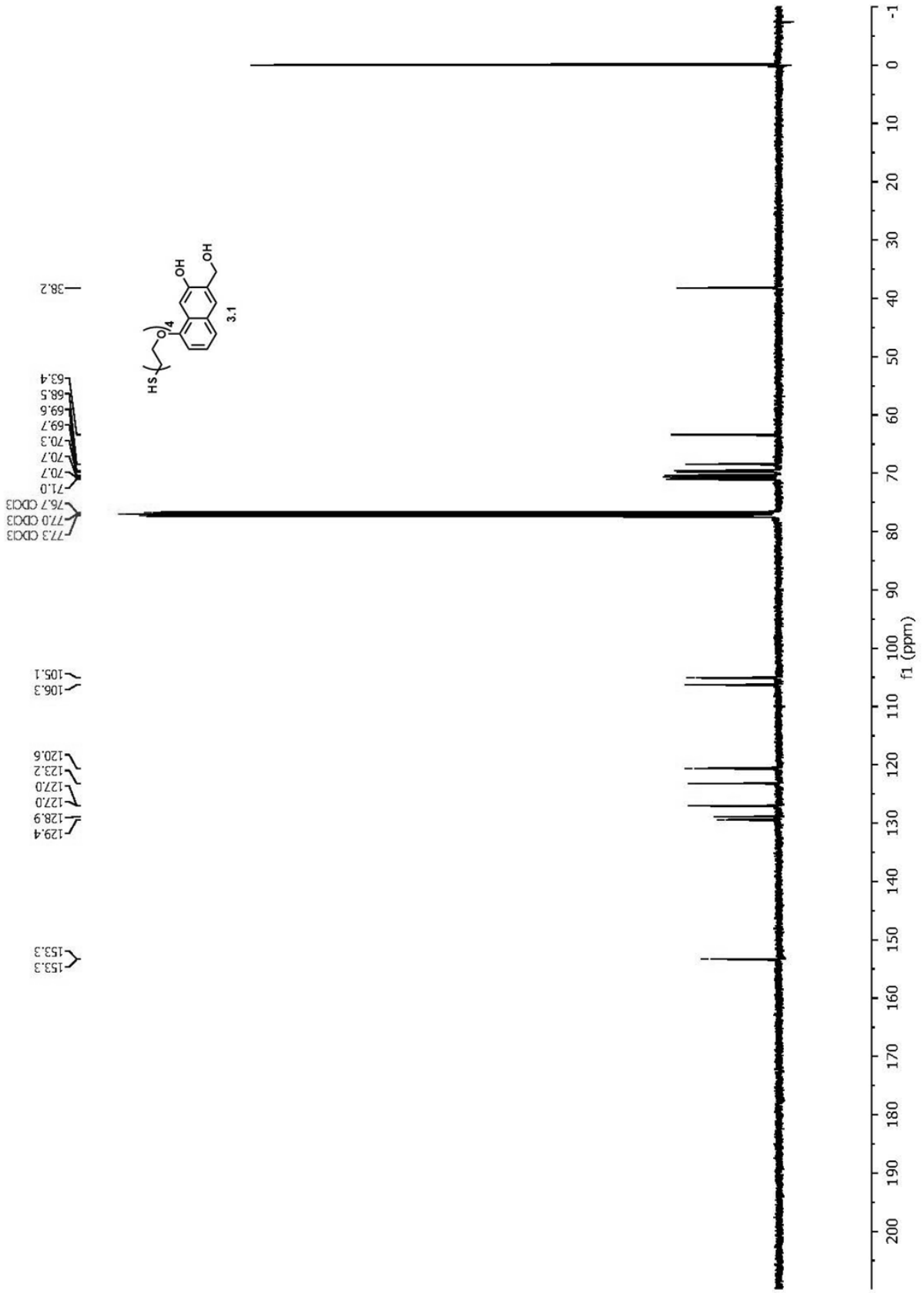
38.2
63.4
68.5
69.6
69.7
70.3
70.7
70.7
71.0
76.7 CDCl3
77.0 CDCl3
77.3 CDCl3
105.1
106.3
120.6
123.2
127.0
127.0
128.9
129.4
153.3
153.3
OH
OH
HS
O
4
3.1
f1 (ppm)

7.555
7.534
7.471
7.260 cdcl3
7.241
7.221
7.217
7.153
7.137
4.853
3.430
3.024
3.008
2.991
2.924
2.908
2.904
2.887
2.869
1.773
1.752
1.732
3.2
HO
HO
SH
O
O
1.00
2.00
0.67
2.01
2.00
2.02
1.00
1.00
1.00
2.00
f1 (ppm)

3.10
1.595
3.587
3.597
3.601
3.609
3.683
3.696
3.704
3.708
3.714
3.720
3.727
3.790
3.797
3.803
3.813
3.961
3.972
3.976
3.985
4.261
4.273
4.285
5.057
5.055
6.716
6.735
7.176
7.196
7.216
7.260 CDCl3
7.286
7.306
7.419
7.654
6.01
2.02
8.26
2.01
2.05
2.00
2.03
1.01
1.01
1.01
1.00
1.00
f1 (ppm)

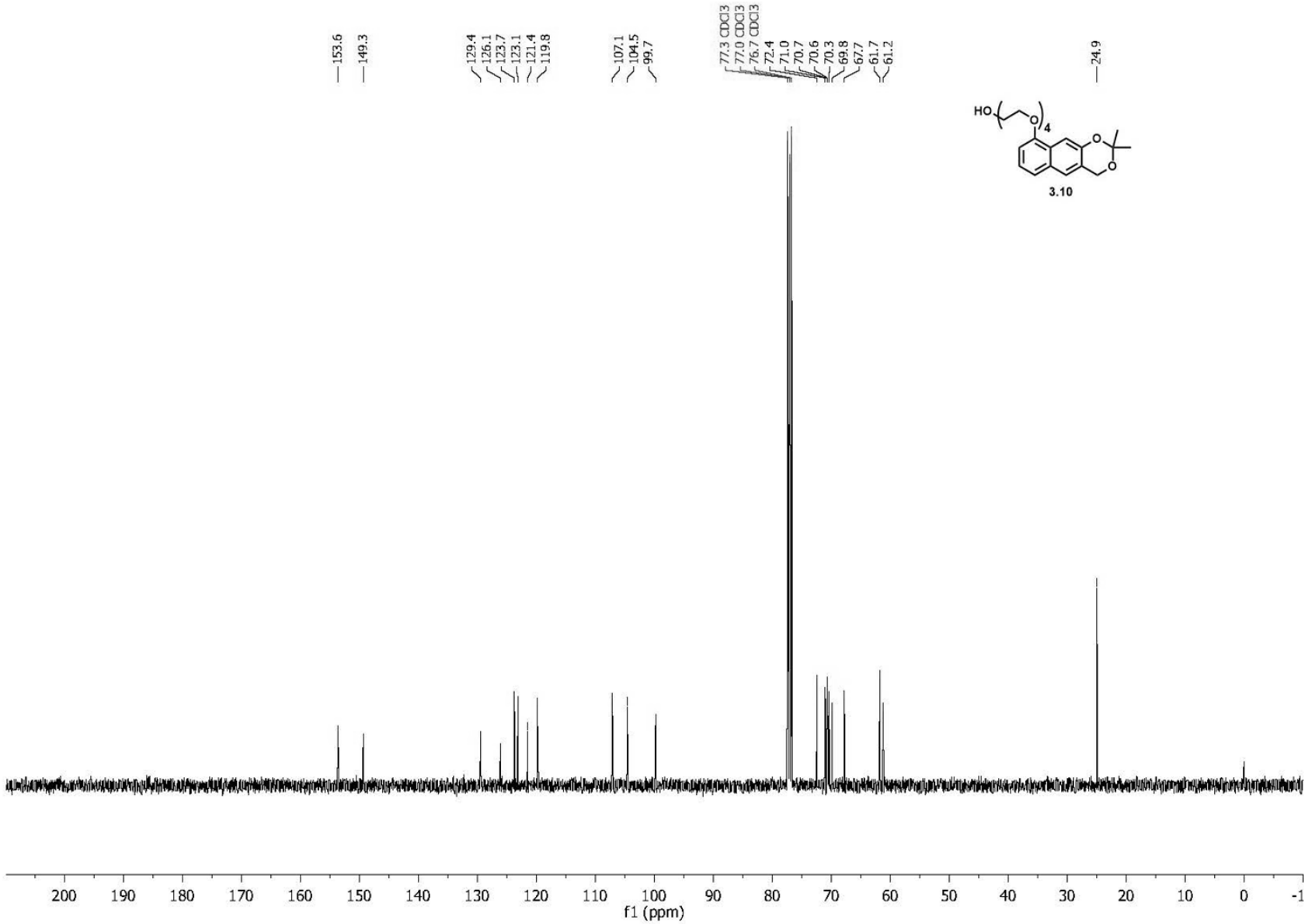
153.6
149.3
129.4
126.1
123.7
123.1
121.4
119.8
107.1
104.5
99.7
77.3 CDCl3
77.0 CDCl3
76.7 CDCl3
72.4
71.0
70.7
70.6
70.3
69.8
67.7
61.7
61.2
24.9
HO
4
O
O
O
3.10
200
190
180
170
160
150
140
130
120
110
100
90
80
70
60
50
40
30
20
10
0
-1
f1 (ppm)

7.781
7.776
7.765
7.760
7.643
7.412
7.309
7.300
7.288
7.279
7.260 CDCl3
7.209
7.189
7.169
6.721
6.702
5.049
5.046
4.263
4.251
4.238
4.136
4.123
4.112
4.104
3.963
3.954
3.950
3.938
3.772
3.762
3.756
3.749
3.667
3.660
3.655
3.644
3.610
3.602
3.595
3.590
3.577
3.571
3.567
3.564
3.557
2.402
1.784 HDO
1.586
TsO
4
3.11
2.00
1.00
1.00
3.00
1.00
1.00
2.00
2.00
2.03
2.02
2.03
4.04
4.03
2.00
1.00
6.03
3.00
2.00
f1 (ppm)

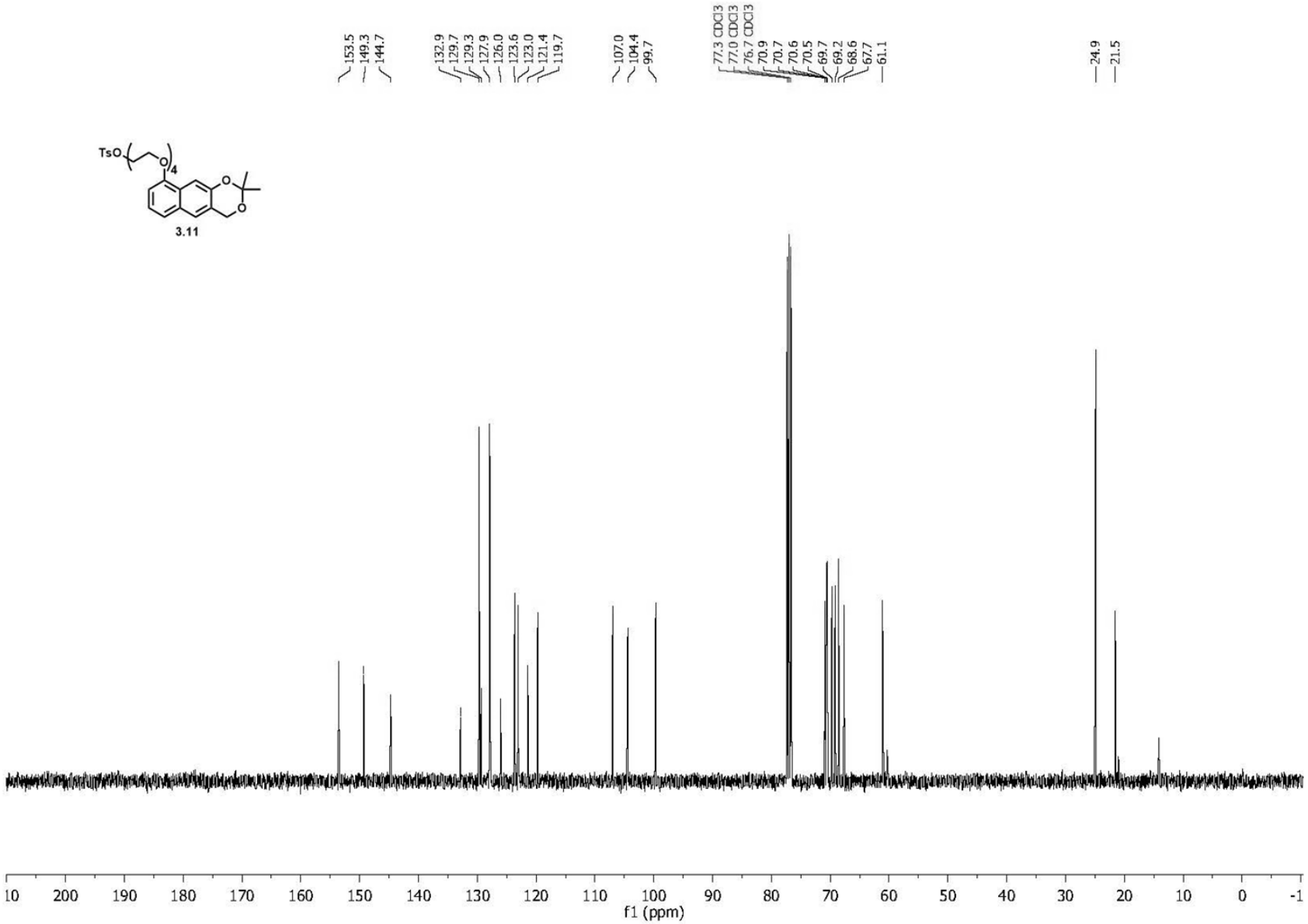
153.5
149.3
144.7
132.9
129.7
129.3
127.9
126.0
123.6
123.0
121.4
119.7
107.0
104.4
99.7
77.3 CDCl3
77.0 CDCl3
76.7 CDCl3
70.9
70.7
70.6
70.5
69.7
69.2
68.6
67.7
61.1
24.9
21.5
TsO
4
3.11
f1 (ppm)

7.653
7.421
7.420
7.418
7.417
7.415
7.305
7.303
7.287
7.284
7.282
7.260 CDCl3
7.215
7.196
7.194
7.175
6.733
6.731
6.714
6.712
5.058
5.054
4.282
4.270
4.267
4.266
4.257
3.987
3.977
3.974
3.973
3.962
3.798
3.796
3.795
3.791
3.783
3.718
3.711
3.706
3.705
3.704
3.694
3.674
3.673
3.670
3.666
3.660
3.658
3.637
3.635
3.629
3.625
3.622
3.621
3.605
3.589
3.573
3.095
3.079
3.063
2.316
3.12
6.00
3.00
2.01
2.01
2.09
2.00
2.00
2.04
2.03
2.03
2.02
1.00
0.99
1.00
1.00
0.88
f1 (ppm)

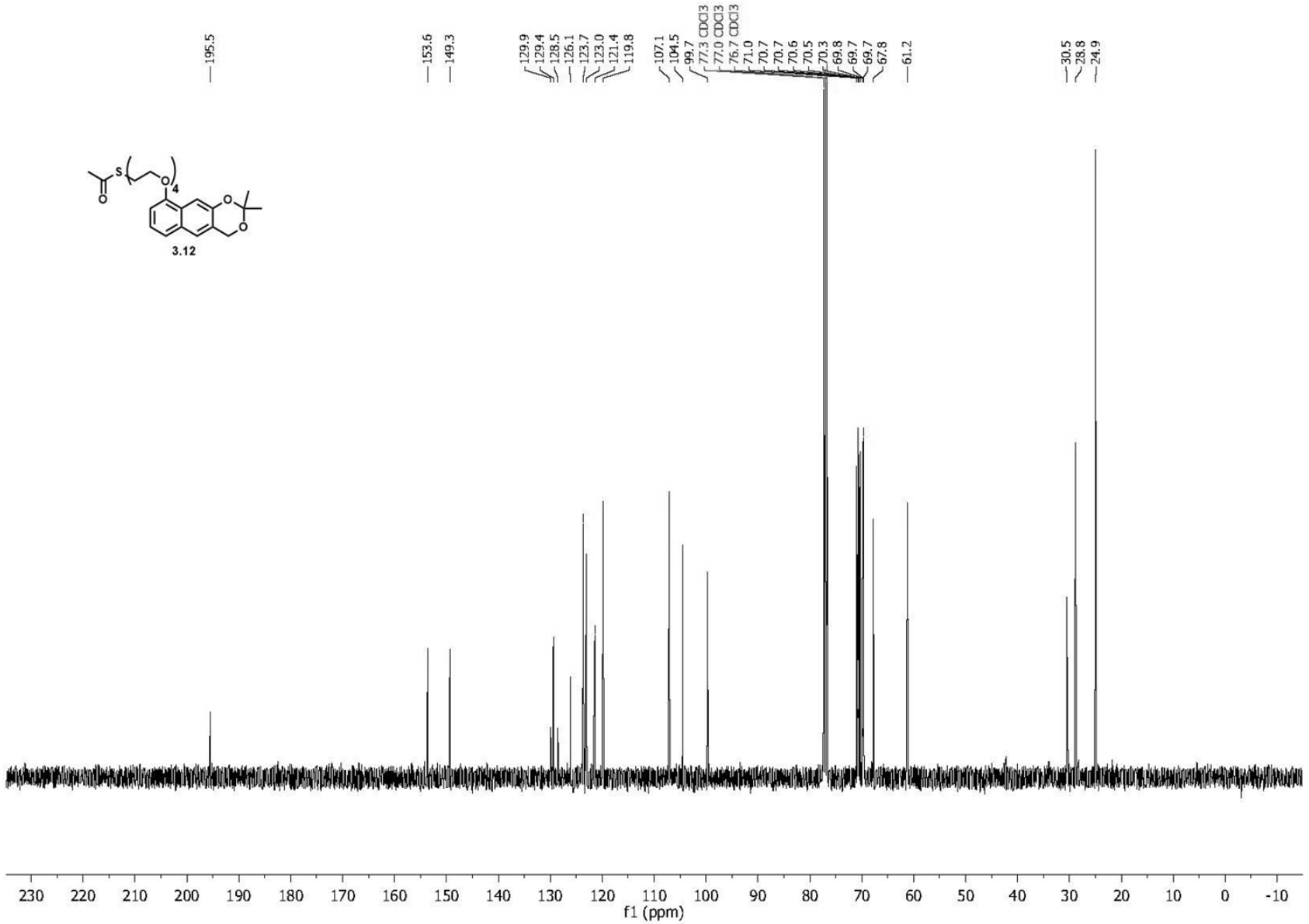
195.5
153.6
149.3
129.9
129.4
128.5
126.1
123.7
123.0
121.4
119.8
107.1
104.5
99.7
77.3 CDCl3
77.0 CDCl3
76.7 CDCl3
71.0
70.7
70.7
70.6
70.5
70.3
69.8
69.7
69.7
67.8
61.2
30.5
28.8
24.9
3.12
f1 (ppm)

3.13
f1 (ppm)

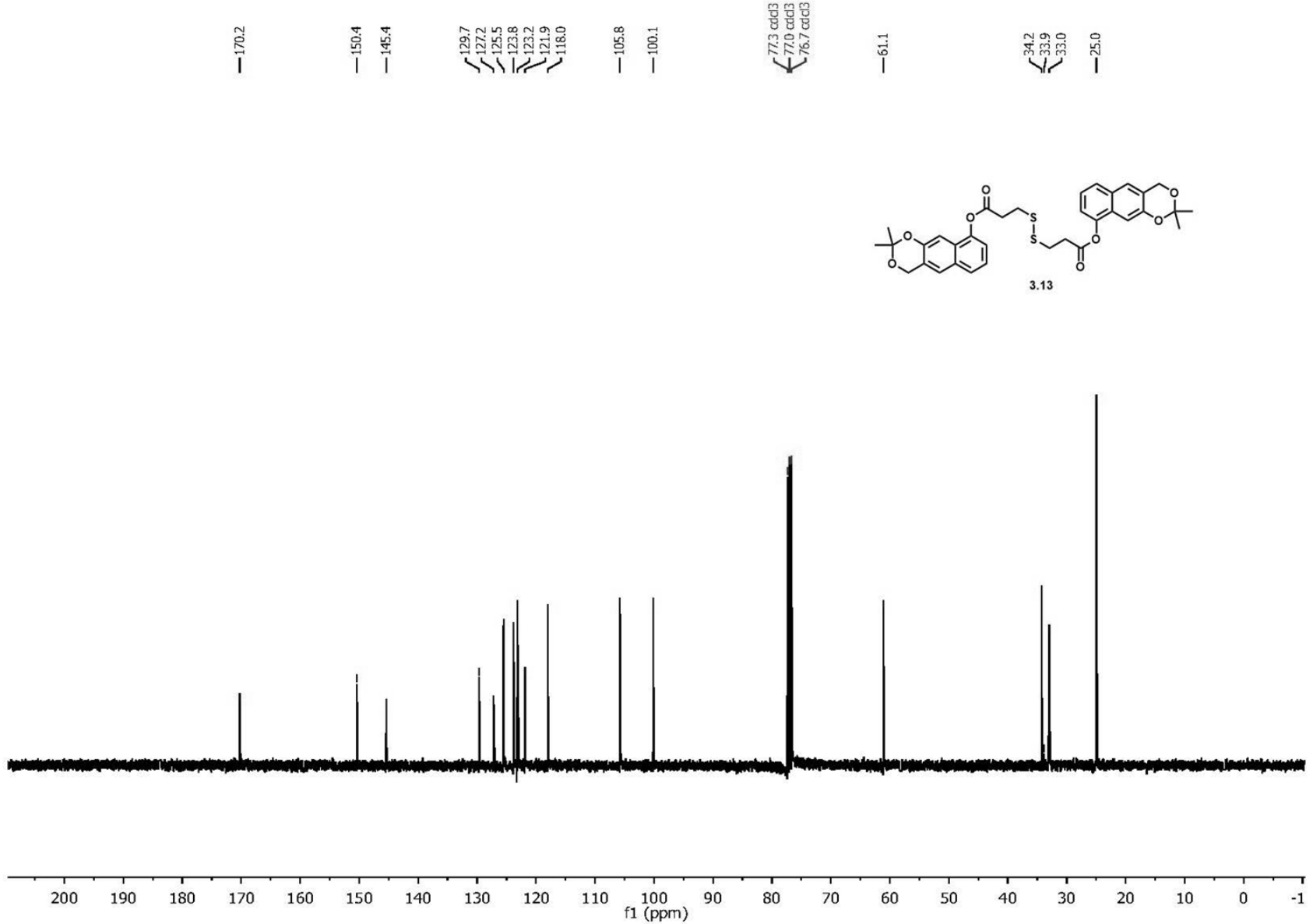
170.2
150.4
145.4
129.7
127.2
125.5
123.8
123.2
121.9
118.0
105.8
100.1
77.3 cdcl3
77.0 cdcl3
76.7 cdcl3
61.1
34.2
33.9
33.0
25.0
3.13
f1 (ppm)

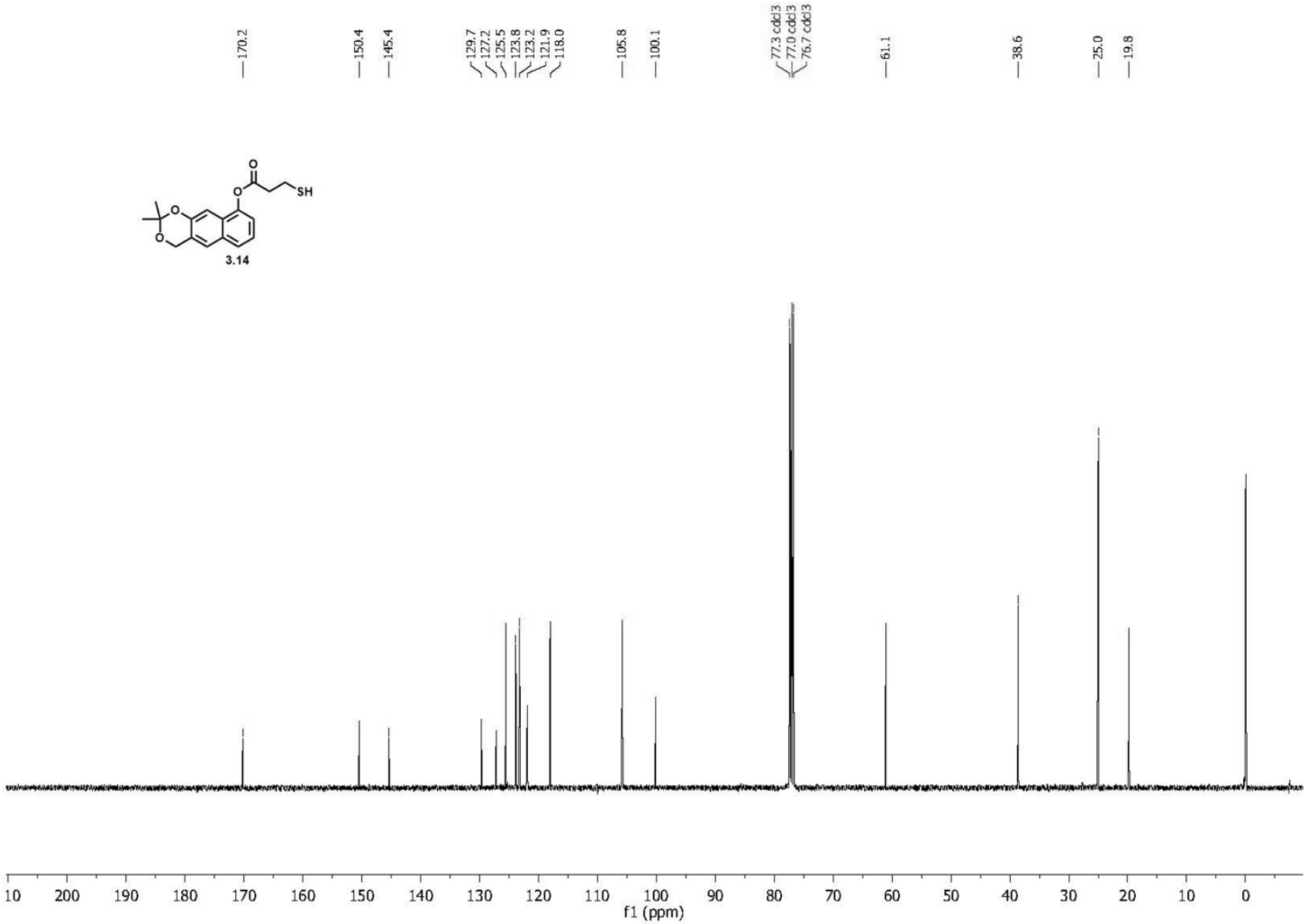
170.2
150.4
145.4
129.7
127.2
125.5
123.8
123.2
121.9
118.0
105.8
100.1
77.3 cdcl3
77.0 cdcl3
76.7 cdcl3
61.1
38.6
25.0
19.8
SH
3.14
f1 (ppm)

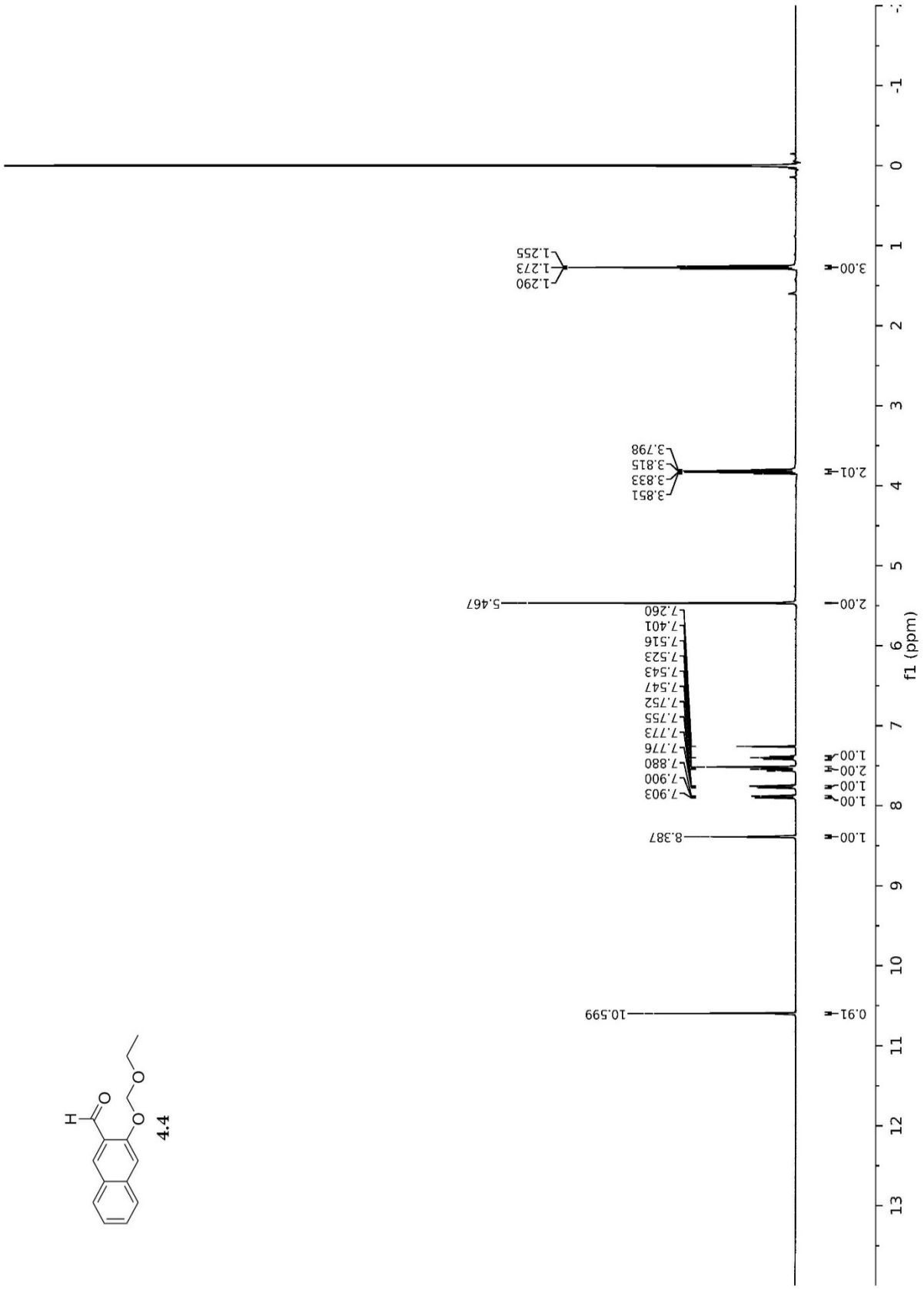
10.599
8.387
7.903
7.900
7.880
7.776
7.773
7.755
7.752
7.547
7.543
7.523
7.516
7.401
7.260
5.467
3.851
3.833
3.815
3.798
1.290
1.273
1.255
0.91
1.00
1.00
2.00
1.00
2.01
3.00
2.00
f1 (ppm)

4.4

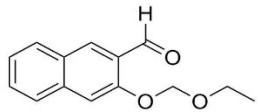

4.4

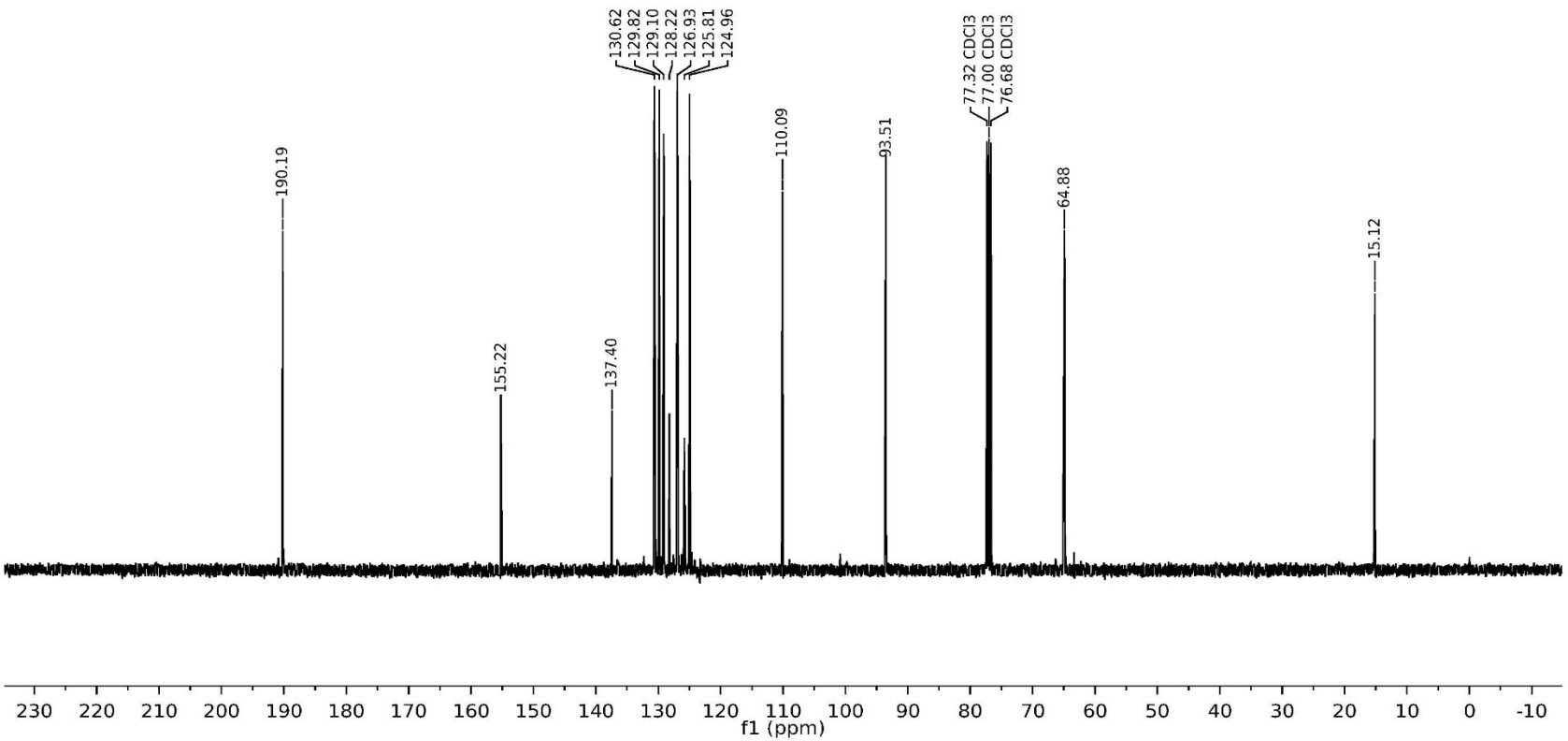
190.19
155.22
137.40
130.62
129.82
129.10
128.22
126.93
125.81
124.96
110.09
93.51
77.32 CDCl3
77.00 CDCl3
76.68 CDCl3
64.88
15.12
230 220 210 200 190 180 170 160 150 140 130 120 110 100 90 80 70 60 50 40 30 20 10 0 -10
f1 (ppm)

HO
OH
O
O
4.6

7.896
7.764
7.743
7.721
7.451
7.448
7.434
7.430
7.427
7.413
7.411
7.370
7.367
7.353
7.350
7.347
7.333
7.330
7.260
5.350
5.257
5.247
5.238
5.228
3.953
3.934
3.925
3.914
3.906
3.756
3.738
3.730
3.721
3.710
3.703
3.682
3.313
3.301
2.657
2.646
2.637
2.627
1.252
1.234
1.217
2.00
1.00
2.00
1.00
1.00
3.01
1.00
1.00
3.00
f1 (ppm)

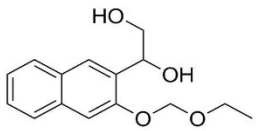
HO
OH
O
O

4.6

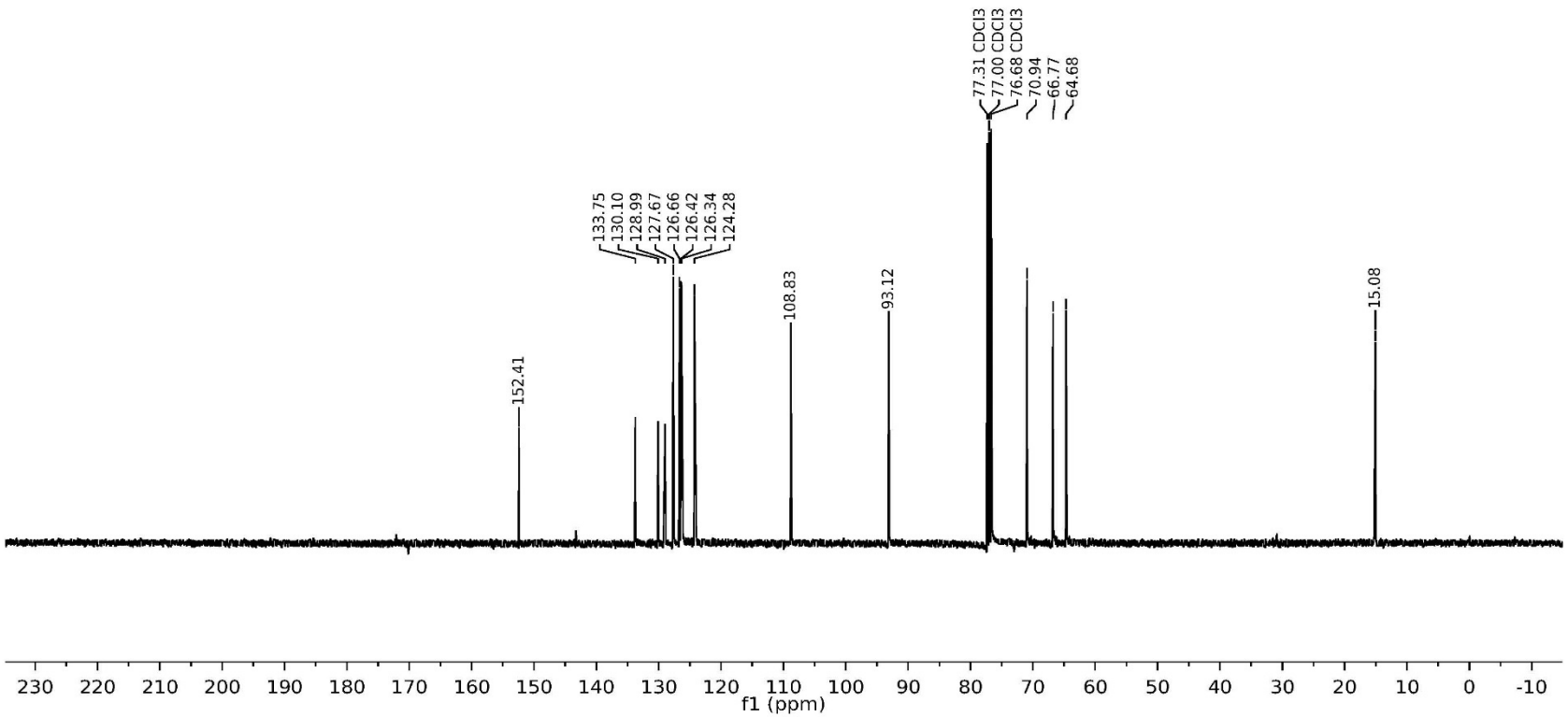
77.31 CDCl3
77.00 CDCl3
76.68 CDCl3
70.94
66.77
64.68
133.75
130.10
128.99
127.67
126.66
126.42
126.34
124.28
108.83
93.12
15.08
152.41
230 220 210 200 190 180 170 160 150 140 130 120 110 100 90 80 70 60 50 40 30 20 10 0 -10
f1 (ppm)

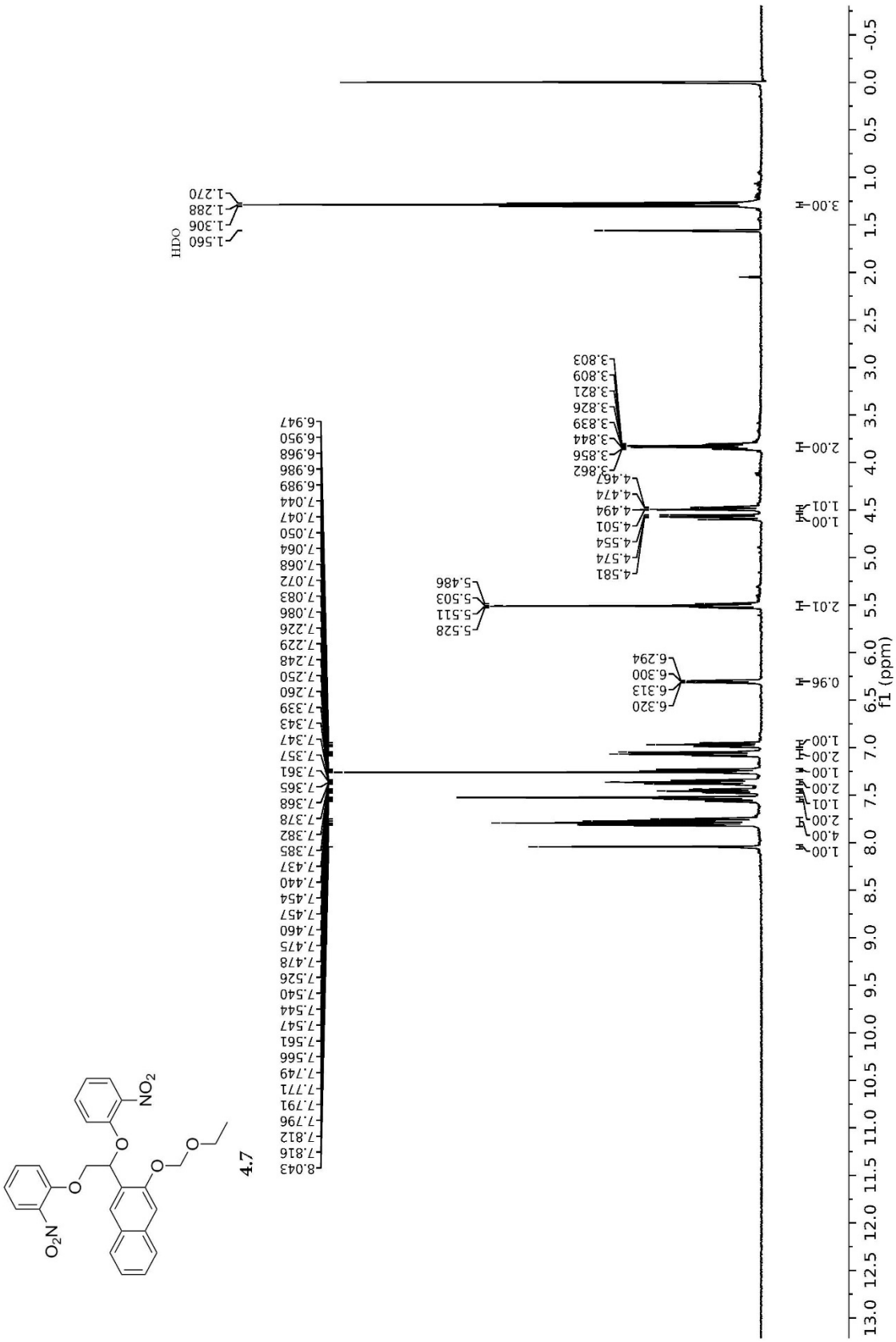
4.7
f1 (ppm)

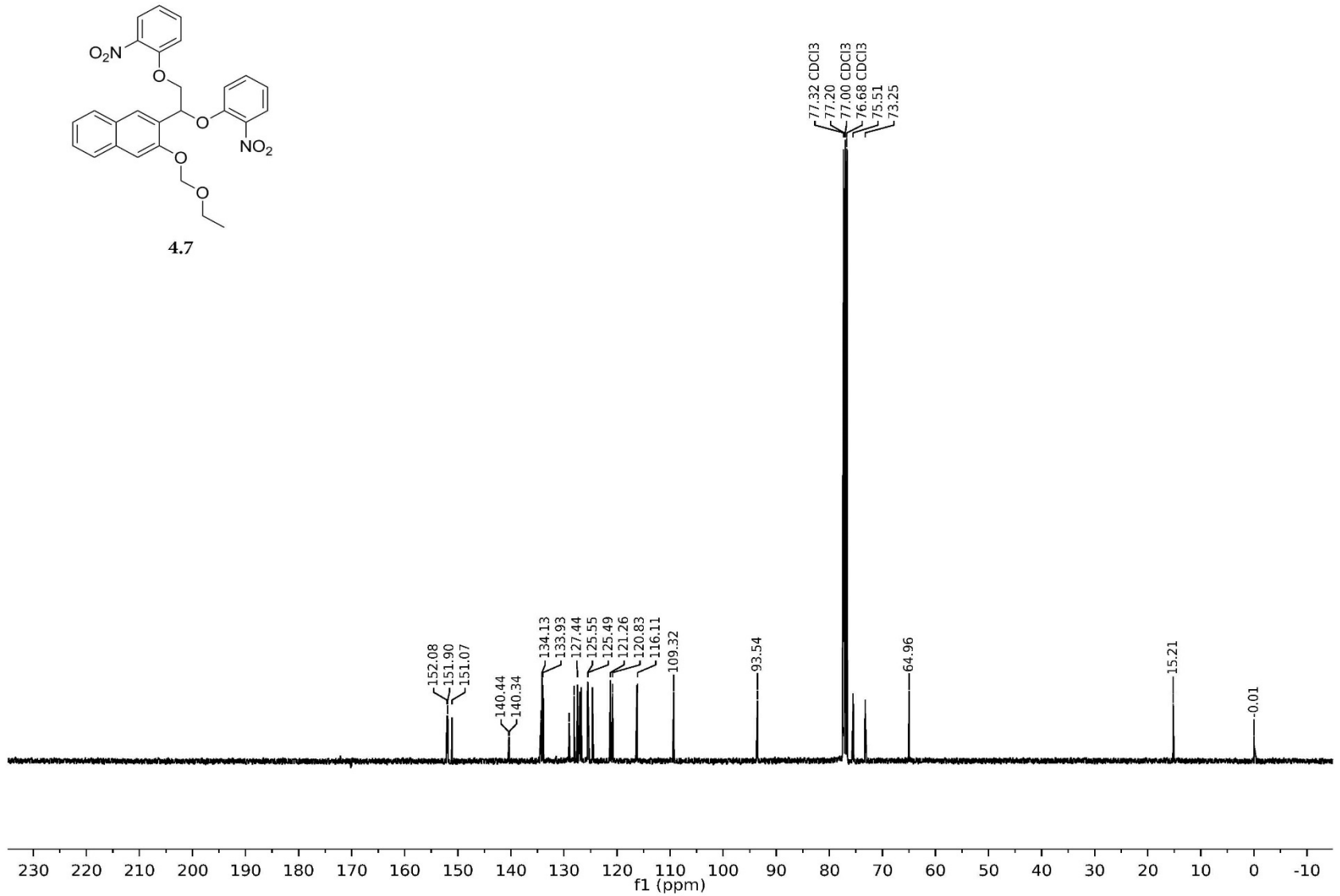
O2N
O
O
NO2
O
O
4.7
77.32 CDCl3
77.20
77.00 CDCl3
76.68 CDCl3
75.51
73.25
152.08
151.90
151.07
140.44
140.34
134.13
133.93
127.44
125.55
125.49
121.26
120.83
116.11
109.32
93.54
64.96
15.21
-0.01
230 220 210 200 190 180 170 160 150 140 130 120 110 100 90 80 70 60 50 40 30 20 10 0 -10
f1 (ppm)

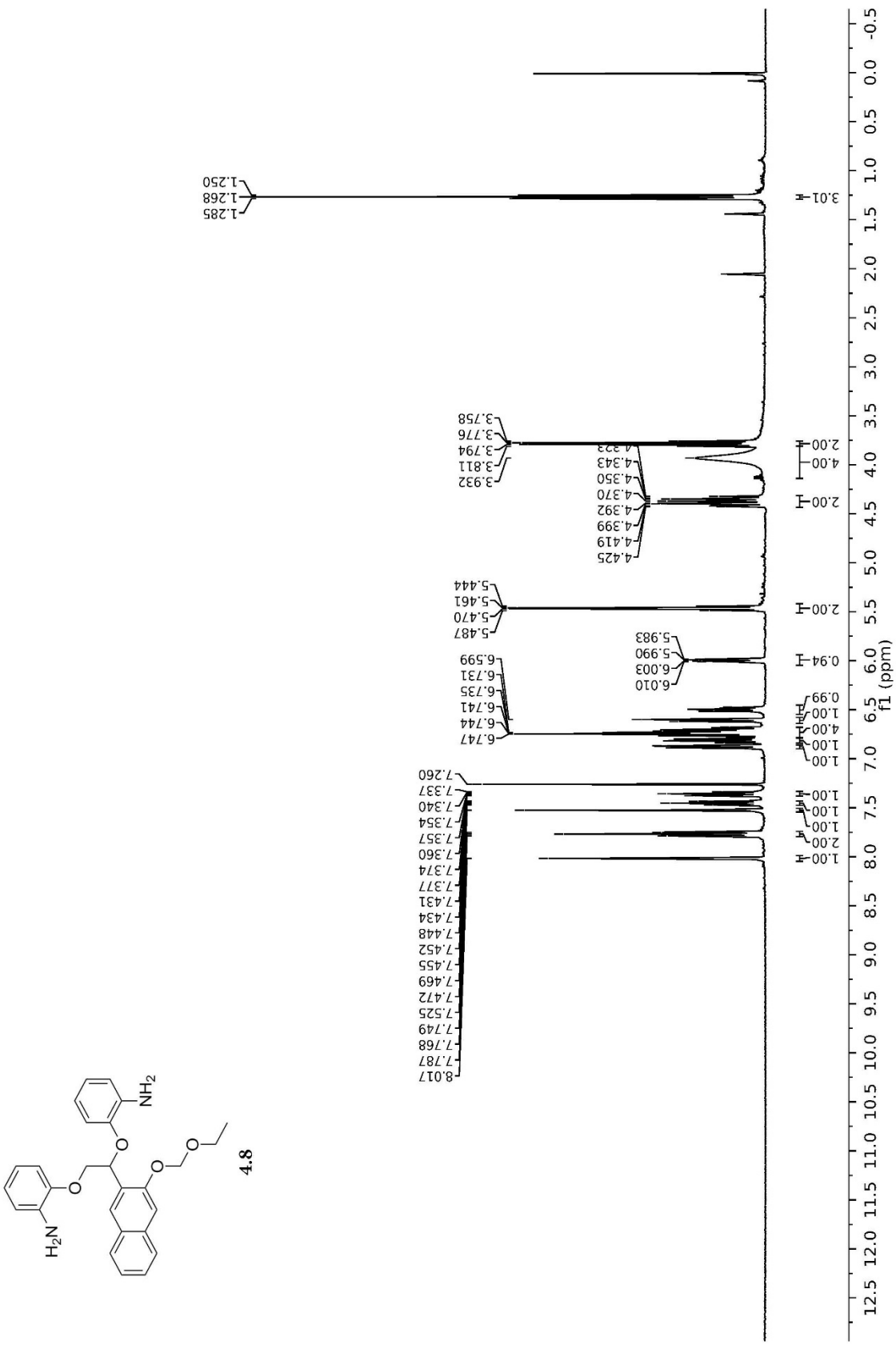
NH2
O
O
O
O
H2N
4.8
8.017
7.787
7.768
7.749
7.525
7.472
7.469
7.455
7.452
7.448
7.434
7.431
7.377
7.374
7.360
7.357
7.354
7.340
7.337
7.260
6.747
6.744
6.741
6.735
6.731
6.599
6.010
6.003
5.990
5.983
5.487
5.470
5.461
5.444
4.425
4.419
4.399
4.392
4.370
4.350
4.343
4.323
3.932
3.811
3.794
3.776
3.758
1.285
1.268
1.250
3.01
2.00
4.00
2.00
2.00
0.94
1.00
4.00
1.00
0.99
1.00
1.00
1.00
1.00
2.00
1.00
f1 (ppm)

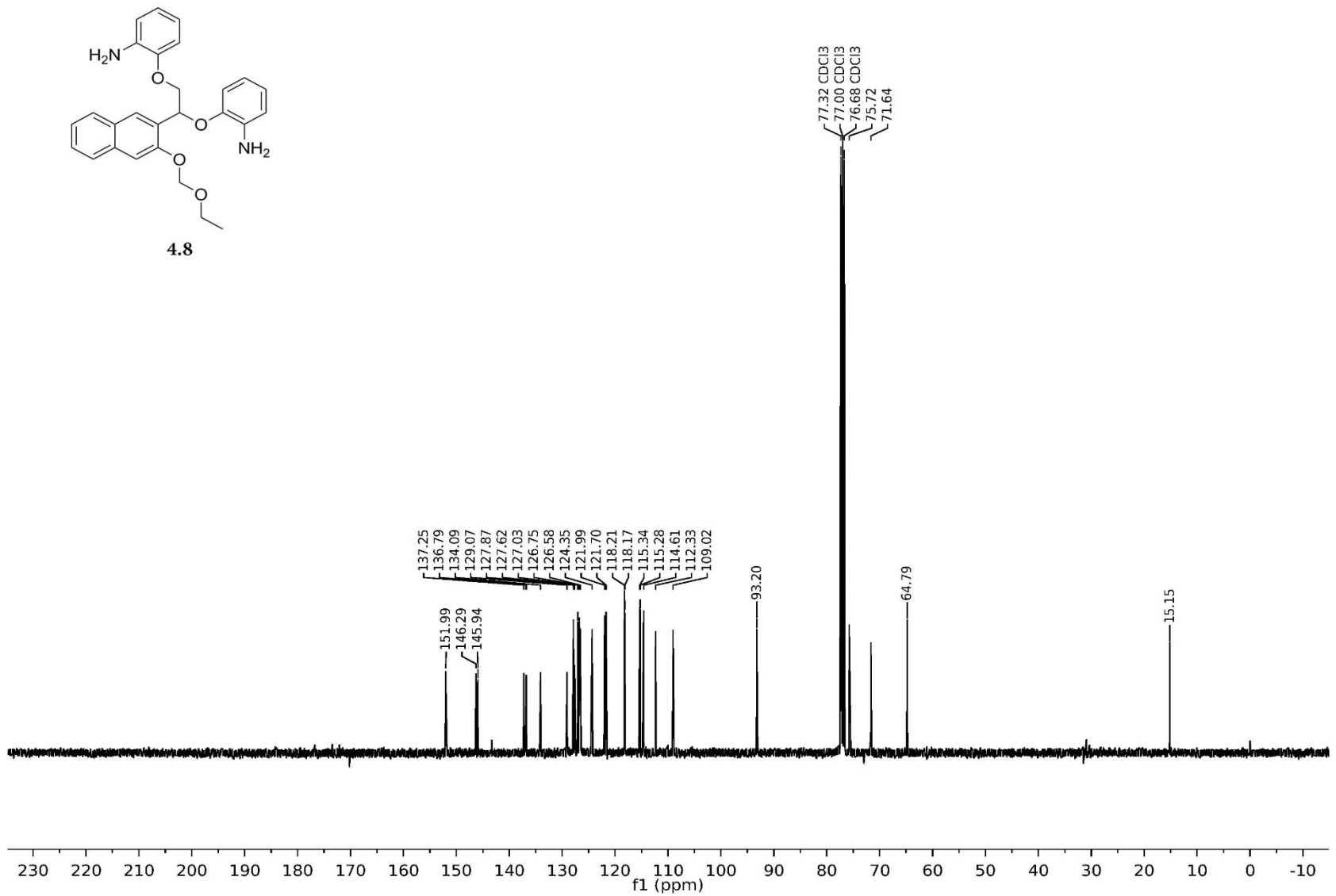
H2N
O
O
O
NH2
O
O
4.8
77.32 CDCl3
77.00 CDCl3
76.68 CDCl3
75.72
71.64
137.25
136.79
134.09
129.07
127.87
127.62
127.03
126.75
126.58
124.35
121.99
121.70
118.21
118.17
115.34
115.28
114.61
112.33
109.02
151.99
146.29
145.94
93.20
64.79
15.15
230 220 210 200 190 180 170 160 150 140 130 120 110 100 90 80 70 60 50 40 30 20 10 0 -10
f1 (ppm)

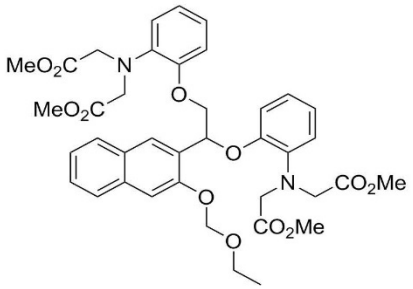
MeO2C
N
MeO2C
O
O
O
N
CO2Me
CO2Me
O
O

4.9

4.302
4.298
4.290
4.244
4.232
4.172
4.127
3.822
3.804
3.787
3.769
3.588
3.444
1.283
1.266
1.248
8.047
7.792
7.772
7.735
7.714
7.485
7.427
7.424
7.411
7.407
7.403
7.390
7.386
7.340
7.336
7.323
7.320
7.316
7.302
7.299
7.260
6.879
6.874
6.866
6.826
6.730
6.713
6.241
6.228
6.214
5.489
5.471
5.461
5.444
1.00
1.00
1.00
1.00
1.00
1.00
3.00
2.00
2.00
1.01
1.00
2.00
8.00
2.02
2.00
6.00
6.00
3.04
f1 (ppm)

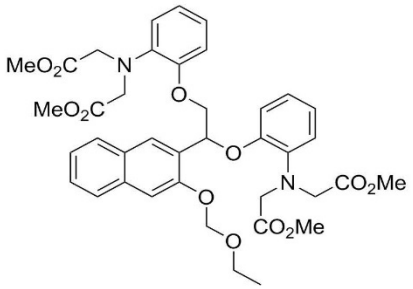
MeO2C
N
MeO2C
O
O
O
N
CO2Me
CO2Me
O
O

4.9

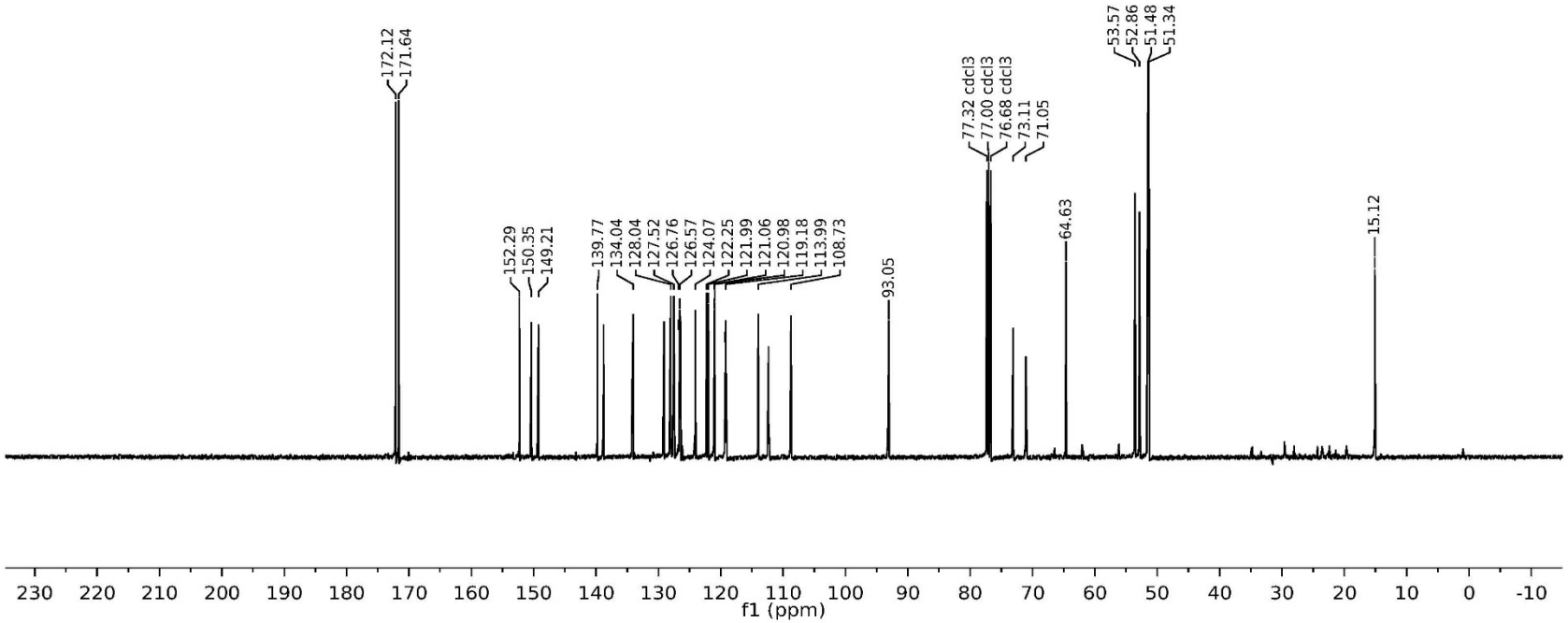
172.12
171.64
152.29
150.35
149.21
139.77
134.04
128.04
127.52
126.76
126.57
124.07
122.25
121.99
121.06
120.98
119.18
113.99
108.73
93.05
77.32 cdcl3
77.00 cdcl3
76.68 cdcl3
73.11
71.05
64.63
53.57
52.86
51.48
51.34
15.12
230 220 210 200 190 180 170 160 150 140 130 120 110 100 90 80 70 60 50 40 30 20 10 0 -10
f1 (ppm)

MeO2C
MeO2C
N
O
O
OH
N
CO2Me
CO2Me
4.10
3.564
3.488
7.790
7.746
7.725
7.634
7.613
7.526
7.401
7.398
7.384
7.381
7.377
7.364
7.360
7.312
7.309
7.295
7.292
7.289
7.275
7.271
7.260
7.207
6.927
6.921
6.912
6.910
6.903
6.893
6.888
6.883
6.879
6.875
6.865
6.823
6.817
6.814
6.803
6.798
6.790
6.777
6.772
6.763
6.754
6.749
4.675
4.651
4.627
4.231
4.223
4.206
4.198
4.167
4.141
6.070
6.062
6.048
6.040
1.00
0.99
1.00
4.00
1.00
6.00
1.00
1.00
1.00
1.00
1.01
1.00
1.00
5.00
3.00
f1 (ppm)

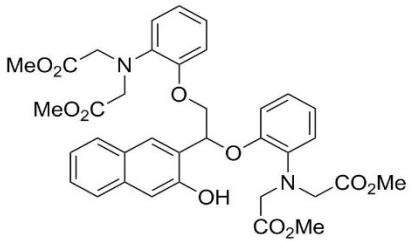
MeO2C
N
MeO2C
O
O
OH
N
CO2Me
CO2Me

4.10

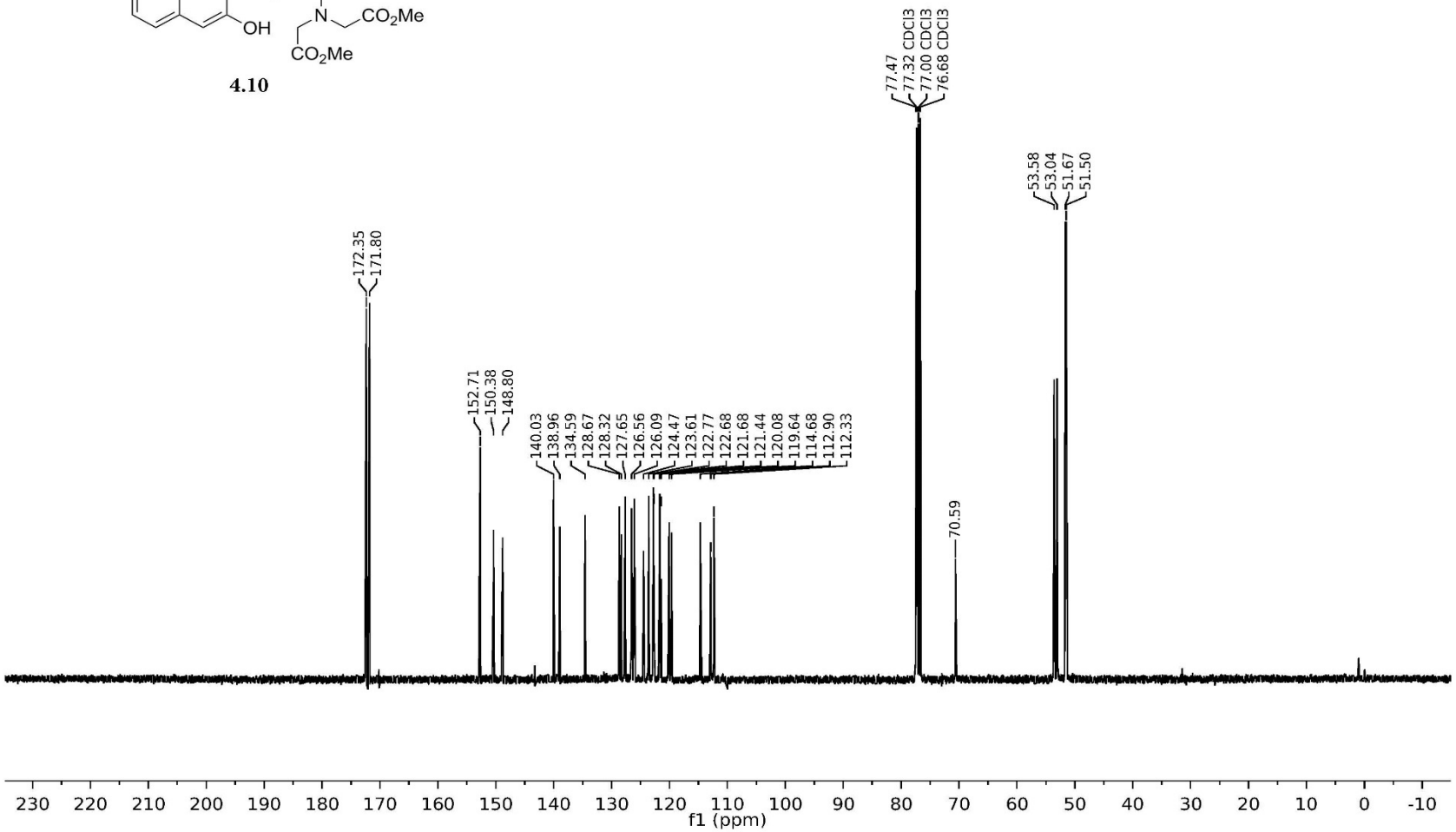
172.35
171.80
152.71
150.38
148.80
140.03
138.96
134.59
128.67
128.32
127.65
126.56
126.09
124.47
123.61
122.77
122.68
121.68
121.44
120.08
119.64
114.68
112.90
112.33
77.47
77.32 CDCl3
77.00 CDCl3
76.68 CDCl3
70.59
53.58
53.04
51.67
51.50
230 220 210 200 190 180 170 160 150 140 130 120 110 100 90 80 70 60 50 40 30 20 10 0 -10
f1 (ppm)

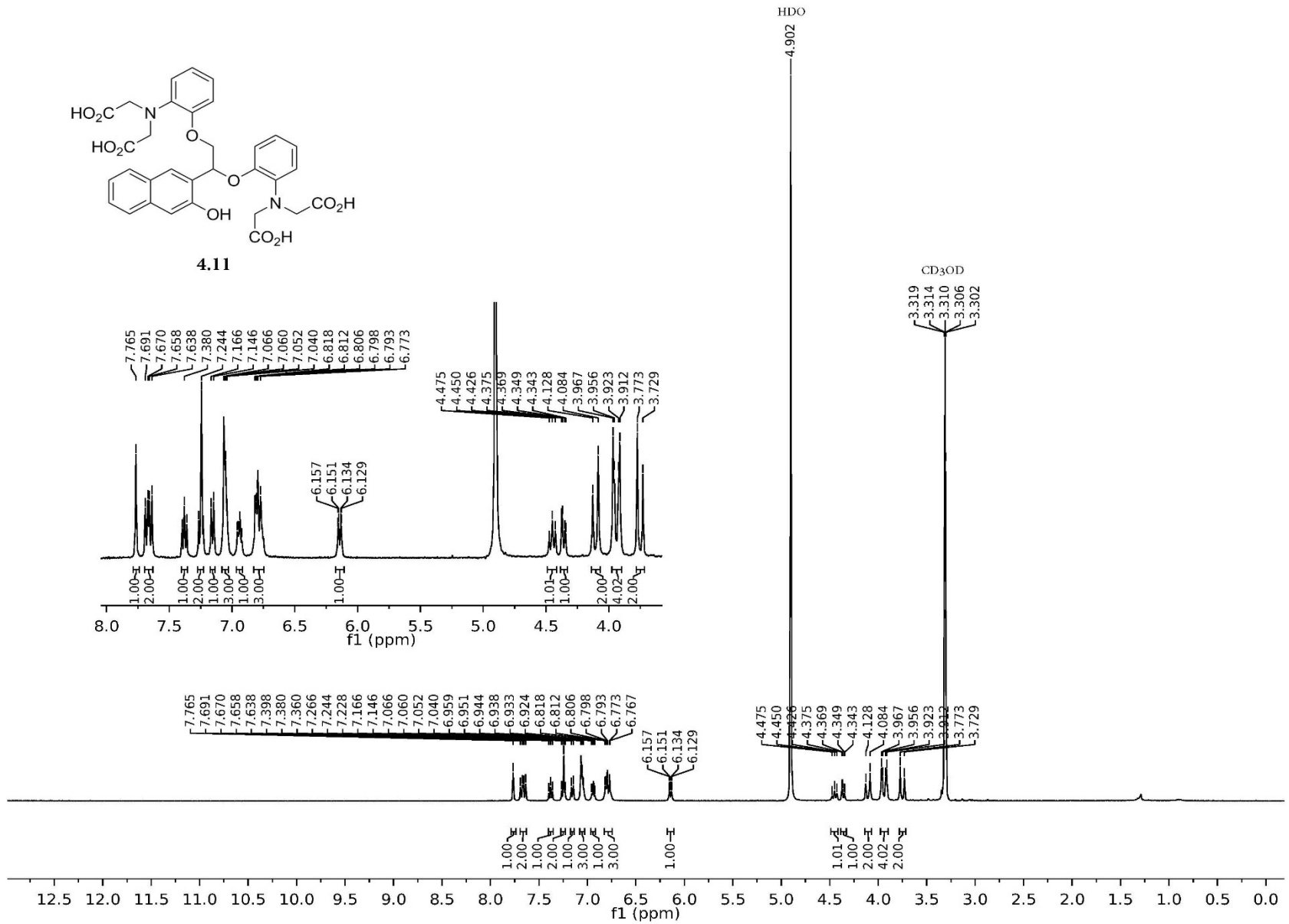
HO2C
N
HO2C
O
O
N
CO2H
OH
CO2H
4.11
HDO
4.902
CD3OD
f1 (ppm)

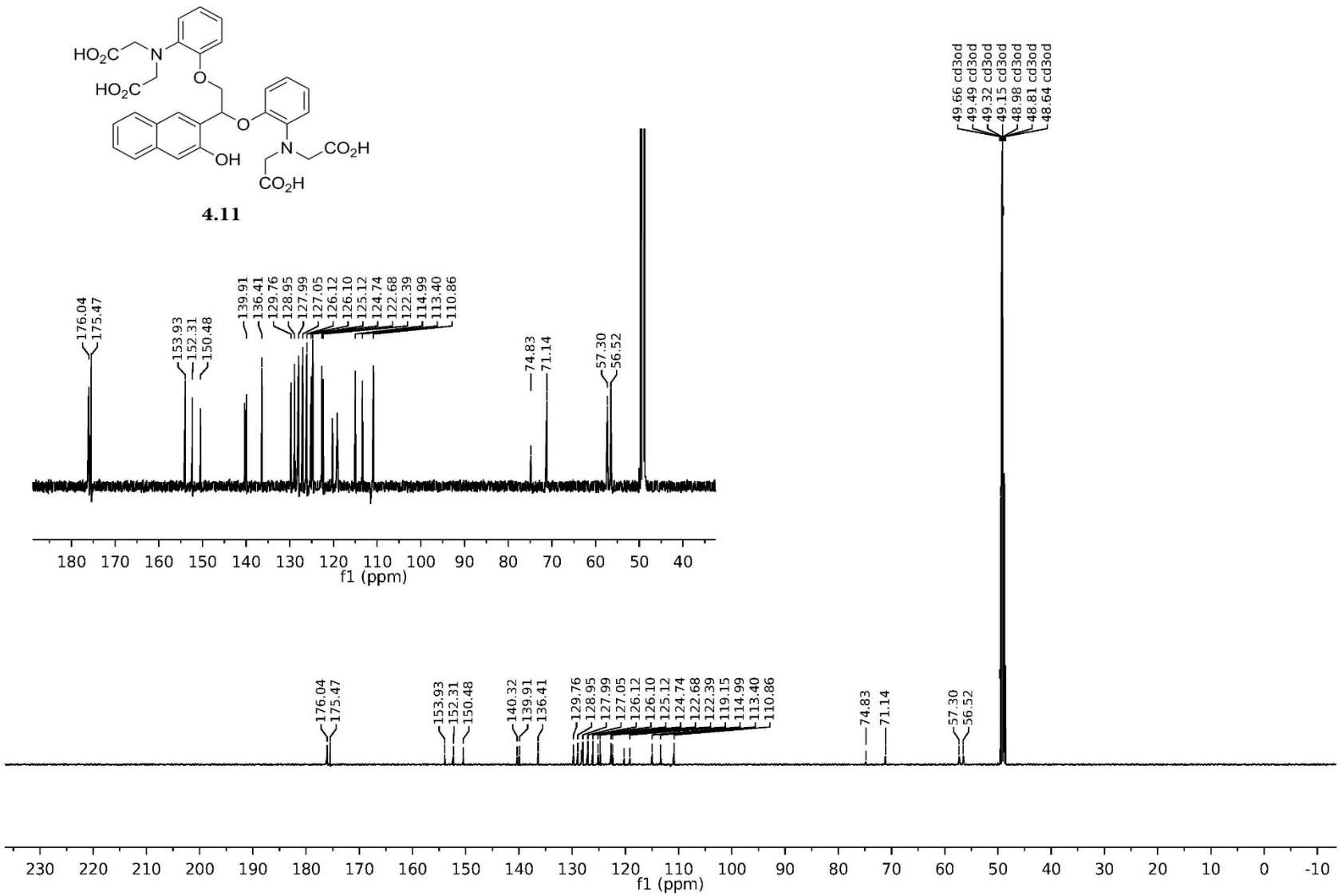
HO2C
N
HO2C
O
O
OH
N
CO2H
CO2H
4.11
176.04
175.47
153.93
152.31
150.48
139.91
136.41
129.76
128.95
127.99
127.05
126.12
126.10
125.12
124.74
122.68
122.39
114.99
113.40
110.86
74.83
71.14
57.30
56.52
49.66 cd3od
49.49 cd3od
49.32 cd3od
49.15 cd3od
48.98 cd3od
48.81 cd3od
48.64 cd3od
140.32
119.15
f1 (ppm)

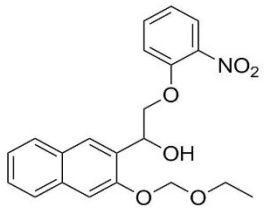
NO2
O
OH
O
O

4.12

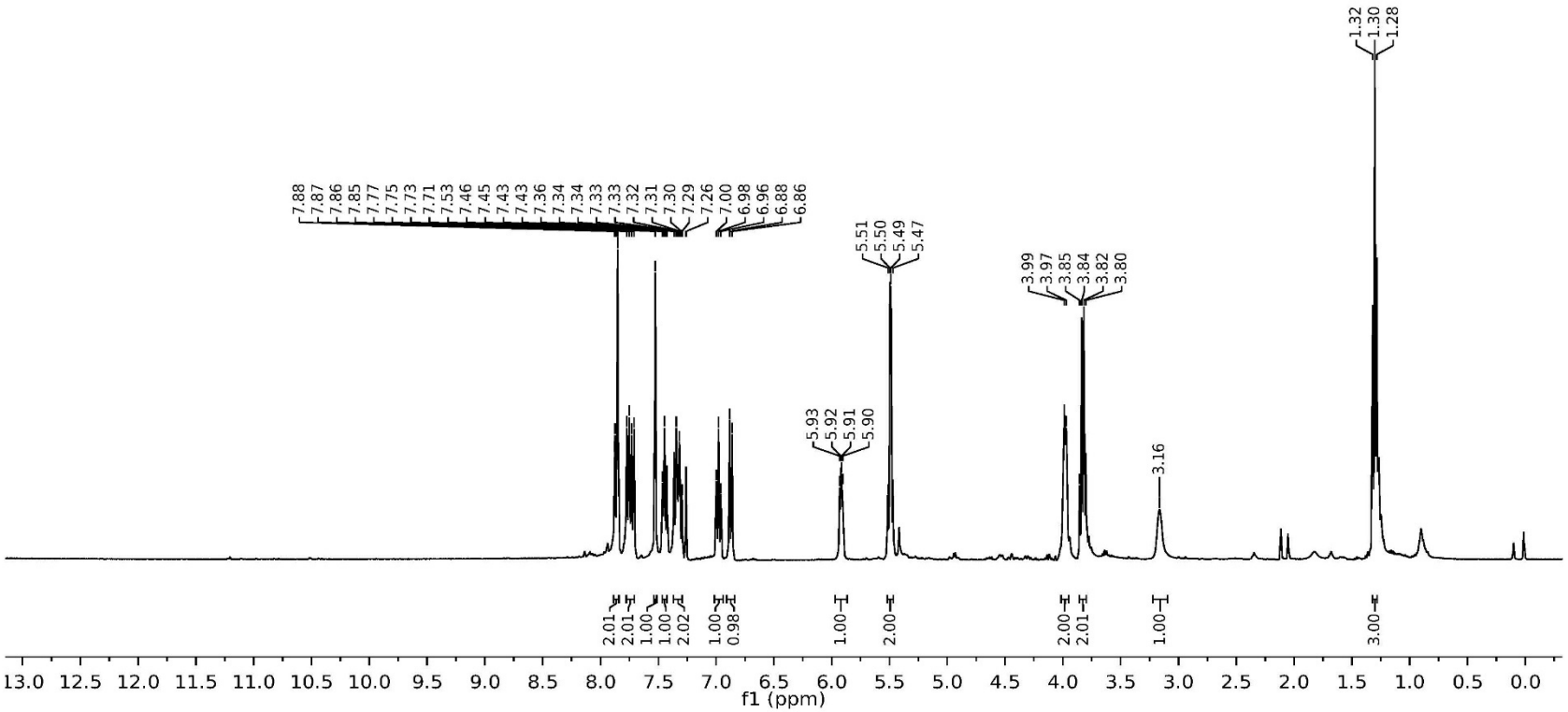
7.88
7.87
7.86
7.85
7.77
7.75
7.73
7.71
7.53
7.46
7.45
7.43
7.43
7.36
7.34
7.34
7.33
7.33
7.32
7.31
7.30
7.29
7.26
7.00
6.98
6.96
6.88
6.86
5.93
5.92
5.91
5.90
5.51
5.50
5.49
5.47
3.99
3.97
3.85
3.84
3.82
3.80
3.16
1.32
1.30
1.28
2.01
2.01
1.00
1.00
2.02
1.00
0.98
1.00
2.00
2.00
2.01
1.00
3.00
13.0 12.5 12.0 11.5 11.0 10.5 10.0 9.5 9.0 8.5 8.0 7.5 7.0 6.5 6.0 5.5 5.0 4.5 4.0 3.5 3.0 2.5 2.0 1.5 1.0 0.5 0.0
f1 (ppm)

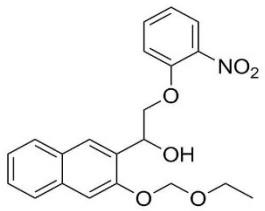
NO2
O
OH
O
O

4.12

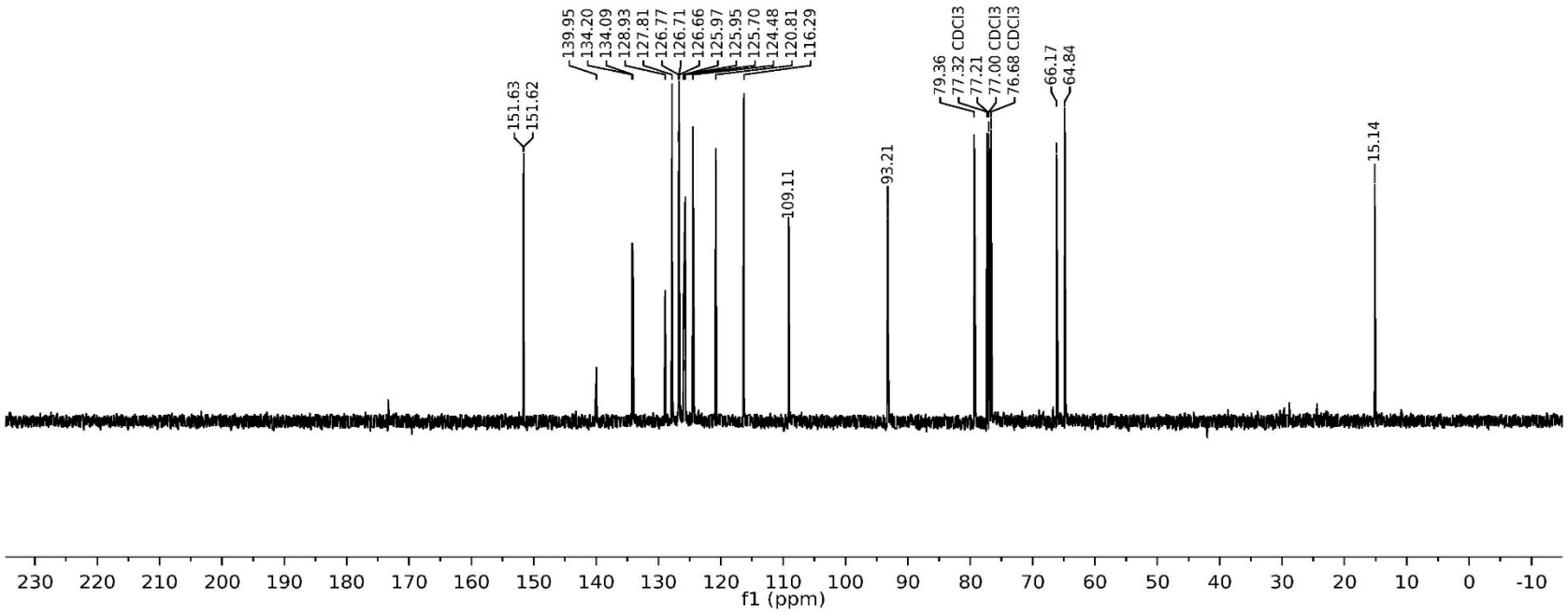
151.63
151.62
139.95
134.20
134.09
128.93
127.81
126.77
126.71
126.66
125.97
125.95
125.70
124.48
120.81
116.29
109.11
93.21
79.36
77.32 CDCl3
77.21
77.00 CDCl3
76.68 CDCl3
66.17
64.84
15.14
230 220 210 200 190 180 170 160 150 140 130 120 110 100 90 80 70 60 50 40 30 20 10 0 -10
f1 (ppm)

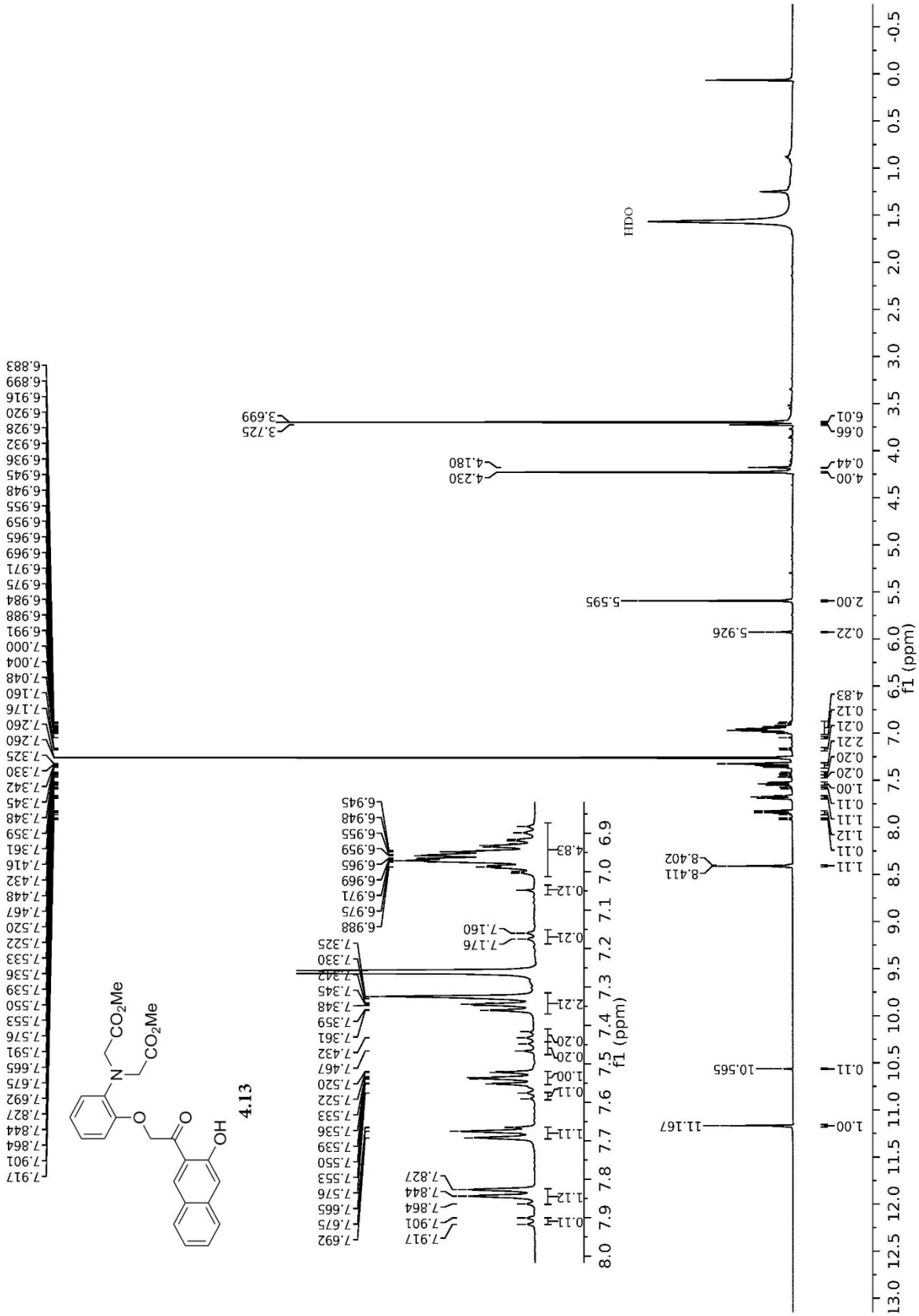
4.13
HDO
f1 (ppm)

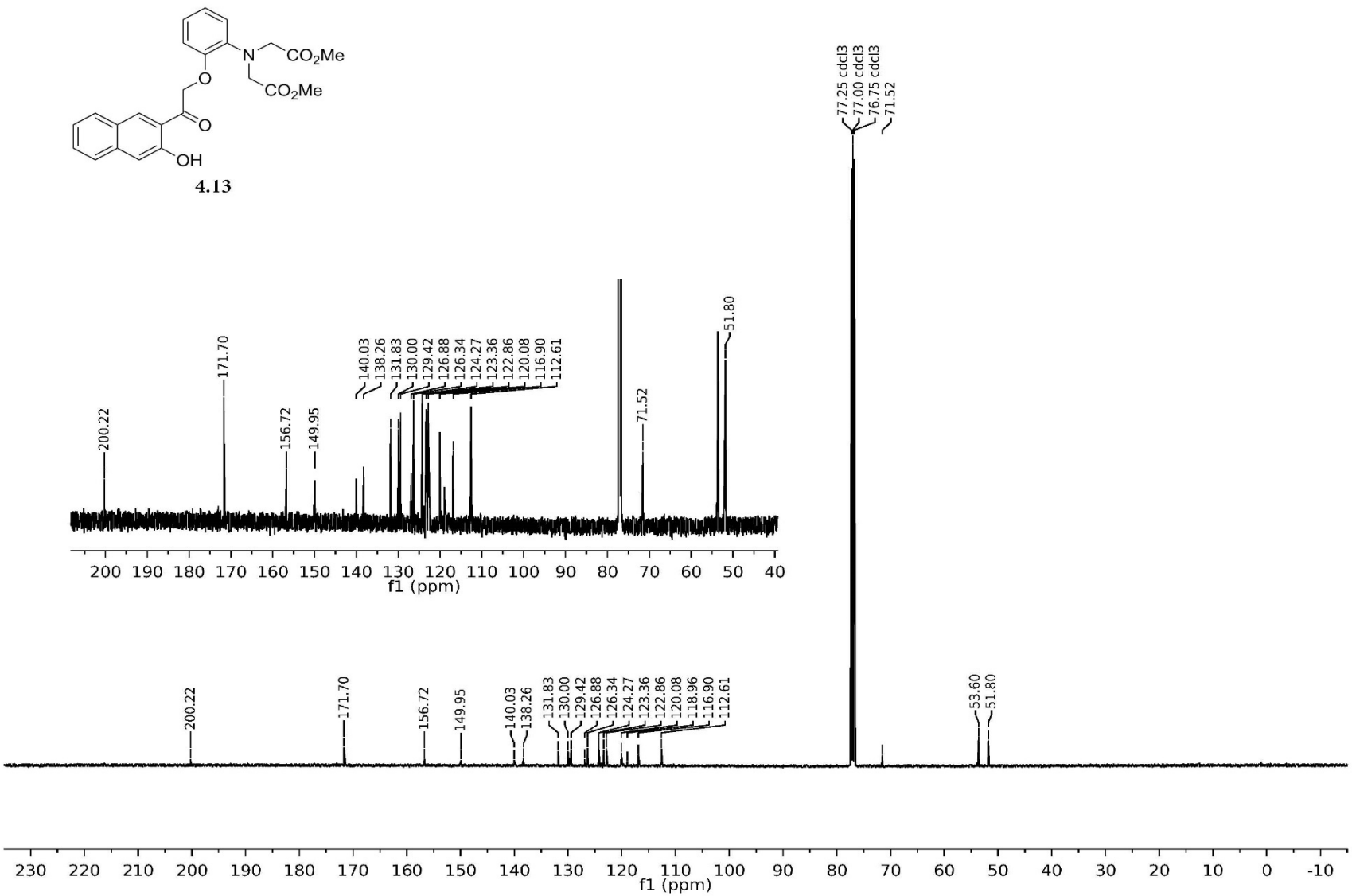
CO2Me
CO2Me
N
O
O
OH
4.13
77.25 cdcl3
77.00 cdcl3
76.75 cdcl3
71.52
51.80
200.22
171.70
156.72
149.95
140.03
138.26
131.83
130.00
129.42
126.88
126.34
124.27
123.36
122.86
120.08
116.90
112.61
71.52
51.80
f1 (ppm)
200.22
171.70
156.72
149.95
140.03
138.26
131.83
130.00
129.42
126.88
126.34
124.27
123.36
122.86
120.08
118.96
116.90
112.61
53.60
51.80
f1 (ppm)

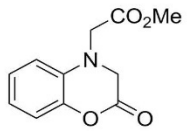
CO2Me
N
O
O

4.15

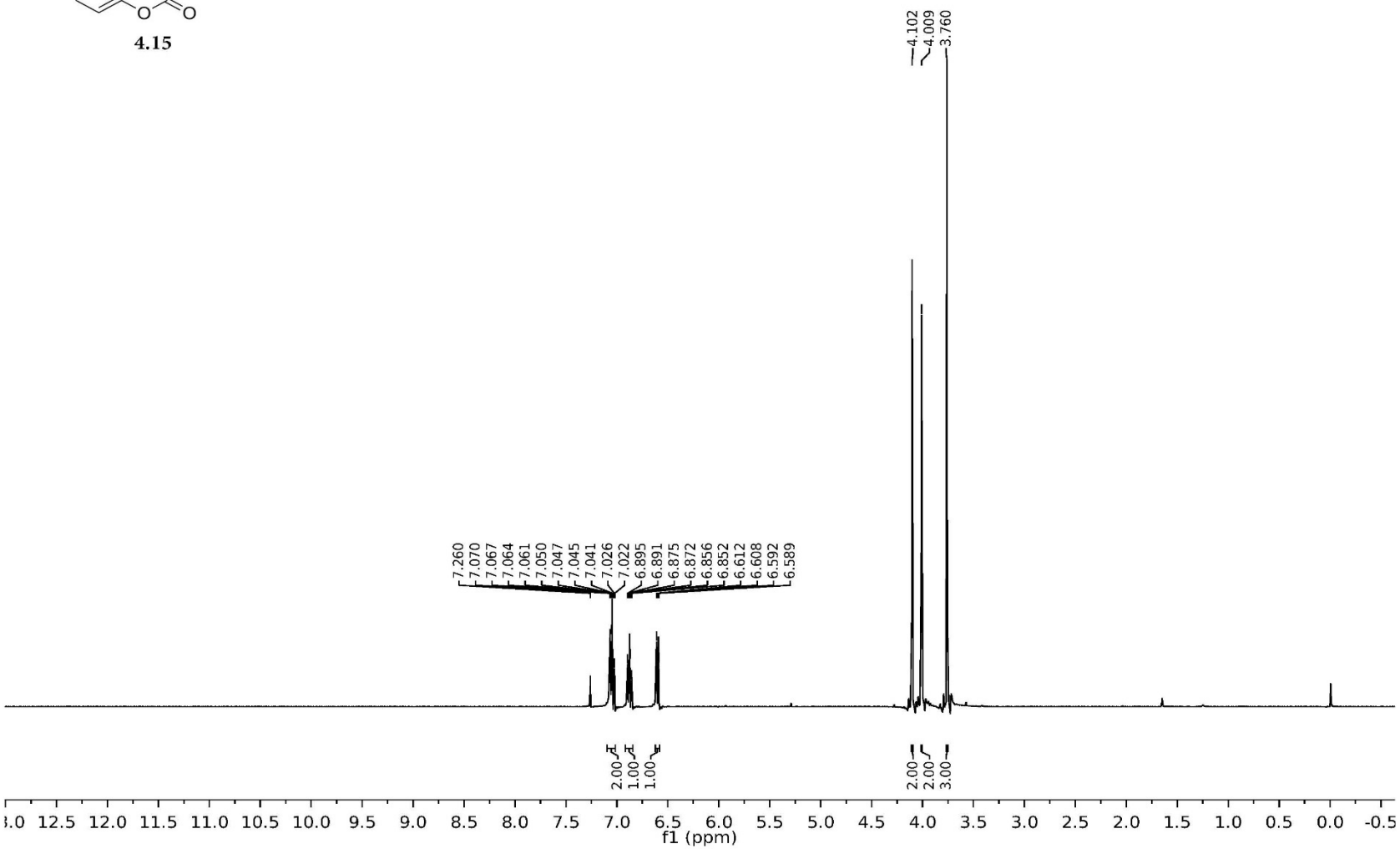
4.102
4.009
3.760
7.260
7.070
7.067
7.064
7.061
7.050
7.047
7.045
7.041
7.026
7.022
6.895
6.891
6.875
6.872
6.856
6.852
6.612
6.608
6.592
6.589
2.00
1.00
1.00
2.00
2.00
3.00
f1 (ppm)

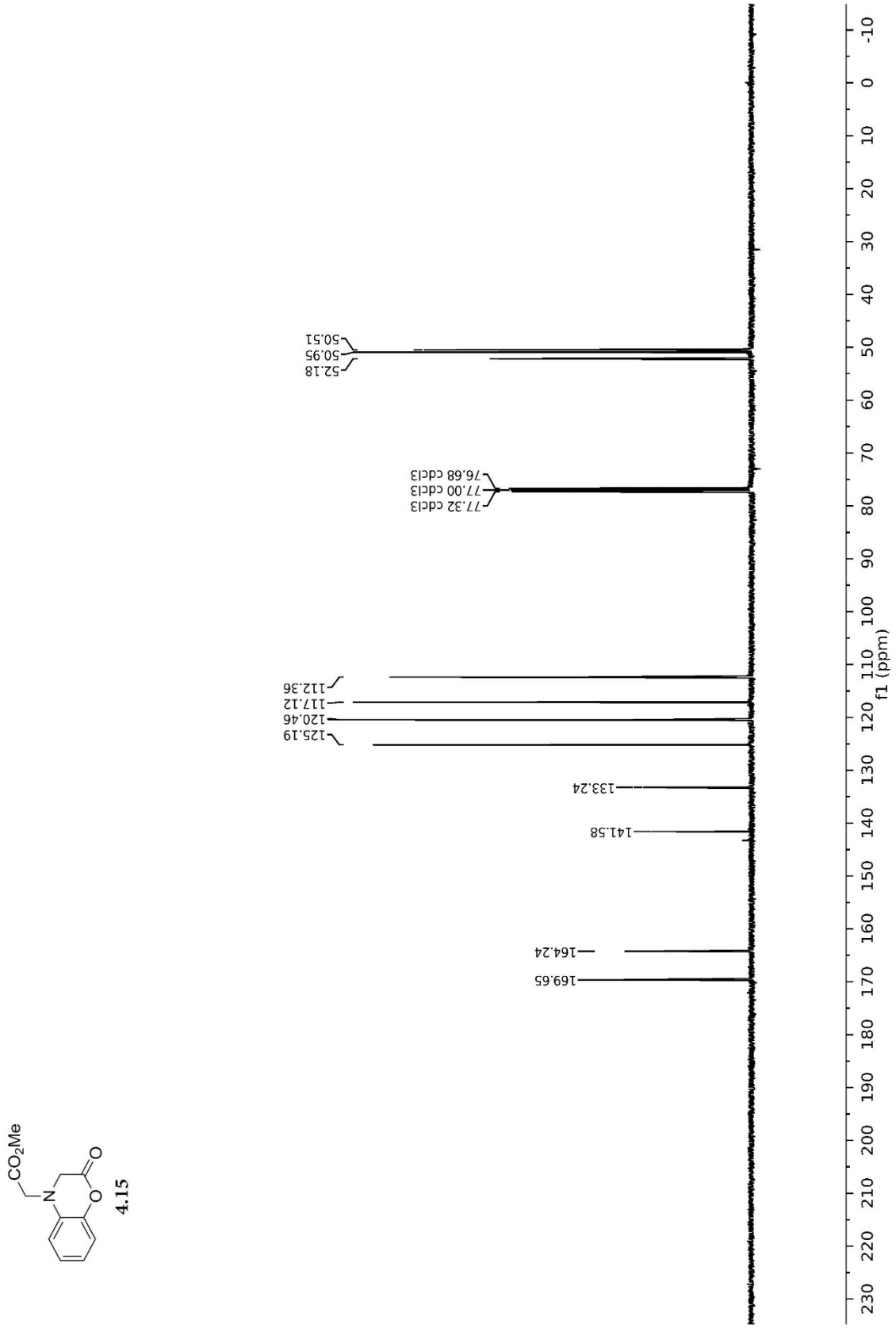
CO2Me
N
O
O
4.15
169.65
164.24
141.58
133.24
125.19
120.46
117.12
112.36
77.32 cdcl3
77.00 cdcl3
76.68 cdcl3
52.18
50.95
50.51
f1 (ppm)

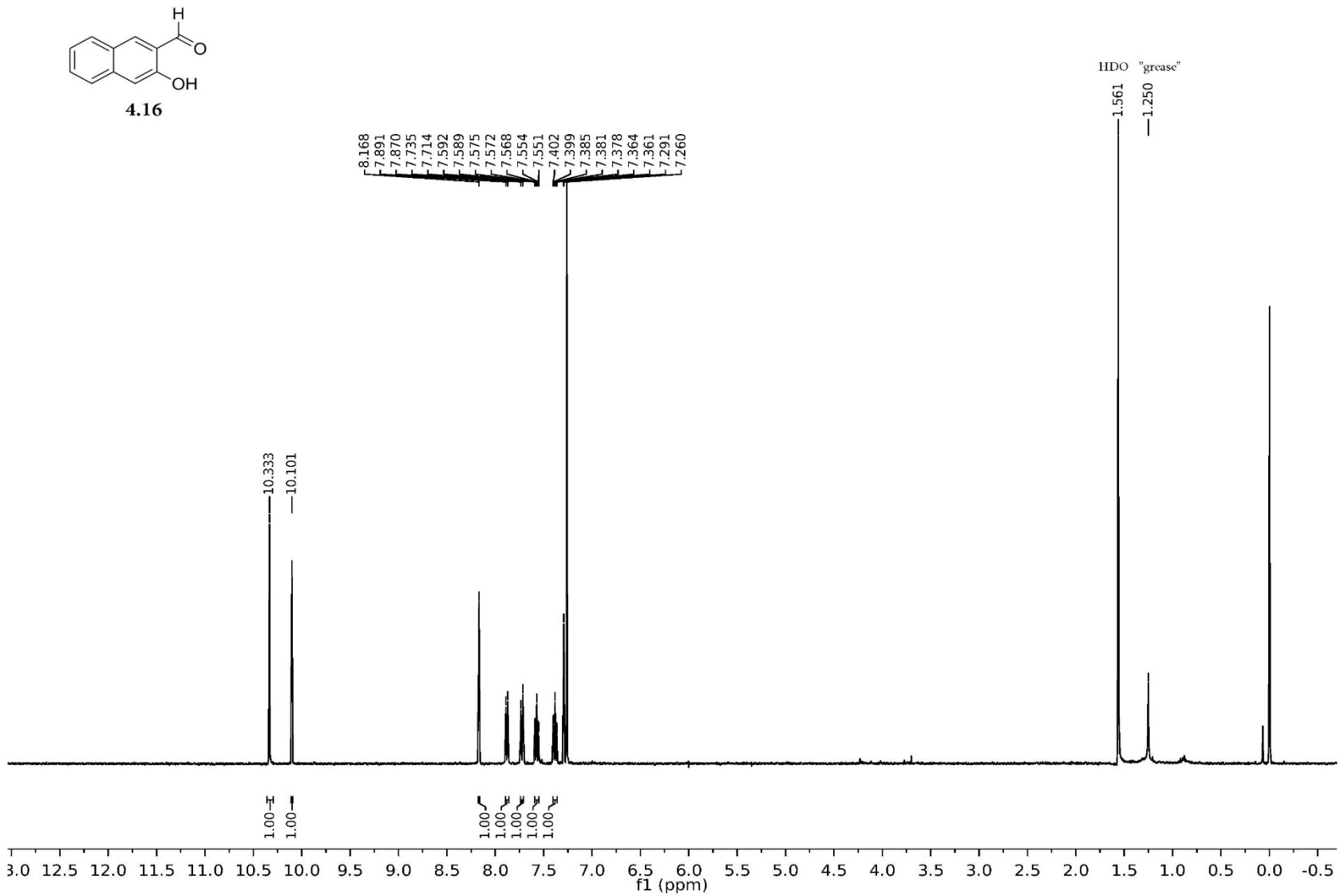
H
O
OH
4.16
HDO
"grease"
1.561
1.250
8.168
7.891
7.870
7.735
7.714
7.592
7.589
7.575
7.572
7.568
7.554
7.551
7.402
7.399
7.385
7.381
7.378
7.364
7.361
7.291
7.260
10.333
10.101
1.00
1.00
1.00
1.00
1.00
1.00
f1 (ppm)

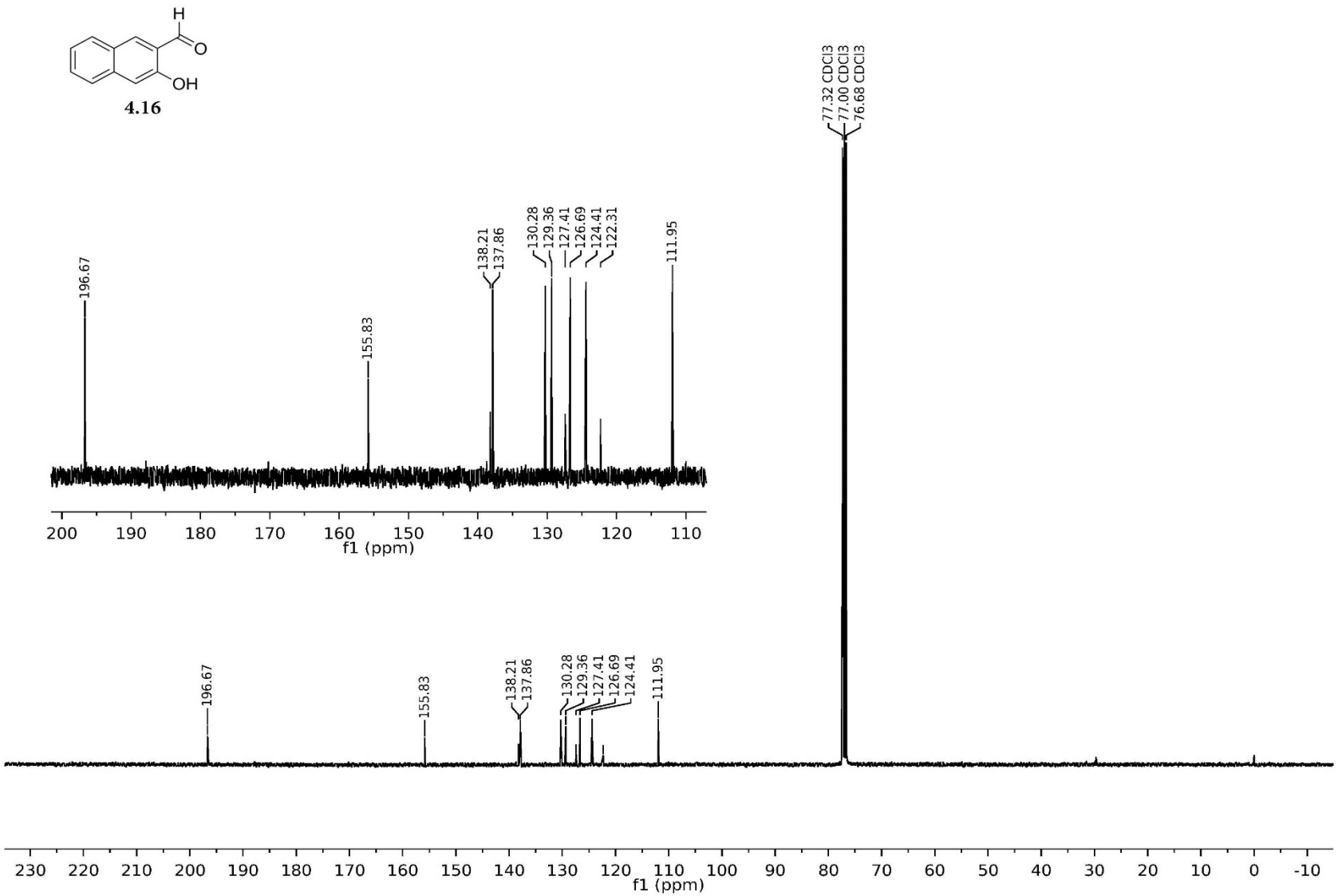
H
O
OH
4.16
196.67
155.83
138.21
137.86
130.28
129.36
127.41
126.69
124.41
122.31
111.95
77.32 CDCl3
77.00 CDCl3
76.68 CDCl3
f1 (ppm)

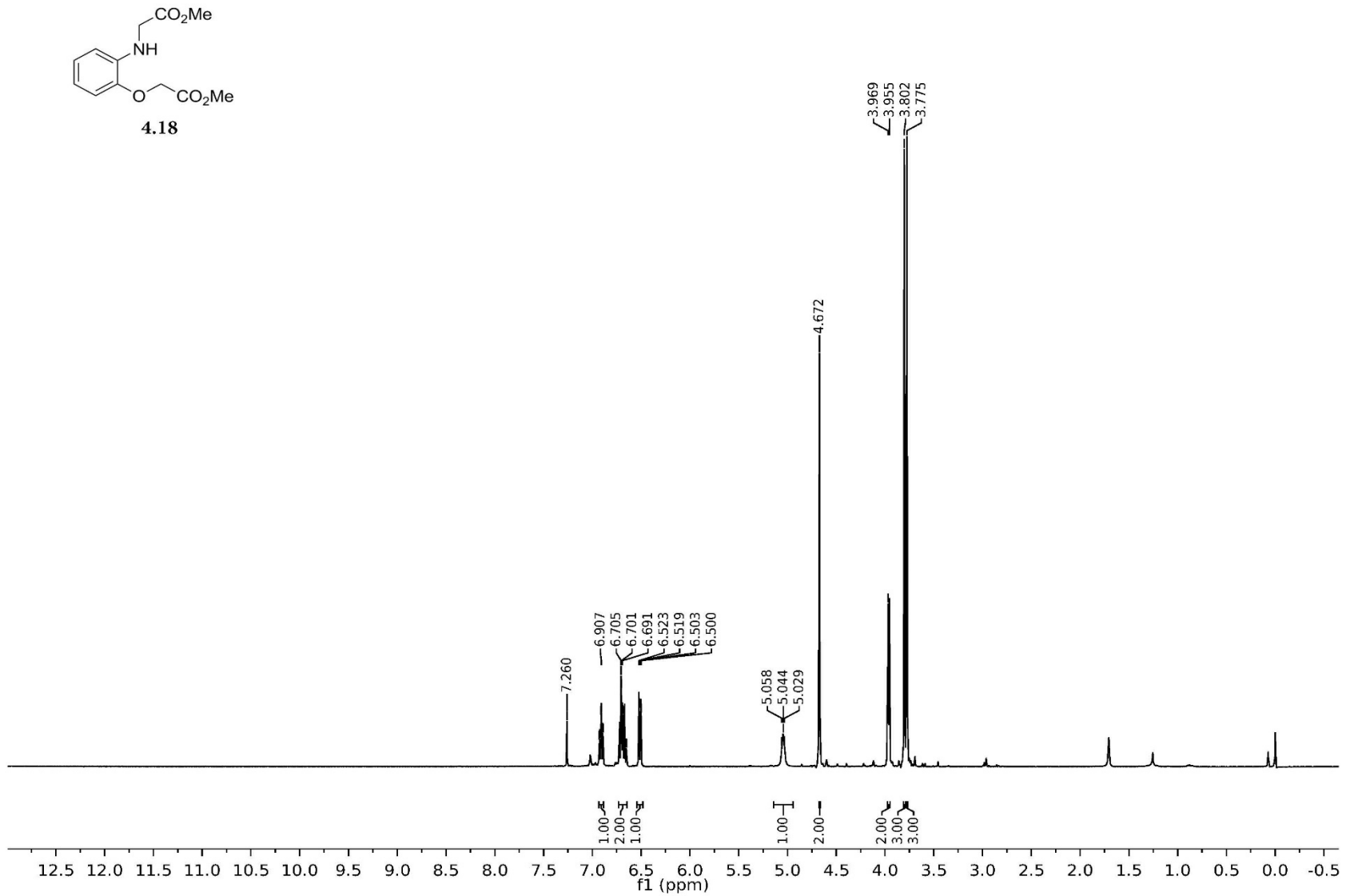
CO2Me
NH
O
CO2Me
4.18
7.260
6.907
6.705
6.701
6.691
6.523
6.519
6.503
6.500
5.058
5.044
5.029
4.672
3.969
3.955
3.802
3.775
1.00
2.00
1.00
1.00
2.00
2.00
3.00
3.00
f1 (ppm)

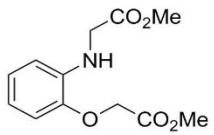
CO2Me
NH
O
CO2Me

4.18

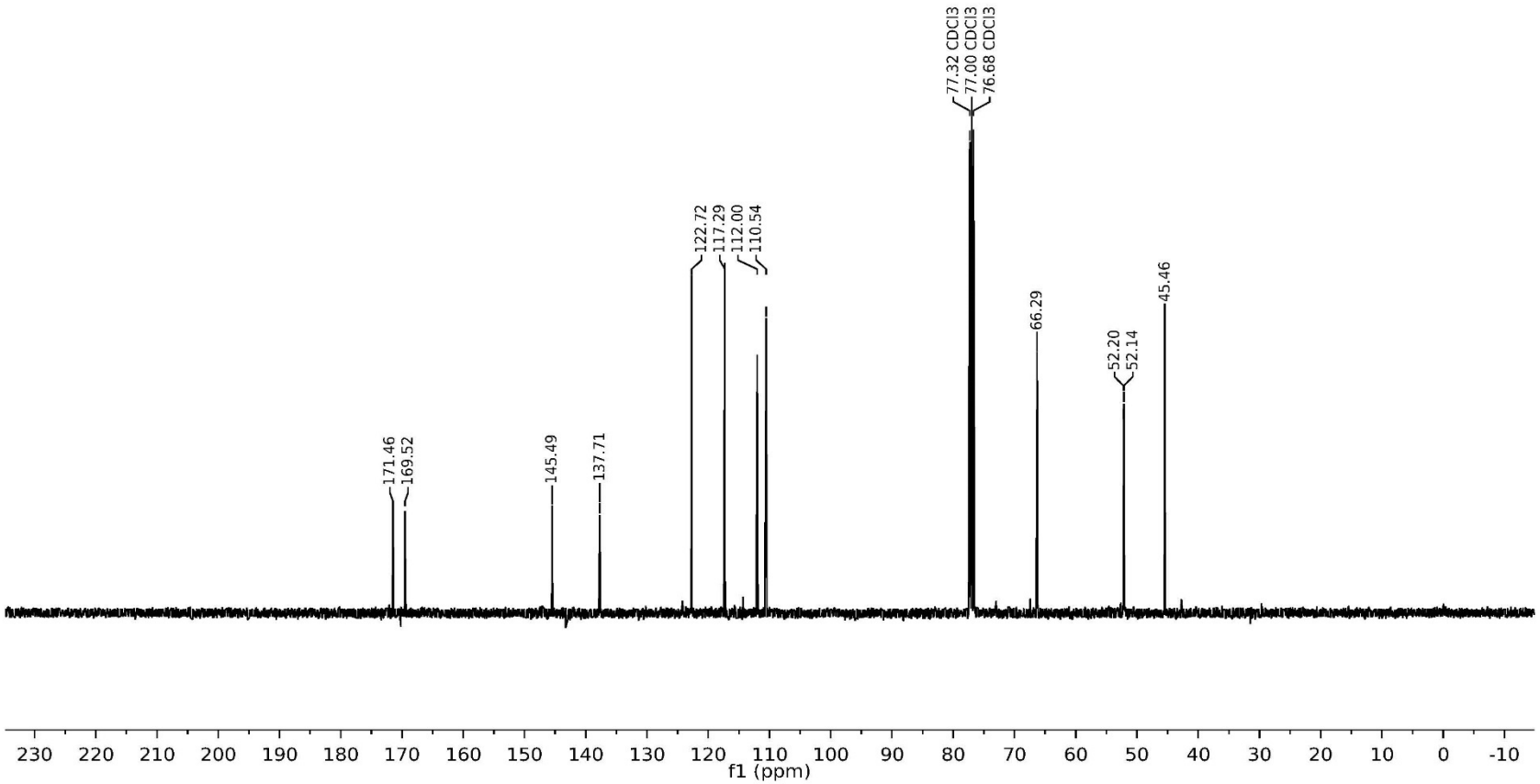
171.46
169.52
145.49
137.71
122.72
117.29
112.00
110.54
77.32 CDCl3
77.00 CDCl3
76.68 CDCl3
66.29
52.20
52.14
45.46
230 220 210 200 190 180 170 160 150 140 130 120 110 100 90 80 70 60 50 40 30 20 10 0 -10
f1 (ppm)

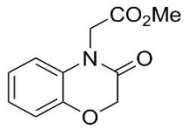
CO2Me
N
O
O

4.19

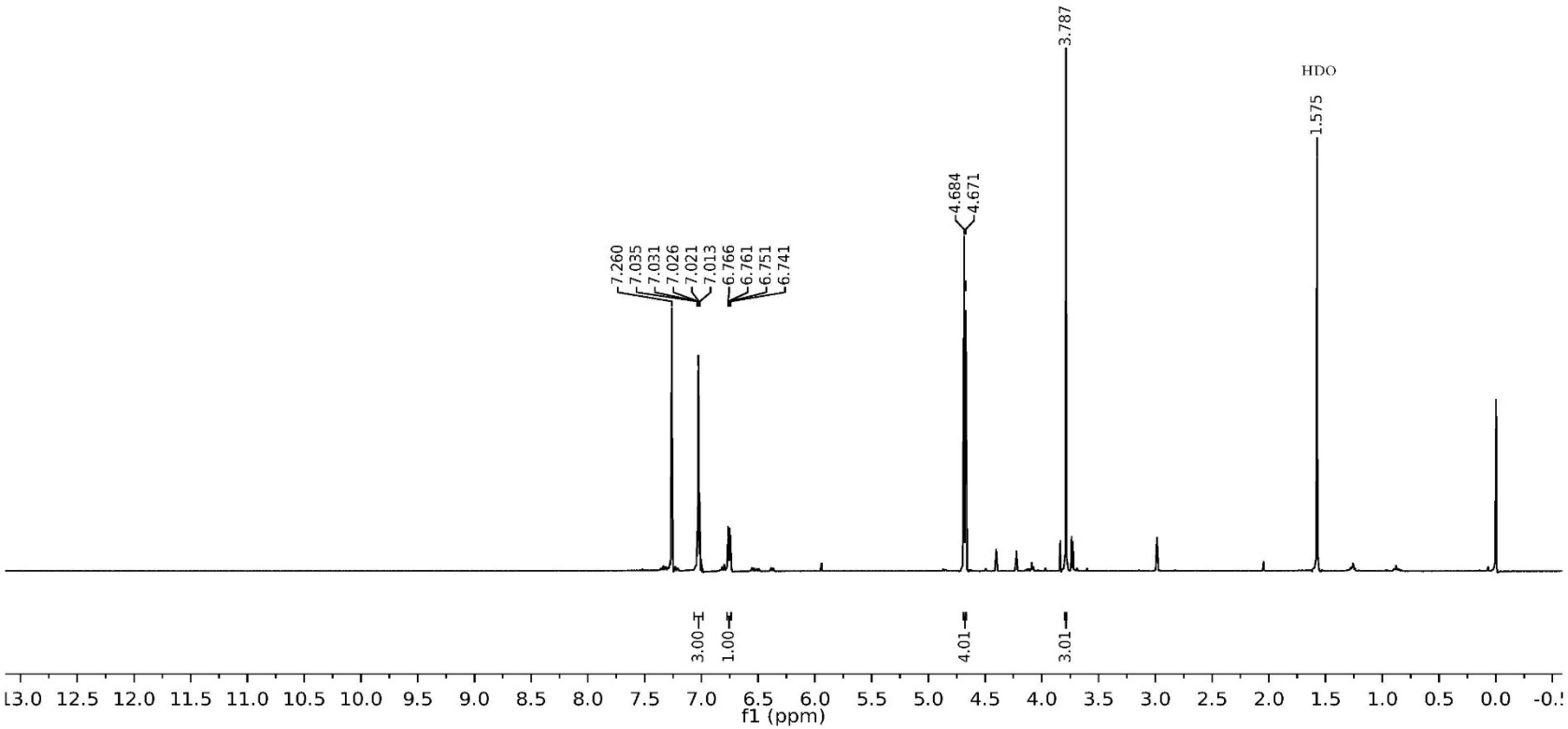
7.260
7.035
7.031
7.026
7.021
7.013
6.766
6.761
6.751
6.741
4.684
4.671
3.787
HDO
1.575
3.00
1.00
4.01
3.01
f1 (ppm)

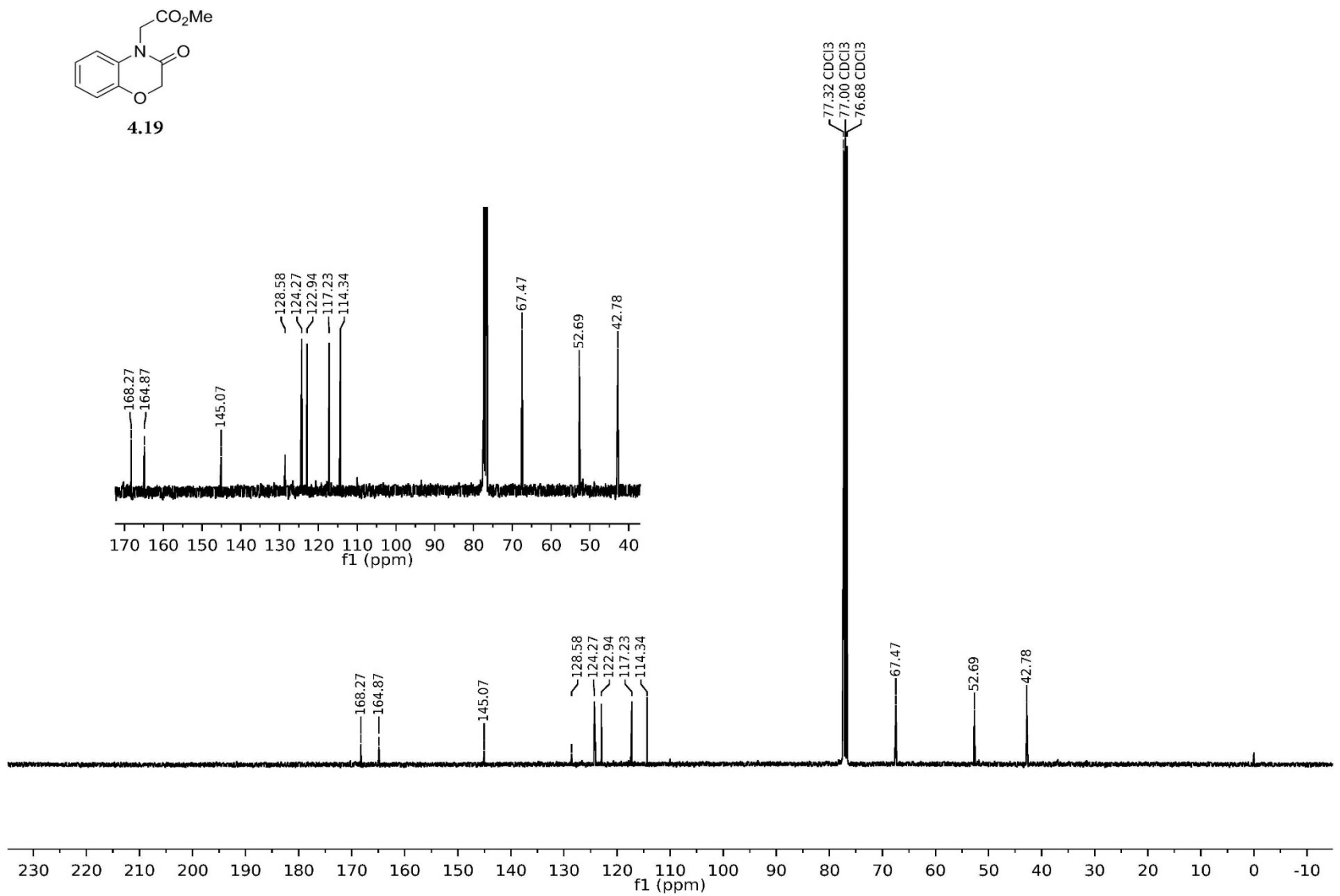
CO2Me
N
O
O
4.19
77.32 CDCl3
77.00 CDCl3
76.68 CDCl3
168.27
164.87
145.07
128.58
124.27
122.94
117.23
114.34
67.47
52.69
42.78
f1 (ppm)

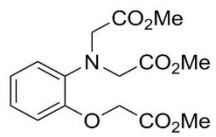
CO2Me
N
CO2Me
O
CO2Me

4.20

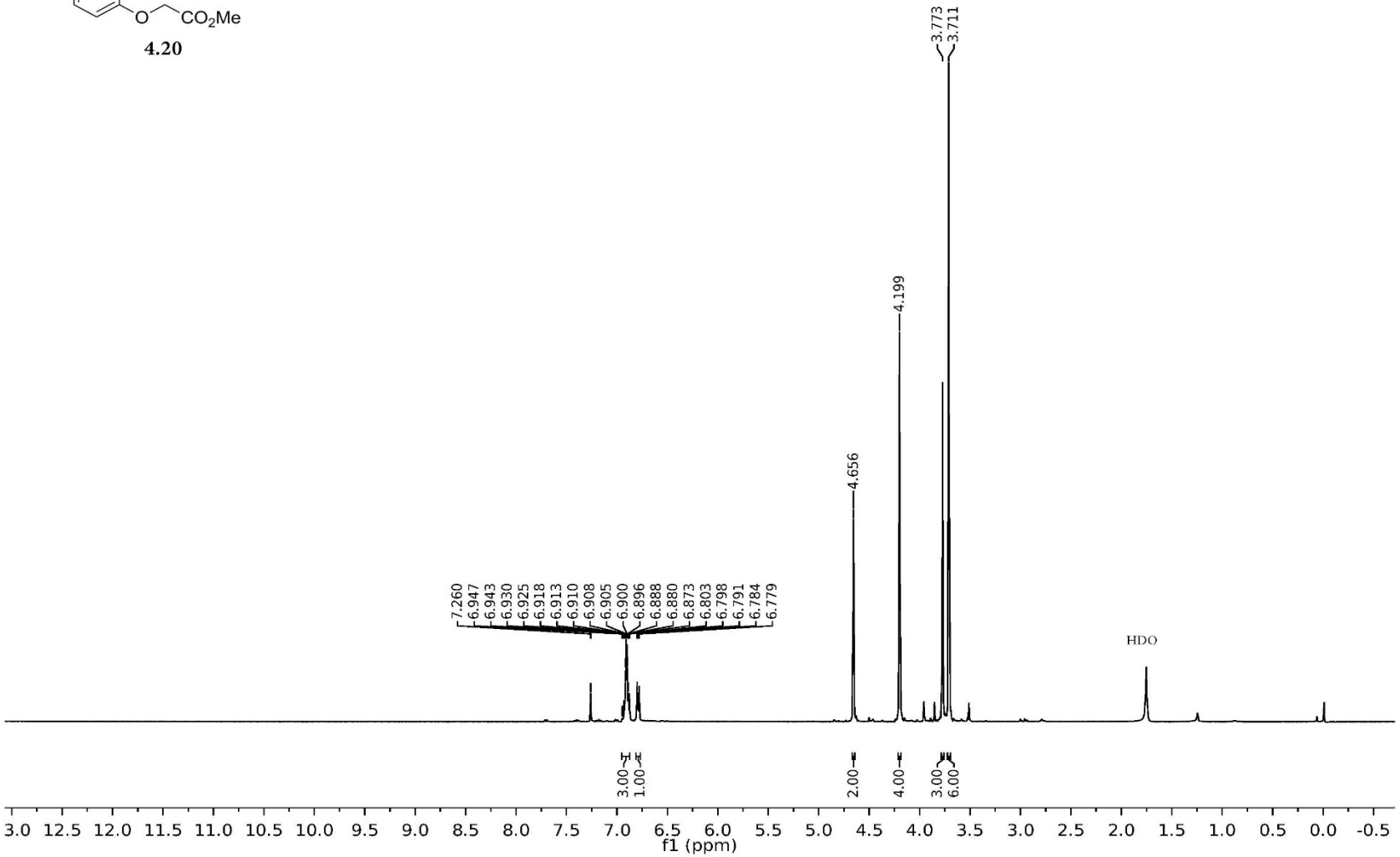
3.773
3.711
4.199
4.656
7.260
6.947
6.943
6.930
6.925
6.918
6.913
6.910
6.908
6.905
6.900
6.896
6.888
6.880
6.873
6.803
6.798
6.791
6.784
6.779
HDO
3.00
1.00
2.00
4.00
3.00
6.00
f1 (ppm)

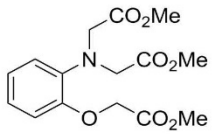
CO2Me
N
CO2Me
O
CO2Me

4.20

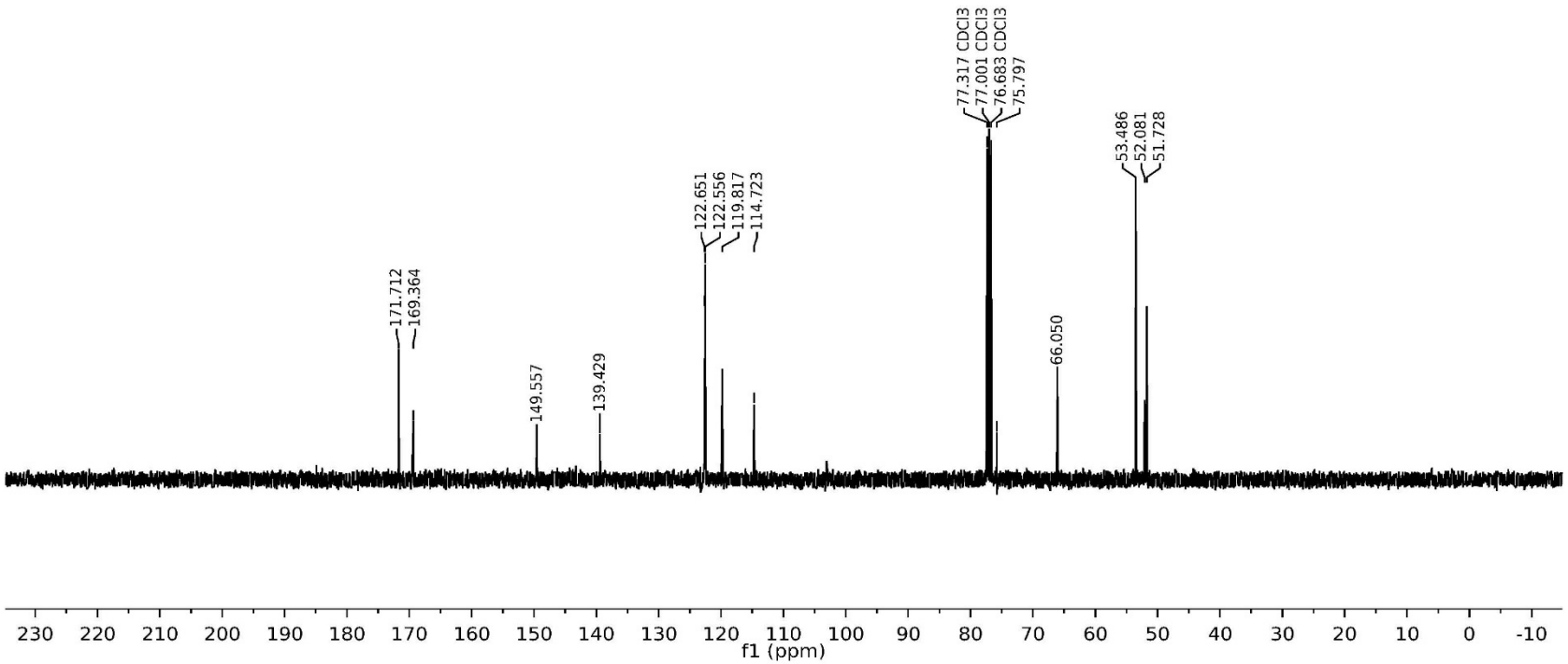
171.712
169.364
149.557
139.429
122.651
122.556
119.817
114.723
77.317 CDCl3
77.001 CDCl3
76.683 CDCl3
75.797
66.050
53.486
52.081
51.728
230 220 210 200 190 180 170 160 150 140 130 120 110 100 90 80 70 60 50 40 30 20 10 0 -10
f1 (ppm)

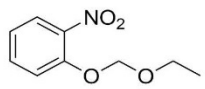
NO2
O
O

4.22

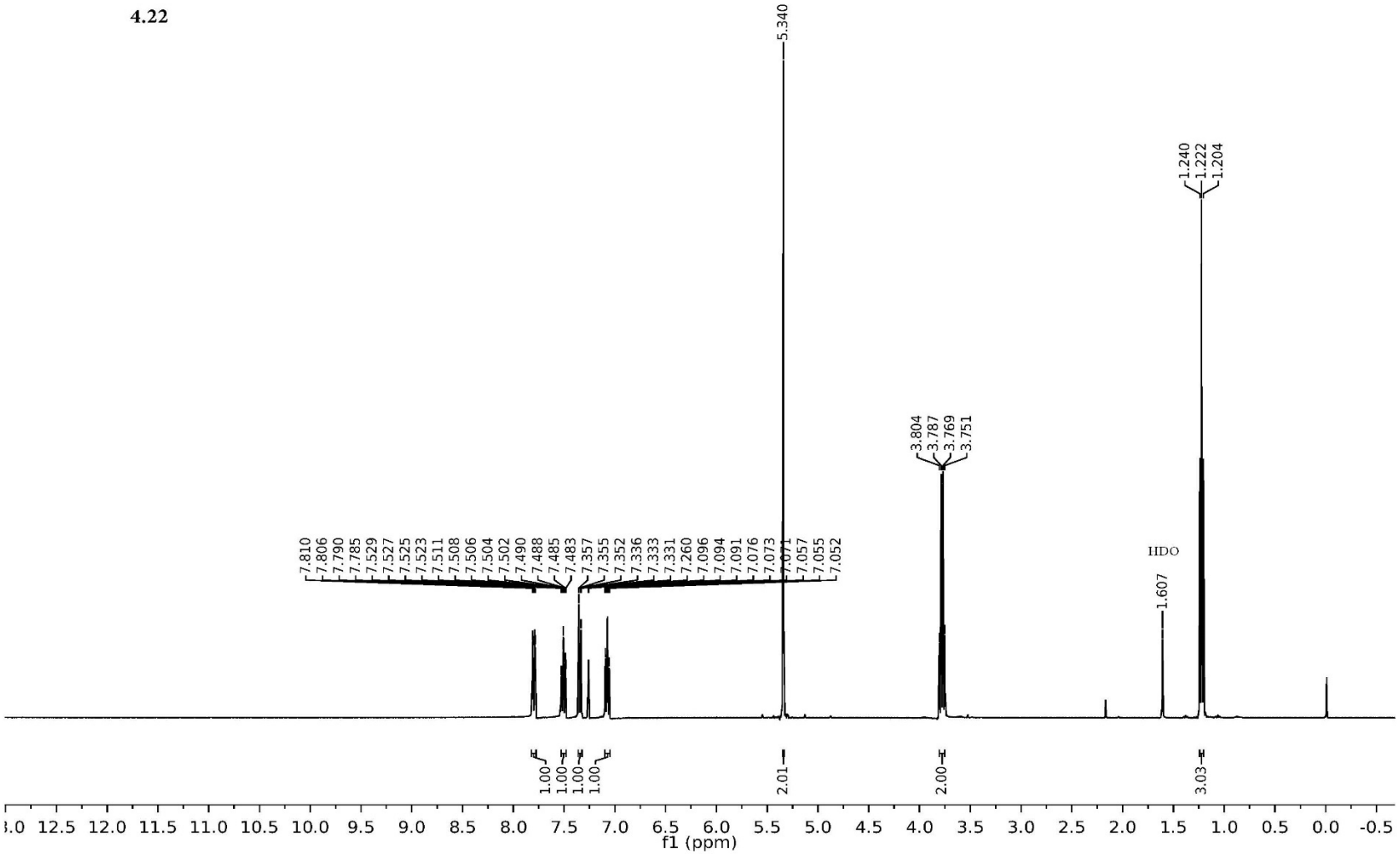
5.340
1.240
1.222
1.204
3.804
3.787
3.769
3.751
HDO
1.607
7.810
7.806
7.790
7.785
7.529
7.527
7.525
7.523
7.511
7.508
7.506
7.504
7.502
7.490
7.488
7.485
7.483
7.357
7.355
7.352
7.336
7.333
7.331
7.260
7.096
7.094
7.091
7.076
7.073
7.071
7.057
7.055
7.052
1.00
1.00
1.00
1.00
2.01
2.00
3.03
f1 (ppm)

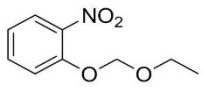
NO2
O
O

4.22

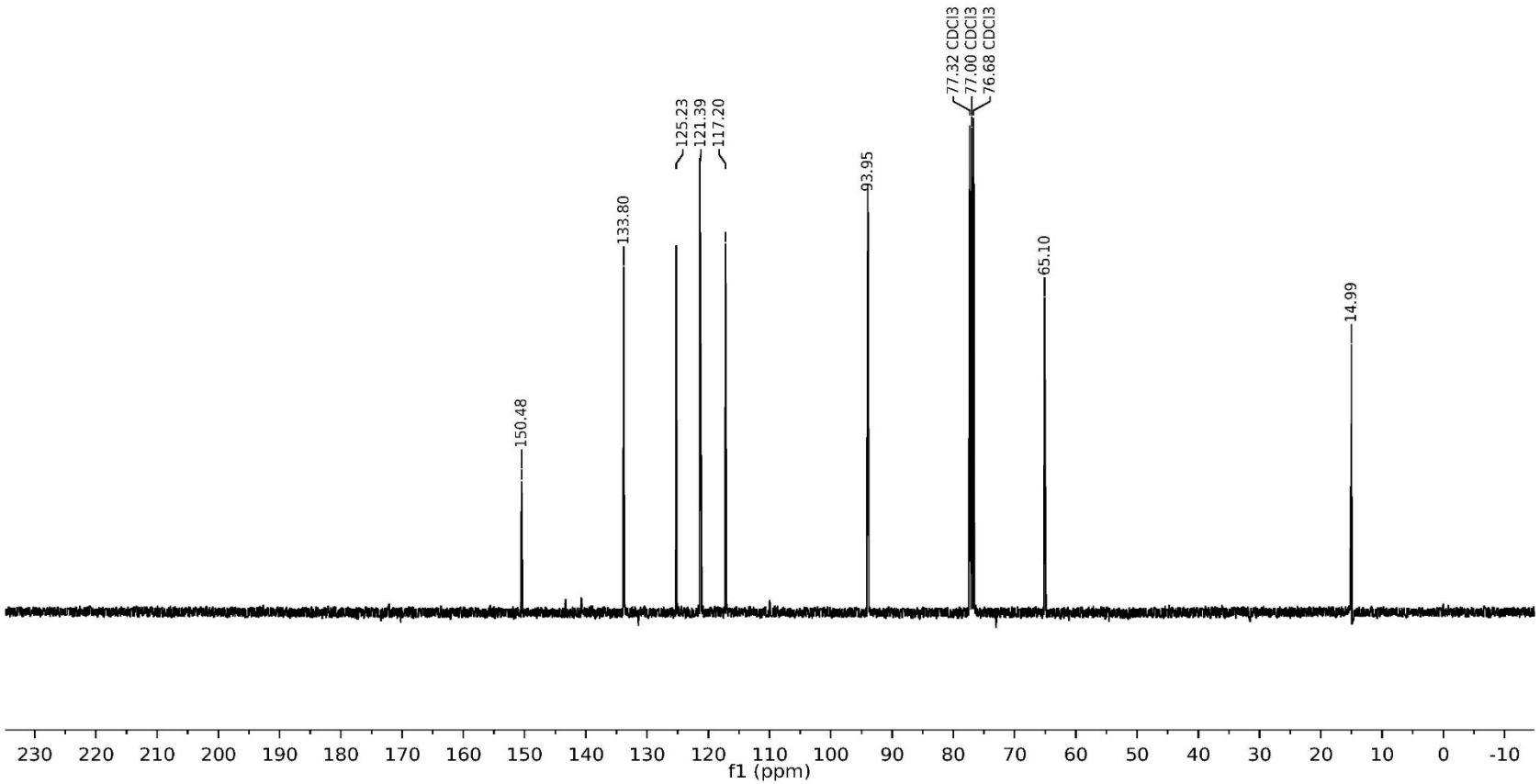
150.48
133.80
125.23
121.39
117.20
93.95
77.32 CDCl3
77.00 CDCl3
76.68 CDCl3
65.10
14.99
230 220 210 200 190 180 170 160 150 140 130 120 110 100 90 80 70 60 50 40 30 20 10 0 -10
f1 (ppm)

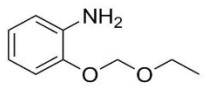
NH2
O
O

4.23

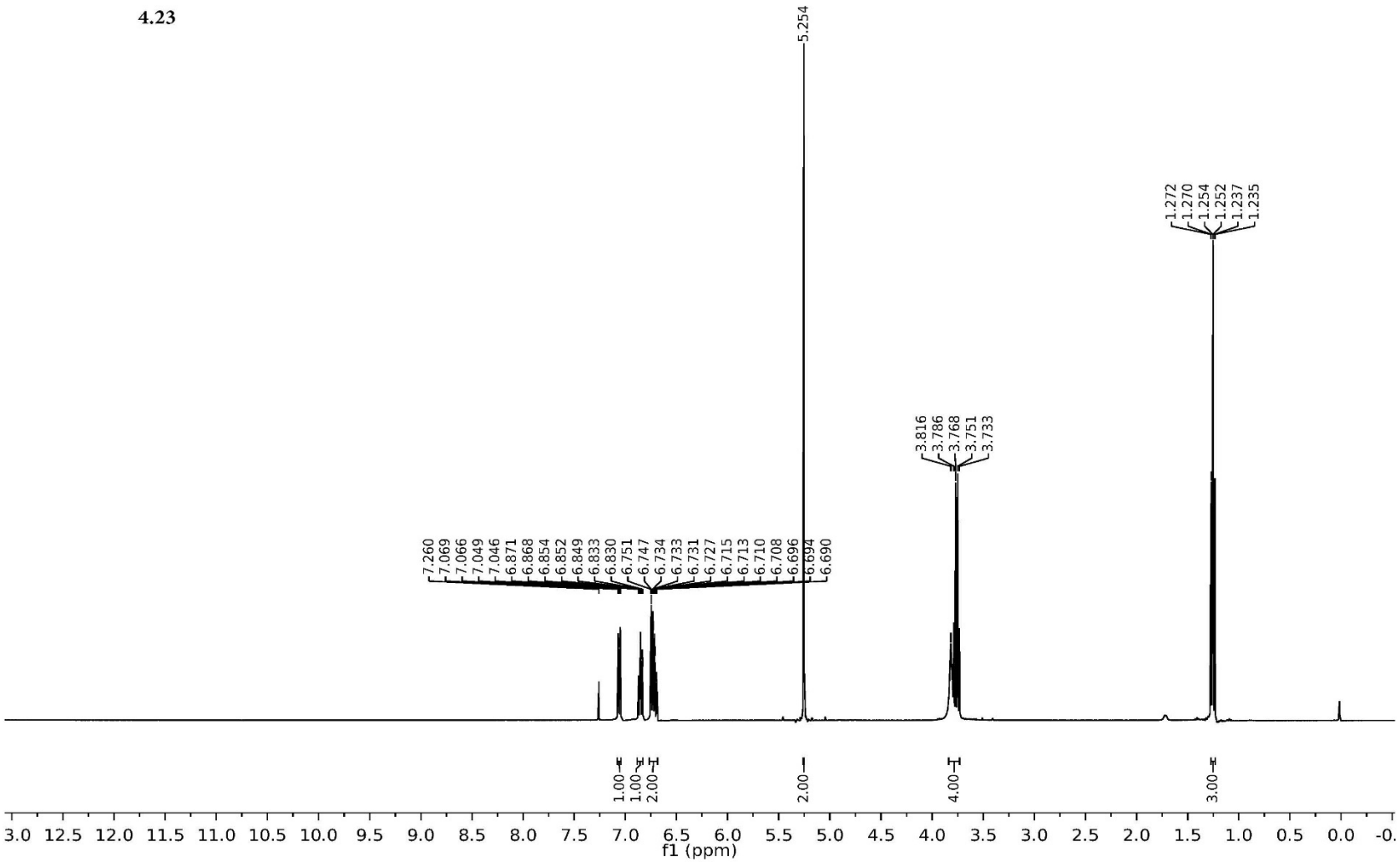
7.260
7.069
7.066
7.049
7.046
6.871
6.868
6.854
6.852
6.849
6.833
6.830
6.751
6.747
6.734
6.733
6.731
6.727
6.715
6.713
6.710
6.708
6.696
6.694
6.690
5.254
3.816
3.786
3.768
3.751
3.733
1.272
1.270
1.254
1.252
1.237
1.235
1.00
1.00
2.00
2.00
4.00
3.00
f1 (ppm)

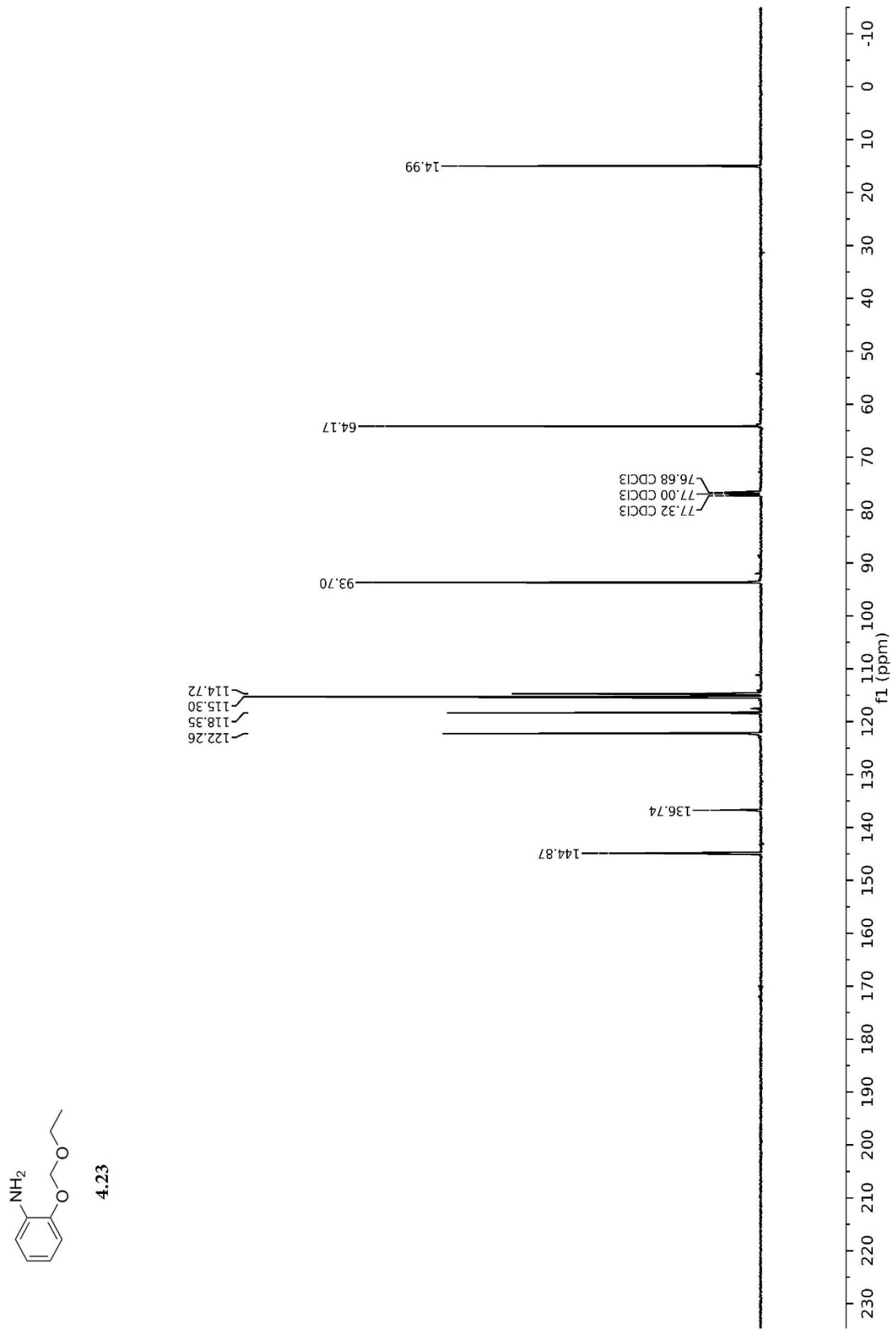
NH2
O
O
144.87
136.74
122.26
118.35
115.30
114.72
93.70
77.32 CDCl3
77.00 CDCl3
76.68 CDCl3
64.17
14.99
f1 (ppm)

4.23

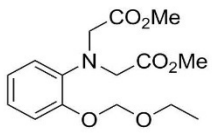
CO2Me
N
CO2Me
O
O

4.24

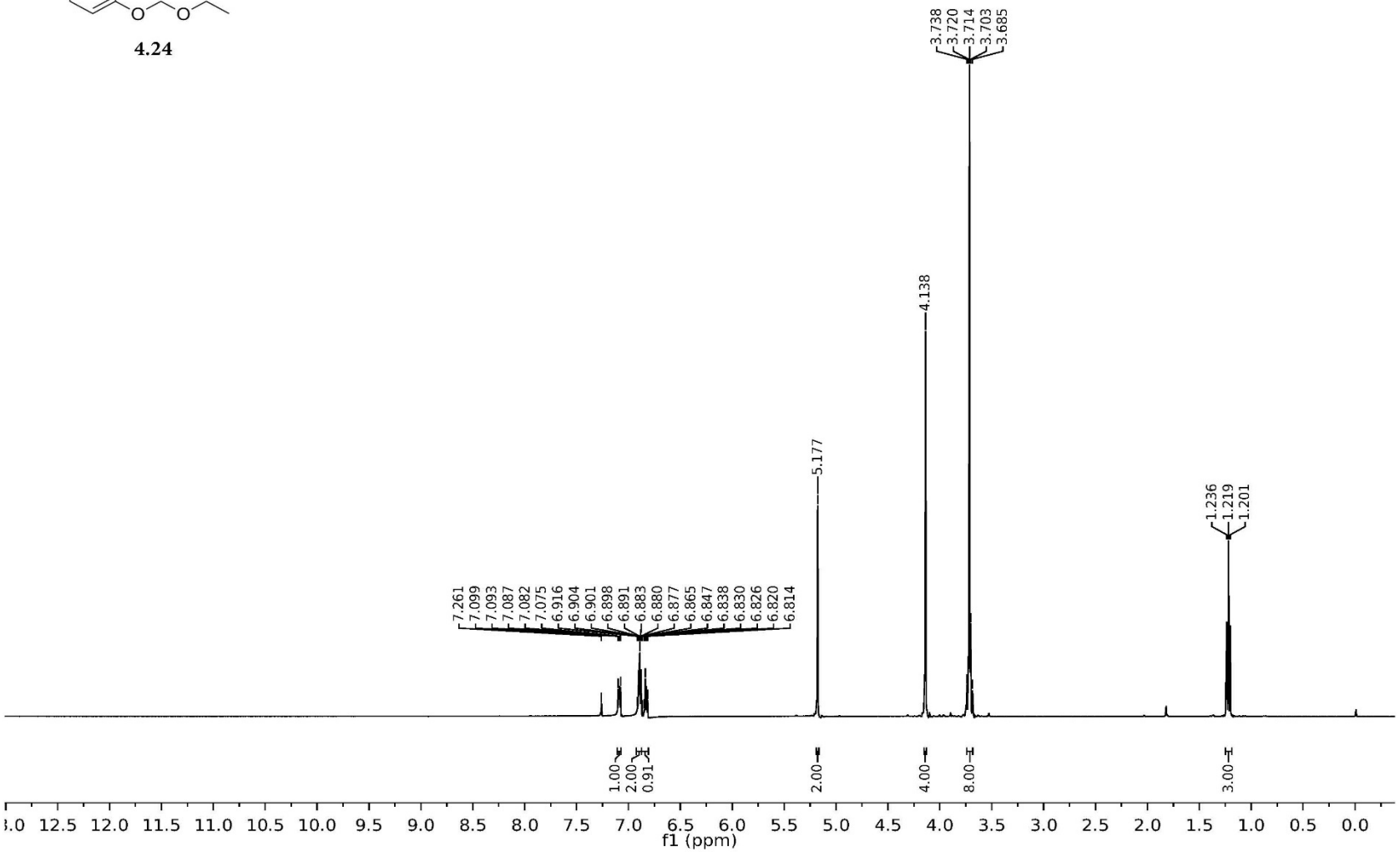
7.261
7.099
7.093
7.087
7.082
7.075
6.916
6.904
6.901
6.898
6.891
6.883
6.880
6.877
6.865
6.847
6.838
6.830
6.826
6.820
6.814
5.177
4.138
3.738
3.720
3.714
3.703
3.685
1.236
1.219
1.201
1.00
2.00
0.91
2.00
4.00
8.00
3.00
f1 (ppm)

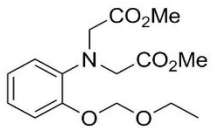
CO2Me
N
CO2Me
O
O

4.24

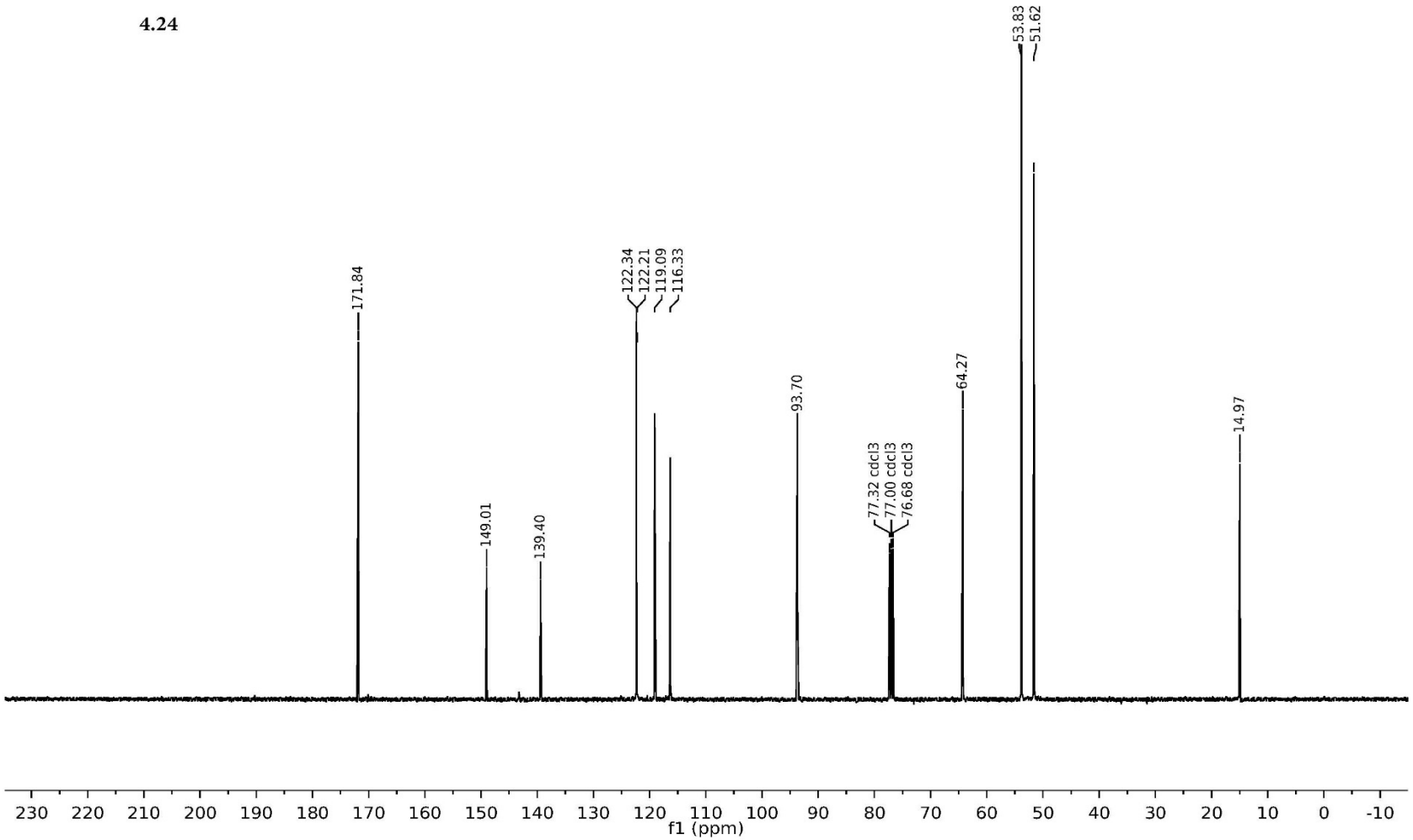
171.84
149.01
139.40
122.34
122.21
119.09
116.33
93.70
77.32 cdcl3
77.00 cdcl3
76.68 cdcl3
64.27
53.83
51.62
14.97
230 220 210 200 190 180 170 160 150 140 130 120 110 100 90 80 70 60 50 40 30 20 10 0 -10
f1 (ppm)

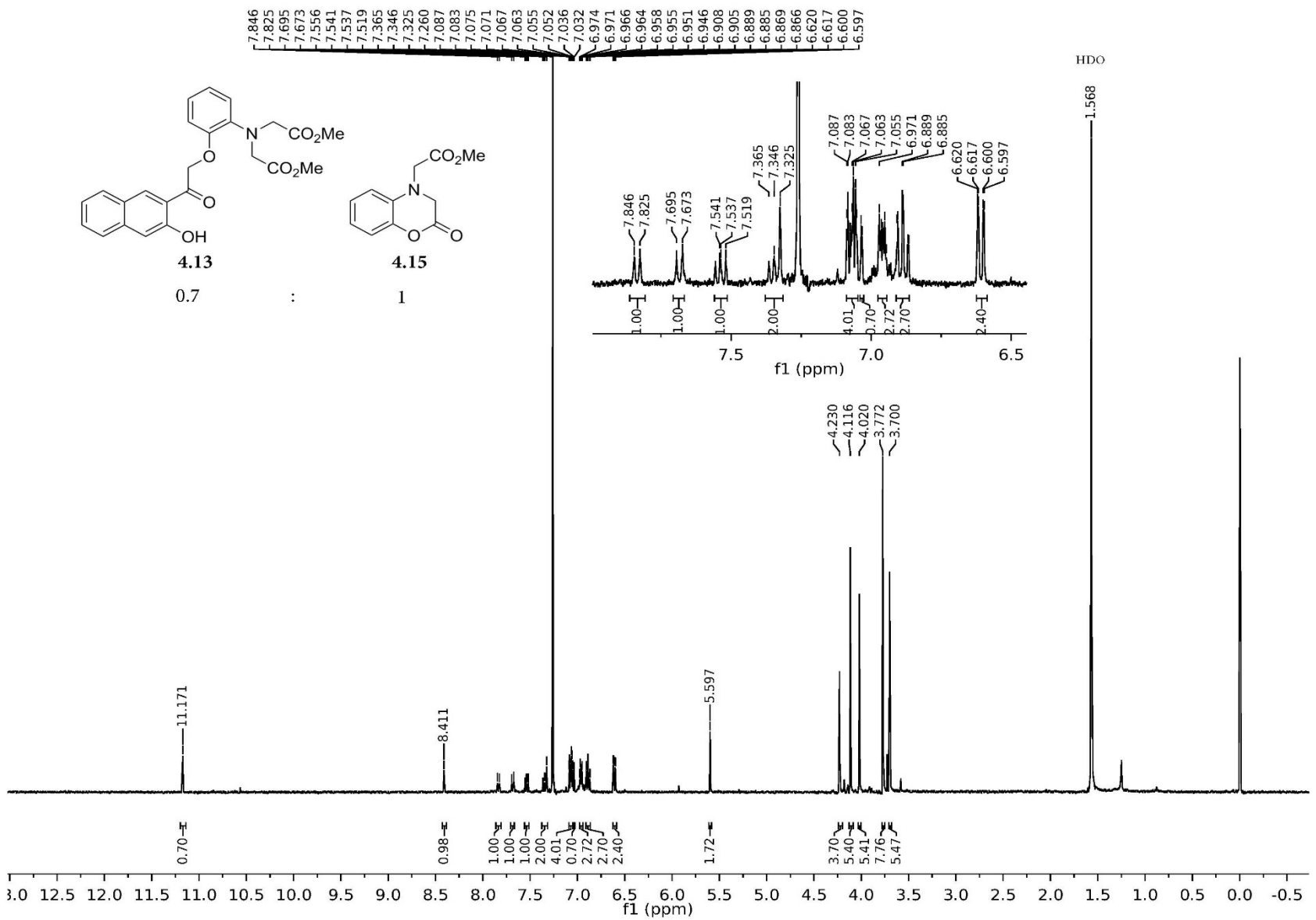
4.13
4.15
0.7 : 1
HDO
1.568
11.171
8.411
5.597
f1 (ppm)

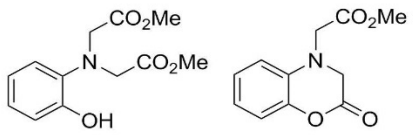
CO2Me
N
CO2Me
OH

4.14

1 : 2

CO2Me
N
O
O

4.15

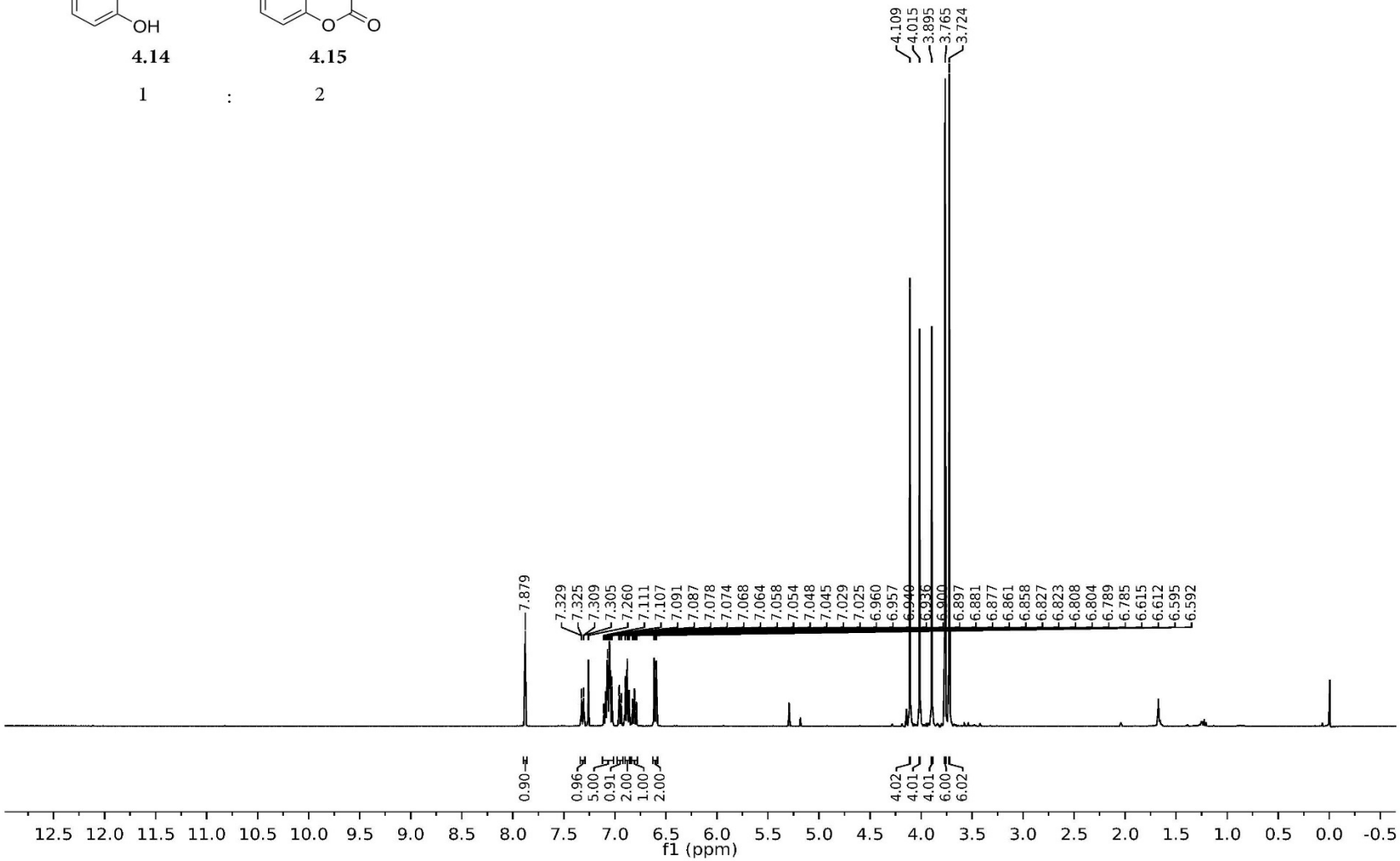
4.109
4.015
3.895
3.765
3.724
7.879
7.329
7.325
7.309
7.305
7.260
7.111
7.107
7.091
7.087
7.078
7.074
7.068
7.064
7.058
7.054
7.048
7.045
7.029
7.025
6.960
6.957
6.940
6.936
6.900
6.897
6.881
6.877
6.861
6.858
6.827
6.823
6.808
6.804
6.789
6.785
6.615
6.612
6.595
6.592
0.90
0.96
5.00
0.91
2.00
1.00
2.00
4.02
4.01
4.01
6.00
6.02
12.5 12.0 11.5 11.0 10.5 10.0 9.5 9.0 8.5 8.0 7.5 7.0 6.5 6.0 5.5 5.0 4.5 4.0 3.5 3.0 2.5 2.0 1.5 1.0 0.5 0.0 -0.5
f1 (ppm)

OCH3
OH
OCH3
OCH3
OCH3
5.31
3.757
5.641
5.620
6.509
6.525
6.669
6.689
7.105
7.122
7.139
7.260
7.260 cddi3
12.10
1.00
4.01
0.88
2.00
f1 (ppm)

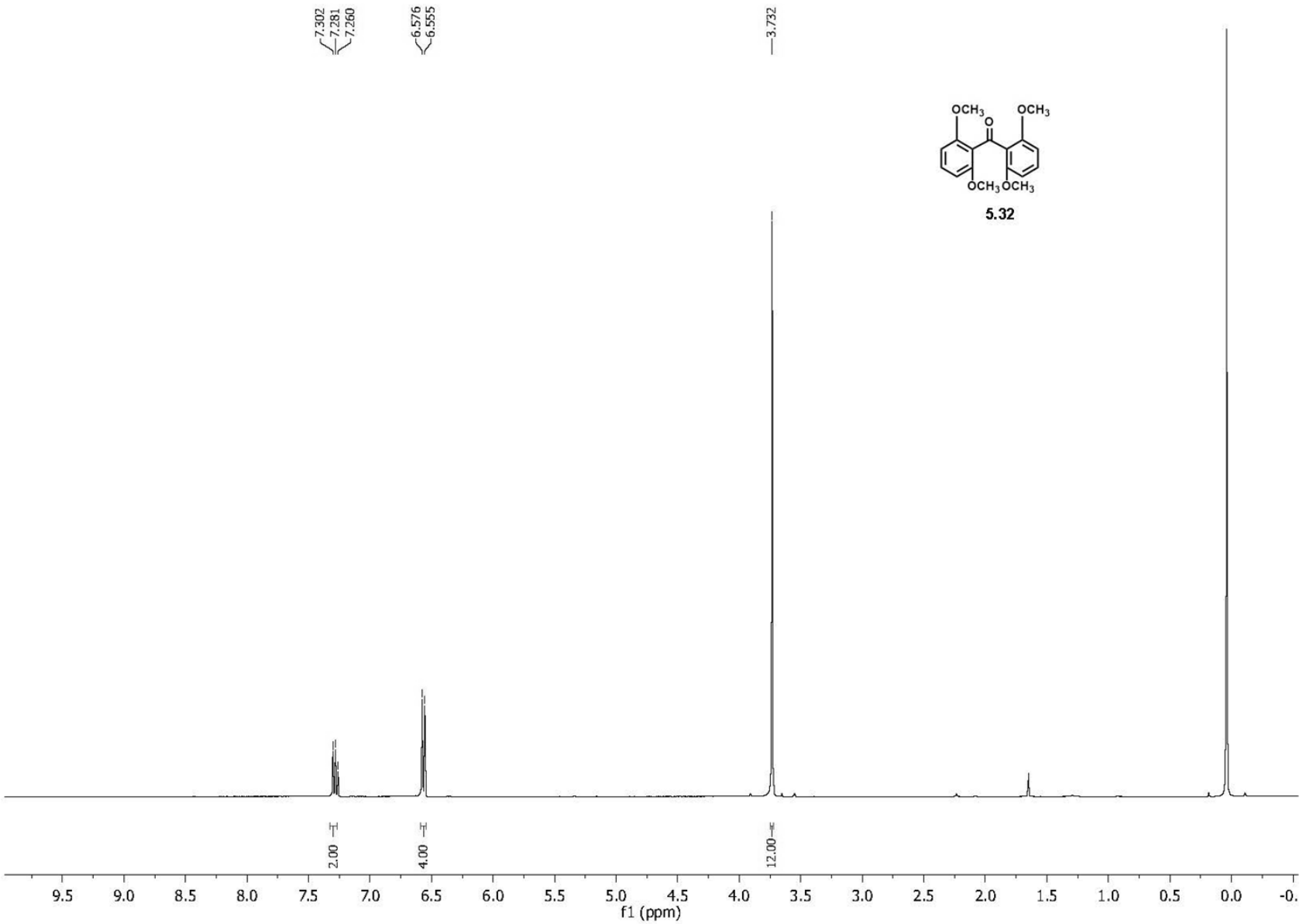
7.302
7.281
7.260
6.576
6.555
3.732
OCH3
OCH3
OCH3
OCH3
O
5.32
2.00
4.00
12.00
f1 (ppm)

193.8
158.4
130.9
121.9
104.5
77.3 CDCl3
77.0 CDCl3
76.7 CDCl3
56.2
0.0
OCH3
OCH3
O
OCH3
OCH3
5.32
f1 (ppm)

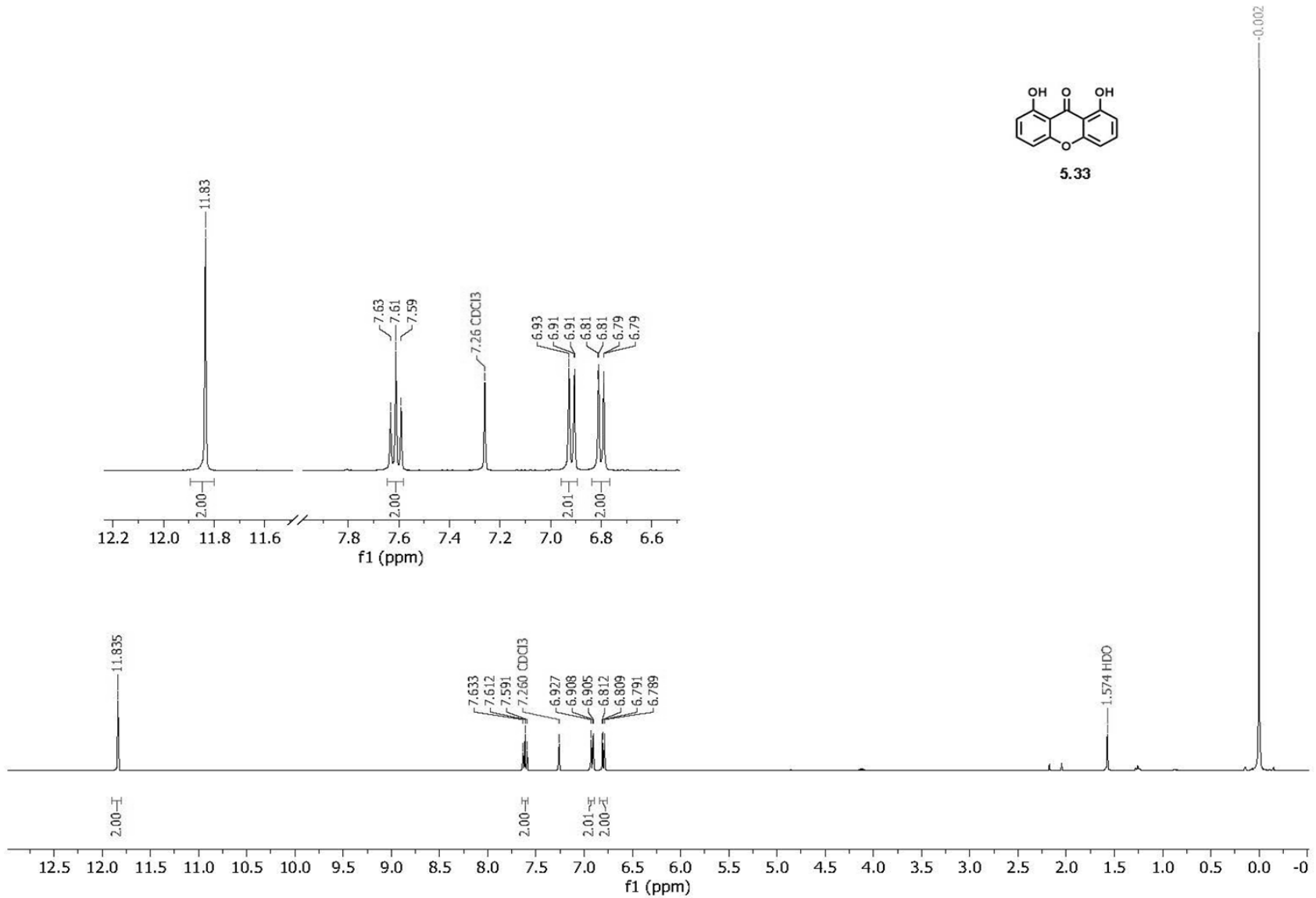
OH
O
OH
O
5.33
11.83
7.63
7.61
7.59
7.26 CDCl3
6.93
6.91
6.91
6.81
6.81
6.79
6.79
2.00
2.00
2.01
2.00
12.2 12.0 11.8 11.6 7.8 7.6 7.4 7.2 7.0 6.8 6.6
f1 (ppm)
11.835
7.633
7.612
7.591
7.260 CDCl3
6.927
6.908
6.905
6.812
6.809
6.791
6.789
1.574 HDO
0.002
2.00
2.00
2.01
2.00
12.5 12.0 11.5 11.0 10.5 10.0 9.5 9.0 8.5 8.0 7.5 7.0 6.5 6.0 5.5 5.0 4.5 4.0 3.5 3.0 2.5 2.0 1.5 1.0 0.5 0.0 -0
f1 (ppm)

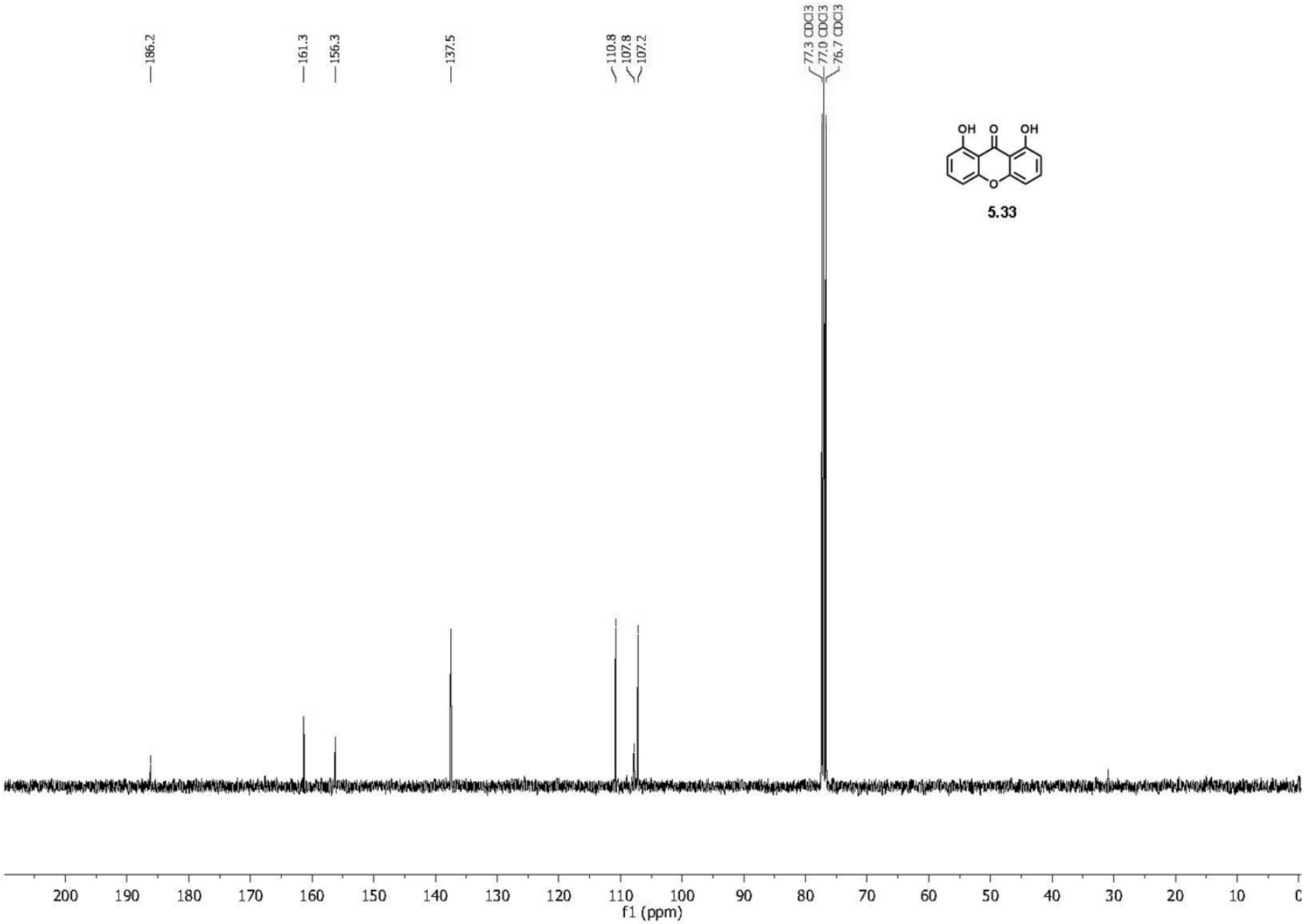
186.2
161.3
156.3
137.5
110.8
107.8
107.2
77.3 CDCl3
77.0 CDCl3
76.7 CDCl3
OH
O
OH
O
5.33
200
190
180
170
160
150
140
130
120
110
100
90
80
70
60
50
40
30
20
10
0
f1 (ppm)

5.34
6.975
6.955
6.935
6.481
6.461
6.452
6.431
4.917 HDO
4.645
3.729
3.330 MeOD
3.318 MeOD
3.314 MeOD
3.310 MeOD
3.306 MeOD
3.302 MeOD
2.00
4.00
1.00
2.00
f1 (ppm)

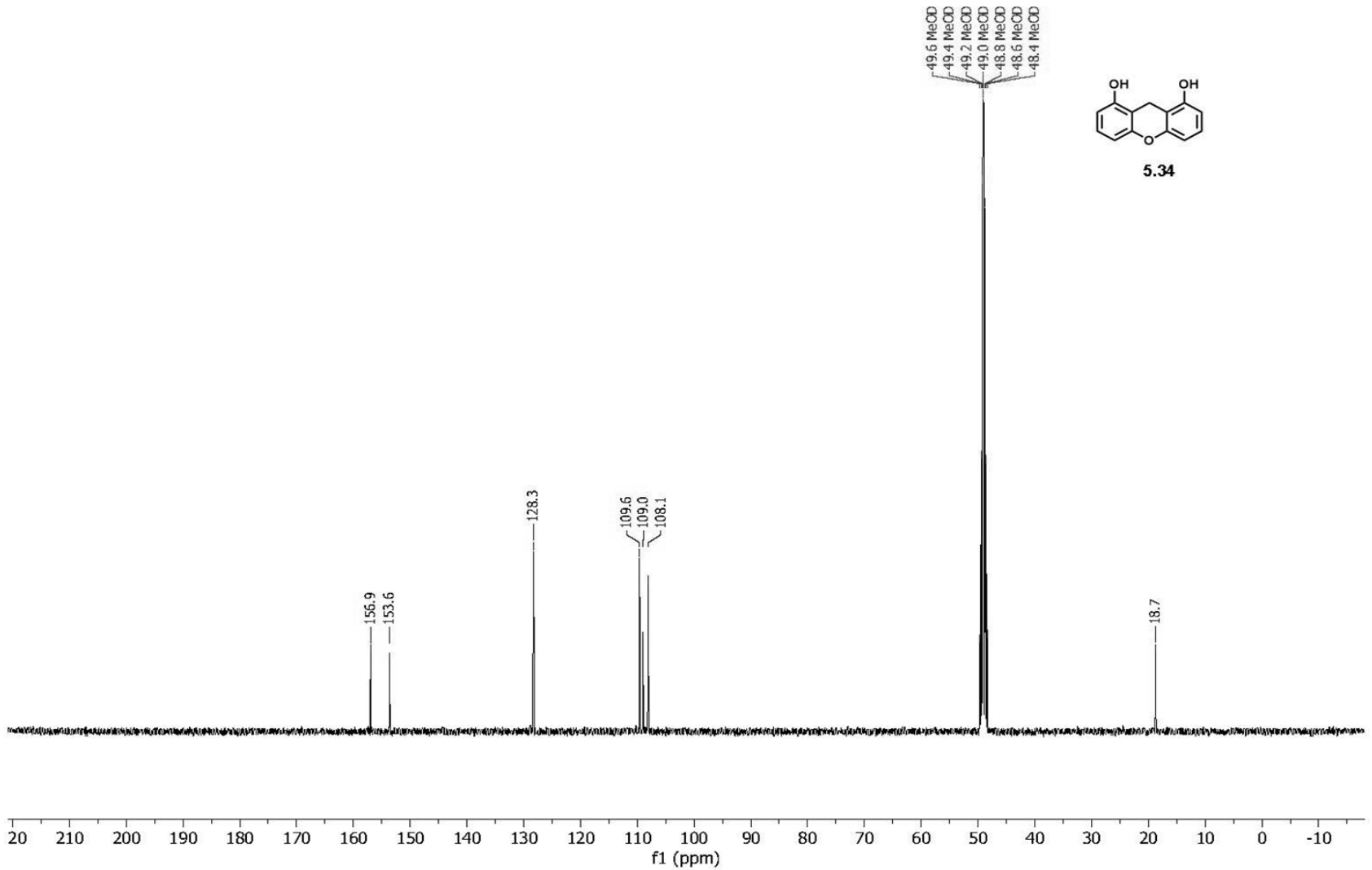
49.6 MeOD
49.4 MeOD
49.2 MeOD
49.0 MeOD
48.8 MeOD
48.5 MeOD
48.4 MeOD
OH
OH
O
5.34
156.9
153.6
128.3
109.6
109.0
108.1
18.7
20 210 200 190 180 170 160 150 140 130 120 110 100 90 80 70 60 50 40 30 20 10 0 -10
f1 (ppm)

1.616 HDO
1.613 HDO
OCH3
OCH3
OH
Ph
OCH3
OCH3
5.35
3.395
6.447
6.450
6.544
6.565
7.107
7.111
7.130
7.148
7.152
7.203
7.222
7.241
7.261 CDCl3
7.452
7.471
12.00
1.00
4.00
2.00
2.99
2.00
2.00
f1 (ppm)

OCH3
OH
OCH3
Ph
OCH3
OCH3
5.35
56.4
79.4
77.3 CDCl3
77.0 CDCl3
76.7 CDCl3
106.8
127.3
126.6
126.5
126.3
125.4
149.3
158.0
f1 (ppm)